The University Of Sheffield.

Role of microRNAs in Determining the Cancer-associated Fibroblast Phenotype

By:

Siti Amalina Bt Inche Zainal Abidin

A thesis submitted in partial fulfilment of the requirements for the degree of Doctor of Philosophy

The University of Sheffield

Faculty of Medicine, Dentistry and Health

School of Clinical Dentistry

November 2017

ACKNOWLEDGEMENTS

Foremost, I am sincerely thankful to my supervisors, Dr Dan Lambert and my co-supervisor, Dr Stuart Hunt for their support and supervision throughout my study. Special thanks to Dr Dan Lambert who constantly guided me in every aspect of this research project; it made my Ph.D. journey really valuable and memorable.

I would like to acknowledge Dr Ryan Pink from Oxford Brookes University who helped me in the analysis of miRNA expression profiling outlined in the thesis. I'm grateful to people who provided help during my study, especially Brenka and Jason for technical assistance. Many thanks to other members of the research group especially Genevieve, Tasnuva, Priyanka, and Amy, for all their help and support around the lab. I would like to thank everyone within the Oral and Maxillofacial Pathology department who directly or indirectly help me during 3 years of my study. Special thanks to my colleagues- Nitin, Zulaiha, Fahmi and Zaki for their kindness, patience and words of wisdom during 'stay back' time in the lab.

I would like to thank Ministry of Education Malaysia and the University of Malaya, Malaysia for funding my study.

Last but not least, I owe my deepest gratitude to my lovely husband and kids for their unconditional love, support, and inspiration. I must say that juggling with study and raising kids is not an easy task. Thanks for always being there for me. Kids, I'll replace the time that I stole from you-that's my promise. Thanks to my parents and in-law family for their continuous prayers for my success. I love you all.

TABLE OF CONTENTS

LIST OF FIGURES

LIST OF TABLES

ABBREVIATIONS

µg	Microgram
µl	Microlitre
ADAM	A disintegrin and metalloprotease
anti-miR/s	miRNA inhibitor/s
ATP	Adenosine triphosphate
B2M	B2-Microglobulin
BCA	Bicinchoninic acid
BSA	Bovine serum albumin
CAF	Cancer-associated fibroblasts
CDKIs	Cyclin-dependent kinase inhibitors
cDNA	Complementary DNA
COL1A1	Collagen type 1A1
CTGF	Connective tissue growth factor
DMEM	Dulbecco's modified Eagle's medium
DNA	Deoxyribonucleic acid
DPBS	Dulbecco phosphate buffer saline
eCAF	Experimentally derived CAF
ECM	Extracellular matrix
EDTA	Ethylene-diamine tetra
EGFR	Epidermal growth factor receptor
EMT	Epithelial-mesenchymal transition
EndMT	Endothelial-mesenchymal transition
FAP	Fibroblast activation protein
FBS	Foetal bovine serum
FN	Fibronectin

FN-EDA1	Fibronectin containing extra domain A
FSP-1	Fibroblast-specific protein 1
GS-OSCC	Genetically stable OSCC
GU-OSCC	Genetically unstable OSCC
h	hour
HGF	Hepatocyte growth factor
HIF-α	Hypoxia-inducing factor α
HNSCC	Head and neck squamous cell carcinoma
HPV	Human papillomavirus
HRP	Horseradish peroxidase
IGF	Insulin-like growth factor 1
IL	Interleukin
kDa	Kilodalton
LDH	Lactate dehydrogenase
LOH	Loss of heterozygosity
M	Molar
Min	Minute
miRNAs/miRs	MicroRNAs
ml	Milliliter
mM	Millimolar
MMPs	Matrix metalloproteases
MMT	Mesenchymal mesenchymal transition
mRNA	Messenger RNA
MSCs	Mesenchymal stem cells
ng	Nanogram
nM	Nanomolar
NOF	Normal oral fibroblasts

OSCC	Oral squamous cell carcinoma
PDGF	Platelet-derived growth factor
pre-miR	miRNA mimic
qRT-PCR	Quantitative real-time polymerase chain reaction
RIPA	Radioimmunoprecipitation assay
RISC	RNA-inducing silencing complex
RNA	Ribonucleic acid
s	Seconds
SASP	Senescence-associated secretory phenotype
SA-βgal	Senescence-associated β galactosidase
SDF-1	Stromal cell-derived factor 1
SEM	Standard error of mean
TAMs	Tumour-associated macrophages
TEMED	Tetramethylethylenediamine
TGF-β1	Transforming growth factor beta 1
TIMPs	Tissue inhibitor of metalloproteinases
TLDA	Tiling low-density array
UTR	Untranslated region
UV	Ultraviolet
V	Volts
v/v	Volume/volume
VEGF	Vascular endothelial growth factor
w/v	Weight/volume
α-SMA	Alpha smooth muscle actin

ABSTRACT

Background: Transforming growth factor beta 1 (TGF-β1), a pro-fibrotic tumour-derived factor, promotes myofibroblast differentiation in the tumour microenvironment and is thought to contribute to the development of pro-tumourigenic cancer associated fibroblasts (CAF). To date, the molecular mechanisms underlying CAF differentiation are poorly characterised. Here, the contribution of a class of small non-coding RNA, miRNA, to myofibroblastic CAF differentiation was examined. The expression profile of miRNA in experimentally-derived CAF (eCAF) was determined compared to normal fibroblasts and CAF derived from oral cancers, and the functionality of selected miRNAs in the reprogramming of normal fibroblasts to eCAF or in tumour-derived CAF was investigated.

Methods: NOF (normal oral fibroblasts) were treated with a range concentration of TGF-β1 (0.05-5 ng/ml) for 24 h and 48 h. The expression of myofibroblast markers, α-SMA and FN-EDA1, were determined using qRT-PCR and western blot. The formation of stress fibres was assessed by fluorescence microscopy, and associated changes in contractility assessed using collagen contraction assays. miRNA expression profiling in NOF, eCAF, and tumour-derived CAF was carried out using tiling low density array (TLDA) cards, with two distinct methods of analysis employed. Candidate miRNAs were validated using qRT-PCR. miRNA inhibitors used in the loss-of-function experiments; anti-miR-424-3p and anti-miR-145-5p while a pre-miR-424-3p used to overexpress miR-424-3p.

Results: TGF-β1 induced a myofibroblastic, CAF-like, phenotype in NOF (termed eCAF) as assessed by expression of molecular markers, the formation of stress fibres and increased contractility. TLDA analysis and qPCR validation demonstrated that miR-424-3p and miR-145-5p were upregulated in eCAF. Overexpression of miR-424-3p inhibited

TGF-β1-induced eCAF phenotype in NOF. Conversely, knockdown of miR-424-3p or miR-145-5p had no effect on eCAF formation. Overexpression of miR-424-3p did not inhibit basal myofibroblast phenotype of CAF or further TGF-β1-induced myofibroblast phenotype in CAF. Neither inhibition of miR-424-3p nor miR-145-5p increased basal myofibroblast phenotype of CAF. Inhibition of miR-424-3p decreased TGF-β1-induced α-SMA stress fibre formation and TGF-β1-induced contractility in CAF. Inhibition of miR-145-5p increased TGF-β1-induced gel contraction, but not other myofibroblast phenotype, in CAF. Reanalysis of TLDA data using a more stringent approach identified other potential miRNA candidates differentially expressed in eCAF and CAF, compared to NOF. The miRNA expression profiles of tumour-derived CAF (two subtypes of OSCC) was distinctly different from that observed in eCAF, suggesting a difference between CAF and fibroblasts artificially induced to become CAF-like cells *in vitro*.

Conclusions: The findings suggest that miR-424-3p might partially participate in TGF-β1-induced CAF-like myofibroblast differentiation. Other miRNA was identified which showed differences in expression between NOF, eCAF and CAF which could be functionally analysed in future studies. Collectively the data suggest that miRNA may play a role in CAF development, and could provide translational benefits in cancer therapy.

CHAPTER 1: Introduction

1.1 Overview

Several lines of evidence demonstrate that altered stroma microenvironment makes a significant contribution to the malignant progression of cancers including oral squamous cell carcinomas (OSCC) (Sobral *et al*., 2011). The tumour microenvironment contains a mixture of cancerous cells together with normal cell populations such as fibroblasts, endothelial cells, inflammatory cells and non-cellular components including extracellular matrix components (ECM) (Baglole *et al*., 2006; Bussard *et al*., 2016). The majority of tumour stromal cells, in most cases, are activated fibroblasts which commonly express alpha smooth muscle actin (α-SMA) and other myofibroblast markers such as fibronectin extra domain A (FN-EDA1) (Sugimoto *et al*., 2006). These cells have been referred interchangeably as carcinoma-associated fibroblasts, cancer-associated fibroblasts but are often called myofibroblasts (Dewever and Mareel, 2003; Bussard *et al*., 2016). TGF-β is the best characterised factor capable of inducing a myofibroblast phenotype (Ronnov-Jessen and Petersen, 1993; Tuxhorn *et al*., 2002). However, other growth factors and cytokines mediate myofibroblast differentiation including interleukin-6 (IL-6), platelet-derived growth factor (PDGF) and hepatocyte growth factor (HGF) (Kalluri, 2016). More recently, Activin A has been reported to provoke myofibroblast differentiation. Nithiananthan and colleagues (2017) demonstrated that Activin A induces dermal fibroblast activation by increasing α-SMA positive stress fibre formation compared to unstimulated cells. Additionally, expression of α-SMA positive stress fibre formation by Activin A in static conditions is similar to that fibroblasts stimulated with TGF-β1.

MicroRNAs (miRNAs) are small noncoding RNA molecules that regulate target gene expression at the posttranscriptional level and are found to be deregulated in many cancer cells (Ambros, 2004; Schickel *et al*., 2008). miRNAs are involved in many

cellular processes such as cell death, cell proliferation and differentiation (Bartel, 2009). Interestingly, some of them have also been classified as oncomiRs and tumour suppressors (Lee and Dutta, 2006). To date, it is not clearly understood whether miRNAs are involved in myofibroblast differentiation in cancer since little is known about the miRNA expression in the stroma microenvironment.

Previous studies have demonstrated that CAF might be a potential target in the treatment of cancer (Micke and Ostman, 2004), due to the genetic stability of these cells and their wide applicability in various tumour types. They regulate the make-up of the tumour ECM and the crosstalk between cancer cells and CAF that favours the survival of tumour cells (Thode *et al*., 2011). Therefore, with this in mind, a study might be conducted to investigate the role of miRNAs in CAF differentiation. In addition, there has been no report comparing miRNA expression profile between TGF-β1-treated NOF with unstimulated NOF in the tumour microenvironment of OSCC. The role of selected miRNA in this study will add a valuable knowledge on how miRNAs regulate CAF differentiation in OSCC.

1.2 Cancer biology

Cancers are a group of diseases in which normal cells proliferate in an uncontrolled fashion and spread throughout the body. Such cells can arise in a variety of tissues and organs and each of these sites contains different cell types that may be affected. The hallmarks of cancer, as reviewed by Hanahan and Weinberg (2011), are the minimum sets of genotypes or phenotypes that a cancer cell must acquire to become malignant. These are; (a) sustaining proliferative signalling, (b) evading growth suppressors, (c) enabling replicative immortality, (d) resisting cell death, (e) sustained angiogenesis and (f) tissue invasion and metastasis.

Carcinogenesis is defined as a multi-step process which involves initiation, promotion and progression (Figure 1.1). It is initiated in a single cell that is exposed to various carcinogens e.g. tobacco smoke, resulting in irreversible changes that will permit malignant transformation. Once a cell has been initiated, it can become a cancer cell if it retains the ability to divide and if the cellular changes that occurred during initiation are enhanced by promotion. A promotion stage occurs where growth enhancement can allow it to form a tumour. Both events resulted in the accumulation of genetic modifications. Finally, at progression stage, the tumour must corrupt the cells around it (the tumour microenvironment) to allow it to develop its own blood supply (angiogenesis) in order to survive.

1.2.1 Cancer prevalence

Cancer is a major public health problem worldwide. Head and neck cancers rank sixth of cancer-related death in the world, with an estimated 500 000 cases annually (Fanucchi *et al*., 2006). The National Cancer Registry of Malaysia reported that head and neck cancer was the third most common cancer among males and accounted for 7.8 % of the total cancers in males (Gerrad and Halimah, 2008). Melanesia, south-central Asia, western and southern Europe and southern Africa are high-risk regions for oral cancer while southern and eastern Europe, south America and western Asia are for laryngeal cancer (Parkin *et al*., 2002). This cancer usually occurs over the age of 60 and is much more common in men, although the incidence of the disease is rising amongst both women and young people, most likely due to lifestyle changes (Mackenzie *et al*., 2000).

1.3 Head and neck cancer and its carcinogenesis

Head and neck cancer is a broad term that consists of heterogeneous groups of tumours that arise in the oral cavity, pharynx, larynx and cervical oesophagus (Figure

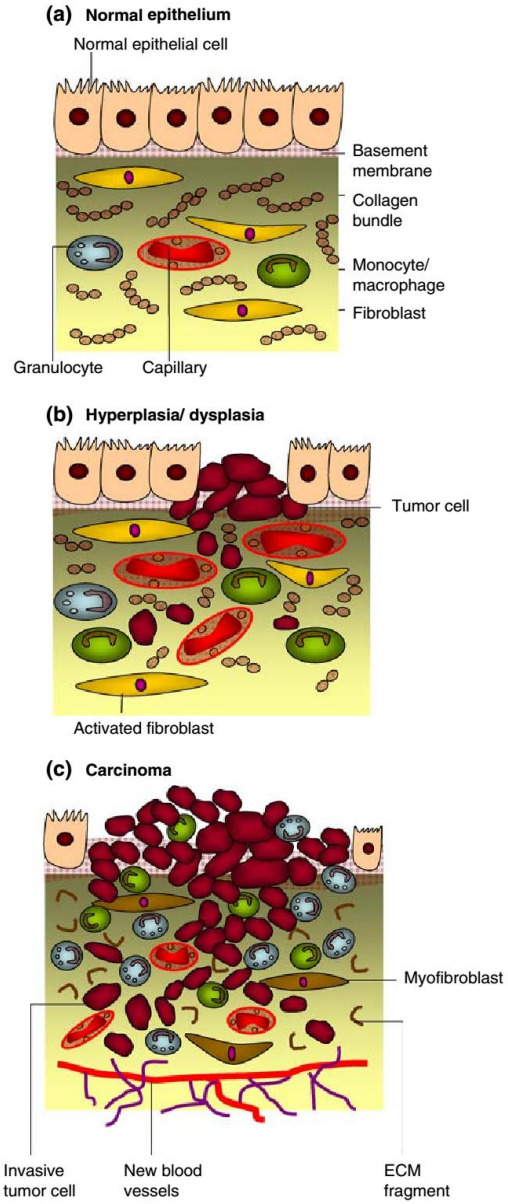

Figure 1.1: Carcinogenesis

A) Epithelial cells are separated by basement membrane from the stroma milieu. The stromal compartment consists of fibroblasts, inflammatory cells, ECM and blood vessels. **B)** During carcinogenesis, epithelial and stromal components undergo genetic modifications that promote cell proliferation. Additionally, fibroblast becomes activated, increases in inflammatory cells homing and formation of new blood vessels. **C)** The stroma becomes reactive and epithelial cells proliferate uncontrollably. Moreover, ECM components are degraded while the number of inflammatory cells and activated fibroblasts increases, resulting in secretion of various growth factors. Angiogenesis is maintained for tumour cells to survive and ultimately metastases to distant site (taken from Mbeunkui and Johann, 2009)

1.2). In most of the cases, this type of cancer mainly presents as squamous cell carcinomas, therefore collectively referred as head and neck squamous cell carcinoma (HNSCC). Although disparate in site, these tumours sometimes share certain molecular characteristics. It has been found that telomerase is reactivated in 90 % of cases of HNSCC (McCaul *et al*., 2002). Meanwhile, inactivation of p16 and loss of 3p contribute to HNSCC carcinogenesis (Rocco and Sidransky, 2001; Perez-Ordonez *et al*., 2006). p53 mutation and loss of heterozygosity of 17p are detected in 50 % of cases of HNSCC (Balz *et al*., 2003). Cyclin-D1 overexpression and amplification of 11q13 are seen in HNSCC which might contribute to tumour aggressive behaviour (Pignataro *et al*., 1998; Cappacio *et al*., 2000). Poor prognosis was detected in patients with tumours overexpressing epidermal growth factor receptor (EGFR). Proangiogenic factors including vascular endothelial growth factor (VEGF) have found to be upregulated in HNSCC (Smith *et al*., 2000). Taken together, these collective events, in concert with changes in the tumour microenvironment, might govern the development of HNSCC.

1.3.1 Risk factors for HNSCC

The major risk factors of HNSCC are smoking and excessive alcohol consumption (Rodriguez *et al*., 2004). Recently a new etiologic factor, human papillomavirus (HPV), was found to be involved in specific subsets of HNSCC (D'Sauza *et al*., 2007). High-risk HPV types such as HPV16 and HPV18 mediate their carcinogenic effect through E6 and E7 oncoproteins, that inactivate the p53 and pRb, respectively (Munger and Howley, 2002). HPV genomic DNA was detected in about 25 % of cases of HNSCC (Kreimer *et al*., 2005). In addition, HPV16 might not depend on other carcinogens to cause HNSCC (D'Souza *et al*., 2007). Therefore, the interaction between HPV and HNSCC is crucial especially for treatment, prognosis and prevention of HNSCC. All cancers are caused by abnormalities in the genetic material of the

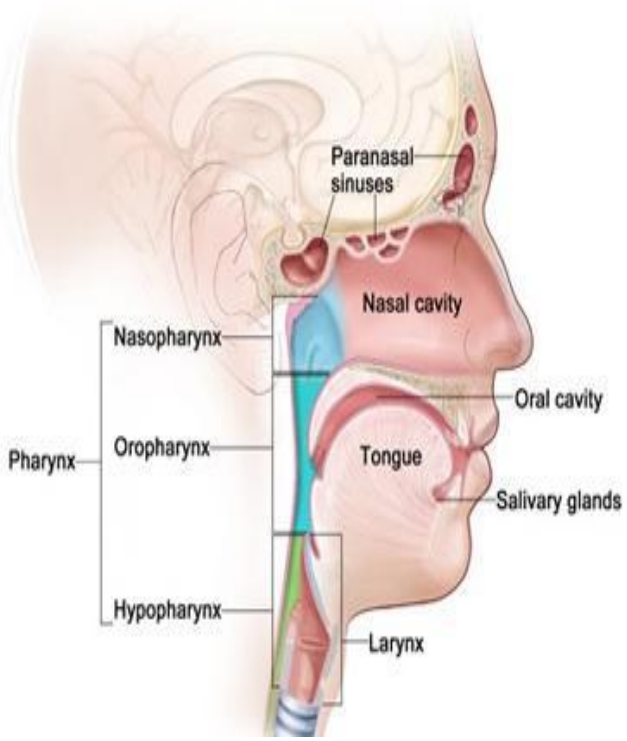

Figure 1.2: Head and neck cancer

A schematic picture highlighting the organs in which head and neck cancer can possibly originate from. Head and neck cancer is generally understood as cancer of heterogeneous group of organs or tissues that originate in oral cavity, pharynx, larynx and cervical oesophagus (taken from the National Cancer Institute: https://www.cancer.gov/types/head-and-neck/head-neck-fact-sheet)

transformed cells. This can happen due to both external factors such as tobacco, infectious organisms, chemicals, and radiation and internal factors such as inherited mutations, hormones and immune conditions (American Cancer Society, 2011). These factors may act together or in sequence to initiate or promote carcinogenesis. In the case of Fanconi Anaemia, patients have mutations in the genes which play a role in the maintenance of DNA stability; in addition to bone marrow failure they are also at high risk to develop squamous cell carcinoma, especially in the oral cavity, compared to others (Suarez *et al*., 2006). Therefore, individuals with cancer susceptibility syndromes are high risk to get HNSCC. Several genetic variations in enzymes that function to metabolise and detoxify the carcinogenic substances in cigarette smoke and alcohol are found to increase cancer risk (Ruwali *et al*., 2009).

1.3.2 Treatments for HNSCC

With the advancements in research and development, a number of invasive and non-invasive treatments for HNSCC have been in practice. Some of the most widely practised treatments are listed below and in each case, therapy will be decided by considering primary tumour site, stage, resectability, patient factors such as swallowing and airway considerations, desire for organ preservation and comorbid illnesses (Argiris *et al*., 2008). Treatment decisions for HNSCC are often complex due to the involvement of specialists such as head and neck surgeons, medical oncologists, radiation oncologists, plastic surgeons as well as dentists.

Surgery- It is a primary treatment for HNSCC but often limited to some extent such as the anatomical extent of the tumour and desire to achieve organ preservation. HNSCC metastasise to a lymph node in the neck via the lymphatic route. Therefore, the presence of lymph nodes metastases and the level in the neck, as well as the number of involved nodes and the presence of extranodal spread are important prognostic factors (Schaaij-

Visser *et al*., 2010). At this stage, the neck should be treated. Surgical excision may be achieved with functional preservation of the involved organ and good oncological results for a small, transorally accessible cancers of the oral cavity, pharynx and larynx (Lefebvre, 2006).

Radiotherapy- It is an essential part of surgery treatment of HNSCC. Radiotherapy itself controls tumour growth for early stage glottic, base of tongue and tonsillar cancer (Argiris *et al*., 2008). Advances in imaging and radiation delivery such as CT scan, MRI or PET datasets have dramatically changed management approaches. The intensity of radiotherapy beams can be optimised by computer-controlled treatment to deliver a high dose of radiation to cancer cells while reducing the dose and toxic effect on healthy tissues (Argiris *et al*., 2008). Advance in radiotherapy methods including heavy particle radiation, proton therapy, brachytherapy and neutron beam radiation can be used, but have not been validated in clinical trials (Ding *et al*., 2005).

Chemotherapy and novel agents- Chemotherapy plays an important role in HNSCC treatment, from palliative care to curative programmes for locally advanced HNSCC (Cohen *et al*., 2004). Different classes of agents such as platinum compounds, antimetabolites as well as taxanes have shown promising activity against HNSCC (Colevas, 2006). Platinum compounds including cisplatin are used in combination with radiation or with other agents. Taxane-based combinations are effective in treating locally advanced HNSCC (Argiris, 2005). EGFR inhibitors such as cetuximab have emerged as a novel treatment for locally advanced HNSCC (Karamauzis *et al*., 2007). In addition, the combination of EGFR with other molecular targeted agents has emerged as a novel strategy (Argiris *et al*., 2008). However, the combination of these novel agents is not yet regarded as a standard treatment for locally advanced HNSCC.

1.4 Tumour Microenvironment

Stroma of the tumour microenvironment (reactive stroma) is fundamentally different from the stroma of normal tissue. Genetic and epigenetic studies indicate that tumour progression is not just determined by cancer cells themselves, but also tumour microenvironment. Paget (1889) proposed "seed and soil" hypothesis; tumour cells (the seed) require the host environment (the soil) for their optimal growth. The tumour microenvironment is a complex network that comprises a multiple cell, soluble factors, signalling molecules and ECM which directs tumour progression (Cukierman and Bassi, 2012). The multiple cells that collectively form the tumour microenvironment are endothelial cells, pericytes, fibroblasts and inflammatory cells (Figure 1.3) (Joyce and Pollard, 2009). Numerous studies have demonstrated that CAF promote tumour growth and progression, although there exist conflicting reports. Paracrine interactions within the tumour microenvironment are responsible for the complexity of the metastatic cascades (Van Zijl *et al*., 2011). For example, matrix metalloproteinase (MMPs) secreted from tumour cells can modify extracellular microenvironment by degrading ECM proteins, cytokines and growth factors secretion including TGF-β (Egeblad and Werb, 2002). In addition, MMPs and members of a disintegrin metalloproteases (ADAM) family can cleave cell surface membrane receptors, thus releasing them into ECM (Zhou *et al*., 2005).

1.4.1 Fibroblasts

As originally described by Tarin and Croft (1969), fibroblasts are non-vascular, non-epithelial, non-inflammatory cells, embedded within the matrix of the connective tissue. Morphologically, fibroblasts are spindle-like shape cells with the prominent actin cytoskeleton and vimentin filaments (Kalluri and Zeisberg, 2006). Fibroblasts play role in ECM deposition, regulation of epithelial differentiation, regulation of inflammation and involvement in wound healing (Parsonage *et al*., 2005). They synthesise ECM

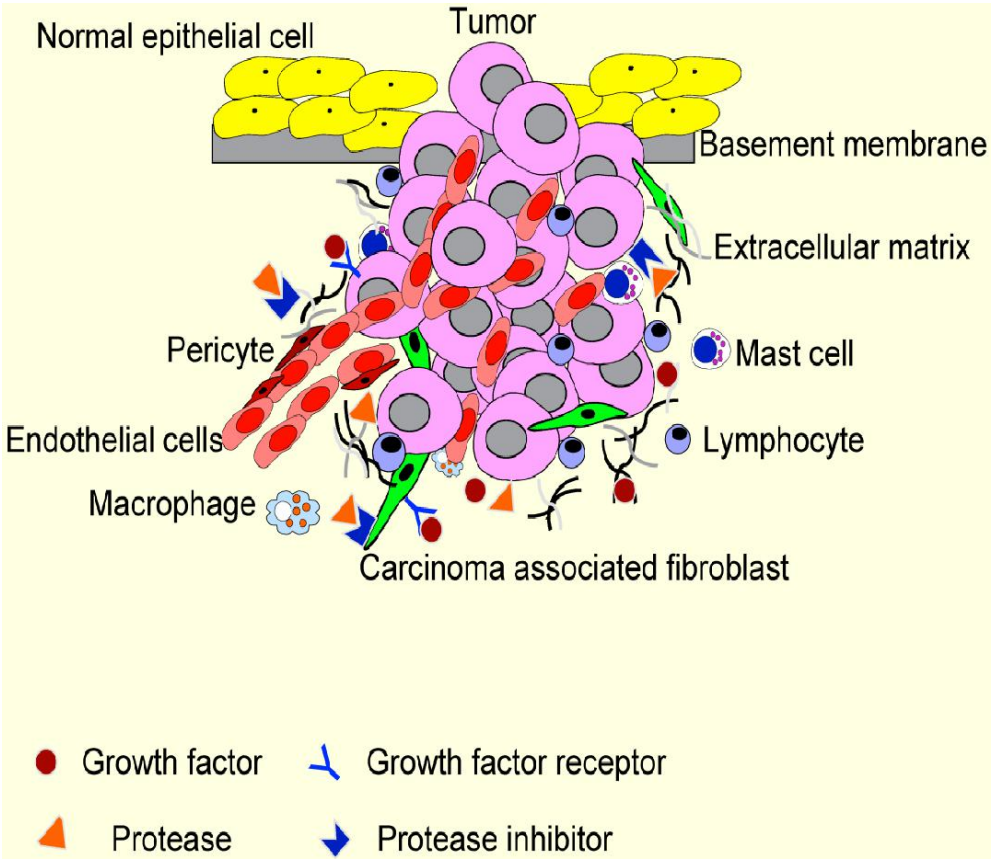

Figure 1.3: Tumour microenvironment

Various cell types within tumour microenvironment in addition to tumour cells. These include cellular components such as endothelial cells, pericytes, CAF and non-cellular components including ECM and various growth factors (taken from Joyce and Pollard, 2009).

constituents including type I, type III and type V collagen and fibronectin (Tomasek *et al*., 2002; Rodemann and Muller, 1991). In addition, they secrete type IV collagen and laminin for basement membrane formation (Chang *et al*., 2002). Fibroblasts are crucial in maintaining an ECM homoeostasis, by producing ECM-degrading proteases such as MMPs (Simian *et al*., 2001).

Fibroblasts in normal stroma are considered inactive with negligible metabolic activity at the molecular level. Therefore, they are assumed to be in the quiescent state. A specific marker for quiescent fibroblast is still unknown, but fibroblast specific protein 1 (FSP-1) has been proposed as a possible candidate (Strutz, 1995). Fibroblasts play important roles in wound healing in which they invade the lesions and generate ECM that acts as a scaffold for tissue regeneration (Rasanen and Vaheri, 2010). These activated fibroblasts become a specialised type of fibroblasts known as myofibroblasts which acquired contractile stress fibres and express α-SMA and FN-EDA1 (Tomasek *et al*., 2002). However, the mechanism of how these myofibroblasts revert to their original phenotype is poorly understood, but it is believed that these myofibroblasts undergo a specific type of programmed cell death called nemosis and removal by granulation tissue (Desmouliere *et al.*, 1995). The differences between quiescent fibroblasts and activated myofibroblasts are listed in Table 1.1. Myofibroblasts in mammals are highly heterogeneous with specific expression depending on where they are isolated in the tissue. Therefore, none of the fibroblasts markers is both exclusive to fibroblasts or present in all fibroblasts (Table 1.2).

1.4.2 Cancer associated fibroblasts

Unlike in normal stroma, fibroblasts in tumour stroma remain activated. These activated fibroblasts are called cancer associated fibroblasts (CAF) (Tomasek *et al*., 2002). In regards to phenotype and function, CAF can be distinguished from normal

Quiescent or resting fibroblasts	Activated fibroblasts
Morphologically bland (spindle-shaped)	Morphologically active (cruciform or stellate-shaped)
Metabolically indolent	Metabolically active
G0/G1 arrest or slow cycling self-renewal	Proliferative
Activated by growth factors	Further activated by growth factors
FSP1+, α1β1 integrin+	αSMA+, PDGFRβ+, FAP+
Non-migratory	Migratory
No ECM production	ECM production and synthetic phenotype
No active secretome	Active and dynamic secretome
Epigenetically stable	Epigenetically modified (e.g. *RASAL1* hypermethylation)
Precursor for activated fibroblasts	Precursor for chondrocytes, adipocytes, myocytes and endothelial cells

Table 1.1: The differences between normal fibroblasts with activated fibroblast

Morphologically, fibroblasts appear as elongated cells with a prominent actin and vimentin filaments. Phenotypically, activated fibroblast often express α-SMA (adapted from Kalluri, 2016)

Marker	Function	Fibroblast types in which it is found	Other cell types in which it is found
Vimentin	Intermediate- filament-associated protein	Miscellaneous	Endothelial cells, myoepithelial cells and neurons
α-SMA	Intermediate- filament-associated protein	Myofibroblasts	Vascular smooth muscle cells, pericytes and myoepithelial cells
Desmin	Intermediate- filament-associated protein	Skin fibroblasts	Muscle cells and vascular smooth muscle cells
FSP1	Intermediate- filament-associated protein	Miscellaneous	Invasive carcinoma cells
Discoidin-domain receptor 2	Collagen receptor	Cardiac fibroblasts	Endothelial cells
FAP	Serine protease	Activated fibroblasts	Activated melanocytes
α1β1 integrin	Collagen receptor	Miscellaneous	Monocytes and endothelial cells
Prolyl 4-hydroxylase	Collagen biosynthesis	Miscellaneous	Endothelial cells, cancer cells and epithelial cells
Pro-collagen 1α2	Collagen1 biosynthesis	Miscellaneous	Osteoblasts and chondroblasts

Table 1.2: Activation markers

Several well-established markers for fibroblasts and their expression in other cell types (adapted from Kalluri and Zeisberg, 2006).

fibroblasts by differential expression of ECM components and growth factors as well as their proliferation rate (Kalluri and Zeisberg, 2006). CAF are characterised by several activation markers including α-SMA, fibroblast specific marker 1 (FSP-1), PDGF and FAP (Garin-Chesa *et al*., 1990; Kalluri, 2016). CAF are often identified by their expression of α-SMA (Ronnov-Jenssen *et al*., 1996; Gabbiani, 2003). In addition, FSP-1 is reported to be specific to CAF *in vivo* (Kalluri and Zeisberg, 2006). The previous study has demonstrated that CAF in different tumours showed two major subsets. One subset was FSP-1 positive but lack expression of α-SMA and PDGF while other, on the other hand, FSP-1 negative with co-expressed α-SMA and PDGF (Sugimoto *et al*., 2006). CAF were found to be one of the most prominent cell type within the tumour stroma of breast, prostate and pancreatic cancers (Kalluri and Zeisberg, 2006; Pietras and Ostman, 2010). The underlying mechanisms that mediate transition of normal fibroblasts to CAF are unclear. Apart of TGF-β, various growth factors such as PDGF, insulin growth factor (IGF) and granulocyte macrophage colony stimulating factor (GM-SCF) were suggested to take part in CAF differentiation (DeWever and Mareel, 2003). Phenotypic features of CAF can be induced by TGF-β *in vitro* which mediates fibroblast activation during wound healing and organ fibrosis (Dumont and Arteaga, 2000).

1.4.3 Myofibroblasts or activated fibroblast-associated with wound healing

Wound healing is a sequence of events that lead to the repair of injured tissue. Wound healing occurs in three phases; inflammatory, proliferative and remodelling phases (Schilling, 1976). Homing of leukocytes including neutrophils, lymphocytes and monocytes to the wound is important to clear dead cells (Kurkinen *et al*., 1980). This phase is known as the inflammatory phase. While in the proliferative phase, collagen deposition occurs as well as the formation of new vasculature (Hunt, 1998). The injured tissue attracts various types of cell such as endothelial cells, pericytes, myofibroblasts

and leukocytes (Witte and Barbul, 1997). In the remodelling phase, wound healing can be accomplished by regeneration of same parenchymal cells or replacement of fibrous extracellular matrix (Madden and Smith, 1970). After completing the wound healing process, myofibroblasts revert to their original phenotype or undergo apoptosis by granulation tissue (Desmouliere *et al*., 1995).

Myofibroblasts are most commonly present in tissue related with mechanical strength such as the oral cavity, the skin, the gastrointestinal tract, the uterus, the testes and the heart (Huang and Lee, 2003; Eyden, 2009). Morphologically, myofibroblasts appears similar to both fibroblast and smooth muscle cells (Oda *et al*., 1988). Myofibroblasts commonly expresses α-SMA, though this marker is expressed in smooth muscle cells (Hinz *et al*., 2007; Eyden *et al*., 2009). However, myofibroblasts is negative for heavy myosin chains, caldesmon and desmin (McAnulty, 2007; Schurch *et al*., 2007; Eyden, 2008). They are also typically negative for cytokeratin, CD68, CD34 and CD31 (DeWever, 2008; Micke and Ostman, 2004). Myofibroblast differentiation is induced by paracrine signalling by various factors including TGF-β, PDGF and IGF 11 (Powell *et al*., 1999; Desmouliere *et al*., 2004; Micke and Ostman, 2004). Morphologically and phenotypically differences between quiescent fibroblasts, wound healing associated fibroblasts and CAF are shown in Figure 1.4.

1.4.4 Senescent fibroblasts

Cellular senescence or replicative senescence is termed as an event in which proliferating cells undergo permanent cell arrest in response to oncogenic events. In 1965, Hayflick and co-workers demonstrated that human fibroblasts had limited ability to proliferate in culture; after many cell passages, cell proliferation was gradually decreased. Many factors contribute to cellular senescence including DNA damage,

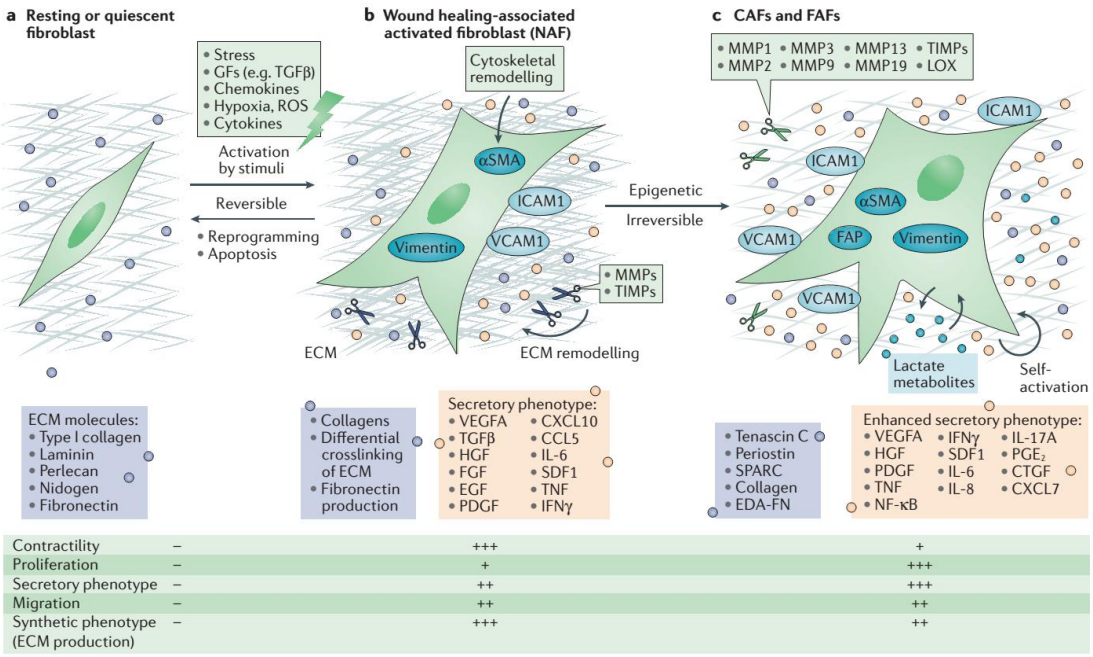

Figure 1.4: Morphologically and phenotypically differences between quiescent fibroblasts, wound healing associated fibroblasts and CAF

A) Quiescent fibroblasts are elongated-shaped single cells, **B)** During wound healing, activated fibroblasts are stellate-shaped cells and express α-SMA. ECM remodelling contributes to their contractility and various secretory molecules amplify their activation and enhance proliferation, **C)** CAF may gain enhanced various secretory molecules and specialised ECM remodelling, adding to the complexity of tumour microenvironment (Kalluri, 2016).

oncogene expression and physiological mitogenic signals. Cellular senescence acts as tumour suppressive mechanism that prevents cells undergo neoplastic transformation (Campisi, j, 2001; Redder, R, 2000). The hallmark of cellular senescence is growth arrest. Senescent cells arrest growth at G1 phase of cell cycle, yet they remain metabolically active (Herbig *et al*., 2004). Unlike quiescence cells, the growth of senescent cells is permanently arrested as the proliferative ability of senescent cells cannot be stimulated by known physiological stimuli. The characteristics of senescence growth arrest depend on the species and genetic background of the cell itself. Senescent cells often express cell-cycle inhibitors; the cyclin-dependent kinase inhibitors (CDK1s) p21 and p16 (Campisi, J, 2001; Braig and Schmitt, 2006). These CDKIs are involved in tumour suppressor pathways that are governed by the p53 and pRB proteins. p53 and pRB act as transcriptional regulators and the pathway they regulated are often interrupted in cancer (Sherr and McCormick, 2002).

Several markers can distinguish senescent cells, both in culture and *in vivo*. Nevertheless, none of them is specific to the senescent state and are normally used in combination to increase confidence. The most common senescence marker was senescence-associated β-galactosidase (SA-βgal) (Dimri *et al*., 1995). This marker can be detected by histochemical staining in senescent cells. Recently p16 also can be used to identify senescent cells (Krishnamurthy *et al*., 2006). p16 is expressed in many (not all) senescent cells (Beausejour *et al*., 2003; Itahana *et al*., 2003). However, it also expressed in some of the tumour cells, particularly those that have lost pRB function (Gil and Peters, 2006).

1.5 Roots of CAF

There is considerable controversy regarding the origin of CAF. It is possible that

they come from multiple origins such as resident fibroblasts, pericytes, epithelial cells, mesenchymal cells, endothelial cells as well as cancer cells (Figure 1.5) (Chirri and Chiarugi, 2011). Thus, their multiple origins contribute to pleiotropic actions in tumour microenvironment milieu.

1.5.1 CAF may derive from normal fibroblasts

CAF possibly originate from resident fibroblasts via mesenchymal-mesenchymal transition (MMT) by cancer-derived growth factors including TGF-β (Kalluri and Zeisberg, 2006). This notion was confirmed by data showing that human mammary fibroblasts convert into CAF in a breast tumour xenograft model and this activation is mediated by TGF-β (Kojima *et al*., 2010). CAF and tumour cells create a cytokinenetwork, working directly on both cells. Additionally, CAF undergo frequent genetic modification (Tsellou and Kiaris, 2008).

The evidence of genetic alteration in CAF is controversial and conflicting. Some of the studies have identified a genetic alteration in CAF. This is exemplified in the work conducted by Littlepage *et al*., (2005) that tumour enhancing characteristics of fibroblast can be maintained without exposure to cancer cells. This indicates that genetic modification may responsible for this stable phenotypes. Indeed, some studies have reported a high frequency of genetic alterations in CAF including point mutations, loss of heterozygosity (LOH) and changes in expression level of oncogenes and tumour suppressors from various human cancers. Surprisingly, LOH frequency of 59.7 % and 66.2% was observed in BRCA1/2-related breast cancer stroma and in the epithelium, respectively (Weber *et al*., 2006). Additionally, LOH frequency was identified in the neoplastic epithelial breast (25-69%) and stromal compartment (17-61%) (Kurose *et al*., 2001). Taken together, the frequency of LOH in stroma was similar to that

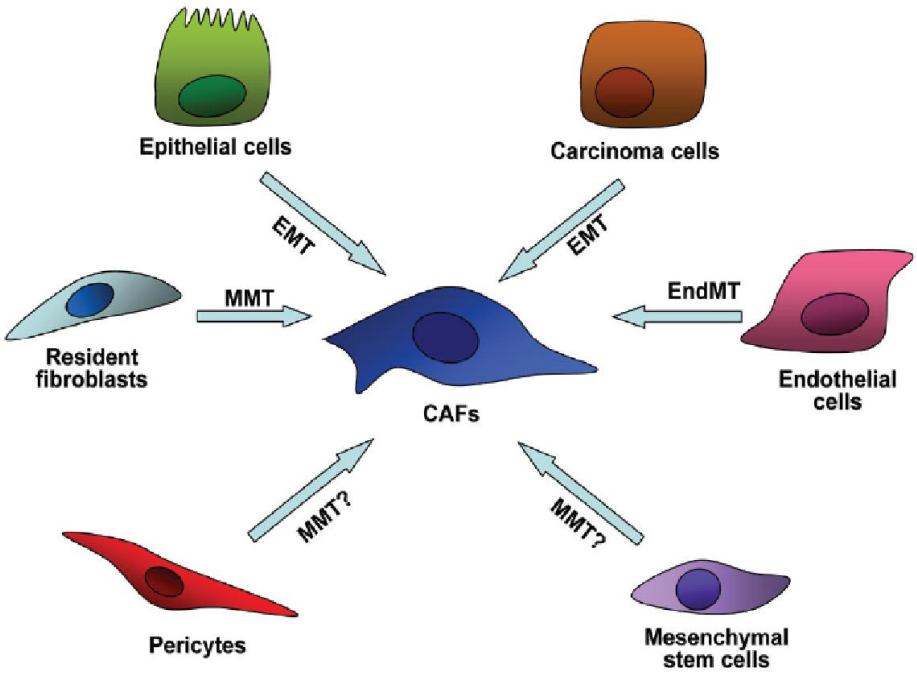

Figure 1.5: Multiple origins of CAF within the tumour microenvironment

CAF may arise from resident fibroblasts, pericytes, epithelial cells, mesenchymal cells, endothelial cells and carcinoma cells via various types of mesenchymal transition process (taken from Chirri and Chiarugi, 2011).

observed in epithelial components. Moreover, LOH signature of CAF is strongly associated with tumour grade in women diagnosed with sporadic breast tumours (Fukino *et al*., 2004). However, one study did not find genetic alterations in CAF isolated from fresh breast cancer biopsies using SNP array analysis (Allinen *et al*., 2004). Similarly, CAF neither show any somatic genetic alterations nor p53 protein expression in pancreatic cancer (Walter *et al*., 2008).

1.5.2 CAF may originate from bone marrow-derived MSCs

CAF may also originate from bone marrow-derived mesenchymal stem cells (MSCs). Both cell types have similarities in the expression of surface markers such as CD29, CD90, CD44, CD73, CD106 and CD117 as well as α-SMA and vimentin. MSCs have capability to differentiate into various cell types including bone, fat, cartilage and muscle in physiological and pathological processes (Bergfeld and DeClerck, 2010; Dominici *et al*., 2006). MSCs exhibit homing and engraftment at injury sites in many conditions, particularly in tissue repair and inflammation (Hall *et al*., 2007). Similar to inflammatory cells in tissue repair, the recruitment of MSCs at the tumour site is mediated by various cytokines and growth factors (Spaeth *et al*., 2008). A study carried out by Spaeth and colleagues (2009) showed that labelled MSCs were localised within the tumour mass and differentiated into CAF. In addition, Direkzi and co-workers (2004) transplanted green fluorescent protein (GFP) α-SMA + MSCs-derived male patient into a female recipient and found that 25% of cells labelled with GFP in the total CAF population. Additionally, osteopontin is able to convert MSCs into CAF. Collectively, these studies indicate that MSCs may act as a potential source for CAF.

1.5.3 CAF may derive from epithelial cells

Alternatively, CAF may originate from epithelial cells via epithelial-

mesenchymal transition (EMT) (Radisky *et al*., 2007). This idea arises from the evidence that epithelial cells undergo DNA oxidation and mutation when exposed to MMP-driven oxidative stress, thereby undergoing specialised EMT in which they become CAF (Spaeth *et al*., 2009). EMT is an event in which epithelial cells with tight junctions become mesenchymal cells with a loose cell-cell adhesion (Hay, 1995). Conversion of epithelial cells into CAF is a special case of EMT (Forino *et al*., 2006). This transition generates CAF instead of cancer cells. Iwano *et al*., (2002) found that 30 % of CAF in the kidney are derived from kidney tubular epithelial cells. Indeed, genetic analysis showed that CAF isolated from human breast cancer biopsies were derived from the epithelial tumour cells (Peterson *et al*., 2003). Even though cancer cells are unable to generate the majority of CAF by EMT, other cells such as normal epithelial cells can act as additional source of CAF through EMT in response to certain stimuli from the microenvironment (Iwano *et al*., 2002; Direkze *et al*., 2004; Direkze and Alison, 2006).

1.5.4 CAF from endothelial cells through endothelial-mesenchymal transition (EndMT)

Proliferating endothelial cells might become CAF via endothelial-mesenchymal transition (EndMT) process by the loss of endothelial markers such as CD31 under stimulation of TGF-β (Zeisberg *et al*., 2007). This type of EndMT expresses both FSP-1 and down-regulation of CD31/PECAM (Potenta *et al*., 2008). During this process, resident endothelial cells disorganise the cell layer and invade the underlying tissue due to loss of E-cadherin (Potenta *et al*., 2008).

1.5.5 CAF from cancer cells

Cancer cells can directly generate CAF through EMT process (Radisky *et al*., 2007). This process allows cancer cells to behave mesenchymal-like phenotype,

characterised by increased in invasiveness. EMT is induced by many factors including TGF-β and is mediated by targeted downstream molecules such as Snail, Slug and Twist (Medici *et al*., 2008).

1.6 Role of CAF in tumorigenesis

CAF affect tumour growth in many ways. Initially, CAF suppress tumour growth by inhibiting early stages of tumour progression through the formation of gap junctions between activated fibroblasts. But, later on, CAF promote tumorigenesis by secreting pro-tumourigenic factors (McAnulty, 2007). Two different pathways are established in the crosstalk between cancer cells and stromal cells. In the efferent pathway, cancer cells cause a reactive response in stroma via secretion of various growth factors and cytokines while in the afferent pathway, the stroma influences cancer cells' behaviour in an analagous way (Figure 1.6; described in more detail in section 1.6.2) (Giannoni *et al*., 2010).

1.6.1 CAF support tumour growth by secretion of growth factors, cytokines and proteases

Tumour cell proliferation is important in order to maintain continuous growth and metastatic properties. CAF directly stimulate cancer cell proliferation by secreting various growth factors, hormones and cytokines such as TGF-β and hepatocyte growth factor (HGF) (Chirri and Chiarugi, 2011). Parallel to this notion, Kuperwasser and colleagues (2004) showed that overexpression of these two growth factors in mouse fibroblasts is able to induce the initiation of breast cancer when co-injected with normal epithelial cells. In addition, FSP-1 secreted by CAF is important in altering tumour microenvironment which favours cancer progression. Metastatic cancer cells transplanted into FSP-1 knockout mice are less likely to form a tumour than when co-injected with

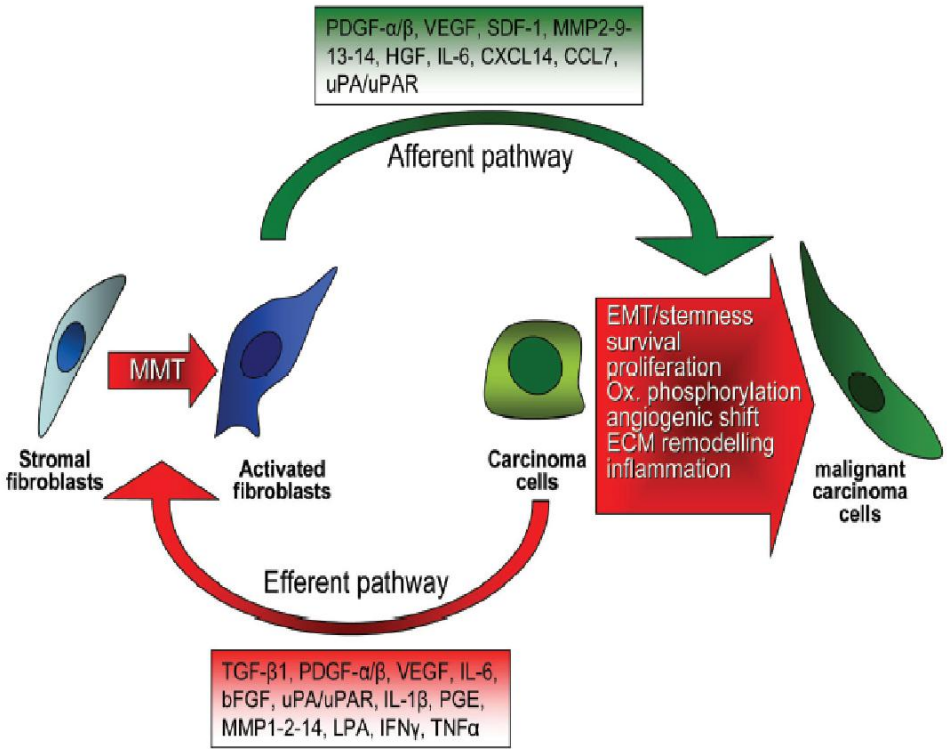

Figure 1.6: Crosstalk between CAF and tumour cells

Cancer cells induce CAF via secretion of various growth factors and cytokines which, in turn, sustain tumour progression by promoting ECM remodelling (taken from Giannoni *et al*., 2010).

FSP-1 positive fibroblasts (Grum-Schewensen *et al*., 2005). Stromal cell-derived factor 1 (SDF-1) derived from CAF is able to promote angiogenesis via binding of SDF-1β or CXCL12 to its receptors, CXCR4 which highly expressed on the cancer cells (Goh *et al*., 2007). Apart from those growth factors, IGF-1 also plays important role in cancer growth. For example, melanoma cells are unable to produce IGF-1 by themselves, thus they rely on surrounding fibroblasts which express N-cadherin to stimulate their growth (Li *et al*., 2003). Of note, CAF can respond to androgen produced by lung and prostate cancer cells to produce growth factors that mediate proliferation of epithelial cells (Cunha *et al*., 2002). CAF also secrete some metabolites such as pyruvate that governs the growth of cancer cells (Koukourakis *et al*., 2006).

1.6.2 CAF regulate motility and stemness

Both clinical and experimental data support the hypothesis that CAF mediate cell motility and metastases to the distant site (Joyce and Pollard, 2009). Two signals are established in the crosstalk between cancer cells and CAF; efferent signal and afferent signal. In efferent signal, several factors secreted by cancer cells such as TGF-β, IL-6, PDGF and VEGF stimulate a response in activated stromal cells. These factors influence fibroblast differentiation and proliferation. In turn, the reactive stromal cells secrete multiple factors including TGF-β, HGF and SDF-1 that influence cancer cells. This signal is known as an afferent signal. CAF and tumour cells create a paracrine network, working directly with each other. The involvement of soluble mediators secreted by CAF influences the progression of cancer cells. *In vitro* coculture studies showed that CAF stimulated by TGF-β increase growth of breast cancer cells and squamous cell carcinoma (Lewis, *et al*., 2004; Casey *et al*., 2008). Additionally, conditioned media from gastric cancer cells induces IL-6 secretion by fibroblasts through IL-1. IL-6 acts in a paracrine manner, promoting the proliferation of gastric cancer cells through STAT3 signalling

(Kinoshita *et al*., 2013). Some studies demonstrated that CAF can induce a cancer stem cell (CSC) phenotype. Vermeulen and co-workers (2010) demonstrated that HGF secreted by CAF enhanced Wnt signalling activity in colon cancer cells, thereby stimulated the CSC features. Additionally, CAF were able to enhance the stem cell-specific phenotype by increasing the CCL-2 expression in breast cancer cells (Tsuyada *et al*., 2012). CAF influence homing and self-renewal capability of cancer cells by increased expression of cancer stem cell markers such as CD44 (Mani *et al*., 2008). Indeed, this induction of cancer stem cells phenotype has been related to EMT through over-expression of either Snail or Twist transcription factors.

1.6.3 Regulation of cancer metabolism

The mechanism of how CAF may regulate tumour metabolism is described in Figure 1.7 (Koppenol *et al*., 2011). The difference between normal and cancer cells is glucose metabolism. Cancer cells use glucose by aerobic glycolysis while normal cells catabolize glucose by oxidative phosphorylation (Jones and Thompson, 2009). Increased glucose consumption produces more intermediate glycolytic metabolites and ATP from glycolysis. Following glycolysis, pyruvate mainly converted into lactate in the cytoplasm by lactate dehydrogenase (LDH) (so-called Warburg effect). The Warburg effect coupled with an increased glucose intake facilitates the growth of cancer cells by generating pyruvate (glycolytic intermediate). This product is more likely secreted rather than being oxidised through mitochondrial metabolism. Aerobic glycolysis and LDH are over-expressed in Caveolin-1 (Cav-1) deficient stromal cells of breast cancer (Pavlides *et al*., 2009). Furthermore, a loss of Cav-1 is correlated with tumour metastases and poor prognoses in breast cancer. In contrast to Warburg effect, Koukourakis *et al*., (2006) proposed that tumour stroma acts as a major buffer of acidity and recycles products of aerobic glycolysis (pyruvate) to sustain its anabolism and growth. These contrast findings

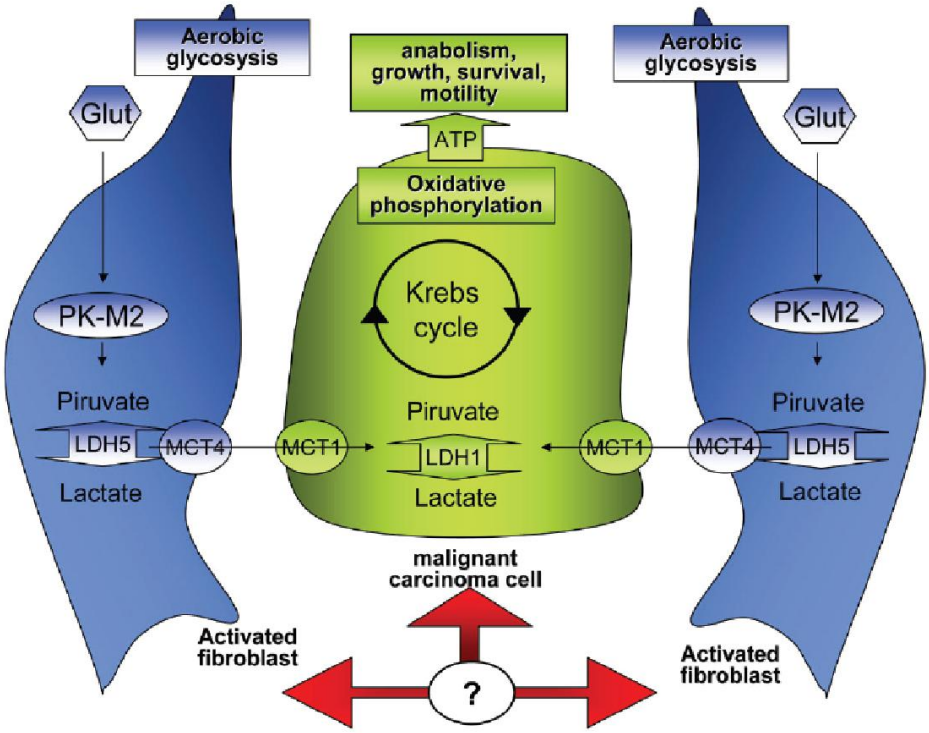

Figure 1.7: Metabolic interactions between cancer cells with CAF

Cancer cells force CAF to undergo aerobic glycolysis that ultimately produces energy-rich nutrients (lactate or pyruvate). This product was used by cancer cells in Krebs cycle for ATP production (taken from Koppenol *et al*., 2011).

need further confirmation especially in an *in vivo* model.

1.6.4 CAF involvement in invasion and metastasis

CAF are able to act as modulators of tumour cell invasion and as regulators for the tumour to metastasise to distant sites. CAF participate in tumour metastases through cell-cell interactions and paracrine signalling (Gupta and Massague, 2006). However, it is also demonstrated that CAF use physical movement; they create a tunnel through the matrix, making a path that allows cancer cells to follow behind (Gaggioli *et al*., 2007). This mechanism poses the role of CAF in ECM remodelling through the secretion of various proteases and metalloproteinases. Moreover, Duda *et al*., (2010) proposed that the stromal cells might travel with tumour cells in the bloodstream, thus protecting tumour cells from apoptosis. CAF have increased ability to degrade matrix, and express palladin which is able to promote *in vitro* and *in vivo* invasion of pancreatic cancer cells (Goicoechea *et al*., 2014). The ECM remodelling by MMPs is one of the important steps in tumour progression. In normal tissues, the balance between MMPs and their inhibitors keeps ECM well-organized. However, in tumours, fibroblasts play a major role by secreting various matrix degrading proteases as well as their activators, urokinase receptor (uPA). The tissue inhibitors of metalloproteinases (TIMPs) can downregulate MMPs activity. In addition, TIMPs can modulate other growth factors without inhibition of the MMPs, suggesting that TIMPs may be involved in some oncogenic signal (Flavell *et al*., 2008). Many MMPs (not all) play important roles in cancer metastases. For example, high levels of MMP2 production in stromal cells indicates pathological neoangiogenesis of glioma (Takahashi *et al*., 2002). Up-regulation of MMP1 is associated with poor prognosis in breast cancer as it cleaves protease-activated receptor-1 (PAR1) on the cancer cell surface, thereby stimulating growth and invasion of cancer cells *(*Poola *et al.,* 2005).

Over the last decades, a large amount of evidence from many different studies demonstrated that CAF produce soluble factors that cause cancer cell migration. For example, HGF, a chemotactic factor released by CAF binds to cMET receptor on the tumour cells, thereby stimulating tumour progression and growth (De Veirman *et al.*, 2014). Karnoub *et al*., (2007) reported that CCL5 is involved in breast cancer metastases. Stanniocalcin 1 (STC1), a protein secreted by CAF stimulates colon cancer cells metastases (Peña *et al.*, 2013). Collectively, these data show that CAF as prominent stromal cell component of tumours create optimal conditions for secondary tumour development.

1.6.5 CAF interact with immune cells in the tumour microenvironment

Pro-inflammatory cytokines secreted by cancer cells and CAF attract excessive immune cells such as leukocytes, monocytes, macrophages and mast cells to the cancer region (Raz & Erez, 2013). CCL2 secreted by CAF showed a role in monocyte/macrophage recruitment in several types of cancer, including lymphoma, breast and melanoma cancer (De Veirman *et al.,* 2014). In addition, several factors secreted by CAF such as IL-6, IL-4, IL-8 and FAP are involved in macrophage differentiation or M2 polarisation, creating an immunosuppressive microenvironment. Once macrophages reach the tumour, they become tumour associated macrophages (TAMs) which further influence growth and metastatic properties of cancer cells (Lin & Pollard, 2007).

1.7 TGF-β and myofibroblasts recruitment

1.7.1 TGF-β signalling

TGF-β superfamily contains over 30 members including three isoforms, TGF-β1, β2 and β-3 that have different potencies but similar properties *in vivo* and *in vitro* and

among of these, TGF-β1 is most related to fibrosis and myofibroblasts differentiation (Ask *et al*., 2008). TGF-β is secreted to ECM as inactive latent complexes consisting of bioactive TGF-β, the latency-associated product and the latent TGFβ-binding-protein 1 (Rifkin, 2005). TGF-β is activated by various proteases and ECM proteins including plasmin, MMP2, MMP9, integrin $\alpha_v\beta_6$ and thrombospondin (Annes *et al*., 2003). TGF-β binds to two transmembrane serine/threonine kinase receptors (TβRI & II), thereby activating downstream molecules, particularly Smads and small G-proteins (Derynck *et al*., 2001). Smad comprises of three classes; the receptor-activated Smads (R-Smads, Smad1, 2, 3, 5 and 8), the common Smads (co-Smad, Smad4) and the inhibitory Smads (iSmads, Smad6 and 7). In TGF-β signalling, the receptor complex binds to Smad2 and 3, which are phosphorylated in their C-terminal tail by the active TβRI. A trimeric complex comprises of the phosphorylated R-Smads, co-Smad and Smad 4 and was transported into the nucleus. This complex recognises specific Smad binding elements located in the enhancer or promoter regions of target genes. TGF-β1 mediates conversion of normal fibroblasts into myofibroblasts. TGF-β1 induces myofibroblast phenotype of MRC-5 human fetal lung fibroblasts, leading to upregulation of miR-21 expression in the myofibroblasts (Yao *et al*., 2011). TGF-β1 treatment caused upregulation of miR-21 expression in primary rat adventitial fibroblasts compared to untreated fibroblasts (Wang *et al*., 2012). TGF-β is important for N-cadherin expression through a JNK-dependent signalling (De Wever *et al*., 2004). Of note, TGF-β is the only growth factor that able to transdifferentiate fibroblasts into CAF *in vivo* and *in vitro* as assessed by abundant expression of α-SMA (Tuxhorn *et al*., 2002). Lewis *et al*., (2004) demonstrated that conditioned media from SCC induces myofibroblast differentiation associated with TGF-β1 treatment. Further, by Matrigel assay, they showed that these activated myofibroblasts produce higher levels of HGF, thereby increasing migration of SCC. Moreover, TGF-β1 produced by CAF is able to increase colony formation in soft agar compared to normal

fibroblast from prostate tissue.

Initially, TGF-β functions as a tumour suppressor by inhibiting early stages of carcinogenesis but, later on, promotes cancer progression and metastases (Arkhurst, 2002). However, the underlying molecular mechanisms are not clear. Under normal conditions, the antiproliferative effect of TGF-β on epithelial cells might limit the growth of normal epithelium and the formation of cancer (Siegel and Massague, 2003). On the contrary, TGF-β facilitates EMT of cancer cells, thus promoting invasiveness and metastasis. High levels of TGF-β1 in tumours is due to an increase in the release of active TGF-β1 from its latent complex that is commonly found in ECM of stromal cells (McCawley *et al*., 2000). Taken together, the role of TGF-β in cancer cells is complex and multifaceted. Therefore, its function should be interpreted with caution.

1.7.2 Canonical TGF-β signalling in myofibroblasts differentiation

Smad signalling was implicated to be involved in myofibroblast differentiation by early studies using knockout models, where mice null for Smad3 was protected from fibrosis in various experimental models (Bujak *et al*., 2007; Flanders *et al*., 2002; Zhao *et al*., 2002). Intriguingly, the proximal promoter of α-SMA contains at least two Smad binding elements (SBEs) and mutation of SBEs prevents TGF-β1 induced activation of this promoter (Hu, Wu and Phan, 2003). Thus, most studies so far, have demonstrated Smad3 as the main Smad mediator of fibrosis associated with TGF-β signalling (Hu *et al*., 2003; Qiu, Feng and Li, 2003; Duan *et al*., 2014). However, other studies showed that both R-Smads are involved in myofibroblasts differentiation (Evans *et al*., 2003). Smad2 and Smad3 are both activated downstream of TβR1 and share similar sequence homology. But these proteins differ in their ability to bind DNA. Unlike Smad3, Smad2 does not binds directly to DNA, thus requires additional co-factors to regulate target

genes (Yagi *et al*., 1999). In line with this, Smad2 and Smad3 null mice show different phenotypes in disease. Smad3 mutant caused colon cancer to metastasise to distant site (Zhu *et al*., 1998). Smad2 signalling determines anterior-posterior polarity of the early mouse embryo (Waldrip *et al*., 1998).

Active Smad complexes can interact with other transcription factors and co-activators in the nucleus that further define target gene competency for expression in a cell. More studies emphasised the interaction between pSmad2/3 and β-catenin at specific cis-elements of fibrotic target genes (Akhmetshina *et al*., 2012; Chen *et al*., 2011; Shafer and Towler, 2009). Upon Wnt signalling activation, β-catenin, the effector of the canonical Wnt signalling pathway, accumulates in the nucleus and binds to the TCF/LEF family of transcription factors (Clevers and Nusse, 2012). The TGF-β and β-catenin signalling pathways display synergistic effects on myofibroblast differentiation and α-SMA expression (Carthy *et al*., 2012; Chen *et al*., 2011). Zhou *et al* (2012) demonstrated that TGF-β signalling can activate β-catenin to form a complex with pSmad3 and the histone acetyl-transferase CREB-binding protein (CBP) at the α-SMA promoter. Furthermore, specifically blocking the interaction of β-catenin with CBP prevents TGF-β-induced expression of α-SMA and fibrosis *in vivo*, suggesting β-catenin connect Smad3 to the catalytic activity of CBP (Hao *et al*., 2011; Henderson *et al*., 2010).

Other crosstalk that exists in Smad signalling is TGF-β-hippo pathways interaction. Some studies showed that YAP and TAZ, the hippo pathway effectors, interact with Smads to control Smad nuclear retention and TGF-β induced cellular responses (Narimatsu *et al*., 2015; Varelas *et al*., 2008). YAP/TAZ accumulates in the nucleus by activated TGF-β signalling (Grannas *et al*., 2015). Inhibition studies of these effectors block the nuclear translocation of active pSmad2/3 complexes, thus inhibit the expression of fibrotic genes associated with TGF-β including α-SMA, COL1A1 and

CTGF (Piersma *et al*., 2015; Szeto *et al*., 2016). Liu and coworkers (2015) demonstrated that YAP/TAZ accumulated in the nuclei of α-SMA positive fibroblasts of lung fibrosis.

1.7.3 Non-Smad signalling: RHO pathway links TGF-β mediated actin polymerisation in myofibroblast differentiation

One of the myofibroblast phenotypes induced by TGF-β is a reorganisation of the actin cytoskeleton and formation of focal adhesion complexes. TGF-β induces these phenotypes, at least in part, through activation of Rho GTPase pathway. The Rho GTPase act as molecular switches, exist in GDP-bound (inactive state) while GTP-bound (active state) and interact with downstream effectors to transmit their signal (Van Aelst and D'souza-Schorey, 1997). TGF-β induces activation of Rho GTPases in various cell types including fibroblasts (Vardouli, Moustakas and Stournaras, 2005), with several studies emphasised on Rho A (Johnson *et al*., 2014; Manickam *et al*., 2014). The mechanism of Rho activation by TGF-β is poorly understood. However, it was postulated to be non-Smad signalling, at least initially, but requires the activity of Tβ1R (Fleming *et al*., 2009; Sandbo *et al*., 2011). The activated Rho GTPase trigger a cascade involving Rho coiled-coiled kinase (ROCK) 1-mediated LIM-kinase 2 activation and inactivation of the actin microfilaments and the formation of stress fibres (Vardouli *et al*., 2005). Both a rapid and delayed activation of Rho Kinase pathway has been observed in response to TGF-β (Edlund *et al*., 2002; Sandbo *et al*., 2011; Vardouli *et al*., 2005). Furthermore, the delayed activation correlates to the prominent stress fibres formation after 18-24 h of TGF-β stimulation and subsequent α-SMA expression. The delayed activation of Rho kinase was postulated to involve a biphasic signalling pathway; initially dependent on Smad signalling but later dependent on cofilin phosphorylation downstream of ROCK (Edlund *et al*., 2002; Sandbo *et al*., 2011). Inhibition of ROCK signalling by pharmacological inhibitor (Y27632) prevents stiffness-induced α-SMA

expression and stress fibres formation in lung myofibroblasts (Htwe *et al*., 2017). Inhibition of actin polymerisation by cytochalasin D prevents myofibroblast transformation of lung fibroblasts (Ni *et a*l., 2013). Inhibition of focal adhesion kinase (FAK) activity by FAK inhibitor attenuates myofibroblast differentiation of cardiac fibroblast (Zhang *et al*., 2017). Collectively, inhibition of Rho kinase signalling prevents myofibroblast phenotype in various tissue fibrosis.

1.7.4 Non-Smad signalling: MAPK pathway and TGF-β induced myofibroblasts

As reviewed by Zhang *et al*., (2017), TGF-β activates a member of MAPK signalling (ERK, c-Jun amino terminal kinase and p38 MAPK) upon receptor-ligand binding. In myofibroblast differentiation, a rapid phosphorylation of ERK1/2 and p38 MAPK have been observed in TGF-β-treated human tenon fibroblasts with p38 showing a biphasic and sustained signal (Carthy *et al*., 2015; Meyer-Ter-Vehn *et al*., 2006). Fra 2, a member of the Fos family of AP1 transcription factors, is believed to be involved in the ERK1/2 activation induced by TGF-β. Pre-incubation of human breast fibroblasts with Fra 2-targeting siRNA inhibits the myofibroblast markers associated with TGF-β such as calponin and SM-22α compared to control siRNA (Carthy *et al*., 2015). However, the exact mechanism on how MAPK signalling links to Smad signalling remains unclear. The pathways that involve in TGF-β-induced myofibroblasts differentiation are illustrated in Figure 1.8.

1.8 Drug resistance induced by tumour stromal cells

Therapeutic resistance is the significant reason for cancer treatment failure, including in HNSCC. Stromal cells including CAF may influence the treatment sensitivity of tumour cells. Several lines of evidence demonstrate that the tumour microenvironment

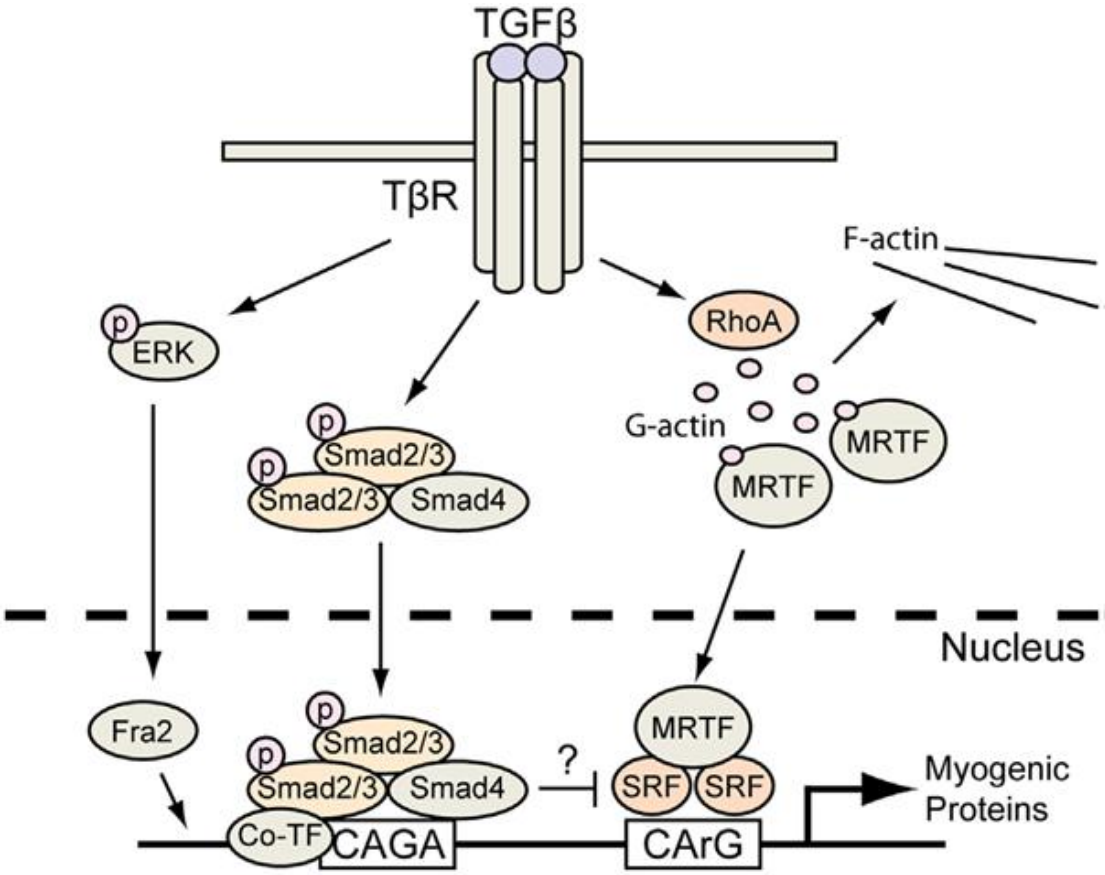

Figure 1.8: TGF-β signalling in myofibroblasts differentiation

TGF-β activates Smad and non-Smad signalling which contribute to the myofibroblasts phenotype. The Smad pathway is characterised by the binding of Smad transcriptional complexes to the Smad binding elements in the specific site of target genes. TGF-β induces non-Smad MAPK signalling via Fra 2, a member of Fos family of AP1 transcription factors (taken from Carthy *et al*., 2015).

confers chemotherapy resistance by releasing soluble factors. Johansson and coworkers (2012) demonstrated that co-culture of HNSCC cell lines with CAF in the presence of cetuximab resulted in an increased proliferation rate of tumour cells and elevated expression of MMP-1. Additionally, the CAF-induced resistance was partly abolished by adding MMP-1 inhibitor into co-culture, suggesting the role of MMP-1 in the development of drug resistance. HGF levels secreted by the stromal cells of melanoma correlates with poor response to anti-cancer drugs (Straussman *et al*., 2012). The cellular (CAF) and non-cellular (ECM) of tumour microenvironment contribute to the anti-apoptotic property of tumour cells (Sebens and Schafer, 2012). The tumour microenvironment also hampers chemotherapy treatments by causing the tumour to develop drug resistance through metabolic effects (Pietras and Ostman, 2010). Moreover, other studies demonstrated that stromal cells promote mitochondrial metabolism in carcinoma cells (Martinez-Outschoorn *et al*., 2010; Martinez-Outschoorn *et al*., 2011). For instance, fibroblasts induce resistance to tamoxifen in breast cancer by amplifying mitochondrial metabolism in cancer cells (Martinez-Outschoorn *et al*., 2011). Additionally, stromal cells induce resistance to cytotoxic chemotherapy such as doxorubicin and docetaxel through lactate production (Martinez- Outschoorn *et al*. 2011; Rong *et al*., 2013). Parallel with this finding, Tavares-Valente and colleagues (2013) demonstrated that lactate release from stromal cells causes a low pH in the tumour microenvironment and this low pH is associated with resistance to paclitaxel and doxorubicin in MCF-7 cells.

1.9 Therapeutic implications

Increasing evidence shows that cancer progression is greatly influenced by its microenvironment, not merely on cancer cells. The concept of targeting CAF as a therapeutic implication is intriguing, however, several obstacles should be overcome.

Successful therapy must solely target the cancer components while avoid targeting the surrounding normal stromal cells such as endothelial cells and inflammatory cells. Moreover, several factors such as insufficient vascular structures, pH alterations and hypoxia may hamper the delivery of agents to the stroma. Therefore, effective approaches are needed to identify the novel targets and successful delivery methods. There are several promising drugs targeting CAF. VEGF inhibitors specifically target the endothelial cells, one of the origins of CAF (Xing *et al*., 2010). Tenascin-C is highly expressed in CAF and able to promote metastases in colon cancer (De Wever *et al*., 2004). Anti-tenascin antibody, 81C6 is now in a clinical trial (phase II) for brain tumour patients (Reardon *et al*., 2006). FAP is abundantly expressed in CAF compared to normal fibroblast. Thus, an antibody called sibrotumab is under clinical trials for colon cancer patients (Scott *et al*., 2003). CTGF is highly expressed in CAF and it promotes tumorigenesis in prostate cancer (Yang *et al*., 2005). Therefore, CTGF inhibitors might be a promising target for cancer therapy. Further understanding of CAF themselves and their pathological role in tumour microenvironment milieu will lead to the development of promising novel agents for cancer therapy.

1.10 MicroRNAs

They are many types of endogenous RNA molecules exist; small transfer RNA (tRNA), ribosomal RNA (rRNA), small nucleolar RNA (snoRNA), small interfering RNA (siRNA) and microRNA (miRNAs). miRNAs are small noncoding RNAs of ~ 22 nucleotides in length that negatively regulate gene expression at the post-transcriptional level. miRNAs regulate cell differentiation since they affect the expression of many genes. Furthermore, they are deregulated in cancer cells (Schickel *et al*., 2008). Generally, it is not clear whether miRNAs are involved in the conversion of normal fibroblasts to CAF. In addition, little is known about miRNAs expression in tumour

stroma, particularly in oral cancer. One study demonstrated that miR-145 was down-regulated in oral fibroblast treated with cigarette smoke condensate (Pal *et al*., 2013).

1.10.1 Expression and function of miRNAs

The expression and function of miRNAs involve a complex set of proteins (Meltzer, 2005). miRNAs commonly located in a non-coding region or in introns of protein coding-genes (Chen, 2005). The mechanism of miRNAs biogenesis and function is described in Figure 1.9 by Barca-Mayo and Lu (2012).

Briefly, a relatively large primary miRNA (pri-miRNA) is produced when the miRNAs gene is transcribed by RNA Polymerase II. This pri-miRNA is cleaved by Ribonuclease III or Drosha to form a precursor miRNA (pre-miRNA) molecule. Then, pre-miRNA is transported to the cytoplasm by Exportin 5 for further steps. In the cytoplasm, the pre-miRNA is converted into short RNA duplex of 18-24 nucleotides in length by Dicer. In most cases, one strand is degraded while the other one is incorporated into the RNA-induced silencing complex (RISC). The RISC complex caused miRNA to bind to the 3' UTR region of mRNA target, leading to degradation of miRNA or inhibition of mRNA translation. Of note, miRNAs might play a role in cell proliferation and apoptosis, thus it is not surprisingly that miRNAs might cause tumorigenesis (Catto *et al*., 2011).

1.10.2 MicroRNAs and cancer

While most microRNA studies have focused on the tumour cell, little is known about microRNA expression in the tumour microenvironment. As mentioned above, the microRNAs are usually deregulated in many cancers. Differential expression of microRNAs in various cancer cells can be identified by high output technologies

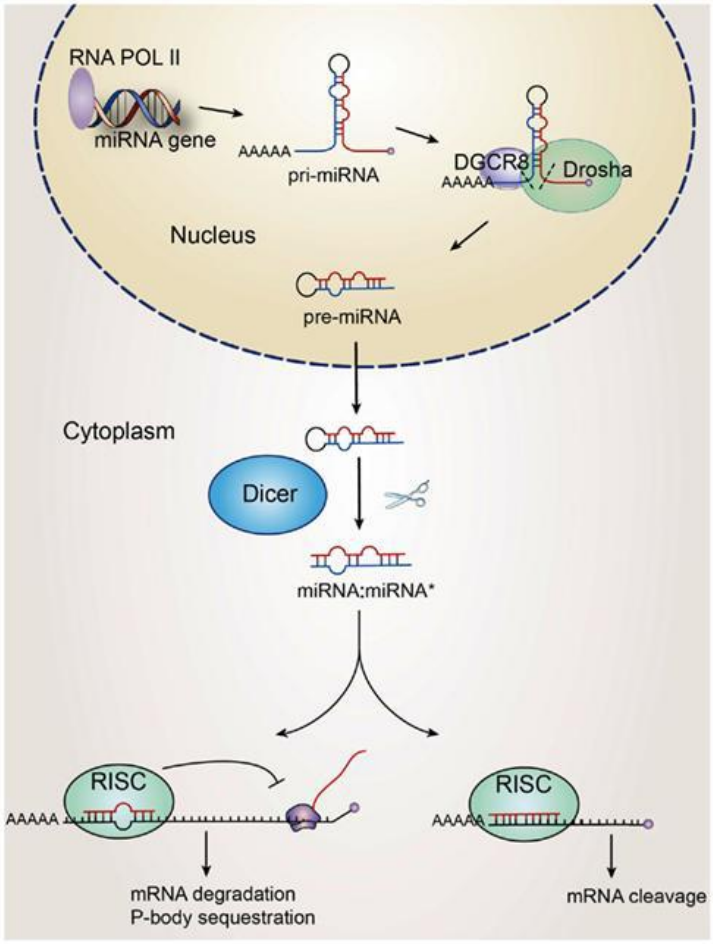

Figure 1.9: Biosynthesis and function of miRNAs

A pri-miRNA is transcribed from miRNA gene by RNA polymerase II and is cleaved by Drosha to produce pre-miRNA. A pre-miRNA is transported into the cytoplasm by Exportin 5. In the cytoplasm, the pre-miRNA is cleaved by Dicer to produce a miRNA duplex. The mature miRNA strand incorporates into the RISC and bind to a specific site of mRNA target. The miRNA complex induces either mRNA degradation or translational repression (taken from Barca-Mayo and Lu, 2012).

including microarray and PCR approaches. For example, down regulated of miR-15a and miR-16-1 in prostate cancer cells and these miRNAs target their downstream molecule, BCL-2 (Calin *et al*., 2002; Cimmino *et al*., 2005). Let-7 family, tumour-suppressor miRNA is found to be down-regulated in several cancers such as lung and gastric cancer (Takamizawa *et al*., 2004). In addition, decreased expression of this miRNA cause increased expression of Ras oncogene in some human lung tumours and is associated with poor prognosis (Johnson *et al*., 2005). Previous studies have shown that oncogenic miRNAs involved in the pathogenesis of some tumours. Overexpression of these miRNAs inactivates tumour suppressor genes. For example, overexpression of miR-155 in breast, lung and colon cancers (Yanaihara *et al*., 2006; Volinia *et al*., 2006). Additionally, overexpression of miR-21 has been shown in glioblastoma cell lines (Chan *et al*., 2005). Taken together, altered miRNAs expression could be involved in the initiation of tumour process.

1.10.3 miRNA in tumour microenvironment (CAF)

Accumulating data indicate that microRNAs are involved in the dramatic changes in the tumour microenvironment, mainly in CAF, which enhances the progression of the tumour (Aprelikova *et al*., 2012). To date, there have been no reports regarding differential miRNA expression profiling in CAF, particularly in HNSCC. A recent study demonstrated that miR-21 expression in CAF is associated with poor prognosis in pancreatic ductal adenocarcinoma (Kadera *et al*., 2013). Overexpression of miR-21 promotes CAF formation in cultured human fibroblast foreskin (Li *et al*., 2013). Yang and colleagues (2014) demonstrated that miR-106b is upregulated in CAF compared with normal fibroblasts established from patients with gastric cancer. Additionally, the expression level of miR-106b is associated with poor prognosis of patients. miR-200 family including miR-200c is down-regulated in CAF compared to normal fibroblast in

breast cancer (Zhao *et al*., 2012). This miRNA has been shown to regulate EMT and cancer cell migration by targeting tumour suppressor E-Cadherin (Gregory *et al*., 2008). miR-31 is down-regulated in CAF of endometrial cancer compared to normal fibroblast and is associated with increased tumour cell motility (Aprelikova *et al*., 2010). Taken together, global gene expression profiling of the stromal compartment, mainly fibroblasts have been shown to effectively predict clinical outcome and therapy response (Finak *et al*., 2008; Farmer *et al*., 2009).

1.10.4 miRNA in fibrosis

Fibrosis is the formation of excess fibrous connective tissue in an organ that ultimately resulted in an imbalance of metabolism of ECM molecule. Fibrosis is probably to result from both; an increased synthesis and decreased degradation of ECM components. For example, MMPs that degrade ECM may be elevated while their inhibitors, TIMPs may be down-regulated. Thus, abnormalities in multiple pathways involved in tissue repair and inflammation can lead to the development of fibrosis. Extensive tissue remodelling and fibrosis can eventually lead to a number of organ failure. Several of evidence that suggest miRNAs are involved in the process of fibrosis in several organs including heart, lung and kidney.

Cardiac fibroblasts are abundant cell type in the heart and crucial in the regulation of cardiac ECM metabolism (Sounders *et al*., 2009). Excess deposition of ECM components in the heart is associated with various cardiovascular diseases such as hypertension, myocardial infarction and cardiomyopathy and miRNAs are believed to involve in the modulation of these conditions (Diez, 2009; Mishra *et al*., 2009). miR-28 was selectively expressed in cardiac fibroblasts and overexpression of miR-28 was observed in heart failure of human, mice and rats (Thum *et al*., 2008). Van Rooij *et al* (2008) demonstrated that the miR-29 family was down-regulated in murine and human hearts during

myocardial infarction.

Pulmonary fibrosis is characterised by excessive deposition of collagen and other ECM proteins within the pulmonary interstitium. In addition, it is commonly associated with the upregulation of TGF-β (du Bois, 2010). Pottier and co-workers (2009) demonstrated that TGF-β caused downregulation of miR-155 expression in human lung fibroblasts. Additionally, studies using a bleomycin-induced mouse model of lung fibrosis demonstrated that upregulation of miR-155 was correlated with the degree of lung fibrosis in C57BL/6 and BALB/C mice (Pottier *et al*., 2009).

Diabetic nephropathy is characterised by progressive fibrosis in the renal glomerulus and tubulo-interstitial region (Brosius, 2008). Treatment of TGF-β in cultured human and mouse mesangial cells caused upregulated of miR-377 expression (Wang *et al*., 2008).

1.10.5 Role of miRNAs in tumour microenvironment

1.10.5.1 CAF differentiation

Mitra and co-workers (2012) demonstrated that miR-155 was upregulated in both fibroblasts isolated from ovarian cancer tissue and in experimentally induced CAF. Upregulation of miR-31 and miR-221 were reported in breast CAF (Zhao *et al*., 2012). However, downregulation of some miRNAs may induce a CAF myofibroblast phenotype. The expression of miR-31 and miR-214 were downregulated in CAF ovarian (Mitra *et al*., 2012). Additionally, they demonstrated that triple transfection of NOF with anti-miR-31, anti-miR-214 and pre-miR-155 promotes fibroblast migration and invasion of co-cultured HeyA8 and SKOV3ip1 cells. Triple transfection of CAF with pre-miR-31, pre-miR-214 and anti-miR-155 reverses these pro-tumourigenic properties of co-cultured ovarian cancer cells to levels similar to those NOF co-cultured with ovarian cancer cells. Tang and colleagues (2016) demonstrated that miR-200 downregulation contributes as a

regulator of CAF differentiation in breast cancer.

1.10.5.2 EMT and ECM remodelling

In order to metastasize to a distant site, cancer cells must break the basement membrane which separates epithelial cells from the stroma. Under normal condition, epithelial cells form a strong connection to each other by gap junction involving E-cadherin, thus limit their migration. Taking this advantage, cancer cells undergo EMT and suppress E-cadherin expression, thus detach from the epithelial layer to metastases (Thiery *et al*., 2009). Furthermore, cancer cells undergoing EMT are fundamentally different in gene expression profiles and are stem-like cells e.g. self- renewal capability (Mani *et al*., 2008). Therefore, as mentioned before, EMT is a crucial process for cancer cells stemness. A mountain of evidence suggests that miRNAs are involved in regulating the EMT process. The first group of miRNAs that regulate EMT are the miR-200 family (miR-200a, miR-200b, miR200c, miR-141 and miR-429) and miR-205 (Zhang *et al*., 2014). These two families were deregulated in various tumours to facilitate EMT progression. Furthermore, suppression of these miRNAs cause increased expression of the transcription factor ZEB family, which modulate the expression of E-cadherin in cancer cells (Gregory, 2008; Korpal *et al*., 2008; Burk *et al*., 2008). Since then, some additional miRNAs have been found to regulate EMT process by targeting EMT-related transcription factors. For example, miR-34, miR-9 and miR-30a modulate Snail1 expression (Kim *et al*., 2011; Liu *et al*., 2012), miR-124, miR-203 and miR 204/211 regulate Snail2 (Xia *et al*., 2012; Zhang *et al*., 2011; Wang *et al*., 2010) whereas miR-214, miR-580 and Let 7d target Twist1 (Li *et al*., 2012; Nairismagi *et al*., 2012; Chang *et al*., 2011). Additionally, miR-138, miR-215 and miR-708 downregulate Zeb2 (Liu *et al*., 2011; White *et al*., 2011; Saini *et al*., 2011).

MMPs are important in ECM remodelling by cancer cells. MMPs are produced

by various cells such as macrophages, mast cells and fibroblasts as well as certain epithelial cells under the appropriate stimuli (Overall and Kleifeld, 2006). It has been demonstrated that some miRNAs affect the expression of MMPs. miR-29b suppresses the expression of prometastatic regulators including MMP2 and MMP9, thereby modifying the tumour microenvironment and reduce metastasis by altering collagen remodelling, proteolysis and angiogenesis (Chou *et al*., 2013). Conversely, upregulation of miR-21 cause increased expression of various MMPs including MMP2 and MMP9 through suppression of PTEN in hepatocellular carcinoma cells and the MMP inhibitors RECK and TIMP3 in glioblastoma cells (Gabriely *et al*., 2008; Meng *et al*., 2007). Additionally, decrease expression of miR-138 induced RhoC expression and increase MMP2/MMP9 production in cholangiocarcinoma (Wang *et al*., 2013).

Taken together, these findings show that many miRNAs involved in EMT and ECM remodelling whereby cancer cells take advantage of tumour microenvironment to facilitate their metastases using these processes.

1.10.5.3 Hypoxia and angiogenesis

In primary tumour, cancer cells proliferate rapidly with outgrowing of its blood supply, leaving many tumour cells in regions deprived of adequate oxygen supply compared to normal tissues. Therefore, to adapt and survive this hypoxic environment, cancer cells have to modify their intrinsic gene expression and form a new vasculature to get enough nutrients and oxygen. Hypoxia-inducing factors (HIFs) are the transcription factors that respond to hypoxia. HIFs arrange a signalling cascade to promote tumour growth and angiogenesis (Semenza, 2012). The most common miRNAs-inducing hypoxia is miR-210. Upregulation of miR-210 under hypoxia is correlated with metastases in breast cancer, melanoma, pancreatic cancer, and ovarian cancer (Ho *et al*., 2010; Giannakakis *et al*., 2008; Camps *et al*., 2008). Theoretically, miR-210 targets

MAX dimerization protein (MNY), a MYC antagonist which allows cancer cells to divert the hypoxia-induced cell cycle arrest (Zhang *et al*., 2009). miR-210 regulates the mitochondrial metabolism of cancer cells through glycolysis by suppressing the expression of iron-sulfur cluster scaffold homolog (ISCU) and cytochrome c oxidase assembly protein (COX10) (Chen *et al*., 2010). miR-424 is also believed as hypoxia-induced miRNAs by suppression of the scaffolding protein cullin 2 (CUL2), which is important to assemble the ubiquitin ligase system, thus stabilise the HIF-α and promote angiogenesis (Ghosh *et al*., 2010). Collectively, these findings have delineated the role of several miRNAs related with HIF signalling to control oxygen homoeostasis inside tumours. Regardless of these findings, recent understanding of the role of hypoxia-induced miRNAs remains limited. Taken together, the communication between miRNA-containing microvesicles with various cell types delineates an additional mechanism of microenvironmental regulation of miRNAs involved membrane and secreted proteins.

1.10.6 Role of miR-424

To date, little is known about the effects of miR-424 in cancer as well as in the stromal microenvironment, particularly in CAF. miR-424 is believed to involve in maintaining physiological vasculature (Kim *et al*., 2013; Chamorro-Jorganes *et al*., 2011) and differentiation of blood cells (Rosa *et al*., 2007). While in cancer, miR-424 expression possibly induces EMT as effectively as miR-200c in prostate cancer (Banyard *et al*., 2013). Low expression of miR-424 correlates with poor prognosis and lymph node metastasis in cervical cancer (Xu *et al*., 2012).

miR-424 is a member of the miR-16 family, which includes miRNA-15/16/195/424/497. Despite different genomic locations, these miRNAs have a ‘seed region’ in the 5’UTR which resulted in some overlapping miRNA targets (Forrest *et al*., 2010). MiR-16 family regulates multiple cell cycle genes such as CCND1, CCNE1 and

targets several oncogenes including BCL-2 in various types of cancer (Liu *et al*., 2008). However, Cimmino and colleagues (2005) demonstrated that miR-16 negatively regulates BCL-2. miR-195 regulates pro-apoptotic activity through targeting BCL-2 expression in colorectal cancer (Huang *et al*., 2010). Additionally, ectopic expression of miR-195 cause down-regulation of cell cycle-related genes such as CCNE1 and CHK1 as well as an accumulation of cells at GI phase (Linsley *et al*., 2007). Similar to miR-195, ectopic expression of miR-497 blocked cell cycle at G1 stage and induced apoptosis in breast cancer (Li *et al*., 2011). Taken together, these findings suggest that miR-16 family has a similar cluster of gene regulation. miR-424 is relatively known as hypoxia-induced miRNA. Ghosh and co-workers (2010) demonstrated that hypoxia-induced miR-424 regulates HIF-α isoforms and promotes angiogenesis. miR-424-5p expression was decreased in liver cancer tissue compared to that normal liver tissue and this downregulation was associated with advance disease progression in liver cancer patients (Zhang *et al*., 2014). Conversely, Wu and co-workers (2013) demonstrated that miR-424-5p was significantly upregulated in pancreatic cancer. To date, there is no published study, which has explored the role of miR-424 in CAF of OSCC. Recent study demonstrated that miR-424 downregulates isocitrate dehydrogenase 3α (IDH3α) in CAF isolated from colon cancer tissue (Zhang *et al*., 2015). miR-424 potentiates TGF-β-induced myofibroblast differentiation through EMT in human lung epithelial cells (Xiao *et al.*, 2015).

1.10.7 miR-145 and tumour microenvironment

miR-145 is a 22 nt in length and located on chromosome 5(5q32-33), well-known cancer associated cancer region (Zhang, 2009; Le Beau *et al*., 1989). miR-145 is co-transcribed with miR-143 and commonly refers as a miR-143/miR-145 cluster (Cordes *et al*., 2009). miR-145 is a well-established tumour suppressor was found to be

downregulated in various types of cancers including bladder, breast and colon cancer (Ichimi *et al*., 2009; Sempere *et al*., 2007; Schepeler *et al*., 2008). The mechanism underlying this downregulation remains unknown. miR-145 involved in regulation of various cellular processes including cell cycle and apoptosis by targeting multiple oncogenes (Zhang, 2009). Additionally, downregulation of miR-145 is associated with poor prognoses for many cancers and have been considered an ideal biomarker in cancer therapy. miR-145 is downregulated in the saliva of the patients with OSCC compared with healthy patients (Zahran *et al*., 2015).

p53 is a tumour suppressor that controls various cellular pathways. Recently, p53 regulates some of the miRNAs such as miR-192/215, miR-34 and miR-145 (Hermeking, 2007; Barlev *et al*., 2010). Sachdeva *et al* (2009) demonstrated p53 regulates the miR-145 promoter activity by directly binding to the p53 response elements-2 (p53RE-2), thereby increases miR-145 expression. Downregulation of miR-145 was demonstrated in prostate cancer tissue and various types of cancer cell lines associated with p53 mutations (Suh *et al*., 2011). Till now, many oncogenic genes have been identified as targets for miR-145, which involves in various biological pathways proliferation, invasion and metastases (Fuse *et al*., 2011; Miles *et al*., 2012; Noh *et al*., 2013). miR-145 inhibits cancer cell proliferation by targeting growth factor-related genes including EGFR (Fuse *et al*., 2013). miR-145 regulates some genes-related to invasion and metastases such as MUC1, FSCN and SOX9 (Guo *et al*., 2013; Miles *et al*., 2012; Noh *et al*., 2013). Apart from that, miR-145 regulates cell differentiation by targeting core reprogramming factors such as OCT4, SOX2 and KLF4 (Xu *et al*., 2009; Hu *et al*., 2012). In addition, miR-145 could inhibit angiogenesis process by targeting VEGF and HIF-1α (Fan *et al*., 2012; Zou *et al*., 2012).

Recently, the roles of miR-145 in the tumour microenvironment, particularly in

the myofibroblast differentiation has gained a lot of attentions. miR-145 was reported to promote myofibroblast phenotype in cardiac and pulmonary fibrosis (Wang *et al*., 2015; Yang *et al*., 2013). Microarray data showed a significant downregulation of miR-145 in CAF isolated from invasive bladder tumours and normal fibroblast from foreskin (Enkelmann *et al*., 2011). However, these data not correlate with validation data from qRT-PCR. Additionally, miR-145 was shown to regulate scarring of skin tissues and TGF-β1-induced myofibroblast differentiation compared to untreated fibroblasts (Gras *et al*., 2015). Collectively, these data suggest that miR-145 plays a role in fibroblast transdifferentiation. Pal *et al*., (2013) demonstrated that miR-145 was downregulated in normal oral fibroblasts in response to cigarette smoke, which promotes migration of OSCC cancer cell lines. This finding highlighted that miR-145 is involved in stromal-epithelial interactions.

1.10.8 miRNA and cancer-related extracellular vesicles

Recent works have demonstrated the role of miRNAs in cellular communication. miRNAs have been detected as circulating biomarkers for various cancers such as breast, pancreatic, colon and lung (Roth *et al*., 2010; Kawaguchi *et al*., 2013; Cheng *et al*., 2011). These circulating miRNAs are generated from cancer cell debris through apoptosis or necrosis and from miRNA-containing extracellular vesicles including exosomes, microvesicles and apoptotic bodies (Valadi *et al*., 2007). Vesicles released from cells are vary from 30 nm to 5 μm in diameter and are collectively called extracellular vesicles. However, exosomes have been extensively studied amongst vesicles as direct carriers of miRNAs mediating cellular communication (Kosaka and Ochiya, 2011). Recent studies have demonstrated that certain miRNAs in this form could influence tumour progression via cancer cell-stroma interactions. For example, in breast cancer cells, miR-210 can be released via nSMase2-dependent exosomal secretion pathway and transported to

endothelial cells, thereby served as angiogenic miRNA in recipient endothelial cells (Kosaka *et al*., 2013). On the other hand, miRNAs also can be transported from stromal cells to cancer cells. In coculture experiment, MiR-233 can be transmitted to breast cancer cells from TAMs. Of note, miR-233 is highly expressed in IL-4-TAMs, not in breast cancer cells (Yang *et al*., 2011). Conversely, transmission of miR-233 from macrophages to hepatocellular carcinoma cells is associated with cellular contact and gap junction, not exosomes. Additionally, miR-1 was shown to mediate extracellular vesicles function. Overexpression of miR-1 in glioblastoma cells decreased *in vivo* tumour growth and angiogenesis associated with extracellular vesicle transport of miR-1 (Bronisz *et al*., 2014).

1.10.9 miRNAs therapies

The rationale of using miRNAs as a therapeutic approach is because 1) miRNAs play important role in basic biological processes and deregulated in various cancer 2) the cancer phenotype can be reversed by targeting miRNAs expression (Calin *et al*., 2002; Motoyama *et al*., 2008). To date, two main approaches have been taken; miRNA inhibition therapy (anti-miR) 2) miRNA replacement therapy (mimic miRNA). Anti-miRs are generated to inhibit endogenous miRNAs that have a gain-of-function in diseased tissues while mimic miRNAs are generated to restore miRNA that have a loss of function.

Anti-miRs approach targets a single gene product such as small molecule inhibitors and short interfering RNAs (siRNAs). Additionally, miRNA sponges and antisense oligonucleotide (ASOs) are also been used as miRNA inhibition therapy. Anti-miRs disrupt the RISC complex, thereby prevent the degradation of mRNA. miRNA sponges have been developed to repress the activity of miRNA families sharing a common seed sequence. Therefore, the disadvantage of miRNA sponges is the limited

homogeneity of transcripts expression resulted in unwanted side effects (Zhang and Wang, 2013). There are hurdles that hamper miRNA-based therapy, especially *in vivo* study. In general, RNAs have low stability *in vivo*. Therefore, miRNA introduced into mice is quickly cleared (30 min) from circulatory system (Trang *et al*., 2011). Unmodified RNA will be degraded by RNAses and rapid renal excretion (Czauderna *et al*., 2003). Thus, the plasma half-life of RNAs needs to be increased for miRNA-based therapy. This can be achieved by higher miRNA stability or protection from RNAses. miRNA stability can be improved by chemically modified oligonucleotides such as locked nucleic acid (LNA) nucleotides (Wahlestedt *et al*., 2000), 2'-O-methyl-oligonucleotides (2'-O-MOE) (Yoo *et al*., 2004) and peptide nucleic acid (PNA) (Hyrup and Nielsen, 1996).

miR-21 is an oncomiRs and highly expressed in solid tumours and haematological diseases (Folini *et al*., 2010; Lakomy *et al*., 2011). Inhibition of miR-21 is able to decrease cell proliferation and increased apoptosis in breast and glioblastoma cancer cells (Mei *et al*., 2010; Corsten *et al*., 2007). Inhibition of miR-21 increased expression of PTEN and decreased tumour cell proliferation, migration and invasion in hepatocellular carcinoma cells (Meng *et al*., 2007).

On the other hand, miRNA mimics are used to restore miRNA that have a loss function by using the oligonucleotide mimics containing the same sequence as the mature endogenous miRNA. Similar to siRNAs, miRNA mimics can be delivered using the same technologies. Therefore, miRNA mimics therapy will face less of a delivery obstacle compared to anti-miRs. Furthermore, miRNA mimics are expected to be more specific and well-tolerated in normal cells. This notion is based on the fact that miRNA mimics have the same sequence as the naturally occurred miRNA and target the same genes. The fact that most of the normal cells already express the targeted miRNA,

delivery of miRNA mimics to normal cells is unlikely cause an adverse effect. This is because the cellular pathways targeted by the mimic are already activated or inactivated by the endogenous miRNA.

The Let-7 family is one of the tumour suppressor miRNAs and commonly downregulated in the tumour (Barh *et al*., 2010). Administration of Let-7 either Let-7 mimic or a virus leads to strong inhibition of tumour growth in human non-small cell lung cancer xenografts (Trang *et al*., 2010). This collective evidence suggests that inhibition of overexpressed oncomiRs or substitution of tumour suppressive miRNAs will become a promising strategy for cancer therapy.

1.11 Aims and hypotheses of the study

As mentioned above, the interaction between stroma and tumour cells contributes to tumourigenesis and it is recognised that inflammatory cells, epithelial cells as well as CAF are involved in promoting tumour growth. Fibroblasts play a pivotal role in maintaining tissue homoeostasis and wound healing. However, the mechanism underlying conversion of fibroblasts into CAF is poorly understood. Recently, miRNA research has become a rising topic in cancer biology. Several studies have revealed miRNA expression profiling in various cancer cells including HNSCC. But, the study of miRNA in tumour stroma is still limited, leading to a paucity of information of how miRNA contribute to malignancy in tumour-stroma interaction. Additionally, it is not clear whether endogenous miRNAs are involved in the conversion of fibroblasts to CAF. Therefore, we hypothesise that miRNAs are involved in the reprogramming of normal fibroblasts to experimentally-derived CAF (eCAF). The present study aimed to determine the miRNA expression profile in eCAF and tumour-derived CAF, and to study the functions of candidate miRNA identified using this approach. To do this, a number of specific aims were addressed as stated below;

1) To characterise the CAF-like myofibroblastic phenotype of stromal oral fibroblasts to utilise later to study miRNA involvement in the development of CAF
2) To determine the miRNA expression profiles of eCAF and further examine the role of selected miRNAs in eCAF and tumour-derived CAF
3) To profile the expression of miRNA using a global miRNA profiling strategy to identify novel miRNA regulations of CAF-like differentiation in eCAF or CAF development in tumour-derived CAF (isolated from two subtypes of OSCC)

Thus, the model for miRNA-induced normal oral fibroblasts into eCAF here opens the possibility of a treatment approach targeting the tumour stroma with miRNA mimics and miRNA inhibitors. The workflow for the study is presented in Figure 1.10.

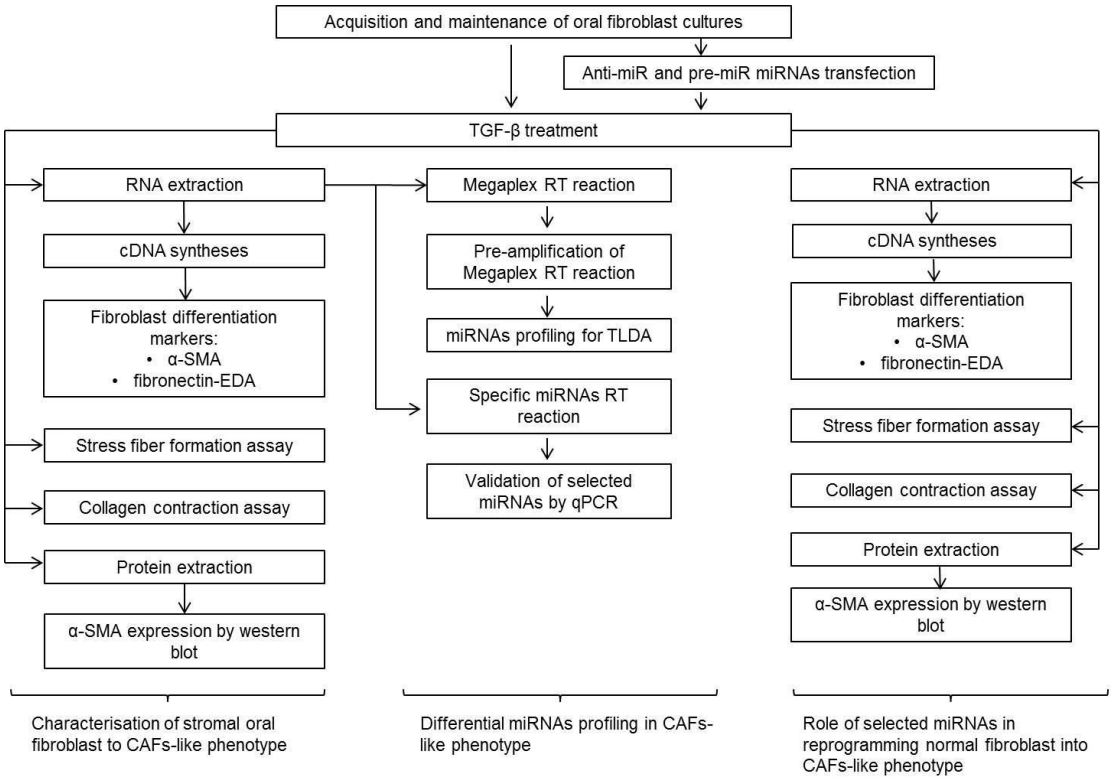

Figure 1.10: A summary of experimental design

Briefly, cells were treated with TGF-β1 (0.05-5 ng/ml) for 24 and 48 h. Fibroblasts differentiation markers such as α-SMA and FN-EDA1 were determined by qPCR. The optimal concentration and time point were used for subsequent experiments including α-SMA protein expression, stress fibre formation, collagen contraction as well as miRNAs expression profiling. Selected miRNAs were validated by qPCR, followed by transfection of cells with selected miRNAs. The responses of transfected cells with or without TGF-β1 were evaluated using the same experiments.

CHAPTER 2: Materials and methods

2.1 Materials and Chemicals

2.1.1 Chemicals and Reagents

All chemicals and reagents used in this study are listed in Table 2.1

Name	Supplier
Acetic acid	Fisher Chemical, UK
Acrylamide 40% solution	Fisher-Scientific, UK
Ammonium Persulphate 99+%	ACROS Organics, USA
Bovine Serum Albumin (BSA)	Fisher-Scientific, UK
CL-Xposure™ film	Thermo Scientific, USA
Complete ULTRA tablets, mini EDTA-free	Roche, UK
Cowbelle ® Dried skimmed milk	ALDI, UK
Dimethyl sulphoxide (DMSO)	Sigma-Aldrich, USA
Dulbecco's Modified Eagle's Medium (DMEM)	Sigma-Aldrich, USA
DMEM (10X)	Sigma-Aldrich, USA
Ethanol	Fisher-Scientific, UK
EZ run pre-stained protein ladder	Fisher-Scientific, UK
Fetal Bovine serum (FBS)	Sigma-Aldrich, USA
Hydrochloric acid (HCl)	Fisher Chemical, UK
Isopropanol	Fisher-Scientific, UK
KlerAlcohol Denatured Ethanol (IMS)	CamLab Limited, UK
L-glutamine	BD worldwide, UK
Methanol	Fisher-Scientific, UK
Nupage antioxidant	Life Technologies, UK
Nupage LDS sample	Life Technologies, UK

Oligofectamine	Life Technologies, UK
Penicillin/streptomycin	BD worldwide, UK
Radioimmunoprecipitation assay (RIPA) buffer	Sigma-Aldrich, USA
Rat tail collagen from tendon	Roche, UK
Recombinant TGF-β1	R&D Systems, USA
Reduced serum-OptiMem medium	Life Technologies, UK
Sodium dodecyl sulphate (SDS)	Fisher-Scientific, UK
Sodium Hydroxide (NaOH)	Sigma-Aldrich, UK
Tetramethylethylenediamine (TEMED)	Applichem, Germany
Trypan blue 0.4%	Life Technologies, UK
Tween-20	Fisher-Scientific, UK
Vectashield mounting medium for fluorescence with DAPI	Vector Laboratories Inc, USA
Virkon (Rely+On™)	DuPont™, UK

Table 2.1 List of chemicals and reagents

2.1.2 Consumables

Table 2.2 shows a list of all consumables used in this study

Name	Supplier
6-well plates	Greiner Bio-one, UK
24-well plates	Greiner Bio-one, UK
Cell scraper Zellschaber	Greiner Bio-one, UK
Cryovials	Greiner Bio-one, UK
Glass coverslips (diameter of 13 mm)	VWR International, UK
IBlot gel transfer stack nitrocellulose	Life Technologies, UK
PCR plates	Qiagen, Germany
Round-bottom tubes	Becton Dickinson, USA
Serological pipette (5, 10 and 25 ml)	Fisher-Scientific, UK
Tubes (15 ml and 50 ml)	Becton Dickinson, USA

Table 2.2 List of consumables

2.1.3 Kits

Table 2.3 shows a list of all commercial kits used in this study

Name	Supplier
BCA Protein Assay	Thermo Scientific, UK
High Capacity cDNA Reverse Transcription	Life Technologies, UK
MirVana™ miRNA isolation	Life Technologies, UK
PCR master mix, no UNG	Life Technologies, UK
Pierce ECL WB	Thermo Scientific, UK
Power SYBR© green PCR master mix	Life Technologies, UK
Preamplification master mix	Life Technologies, UK
RNeasy® Mini Kit	Qiagen, Germany
Taqman Universal PCR Master Mix	Thermo Fisher Scientific, UK

Table 2.3 List of commercial kits

2.1.4 Laboratory equipment

All laboratory equipment used in this study are listed in Table 2.4

Name and Brand	Supplier
Belly dancer-Stuart SRT6 Biocote	ESP Chemical Inc, UK
Class 2 MSC Walker Safety Cabinets	Scientific-Lab Supplies, UK
Compact X4 Xograph imaging system	Xograph Healthcare Inc, UK
Fridge/Freezer	Proline, UK
Galaxy R Co_2 Incubator	Scientific-Lab Supplies, UK
IBlot TM	Life technologies, UK
Integra pipet boy 2	Sigma-Aldrich, UK
JB series water bath	Scientific-Lab Supplies, UK
Neubauer improved optic labor	Fisher-Scientific, UK
Nikon Eclipse TS100 inverted microscope	Nikon, Japan
Real-time PCR machine (Fast Real-time PCR System)	Applied Biosystems, USA
Spectrophotometer (NanoDrop)	Thermo-Scientific, UK
Thermal cycler PCR machine (GeneAmp PCR System 9700)	Applied Biosystems, USA

Table 2.4 List of laboratory equipment used

2.1.5 Antibodies

All antibodies used in this study are listed in Table 2.5

Name	Supplier
Anti-mouse Horseradish peroxidase (HRP) antibody (anti-mouse IgG)	Cell Signaling Technology, USA
Monoclonal α-smooth muscle actin antibody, mouse	Sigma-Aldrich, USA
Mouse β-actin antibody	Sigma-Aldrich, USA
Monoclonal anti-actin, α-smooth muscle FITC antibody in mouse	Sigma-Aldrich, USA
Monoclonal anti-fibronectin antibody, mouse	Sigma-Aldrich, USA

Table 2.5 List of antibodies used

2.1.6 Primers

All primers used in this study are listed in Table 2.5

Name	Sequence	Supplier
U6 Forward	5’ CTCGCTTCGGCAGCACA 3’	Sigma-Aldrich, USA
U6 Reverse	5’ AACGTTCACGAATTTGCGT 3’	Sigma-Aldrich, USA
α-SMA Forward	5’ GAAGAAGAGGACAGCACTG 3’	Sigma-Aldrich, USA
α-SMA Reverse	5’ TCCCATTCCCACCATCAC 3’	Sigma-Aldrich,USA
Fibronectin 1 with EDA (FN-EDA1) Forward	5’ TGGAACCCAGTCCACAGCTATT 3’	Sigma-Aldrich, USA
Fibronectin 1 with EDA (FN-EDA1) Reverse	5’ GTCTTCCTCCTTGGGGGTCACC 3’	Sigma-Aldrich, USA
B2M Control Mix (20X mix of probe with forward and reverse primers)	Pre-designed probe and primer sets	Life Technologies, UK
Collagen 1a (COLA1) Forward	5’ GTGGCCATCCAGCTGACC 3’	Sigma-Aldrich, USA
Collagen 1a (COLA1) Reverse	5’ AGTGGTAGGTGATGTTCTGGGAG 3’	Sigma-Aldrich, USA
miR-424-3p	CAAAACGUGAGGCGCUGCUAU	Life Technologies, UK
miR-145-5p	GUCCAGUUUUCCCAGGAAUCCCU	Life Technologies, UK
miR-424-5p	CAGCAGCAAUUCAUGUUUUGAA	Life Technologies, UK

Table 2.6 List of primers used

2.1.7 Oligonucleotides

All oligonucleotides used in this study are listed in Table 2.7

Name	Part number	Supplier
Negative premiR control #2	AM17111	Life technologies, UK
premiR miRNA precursor 424-3p	AM17100	Life Technologies, UK
mIRCURY LNA™ miRNA power inhibitor 424-3p	4100783-101	Exiqon, UK
mIRCURY LNA miRNA power inhibitor 145-5p	4101574-101	Exiqon, UK
mIRCURY LNA power Negative control A	199006-101	Exiqon, UK
mIRCURY LNA power Negative control B	199007-101	Exiqon, UK

Table 2.7 List of miRNA mimics and inhibitors used

2.2 Cell Culture

2.2.1 Normal buccal oral fibroblasts (NOF)

Three types of NOF cultures were used throughout this study. NOF1, NOF2 and NOF5 cultures were obtained from Prof EK Parkinson (QMUL) and ethics approval had also been obtained (Lim *et al*., 2011). NOF804 and CAF003 were kindly provided by Dr. Helen Colley. All cells were maintained in DMEM medium. Cell passages from 1 to 7 were used in this study.

2.2.2 Reagents for cell culture work

2.2.2.1 Dulbecco's Modified Eagle's Medium

DMEM was purchased as ready-to-use without L-glutamine and antibiotics.

2.2.2.2 Foetal Bovine Serum (FBS)

The serum was aliquoted into sterile 50 ml tubes and kept at -20 ^{0}C.

2.2.2.3 Dulbecco's Phosphate-buffered Saline (DPBS)

DPBS without calcium chloride and magnesium chloride was purchased as ready-to-use.

2.2.2.4 Penicillin/ streptomycin stock solution (100X)

An antibiotic stock solution containing 10 000 U/ml penicillin and 10 mg/ml streptomycin was purchased as ready-to-use. The solution was diluted in DPBS and aliquoted into sterile 1.5 ml tubes before being stored at -20 ^{0}C.

2.2.2.5 Trypsin/EDTA solution (1x)

Cultured cells were detached from the flask surface using trypsin from porcine free-parvovirus. Trypsin-EDTA solution was purchased as ready-to-use and aliquoted into 15

ml tubes and stored at -20 ^{0}C.

2.2.2.6 Complete growth medium

A complete growth medium was used in this study to culture and maintain the cell cultures. The medium consists of DMEM solution supplemented with 10 % (v/v) FBS, L-glutamine and 100 U/ml penicillin and 100 μg/ml streptomycin. The medium was stored at 4 ^{0}C.

2.2.2.7 Assay medium (serum starvation and TGF-β1 treatment)

The assay medium used was DMEM medium without FBS. To prepare 100 ml assay medium, 1 ml L-glutamine and 1 ml penicillin/streptomycin stock solution were mixed with 98 ml of DMEM medium. The medium was kept at 4 ^{0}C.

2.2.2.8 Cryoprotectant medium

This medium contained 10 % (v/v) dimethyl sulphoxide (DMSO) in FBS and was used to store ampoules of cells in liquid nitrogen. The cryoprotectant medium (20 ml) was prepared by mixing 2 ml DMSO in 18 ml FBS. This medium was prepared fresh and kept cold prior to use.

2.2.2.9 Trypan blue 0.1 % (w/v) solution

Trypan blue solution (20 ml) was prepared by diluting 5 ml ready-made 0.4 % (w/v) Trypan blue in 15 ml DPBS. The solution was kept at room temperature until use.

2.2.3 Culture procedures and conditions (routine cell culture)

All tissue culture procedures were carried out under sterile conditions (Class ll biohazard cabinet) and aseptic technique was used in order to avoid any contamination. Good cell culture practice (GCCP) guidelines were exercised during the whole process.

2.2.3.1 Thawing of cells from frozen storage

A frozen ampoule of cells was retrieved from the liquid nitrogen storage vessel and was left at room temperature for approximately 1 min before being transferred to a 37 ^{0}C water bath for 1-2 min to thaw the cells fully. The ampoule was then wiped with a gauze sprayed with 70 % (v/v) IMS prior to opening. The entire content of the ampoule was gently pipetted into a 15 ml centrifuge tube containing 6 ml of DPBS and 1 ml pre-warmed growth medium. The content was centrifuged at 1000 rpm for 1 min to remove the DMSO. The cell pellet was then re-suspended in 5 ml of pre-warmed growth medium. The cell suspension was then slowly pipetted into a 25-cm^2 tissue culture flask. The cell morphology was observed using an inverted phase contrast microscope to check for cell viability. The culture flask was incubated in a humidified atmosphere containing 5 % CO_2 at 37 ^{0}C. The growth medium was replaced every 2-3 days.

2.2.3.2 Sub-culturing of cells

Cells were passaged at intervals of 2-3 days (80-90 % confluence). Subculturing was performed by removal of the medium from the flask. The adherent cells were first rinsed with 2 ml DPBS. After removal of the DPBS, 1 ml trypsin-EDTA solution was added into the flask. The flask was incubated at 37 ^{0}C for approximately 5 min in the CO_2 incubator for detachment of the adherent cells from the flask. The flask was gently shaken to ensure complete detachment of cells and observed under the inverted microscope until the cell layer was dispersed. One ml of fresh medium was added into the flask to inactivate the trypsin activity and followed by repeated gentle pipetting to break apart the clusters of cells. The medium (containing cells) was aspirated and transferred to a sterile 15 ml centrifuge tube. The tube was centrifuged at 1000 rpm for 5 min. The supernatant was then removed and the cell pellet was re-suspended in 5 ml growth medium. The mixture containing cells was aspirated and dispensed into 3-4 new

flasks. The medium volume in each new flask was made up to 5 ml by adding fresh growth medium and the cultures were incubated in humidified atmosphere containing 5 % CO_2 at 37 ^{0}C.

2.2.3.3 Determination of cell number/concentration

Cell counting was performed by Trypan blue dye exclusion to ensure uniformity of the number of viable cells to be added to each flask. Cells were grown in 75-cm^2 tissue culture flasks to obtain stock cultures. The cells were collected as described in Section 2.2.3.2 and re-suspended in 2-5 ml growth medium (depending on the size of the pellet). Cell suspension (10 µl) was then added to 90 µl Trypan blue solution in 1.5 ml tube. The mixture was then mixed well and left for 1 min at room temperature. The number of stained and unstained cells was determined using a haemocytometer. Living cells exclude the dye, whereas dead cells take up the blue dye. The number of viable cells was estimated as follows:

$$\text{Number of viable cells/ml} = \frac{n \times \text{dilution factor} \times 10^4}{5}$$

n = total number of the cell in five squares

2.2.3.4 Freezing down of cells

When required (in order to maintain low passage stocks of primary fibroblasts) cells were frozen down when they reached 70 % confluence. Normally, three or four flasks of cells of the same passage were processed for batch freezing. Cells were detached from flasks using trypsin/EDTA solution as described in Section 2.2.3.2. The cells were then pelleted by centrifugation at 1000 rpm for 2 min to remove the trypsin/EDTA solution. The supernatant was then removed and 10 ml of cryoprotectant medium (Section 2.2.2.8)

was added slowly to resuspend the pelleted cells. The cell suspension was then dispensed into 6 cryovials labeled with cell name, passage number, and date. The vials were placed in a Mr. Frosty for 24 or 48 h at -80^{0}C before being moved into a cryobox where they finally stored in liquid nitrogen in the vapour phase.

2.3 Preparation of collagen

Rat tail collagen (10 mg) was dissolved in 3.3 ml of sterile 0.2 % acetic acid, which results in a final concentration of 3 mg/ml. The collagen then was stored at 4 ^{0}C.

2.4 Preparation of TGF-β1 stock solution

TGF-β1 was supplied in crystalline form and with a purity of more than 99.9 %. The stock solutions of 20 μg/ml were prepared by dissolving 2 μg of TGF-β1 in 0.1 ml of 4 mM HCl. The solution was mixed well and aliquoted into sterile microcentrifuge tubes and stored at -20 ^{0}C. The working solution of TGF-β1 (0, 0.05, 0.5 and 5 ng/ml) was prepared from stock solutions of 20 μg /ml fresh in assay medium prior to use.

2.5 Gene expression of α-SMA and FN-EDA1

2.5.1 Treatment of cells

Cells (2.5 x 10^5/well) were seeded into 6-well plates and incubated overnight in 5 % CO_2 at 37 ^{0}C for cell attachment. The cells were serum starved overnight and were treated on the following day with a range of concentrations of TGF-β1 (0, 0.05, 0.5 and 5 ng/ml) for 24 or 48 h.

2.5.2 Extraction of total cellular RNA

The MirVana miRNA isolation kit was used for total RNA extraction according to the manufacturer's instructions. Briefly, growth medium in culture flasks containing TGF-β1-treated or untreated cells at 24 and 48 h was aspirated and the cells were collected as

described in Section 2.2.3.2. The cells were pelleted by centrifuging at 1000 rpm (168 x g) for 5 min, and pellets lysed with 300 µl of Lysis/Binding solution. The resultant mixture was vortexed to completely lyse the cells and obtain a homogenous lysate. miRNA Homogenate Additive (30 µl) was added to the cell lysate and vortexed to mix. The mixture was incubated on ice for 10 min. Following incubation, 300 µl of Acid-Phenol:Chloroform was added to the lysate. The mixture was vortexed for 30 s to mix and centrifuged for 5 min at 10 000 x g at room temperature to separate the aqueous (upper) and organic phases. The aqueous phase was removed carefully without disturbing the organic phase and was transferred into a fresh microcentrifuge tube. Ethanol (100 %; 375 µl) at room temperature was added into the aqueous phase and vortexed to mix. A filter cartridge was placed into the collection tube for each sample. The mixture was added to the filter cartridge and was centrifuged for 30 s at 10,000 x g to pass the mixture through the filter. The flow-through was discarded and the filter cartridge was placed on same collection tube for washing step. Wash solution 1 (500 µl) was added to the filter cartridge and was centrifuged for 30 s at 10 000 x g to pass the solution through the filter. The flow-through was discarded from the collection tube and the filter cartridge was replaced into the same collection tube. Wash Solution 2/3 (500 µl) was added into the filter cartridge and the solution was drawn through the filter cartridge as in the previous step. The washing step was repeated using 500 µl of Wash Solution 2/3 and the solution was drawn through the filter as in the previous step. The filter cartridge was placed in the same collection tube and was centrifuged for 1 min at 10,000 x g to remove residual fluid from the filter. The filter cartridge was transferred into a fresh collection tube and 20 µl of pre-heated (95 ^{0}C) nuclease free water was added to the center of the filter cartridge and centrifuged for 30 s at 10,000 x g to recover the RNA. The eluate (containing the RNA) was collected and stored at -80 ^{0}C.

2.5.3 Measurement of RNA concentration and purity

RNA purity and concentration were measured using a spectrophotometer (Nanodrop) according to the manufacturer's instructions. For the blank, 2 µl of RNase-free water was pipetted onto the pedestal. The pedestal was then wiped and 2 µl of the samples were then pipetted onto the pedestal. The RNA concentration was recorded in ng/µl. The A_{260}:A_{280} reading was recorded and A_{260}:A_{280} ratio values of 1.8 to 2.0 were deemed to be of sufficient purity for RNA. An OD 260/280 ratio between 1.8 to 2.0 is considered as a good RNA quality (Sambrook *et al*., 2001).

2.5.4 Synthesis of the first-strand cDNA

The High-Capacity cDNA reverse transcription kit was used for cDNA synthesis according to the manufacturer's instructions. Briefly, all reagents were pulsed in a microcentrifuge for 10-15 sec. The RT master mix (20 µl reaction) was prepared in which the mixture contained 1 µl of Multiscribe Reverse Transcriptase, 2 µl of 10X RT buffer, 2 µl of 10X RT Random primers, 0.8 µl of 25X dNTP mix (100 mM) and 4.2 µl of nuclease-free water. Then, 10 µl of RT mixture was added to each RNA sample (100 ng diluted to 10 µl in nuclease-free water) in a PCR tube. The mixture was briefly centrifuged and placed in a thermal cycler. As for a control, a no RT control was performed containing of RNA sample with all other reagents except RT enzyme. The reaction mixture was started by incubating at 25 ^{0}C for 10 min and was terminated by heating at 85 ^{0}C for 5 min. The cDNA products were stored at -20 ^{0}C.

2.5.5 Quantitative real-time RT-PCR (qPCR)

Primers for quantitative real-time reverse transcription polymerase reaction qRT-PCR were designed using Primer Blast (NCBI; https://blast.ncbi.nlm.nih.gov/Blast.cgi). Briefly, primers were dissolved in TE buffer at 100 µM and then diluted to 5 µM in

sterile distilled water. The final concentration of all the primers used was 0.25 µM. Real-time PCR was performed with a 10 µl reaction mixture containing 5 µl Power SYBR Green PCR master mix, 0.5 µl forward and reverse primers, 3.5 µl nuclease-free water and 0.5 µl cDNA sample. The primer pair for human small nuclear RNA U6 was used as an endogenous control. Previous data accrued in the lab had demonstrated the suitability of this as a reference gene for TGF-β1-induced differentiation of NOF. For each primer pair, a no-template control (NTC) was included to control for possible contamination of reagents. The mixture was assembled in 96 well optical reaction plates and the plates were sealed with optical adhesive film. Each gene and cDNA was analyzed in triplicate. The reaction plates were placed on 7900 HT fast real-time PCR. The reaction involved an initial heating for 2 min at 50^0C to eliminate carryover contamination, followed by a denaturing step at 95 ^{0}C for 15 s and annealing/elongation at 60 ^{0}C for 1 min. Reactions were run for 40 cycles. The amplification plot and CT values produced were analyzed by linear regression analysis using SDS Manager programme.

2.5.6 qRT-PCR analysis

Relative quantitation of targets in different samples was calculated by the ΔΔCt method (Livak and Schmittgen, 2001). The amplification of the reference gene must be the same as the efficiency of the target (Melling, 2015). Relative expression levels between the treated samples and untreated samples can be calculated by arithmetic formulas. The treated sample and untreated sample are compared to a reference gene to normalize for variation in sample quality and quantity. These normalized values are known as ΔCt values are then used to calculate ΔΔCt values as follows:

ΔCt values for the treated samples and untreated samples:

$\Delta Ct_{\text{treated}} = Ct\ \text{target}_{\text{treated}} - Ct\ \text{reference}_{\text{treated}}$

$\Delta Ct_{untreated} = Ct\ target_{untreated} - Ct\ reference_{untreated}$

$\Delta\Delta Ct$ value for each of the treated samples:

$\Delta\Delta Ct_{treated\ sample} = \Delta Ct_{treated\ sample} - \Delta Ct_{untreated\ sample}$

$RQ = 2^{-\Delta\Delta Ct}$

Fold difference = Log 2 (RQ) = $-\Delta\Delta Ct$

2.6 Stress fibre formation assay

2. 6.1 Treatment of the cells

Cells (2.5 x 10^5 /well) were seeded onto glass coverslips and incubated overnight in 5 % CO_2 at 37 ^{0}C for cell attachment. Cells were serum starved overnight and were treated on the following day with 5 ng/ml of TGF-β for 48 h.

2.6.2 Immunocytochemistry

Cells grown on coverslips (as described in 2.6.1) were washed twice with DPBS for 5 min and fixed using 100 % methanol for 20 min at room temperature. Following incubation, the fixative was removed and the cells were washed using DPBS for 5 min. Then, the cells were washed with 0.5 ml 4 mM of sodium deoxycholate. The cells were permeabilized using the same solution for 10 minutes. Non-specific antigens were then blocked in a solution of 2.5 % of BSA in DPBS for 30 min. After that, cells were incubated with 25 µl of FITC-conjugated anti α-SMA antibody (dilution 1:100) overnight at 4 ^{0}C and protected from light. The primary antibody was aspirated and coverslips washed twice with DPBS for 10 min before being mounted on slides using mounting medium containing DAPI (Vector Laboratories) and the edges were sealed with nail polish. The slides were viewed under a fluorescence microscope at 40x or 100x magnification and the images were photographed using Pro-plus 7 imaging software. Cells were observed under a fluorescence microscope using a bandpass FITC filter

(excitation 490 nm, emission > 520 nm) to view the green fluorescence of α-SMA positive cells. Nuclei were visualised using a DAPI filter with excitation at 365 nm and emission at 480 nm. Three independent experiments were carried out.

2.7 Contraction assay

Cells (2.5 x 10^5 cells/well) were seeded in 150 µl of DMEM containing 10 % FBS. Meanwhile, 75 µl of collagen (3 mg/ml) was mixed with 10X solution of DMEM. The mixture was mixed with cells immediately. Then, 0.1 mM NaOH was added into the mixture until the colour changes to a slight pink. After that, 300 µl of the collagen mixture containing cells was seeded in each well of 24-well plates. The mixture was incubated for 45 min at 37 ^{0}C. Following incubation, 500 µl DMEM containing 10 % FBS was added to each well. The plates were incubated for another 4 h at 37 ^{0}C before the media were removed without disturbing the collagen lattice. Finally, 500 µl of serum free media was added to each well and incubated overnight at 37 ^{0}C. The next day, the media were removed from each well and the collagen lattice was carefully detached using a scalpel. Then, the lattice was treated with 500 µl of serum free media containing 5 ng/ml of TGF-β1 for 48 h. The lattices were photographed with a digital camera and the surface area for each lattice was calculated using the Image J. For each lattice, collagen contraction was determined in triplicate and the experiments were repeated at least three times.

2.8 Western blot

2.8.1 Treatment of cells

Cells (5 x 10^5/flask) were seeded in culture flasks and incubated in 5 % CO_2 incubator for cell attachment. The cells were serum starved overnight and were treated on the following day with 5 ng/ml of TGF-β1 for 48 h.

2.8.2 Protein extraction

Cells were washed twice with cold DPBS and lysed using RIPA buffer containing 1X complete EDTA-free protease inhibitor. Cells lysates were vortexed briefly, incubated on ice for 30 min and then centrifuged for 15 min at 14 000 rpm at 4^0C. The supernatants were collected and kept at -80 ^{0}C until required.

2.8.3 Protein quantification

Protein quantification was carried out using the Pierce BCA kit. Briefly, 10 µl of each sample or protein standard (2, 1.5, 1, 0.75, 0.5, 0.25, 0.125, 0.025, 0 mg/ml of BSA) were mixed with 200 µl BCA working reagent (consisting of 50 parts reagent A and 1 part of reagent B). The samples were mixed well and incubated at 37 ^{0}C for 30 min. Each sample and standard were run in triplicate. Following incubation, the optical density of the samples and standards were measured by spectrophotometer at a wavelength of 562 nm. The protein concentration of samples was determined from a standard curve on the basis of absorption at 562 nm of the BSA standards.

2.8.4 SDS polyacrylamide gel electrophoresis

Proteins were separated with a 12 % resolving gel consisting of 3 ml of 40% (w/v) acrylamide, 4.3 ml distilled water, 4 ml of 1.5 M Tris-HCl pH 8.8, 0.16 ml of 10% (w/v) SDS, 0.005 ml of TEMED and 0.35 ml of 10% ammonium persulphate. The catalyst ammonium persulphate and TEMED were added last to initiate polymerization. The mixture was immediately poured into the gel cassettes to approximately three-quarters of the total height of the cassettes. Immediately after pouring the gel mixture, a small colume of isopropanol was added into the cassettes to cover the gels. The gels were allowed to solidify for 10 min. The 4 % stacking gels contained 1 ml of 40% (w/v) acrylamide, 2.5 ml of 0.5 M Tris-HCl pH 6.8, 0.1 ml of 10% (w/v) SDS, 6.3 ml of distilled water, 0.01 ml of TEMED and 0.1 ml of 10% ammonium persulphate. Before

pouring the mixture, the isopropanol was removed by filter paper from the gel. The mixture was immediately poured into the top of the cassettes and a sample comb inserted, before allowing the gels to polymerize.

2.8.5 Loading the samples onto the gel

Briefly, 30 µl of the mixture contained 20 µg of samples, 7.5 µl of 4X LDS sample, 3 µL of 1X reducing agent and 13.8 µl of distilled water was prepared and heated for 5 min at 95 ^{0}C. Then, 20 µl of protein samples were loaded into the wells. Five microlitres of pre-stained protein markers were electrophoresed alongside the samples. 1X Running buffer consisted of 25 mM Tris, 192 mM glycine and 0.1% SDS. The gels were electrophoresed with 1X Running buffer at 120 V for 1 h.

2.8.6 Blot transfer

The iBlot™ filter paper was soaked in distilled water. Meanwhile, iBlot ™ anode stack was placed on the blotting surface of iBlot™ apparatus. Then, the pre-run gel was placed on nitrocellulose membrane of the anode stack. The gel was rolled by blotting roller to remove any trapped bubbles. The pre-soaked filter paper was placed on the gel and rolled with a roller to remove any bubbles. After that, the iBlot cathode™ stack was placed on top of it. Again, the bubbles were removed by blotting roller. Lastly, the disposable sponge was placed on the cathode stack and the blotting was performed for 7 min at 23 V.

2.8.7 Ponceau S staining

The membranes were soaked with Ponceau S solution and washed at least two times with distilled water, to visualise protein transfer to the nitrocellulose membrane.

2.8.8 Blocking the membrane

The membranes were blocked by using 5 % non-fat milk and 3 % BSA. The blocking buffer was prepared by dissolving 2.5 g of non-fat milk and 1.5 g BSA in 50 ml 0.1 %

TBS-Tween-20 (TBST). The membranes were blocked with this solution overnight on an orbital shaker at 4 °C.

2.8.9 Incubation with the primary antibody

The blocking buffer was discarded and the membranes were washed with TBST for 5 min. The membranes were incubated overnight with α-SMA or β-actin antibody diluted in blocking buffer on an orbital shaker at 4^0C. The recommended dilution for α-SMA antibody was 1:1000 while for β-actin antibody was 1: 10 000.

2.8.10 Incubation with the secondary antibody

Following overnight incubation, the primary antibodies were discarded and membranes were washed three times for 10 min in TBST. Then, the membranes were incubated with anti-mouse antibody conjugated to horseradish peroxidase (HRP) (1:3000) for 1 h at room temperature on an orbital shaker.

2.8.11 Stripping and reprobing of membranes

Membranes were incubated with 50 ml of stripping buffer made up from 62.5 mM Tris pH 6.7, 2 % of SDS and 100 mM of 2-βmercaptoethanol at 50 ^{0}C for 30 min. Membranes were washed four times with TBS-Tween at 15 min intervals and reprobed as in Section 2.8.9 and Section 2.8.10.

2.8.12 Film development

The membranes were incubated in Pierce ECL substrate working solution containing equal parts of Detection reagent 1 and 2. The membranes were incubated with the working solution for 1 min at room temperature. The blots were placed in the clear plastic wrap and excess working solution was removed using an absorbent tissue. Then, the protected membranes were placed on X-ray cassette and exposed to X-ray film in a dark-room. The film was developed using film developer.

2.8.13 Densitometry

Quantification of protein bands from western blot was carried out using Image J analysis software. The original blot picture was converted to an 8-bit image. The boxes were drawn using the same size around each band. The area of each analyzed lane corresponds to the pixel density of the band. The final step is to calculate the relative protein quantification by adjusting the size of the bands relative to loading control bands.

2.9 MicroRNAs expression profiling

RNA was extracted as described in Section 2.5.2. The RNA purity and concentration was measured as described in Section 2.5.3.

2.9.1 Taqman Tiling Low-Density Array (TLDA)

MicroRNA expression profiling was performed by using Megaplex™ pool kit. The RT reaction master mix was prepared according to Table 2.8. The mixture was mixed well in sterile PCR tubes and was incubated on ice for 5 min. The tubes were placed on thermal cycler and the reverse transcription was performed as follows: 16^0C for 2 min, 42^0C for 1 min and 50^0C for 1 s for 40 cycles and then incubation at 85^0C for 5 min. The Megaplex products were kept at -80^0C. TLDA consists of two arrays, each array containing 384 wells of pre-designed Taqman probes and exon-spanning primers including two endogenous controls and a negative control.

2.9.2 Pre-amplification of cDNAs

The pre-amplification reaction mix contained 12.5 µl of 2X TaqMan preamp master mix, 2.5 µl of Megaplex pre-amp primers pool A or pool B, and 7.5 µl of nuclease-free water. The mixture was mixed well in sterile PCR tubes and incubated on ice for 5 min. The tubes were placed on thermal cycler and the pre-amplification was performed by heating

RT reaction mix components	Volume for one sample (µl)
Megaplex RT primers (pool A or pool B)	0.80
dNTPs with dTPP (100 mM)	0.20
MultiScribe Reverse Transcriptase (50 U/µl)	1.50
10X RT buffer	0.80
MgCl2 (25 mM)	0.90
RNase inhibitor (20 U/µl)	0.10
Nuclease-free water	0.20
Total RNA (3 ng)	3.0
Total	7.5

Table 2.8: List of RT reaction mix components

the samples at 95^{0}C for 10 min, followed by 12 cycles of 95^{0}C for 15 s and 60^{0}C for 4 min and finally heated at 95^{0}C for 10 min. Following pre-amplification, 75 µl of 0.1 X TE pH 8.0 was added to each tube. The tubes were briefly centrifuged to mix them. The pre-amplification products were kept at -80^{0}C.

2.9.3 TaqMan microRNA array

The PCR reaction mix contained 450 µl TaqMan Universal PCR Master Mix, no UNG, 9 µl diluted pre-amplification product and 441 µl of nuclease-free water. The mixture was briefly centrifuged to mix them well. Finally, 100 µl of the mixture was added into each port of TaqMan MicroRNA array plate. The plates were briefly centrifuged and sealed well. The reaction involved an initial heating for 2 min at 50^{0}C to eliminate carryover contamination, followed by a denaturing step at 95^{0}C for 15 s and annealing/elongation at 60^{0}C for 1 min. Reactions were run for 40 cycles.

2.10 Validation of miRNA expression by qRT-PCR

2.10.1 microRNA reverse transcription reaction

RNA was extracted as described in Section 2.5.2. The RNA purity and concentration was measured as described in Section 2.5.3. The expression of specific miRNAs of interest was validated using TaqMan MicroRNA assay. The RT master mix was prepared according to Table 2.9 and dispensed into each PCR tube. The mirRT reaction was performed under optimised cycling condition, starting by incubating at 25 ^{0}C for 10 min and was terminated by heating at 85 ^{0}C for 5 min.

2.10.2 Targeted microRNA quantitation

The reaction mix contained 5 µl of 2X Taqman® Universal PCR master mix, no UNG, 0.5µl of probe and 3.7µl of nuclease-free water. Following that, 0.8 µl of diluted preamp product or miRT product was added to the well. The plate was briefly centrifuged at

RT reaction mix components	Volume per reaction (µl)
dNTPs with dTPP (100 mM)	0.15
MultiScribe Reverse Transcriptase (50 U/µl)	1.00
10X RT buffer	1.50
5X probe	3.00
RNase inhibitor (20 U/µl)	0.19
Nuclease-free water	4.16
Total RNA (10 ng)	5.00
Total	15.0

Table 2.9: Reaction mix for targeted miRNA Transcription

1000 rpm for 2 min. The reaction mix was run on a thermal cycler with an initial heating for 2 min at 50^0C to eliminate carryover contamination, followed by a denaturing step at 95^0C for 15 s and annealing/elongation at 60^0C for 1 min. Reactions are run for 40 cycles. RNU48 was used as a miRNA endogenous control as it is a small nuclear RNA shown previously in the lab to be uniformly and robustly expressed in fibroblasts and myofibroblasts.

2.11 Transfection of anti-miR microRNA inhibitors and pre-miRNAs

Untransfected or transfected cells (2.5 x 10^5/well) were seeded onto a 6-well plate which gives around 60-70 % confluency and incubated overnight in 5 % CO_2 incubator for cell attachment. The concentration for all oligonucleotides used in this study was 50 nM (Kabir *et al*., 2016). Anti-miR-145-5p, anti-miR-424-3p and pre-miR424-3p were transiently transfected into the cells using Oligofectamine reagent while anti-miR negative control A and negative pre-miR #2 were used as controls. 5 ul of Oligofectamine was added into Opti-MEM medium to a final volume of 50 ul. 50 nM of synthetic precursor miRNA or miRNA inhibitor were mixed with Opti-MEM to a final volume of 50 ul. The transfection mixture and anti-miR or pre-miR mixture was incubated together for 30 min at room temperature. Prior to transfection, cells were washed twice with 500 ul of Opti-MEM medium and washed cells were added 800 µl of Opti-MEM medium. After incubation, the transfection mixture-miRNAs was mixed with 100 ul of Opti-MEM medium. Then, the transfection mixture-miRNAs (200 µl) was added to the washed cells and incubated for 4 hrs in 5 % CO_2 incubator at 37 ^{0}C. Following incubation, transfection mixture-miRNAs was removed and was replaced with fresh DMEM culture and further incubated for 48 h. The cells were subjected to serum starvation overnight and TGF-β1 treatment for another 48 h.

2.12 Statistical analyses

The experiments carried out in the present study were repeated three times to calculate the mean of each sample tested. The Shapiro-Wilk ($n < 50$) normality test by Graph Pad Prism 7 was done to determine data distribution. However, this test is less powerful to detect normal distribution in a small sample size. The significant differences in the mean of treated and untreated cells were calculated using unpaired, equal variance of Student T-test, performed using Graph Pad Prism 7. The error bars on graphs represent the standard error of mean (SEM) unless otherwise stated.

2.13 Ethical approval

The isolation and use of human primary buccal fibroblast (NOF804) and CAF003 isolated from OSCC have been ethically reviewed and approved by Sheffield Research Ethics Committee with reference number 09/H1308/66 and 13/NS/0120.STH17021, respectively. CAF isolated from genetically stable OSCC (BICR70, BICR73, BICR59) and CAF isolated from genetically unstable OSCC (BICR31, BICR18, BICR3) had been reviewed and ethically approved (Lim *et al*., 2011).

CHAPTER 3: Characterisation of the CAF-like myofibroblastic phenotype in oral fibroblasts

3.1 Aim and objectives

Over the years, increasing evidence has shown interactions between cancer cells with stroma and how this interaction can influence cancer cell biological behaviour (Goubran *et al*., 2014). CAF, one of the predominant cells of tumour stroma, have been shown to impact many aspects of tumour progression (e.g cancer cell invasion, ECM remodelling, angiogenesis and inflammatory cell infiltrate) in various malignancies (Pietras and Ostman, 2010). In OSCC, the presence of CAF is positively correlated with invasive phenotype (Fujii *et al*., 2012), presence of cancer recurrence (Kellermann *et al*., 2007), and poor prognoses of the patients (Dhanda *et al*., 2014). The origins of CAF *in vivo* are unclear, but increasing of evidence suggests at least a proportion of them arise from differentiation of resident fibroblasts. The molecular mechanisms underlying this differentiation remain largely unknown, however several recent studies in other cancers have implicated the involvement of miRNAs (Mitra *et al*., 2012; Shen *et al*., 2016). Therefore, understanding the molecular mechanism of CAF-myofibroblastic differentiation holds promise as a source of novel approaches to inhibit the pro-tumourigenic properties of CAF.

The work outlined in this chapter aimed to characterise the response of NOF to TGF-β1 stimulation. TGF-β1, a profibrotic cytokine with pleiotropic functions within the tumour microenvironment (Bowen *et al*., 2012), has been used to convert the oral fibroblast into myofibroblast in previous studies (Smith *et al*., 2006; Marsh *et al*., 2011; Sobra *et al*., 2011). Here, the aim was to verify and further characterise the response of NOF to TGF-β1 with the specific aim of developing a model of CAF (cancer-associated fibroblast)-like myofibroblastic differentiation (henceforth termed eCAF) to utilise later in the project to study the contribution of miRNA to the development of CAF. To achieve the aim, a number of specific objectives were addressed as stated below:

1. To determine the appropriate TGF-β1 concentration and treatment time for activation of NOF into eCAF.

2. To determine the gene expression of myofibroblastic CAF markers, α-SMA and FN-EDA1, in untreated and TGF-β1-treated NOF by qPCR.

3. To determine the protein abundance of α-SMA in untreated and TGF-β1-treated NOF cells by western blot.

4. To study cytoplasmic stress fibre formation in untreated and TGF-β1-treated NOF by fluorescence microscopy.

5. To study the contractility of untreated and TGF-β1-treated NOF by collagen contraction assay.

3.2 Results

3.2.1 TGF-β1 induces α-SMA expression in eCAF

Dose response and time course experiments were carried out to optimise the appropriate TGF-β1 concentration and time point required for primary fibroblast activation to a myofibroblastic, CAF-like phenotype (henceforth referred to as experimentally-derived CAF; eCAF). Since CAF are commonly characterised by the expression of α-SMA as well as FN-EDA1, these markers were used experimentally to examine activation of normal resting oral fibroblasts to eCAF. Optimisation of TGF-β1 treatment was carried out by using a dose and time-response experiment. Three primary oral fibroblast cultures; NOF1, NOF5 and NOF804 (derived from different subjects to assess heterogeneity of response), were treated with TGF-β1 at concentrations ranging from 0.05-5 ng/ml for 24 h and 48 h (these concentrations were selected from searching the literature, e.g. Walker *et al*., 2004, and from data previously accrued in the lab

(Melling, Abidin *et al*, in revision)).

As shown in Figure 3.1, TGF-β1 induced expression of α-SMA in a dose- and time-dependent manner in all cultures with maximum α-SMA expression occurring at 48 h post-treatment at a concentration of 5 ng/ml. The increase in α-SMA expression was 5 ±1.9-fold (at 0.05 ng/ml of TGF-β1) and 5.1±1.4-fold (at 0.5 ng/ml of TGF-β1) in NOF1 cells and reached 20±4-fold at 5 ng/ml of TGF-β1 at 24 h, compared to untreated controls. TGF-β1 increased expression of α-SMA at 48 h by 4±1.2-fold and 12±3.9-fold at 0.05 ng/ml and 0.5 ng/ml of TGF-β1, respectively. Treatment with the highest concentration of TGF-β1 increased α-SMA expression by 29±4.1-fold at 48 h (Figure 3.1). Similar to NOF1 cells, TGF-β1 at 24 h induced α-SMA expression by 5±0.9-fold and 12±2.3 -fold at 0.05 and 0.5 ng/ml in NOF5 cells, respectively. However, the induction of α-SMA at 5 ng/ml of TGF-β1 at 24 h was not as great as NOF1 (13±2.4 -fold), but a significant induction (55±3-fold; $p < 0.005$) in expression of α-SMA compared to untreated cells was observed at 48 h (Figure 3.1). Likewise, TGF-β1 induced α-SMA expression in NOF804 cells, a primary fibroblast culture isolated independently (in Sheffield, rather than NOF1 and NOF5 which were isolated at Queen Mary, University of London). At 24 h TGF-β1 significantly induced 5±0.4 -fold and 7±0.7-fold increases in α-SMA expression at 0.05 and 0.5 ng/ml, respectively. The expression level of α-SMA slightly increased at 5 ng/ml compared to 0.5 ng/ml at 24 h (9±0.5-fold). Treatment with TGF-β1 produced a proportional increase in α-SMA expression at 48 h with the 5 ng/ml dose significantly increasing expression by 16±1.0 -fold ($p<0.0001$) compared to untreated controls. Nevertheless, the increase in expression of α-SMA at 5 ng/ml is not as remarkable in NOF804 as for NOF5 and NOF1 at 48 h. In spite of the observed heterogeneity between the responses of cultures from different subjects, overall the results indicate that 5 ng/ml is the optimal concentration of TGF-β1

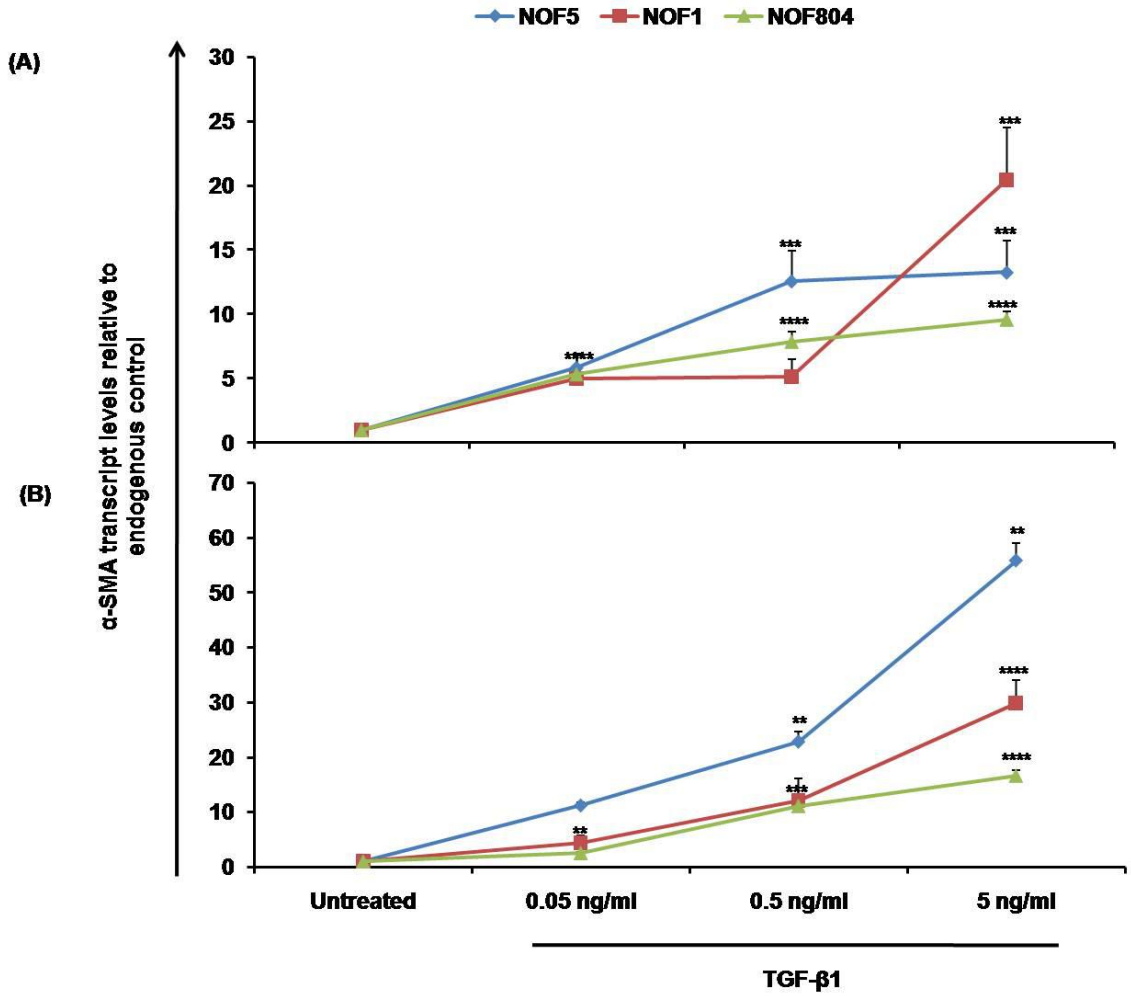

Figure 3.1: α-SMA expression reaches a peak at 48 h after 5 ng/ml of TGF-β1 treatment

Cells were seeded, serum starved and treated with TGF-β1 (0.05-5 ng/ml) or serum-free medium (untreated), for **(A)** 24 h and **(B)** 48 h. After that, cells were subjected to RNA extraction and cDNA preparation. The expression of α-SMA was determined using qPCR and U6 was used as a reference gene. Each data represents the mean ± SEM from three independent experiments. Statistical significance was determined using two-tailed Student T-test with *p < 0.05, **p < 0.005, ***p < 0.001, ****p < 0.0001 compared to untreated.

and 48 h as an optimal time point to induce a CAF-like cell phenotype. This TGF-β1 concentration and time point was also used in the previous studies to induce fibroblast conversion into myofibroblast *in vitro* (Yao *et al*., 2011; Chen *et al*., 2011; Ina *et al*., 2012). Thus, this concentration and time point was used for subsequent experiments. From the body of literature, it is likely that the TGF-β1 concentration used in this study are within the physiological range fibroblasts may be exposed to *in vivo*; 2 ng/ml (Yang *et al*., 2013) and 8 ng/ml (Li *et al*., 2013).

3.2.2 FN-EDA1 expression is increased in eCAF

In order to further characterise the response of NOF to TGF-β1, expression of another myofibroblast marker, extra domain A-containing fibronectin (FN-EDA1), a matrix protein, was also determined in this study. This marker has also been detected in CAF (Serini *et al*., 1998). Each primary oral fibroblast culture was treated with different concentrations of TGF-β1 (0.05-5 ng/ml) for 24 h and 48 h, as described in the previous section. Similar to α-SMA, TGF-β1 induced FN-EDA1 expression in all cultures, with the highest expression observed at 48 h at 5 ng/ml. As shown in Figure 3.2, expression of FN-EDA1 increased in all cultures at 24 h and 48 h. TGF-β1 significantly induced FN-EDA1 expression in NOF1 cells with 2±1.8-fold (0.05 ng/ml), 3±2.6-fold (0.5 ng/ml) and 6±2.6-fold (5 ng/ml) changes at 24 h. At 48 h, TGF-β1 significantly induced FN-EDA1 expression (12±5.0-fold) at a concentration of 5 ng/ml. In NOF5, TGF-β1 significantly induced expression of FN-EDA1 with 2±0.1 -fold (0.05 ng/ml), 3±1.6-fold (0.5 ng/ml) and 4±1.1-fold (5 ng/ml) increases at 24 h, and further significantly increased FN-EDA1 expression at the highest concentration (5 ng/ml) with 12±2.1-fold ($p < 0.0001$) at 48 h (Figure 3.2). The induction of FN-EDA1 expression by TGF-β1 at 5 ng/ml was lower in NOF804 cells at 48 h compared to both NOF1 and NOF5 (Figure 3.2). The FN-EDA1 expression level fluctuated upon treatment with TGF-β1 at 24 h;

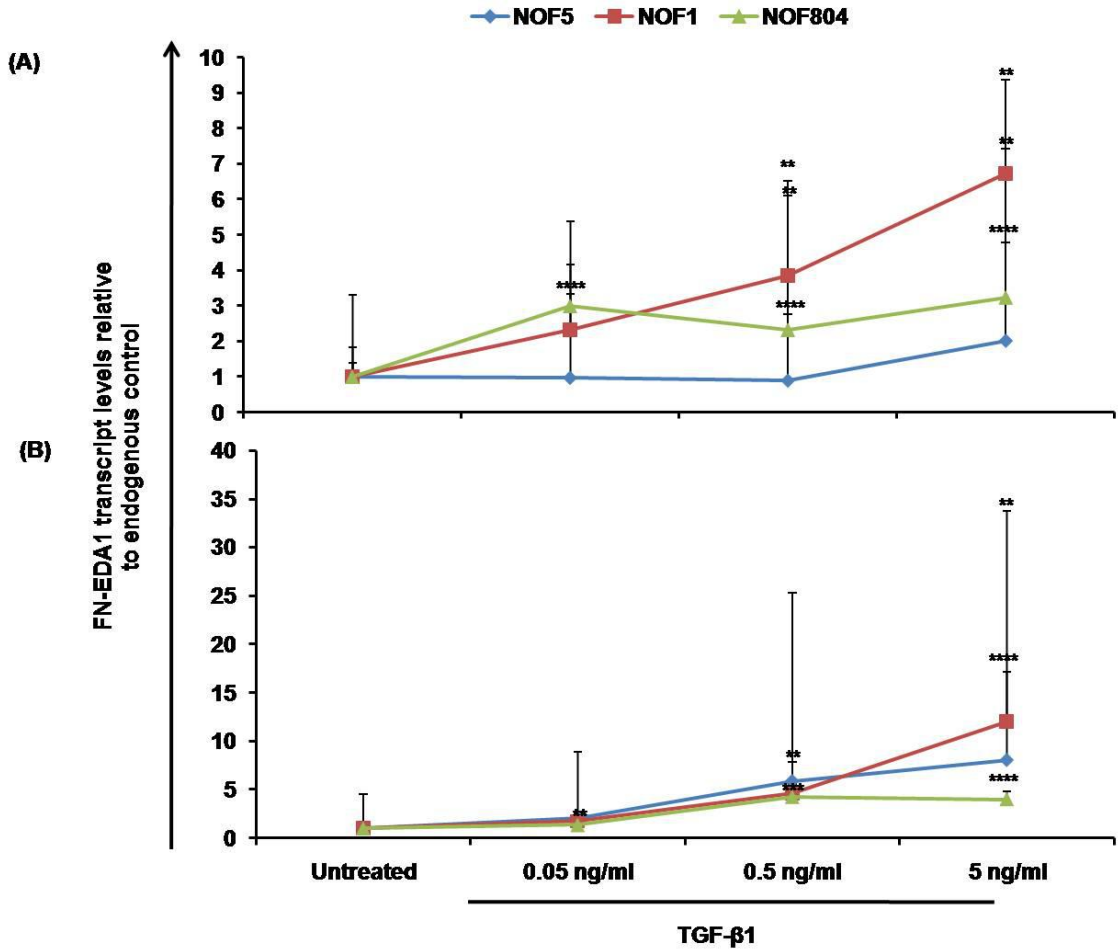

Figure 3.2: FN-EDA1 expression reaches a peak at 48 h of TGF-β1 treatment

Cells were seeded, serum starved and treated with TGF-β1 (0.05-5 ng/ml) or serum-free medium for untreated, for **(A)** 24 h and **(B)** 48 h. After that, cells were subjected to RNA extraction and cDNA preparation. The expression of FN-EDA1 was determined using qPCR and U6 was used as a reference gene. Each data represents the mean ± SEM from three independent experiments. Statistical analysis was determined using two-tailed Student T-test with *p < 0.05, **p < 0.005, ***p < 0.001, ****p < 0.0001 compared to untreated.

3±0.3-fold (0.05 ng/ml), 2±0.4-fold (0.5 ng/ml), 3±1.5-fold (5 ng/ml). At 48 h, TGF-β1 significantly induced FN-EDA1 expression at 0.5 ng/ml and 5 ng/ml (4.5±1.3 -fold and 4±0.8-fold expression of untreated cells, respectively). Unlike NOF1 and NOF5, the induction of FN-EDA1 expression did not display a dose-dependent response in NOF804.

3.2.3 TGF-β1 increases protein abundance of α-SMA in eCAF

Next, α-SMA abundance was also quantified at the protein level. Two primary oral fibroblasts were treated with 5 ng/ml TGF-β1 for 48 h (determined as the optimal concentration of TGF-β1 and optimal time point). Protein extracts were prepared from the cells and analysed by western blot with an anti-α-SMA antibody as described in Section 2.8. The results of western blot analyses of TGF-β1 treatment of NOF5 and NOF804 cells are shown in Figure 3.3. The α-SMA antibody recognized a single protein band of ~42 kDa. The intensity of this protein band was much greater after stimulation of both cells with 5 ng/ml of TGF-β1 compared to untreated cells. An equal amount of β-actin (42 kDa) was detected in the sample analysed which confirmed that equal amounts of protein had been loaded in each lane (Figure 3.3). Image J software was used to quantify the band densities. The densities of the bands corresponding to α-SMA were divided by the densities of the bands representing the internal control, β-actin, to adjust for any differences in the amount of sample loaded in each well. The effect of TGF-β1 stimulation was expressed as the fold difference between the treated and untreated samples. As shown in Figure 3.3, TGF-β1 caused statistically significant 2±0.1-fold ($p < 0.05$) and a 6±0.1-fold ($p < 0.05$) increases in α-SMA protein in NOF804 and NOF5, respectively. Additionally, α-SMA was detected at protein level in unstimulated cells, suggesting a low level of basal activation of α-SMA.

3.2.4 TGF-β1 induces stress fibre formation in eCAF

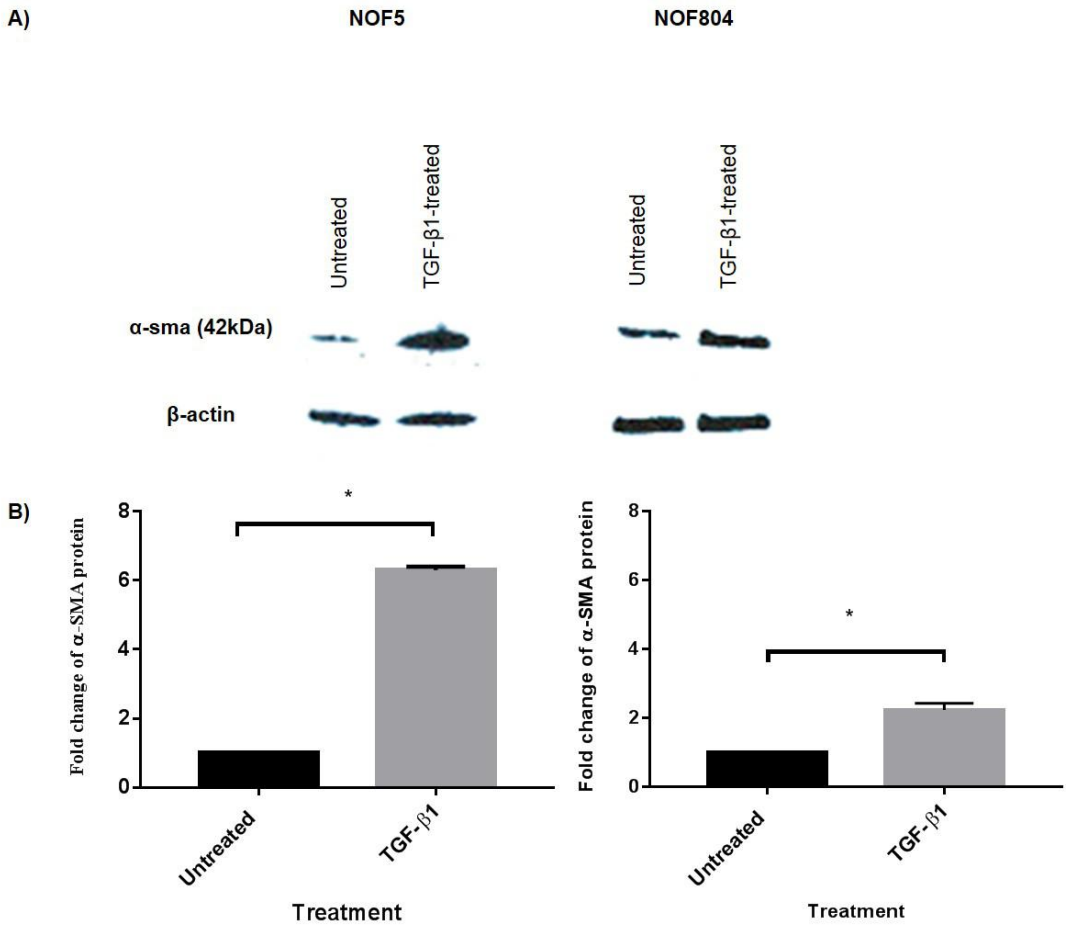

Figure 3.3: TGF-β1 treatment transformed normal fibroblasts into eCAF

Cell lysates were immunoblotted against α-SMA and β-actin **(A)** Western blot bands **(B)** α-SMA band densities were quantified by Image J analysis and normalized to total β-actin. Total protein lysates (20µg) were resolved by 12 % SDS-PAGE and transferred onto nitrocellulose membrane for immunoblotting. Each data represents the mean ± SEM from three independent experiments. Statistical analysis was determined using two-tailed Student T-test with *$p < 0.05$.

It has been demonstrated that in α-SMA-positive fibroblasts, the formation of stress fibres was more prominent compared with α-SMA-negative fibroblasts (Hinz *et al*., 2001). Treatment of 5 ng/ml of TGF-β1 provokes α-SMA-positive stress fibre formation in human primary lung fibroblast compared to unstimulated fibroblasts (Yao *et al.*, 2011). Thus, immunocytochemistry was conducted to next determine whether TGF-β1 was able to induce α-SMA-positive stress fibre formation in primary oral fibroblasts. NOF were seeded onto coverslips, serum starved and were treated with 5 ng/ml of TGF-β1 for 48 h (the dose and time identified as generating the maximal dose of α-SMA expression in Section 3.2). The cells were fixed with methanol, permeabilised and α-SMA was visualised using a FITC conjugated monoclonal anti-SMA antibody. Fluorescence microscopic analysis demonstrated that TGF-β1 increased the number of α-SMA positive cells (green) in all cultures (Figure 3.4 (A). However, not all the different cultures of NOF responded equally to TGF-β1; NOF5 appears unresponsive and NOF1 shows diffuse staining (even some nuclear). Only NOF804 displayed a vivid staining of stress fibres compared to both NOF1 and NOF5 (Figure 3.4 (B). Staining of NOF804 cell with α-SMA-conjugated FITC was better than NOF1 and NOF5 due to more experience with the fluorescence microscope. None of the untreated cells had detectable stress fibres.

3.2.5 TGF-β1 enhances contraction of eCAF

The incorporation of α-SMA in stress fibres is associated with increases in contractility (Arora and McCulloch, 1994; Hinz *et al*., 2001). Myofibroblasts acquire a contractile phenotype to promote wound closure, before re-epithelisation (Skalli and Gabbiani, 1988). Therefore, the contractile ability of fibroblasts is considered one of the hallmarks of the myofibroblast phenotype, and by extension the CAF phenotype. Collagen gel contractility assays are commonly used to study cellular contraction *in vitro*

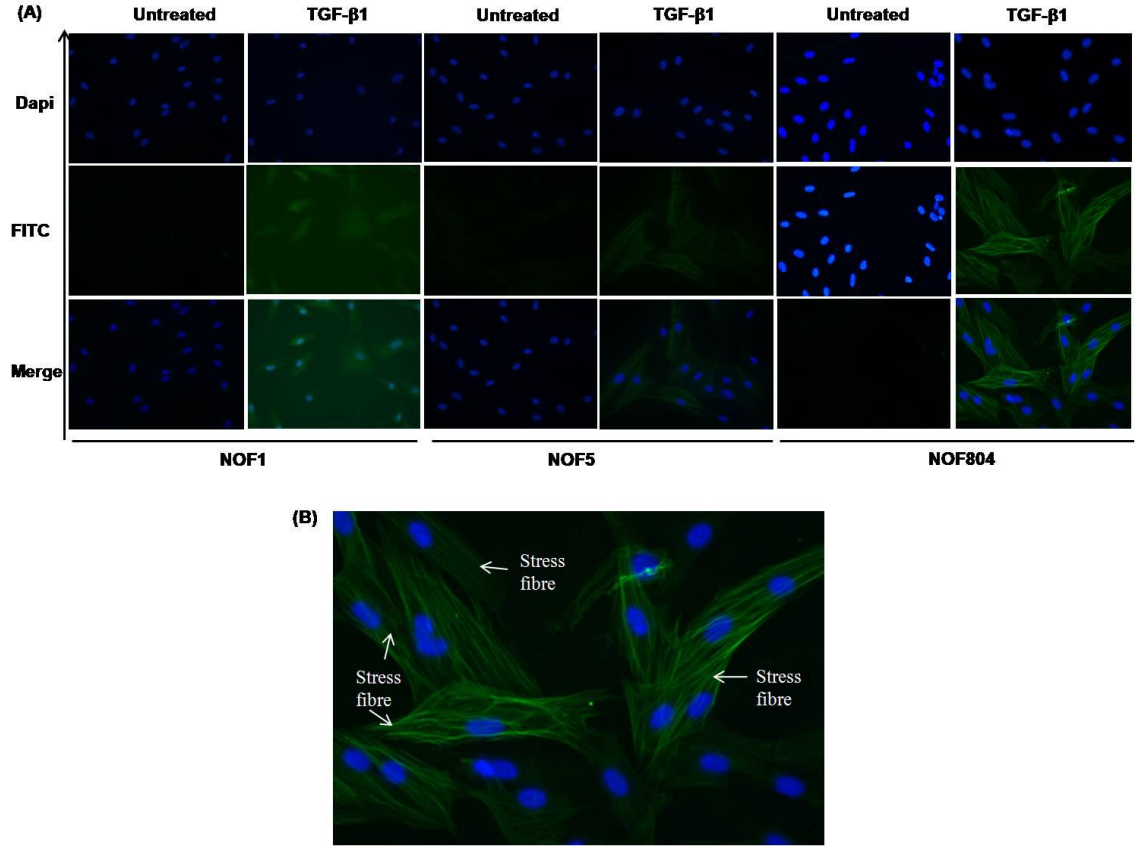

Figure 3.4: Stress fibre formation in NOF in response to TGF-β1

(A) Stress fibres formation in NOF1, NOF5 and NOF804 after treated with 5 ng/ml of TGF-β1 for 48 h, **(B)** NOF804 shows clear stress fibres formation after TGF-β1 treatment and this image was produced by digital zoom of the image at 40x magnification. Cells were seeded onto coverslips and treated with TGF-β1. The coverslips were washed with PBS, fixed in 100 % methanol for 20 min and permeabilised with 4 mM sodium deoxycholate for 10 min. Then, the coverslips were blocked with 2.5 % (v/w) BSA in PBS for 30 min. Cells were observed under a fluorescence microscope after being stained with the α-SMA-FITC antibody (green) and Dapi (blue). The images were taken using fluorescence microscope and were processed using Pro-plus 7 imaging software. The images are representative of three independent experiments except for NOF1 for which n=1.

(Bogatkevich *et al*., 2001). While α-SMA expression is a quantitative measure at cellular level, the gel contractility assay is a functional analysis method measuring the magnitude of contractility. A gel collagen contractility assay was therefore performed to determine whether TGF-β1 treatment of primary oral fibroblasts can promote increased generation of contractile force. To do this, two primary oral fibroblast cultures (unfortunately it was not possible to generate data for this experiment from NOF1 cells as the cells died) were resuspended in collagen mixed with media (1:1) and added to a 24-well plate as described in Section 2.7. The cells were treated with 5 ng/ml of TGF-β1 for 48 h. Cells cultured with 10 % FBS were used as a positive control. Following incubation, the collagen lattices were detached from the edge of wells. The gels were photographed and the area of gel surface was measured with Image J software. A decrease in lattice area correlates with an increase in contractility (Bell *et al*., 1979; Yang *et al*., 2015).

As shown in Figure 3.5, TGF-β1 significantly enhances contraction of NOF5 and NOF804 cells compared to untreated controls. Treatment of NOF5 cells with TGF-β1 significantly decreased lattice surface area (157±8.7 mm^2; $p < 0.001$) compared to untreated cells (267±5.5 mm^2). While TGF-β1 stimulates remarkable gel contraction in NOF804 with decreased lattice surface area (208±4.1 mm^2) compared to untreated cells (382±5.5 mm^2).

3.3 Discussion

Myofibroblasts are characterised by expression of activation markers, α-SMA (Honda *et al*., 2010), collagen 1A1 (COL1A1) and other matrix proteins (Pan *et al*., 2013), as well as the presence of cytoplasmic stress fibres and enhanced contractility. However, some fibroblasts exhibit some features of myofibroblast phenotype without expressing α-SMA or cytoplasmic stress fibres. These cells, which are thought to be *en route* to complete myofibroblast differentiation, termed proto-myofibroblast (Tomasek *et*

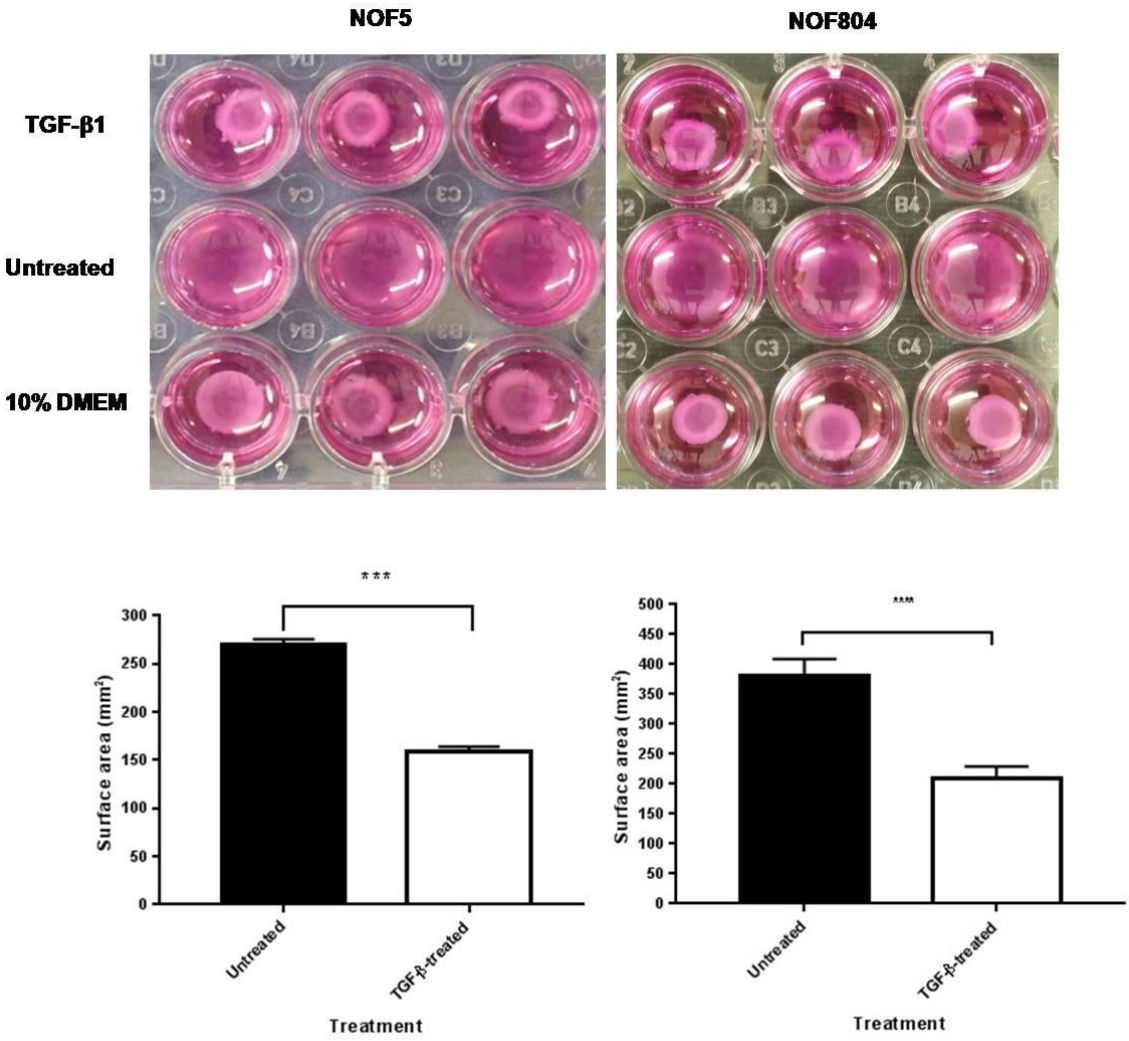

Figure 3.5: The effects of TGF-β1 on collagen gel contractility of NOF5 and NOF804 cells

(A) Images of detached lattices at 48 h, **(B)** the collagen gel contractility were assessed by measuring the gel surface area (n = 3 replicates/group). Cells were counted and mixed with 1:1 collagen mixture of collagen with 10x DMEM. pH was neutralised using NaOH and gel was set to polymerise for 45 min. Growth medium was added to the cells and after 4 h was replaced with serum free medium. The gels were detached from the side of the wells and were subjected to TGF-β1-treatment. Cells were cultured in growth medium as a positive control. The images are representative of three independent experiments. Statistical analysis was determined using Two-tailed Student T- test with ***$p < 0.001$ and ****$p < 0.0001$ compared to untreated.

al., 2002). Myofibroblasts are activated fibroblasts found in wound healing or fibrosis, while CAF are activated fibroblasts found in tumour. Activated fibroblasts are commonly express α-SMA, therefore α-SMA marker is likely the one really consistent feature of CAF. The myofibroblast differentiation model was used to confirm that the phenotype assessed in this study were CAF-like myofibroblastic cell.

TGF-β1 is reported to induce conversion of resting fibroblasts into myofibroblasts *in vitro* (Kalluri and Zeisberg, 2006). However, the mechanisms underlying this conversion, and particularly the relevance of this to CAF development, are poorly understood. *In vitro* studies have demonstrated that TGF-β1 causes conversion of normal primary breast fibroblasts into CAF (Ronnov-Jessen and Petersen, 1993). Thus, TGF-β1 treatment of primary oral fibroblasts from healthy subjects was used in this study to establish an experimental model of CAF (eCAF) and to later in the study use this model to examine the contribution of miRNA to CAF development.

In this study, the optimal TGF-β1 dose for inducing eCAF was determined to be 5 ng/ml at 48 h. TGF-β1 induced upregulation of α-SMA at both the mRNA and protein level. The magnitude of induction of α-SMA expression by TGF-β1 differed between different cultures. This might be due to the TGF-β1 freshness (although great care was taken over storage conditions) as well as the passage number of fibroblast used in the experiments (efforts were made to use a small number of passages). Cell-to-cell variation might also contribute to the differences of α-SMA expression in NOF upon TGF-β1 treatment. Single cells in a tissue contain a diverse population of cells characterised by different morphologies, functions and gene expression profiles (Yuan *et al*., 2017). Myofibroblasts derived from various origins showed different level of α-SMA expression, as do myofibroblasts arising from same origin or same microenvironment conditions (Xu *et al*., 1997; Dugina *et al*., 1998; Hinz *et al*., 2001). The induction of α-SMA protein

level by TGF-β1 was not greater as mRNA level in NOF cultures. This might due to post-transcriptional and post-translational modifications of TGF-β1 in regulating α-SMA expression in fibroblasts. A similar trend of α-SMA protein abundance in response to TGF-β1 were observed in other previous phD project (Melling, 2015). Additionally, a reduction of α-SMA protein level was observed after 48 h when fibroblasts transfected with α-SMA siRNA, indicating a short α-SMA half-life in fibroblasts (Melling, 2015). α-SMA mainly expressed in normal adult smooth muscle and temporary expressed during development of skeletal muscle and cardiac (Ruzicka & Schwartz, 1988; Woodcock-Mitchell *et al.,* 1988). Even though it is a differential marker for smooth muscle cells, its expression also detected in myofibroblasts (Darby *et al.,* 1990; Roy *et al*., 2001). Collectively, these findings showed that α-SMA expression is the hallmark of myofibroblast and CAF differentiation. However, how it regulates fibroblast differentiation is still unclear.

TGF-β1 treatment is reported to cause fibroblasts to alter their ultrastructure with an increase in cytoskeletal stress fibre formation (Vaughan *et al*., 2000). TGF-β1 stimulation enhanced α-SMA-rich stress fibres formation in all NOF cultures. As stated in Section 3.2.4, there was technical issue regarding the staining of NOF5 with α-SMA-conjugated FITC, thus reflects little stress fibre formation compared to the remarkable induction of α-SMA at mRNA level. The α-SMA stress fibre formation can be quantified by fluorescence intensity per cell by Image J, however, the analysis could not be performed due to the images taken were at 40x magnification, resulting an overlapping stress fibre formation compared to images at 100x magnification which only focus on single cell.

TGF-β1 also induced upregulation of other myofibroblast differentiation marker, FN-EDA1 at transcript levels. Fibronectin (FN) is a 440 kDa dimeric glycoprotein and a

major component of ECM. It plays a role in differentiation, adhesion, and migration. FN presents in two main forms; plasma and cellular. Plasma FN is mainly secreted by hepatocytes while cellular FN is abundantly secreted by activated fibroblasts (Muro *et al*., 2003). FN is composed of three different types of homologous; type 1, type II, and type III (Hynes, 1990). It has two alternatively spliced domains which are EDA and EDB (Kornblihtt *et al*., 1996). Only cellular FN has EDA and EDB (Vartio *et al*., 1987; Ina *et al*., 2012). Both isoforms are mainly expressed in embryonic tissue and rarely found in normal adult tissue. Nevertheless, FN-EDA are re-expressed in various fibrotic and pathological processes, including wound healing (Ffrench-constant *et al*., 1989; Ina *et al*., 2012). Although FN-EDA1 promotes myofibroblast differentiation, the mechanism behind it is still unclear. It would be interesting to determine other CAF markers such as FAP, if more time had given. However, none of the markers are exclusive to CAF due to their heterogeneous nature and the expression of many of these markers by other cell types (for example pericytes).

In this study, TGF-β1 promoted fibroblast contraction in NOF cultures. The matrix reorganization that occurs during floating collagen lattice contraction is similar to what occurs during the early phases of wound closure (Tomasek *et al*., 2002). In floating and unattached gels, any tension that caused fibroblast contraction is transferred to the gel matrix, resulting in gel contraction. In this condition, fibroblast is not under continuous tension and stress fibre formation is not observed (Bell *et al*., 1979). Conversely, fibroblasts populated in collagen lattice are attached and unable to contract, thus the formation of stress fibres is seen (Farsi and Aubin, 1984). Subsequent release of the lattices from attachment cause actin stress fibre disassembly (Tomasek *et al*., 1992). These results suggest that the transmission of tension to fibroblast is crucial to induce actin cytoskeleton, thereby promoting myofibroblast phenotype (Hinz *et al*., 2001a).

Induction of α-SMA expression by TGF-β1 at transcript levels was greater in NOF5 compared to NOF804, however, less magnitude of contraction was seen compared to NOF804. It is possible that batch or freshness of TGF-β1 and the fibroblast passage number used in this study contribute to these differences. However, evidence in literature of quantitative correlation between α-SMA mRNA level with the contraction magnitude is limited, suggesting the involvement of other factors, which may also contribute to the lack of correlation observed. Furthermore, although the collagen contractility model provides a simple, yet effective way to study fibroblasts contraction and is widely used, some limitations exist. This assay provides a semi-quantitative measurement of contraction and able to quantify contraction of populations of cells, not of individual cells. Other method such as Traction force microscopy (TFM) is used to measure the contraction of single cells by observing collagen gel embedded with multiple fluorescence microbeads (Dembo and Wang, 1999; Butler *et al*., 2002).This method is technically challenging and measurements of contraction do not provide a true cell contraction model, however. TGF-β1 induced α-SMA expression and FN-EDA1, followed by an increase in collagen contractility in diabetic renal fibrosis (Ina *et al*., 2012). Hinz and colleagues (2001b)) demonstrated that α-SMA modulates fibroblast contractile activity and plays an important role in focal adhesion maturation (Hinz *et al*., 2003).

Alternatively, the statistical analysis for α-SMA and FN-EDA1 transcript levels in NOF cultures could have been done with analysis of variance (ANOVA) by using Tukey's test as a post-hoc test. T-test is a special type of ANOVA that commonly used to compare two different means while ANOVA compares more than two groups of mean.

3.4 Summary

Fibroblasts are the most numerous cellular constituent within the tumour

microenvironment. Activated fibroblasts have been reported to play a role in promoting stromal remodelling and disease progression (Kalluri and Zeisberg, 2006). Although there are many potential sources of CAF within the tumour microenvironment, it is likely that myofibroblastic differentiation of resident fibroblasts accounts for at least some of this population. In this chapter, normal buccal fibroblasts were exposed to factor that are known to promote myofibroblast phenotype *in vitro* in order to model myofibroblastic CAF surrounding tumours for subsequent miRNA profiling and mechanistic studies. In this study, the optimal TGF-β1 dose for inducing differentiation of normal oral fibroblasts to a myofibroblastic CAF-like phenotype (experimental CAF; eCAF) was determined to be 5 ng/ml at 48 h. TGF-β1 treatment of normal primary oral fibroblasts induces the expression of α-SMA as well as promoting FN-EDA1 expression. TGF-β1 also enhances the formation of α-SMA-rich stress fibre in eCAF. In addition, TGF-β1 promotes contractility of collagen in eCAF. These findings suggest that TGF-β1 successfully converts NOF into eCAF and this differentiation model was used later to study any involvement of miRNAs in the development of CAF.

CHAPTER 4: Examination of the roles of miR-424-3p and miR-145-5p in eCAF differentiation

4.1 Aim and objectives

The previous chapter demonstrated that TGF-β1 treatment of normal human primary fibroblasts resulted in differentiation to a myofibroblastic eCAF. The aim of this chapter was to profile the expression of miRNAs in eCAF. To do this, the following objectives were addressed:

1) to determine the differential miRNAs expression of eCAF using TaqMan tiling low density array (TLDA) and validation of selected miRNAs by qRT-PCR.

2) to examine a role selected miRNAs may play in this TGF-β1-induced differentiation by doing loss-of-function and/or gain-of-function experiments in NOF or tumour-derived CAF.

4.2 Results

4.2.1 miRNAs are differentially expressed in eCAF (a preliminary study)

As described detail in Chapter 1, miRNAs are small noncoding RNA molecules (~22 nucleotides) that regulate gene expression at posttranscriptional level (Scaria *et al*., 2007). miRNAs relatively bind to 3'-untranslated region of target mRNA, stimulating degradation or translational inhibition (Breving *et al*., 2010). miRNA bind 7-8mer sequences which may be present in more than one transcript, and also tolerate a degree of base mismatch, resulting in the ability of a single miRNAs to repress the expression of a number of genes (Nam *et al*., 2014). It is thought that, rather than this resulting in non-specific gene expression regulation, this confers on miRNA the ability to target several genes within the same functional pathway, resulting in profound phenotypic changes despite relatively mild effects on the expression of individual genes. This enables a relatively small number of miRNA to play important roles in critical cellular processes, such as differentiation.

Relatively little is known about the role of miRNAs in regulating myofibroblast differentiation in response to TGF-β1, particularly in the context of tumour-stromal interactions. miRNAs are thought to play a role in regulating TGF-β1 signalling; most members of the TGF-β1 pathway are known or predicted to be targeted by one or more miRNAs (Butz *et al*., 2012). Furthermore, TGF-β1 directly regulates the biogenesis of miRNAs through Smads (Zhong *et al*., 2010), suggesting the existence of feedback loops.

To determine TGF-β1-induced eCAF differentiation was associated with changes in miRNA expression, three primary NOF cultures were seeded, serum starved and treated with or without 5 ng/ml of TGF-β1 for 48 h. RNA was isolated from untreated and TGF-β1-treated NOF was used for cDNA synthesis. The cDNA samples were amplified to enhance the sensitivity of the qRT-PCR in detecting the low abundance of miRNAs. Pre-amplified cDNA was subjected to TLDA analysis (Section 2.9.3) and the data obtained were analysed using DataAssist software v2.0. TLDA cards contained 384-wells per card (2 cards) pre-loaded with miRNA targets, including endogenous controls.

In this study, approximately 700 miRNA were differentially expressed in eCAF compared to normal fibroblasts when fold change of <1 is considered downregulated and fold change >1 is considered upregulated (Appendix 1). To identify differentially expressed miRNA to take forward for further study, the fold change of each miRNA were determined using DataAssist software v2.0. For the analysis, the maximum Ct cut-off value of miRNAs was set at 34; Ct value more than 34 are excluded from the analysis.

As shown in Figure 4.1, miR-145-5p, miR-424-5p and miR-424-3p were upregulated 3.1-fold, 1.5-fold and 3.2-fold in NOF1 following TGF-β1-induced myofibroblast differentiation compared to unstimulated cells, respectively. Similarly,

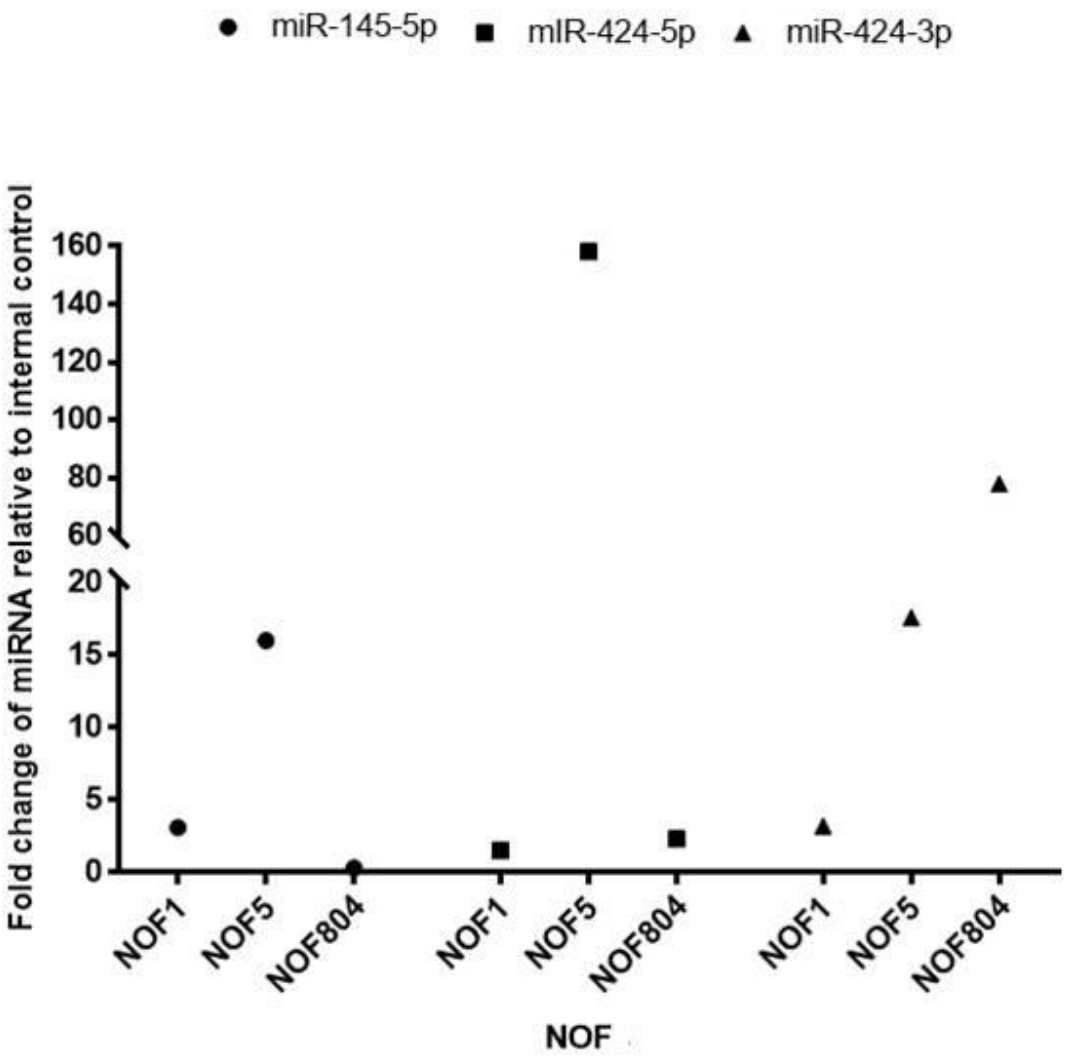

Figure 4.1: Expression of miR-145-5p, miR-424-5p and miR-424-3p are deregulated in eCAF

Three primary NOF cultures were seeded and serum starved for overnight. Following that, fibroblasts were treated with or without TGF-β1 FOR 48 h. RNA was extracted and was used for cDNA synthesis. cDNA was amplified by PCR and the pre-amplified products were used for TLDA analysis by qRT-PCR. The data obtained from qRT-PCR were analysed using DataAssist v2.0 software. The fold difference between the treatment group and the untreated group are plotted. N=1 for TLDA.

miR-145-5p, miR-424-5p and miR-424-3p were found to be highly upregulated in NOF5 after TGF-β1 treatment with 16-fold, 158-fold and 18-fold increases over unstimulated cells, respectively. TGF-β1 treatment upregulated miR-424-3p expression (78-fold) and miR-424-5p expression (2.3-fold) while miR-145-5p was downregulated by 0.3-fold in NOF804 over unstimulated cells. Thus, miR-424-5p, miR-424-3p and miR-145-5p were chosen for validation. In this preliminary study, an attempt to validate some of the other miRNA that highly upregulated in eCAF from both cultures was unsuccessful (data not shown). This might be due to false positives having been identified as a result of only performing one repeat of the TLDA analysis - this deficiency is addressed in Chapter 5.

4.2.2 Validation of selected miRNAs expressed in eCAF

The selected miRNAs were further verified by qRT-PCR. To do this, independent RNA samples treated in the same way as the samples used for TLDA were used to generate specific miR-145-5p, miR-424-5p, miR-424-3p and RNU48 cDNA. They were used in a qRT-PCR reaction using stem-looped primers designed to amplify miR-145-5p, miR-424-5p, miR-424-3p and RNU48. RNU48 was used as reference gene. The qRT-PCR analysis demonstrated that the expression levels of certain selected miRNAs more or less similar with the values observed in the TLDA experiment for NOF1 (Figure 4.2 (A)) and NOF5 (Figure 4.2 (B)), although the magnitude of change observed in some cases differed; for example, the increase in expression level of miR-424-3p detected by qRT-PCR (5.2-fold) was lower than that detected by TLDA (78-fold) (Figure 4.2 (C) and Figure 4.2 (D)).

4.2.3 Overexpression of miR-424-3p attenuates TGF-β1-induced α-SMA and FN-EDA1 markers, not COL1A1 marker in NOF

As NOF5 grew slowly and subsequently died, data for the subsequent

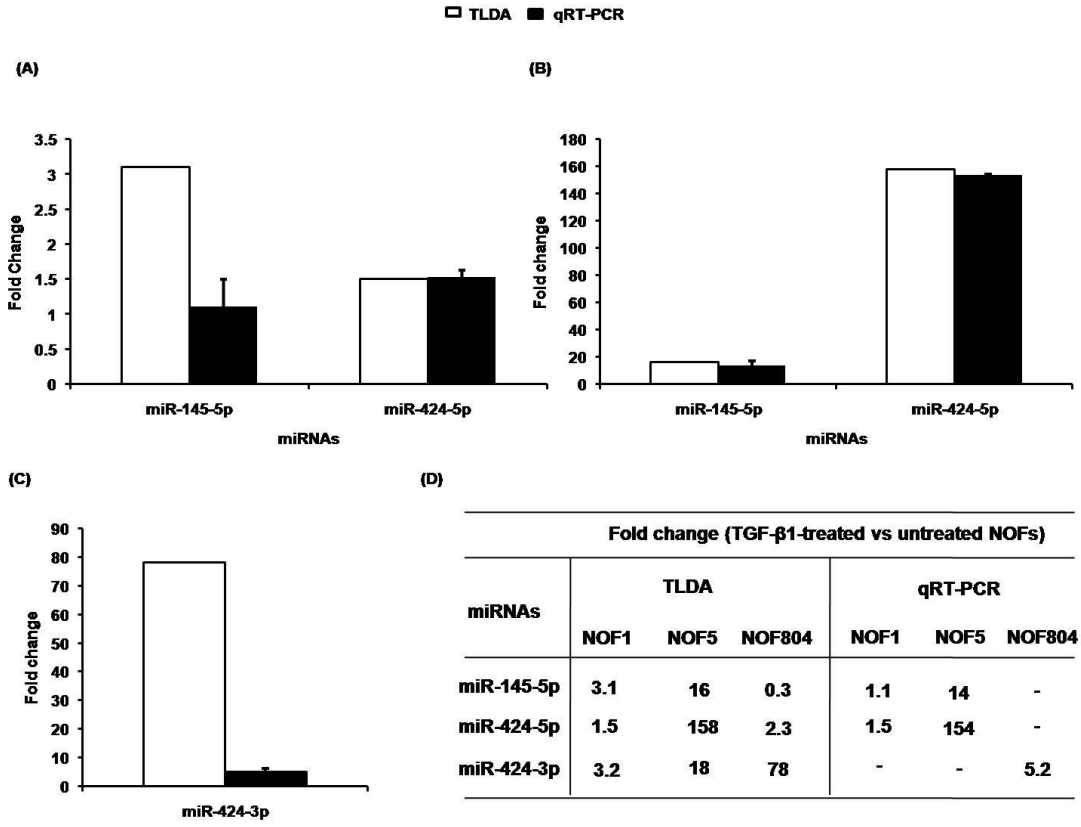

	Fold change (TGF-β1-treated vs untreated NOFs)					
miRNAs	TLDA			qRT-PCR		
	NOF1	NOF5	NOF804	NOF1	NOF5	NOF804
miR-145-5p	3.1	16	0.3	1.1	14	-
miR-424-5p	1.5	158	2.3	1.5	154	-
miR-424-3p	3.2	18	78	-	-	5.2

Figure 4.2: Validation of miRNA expression in eCAF by qRT-PCR

Fibroblasts were seeded and serum starved overnight. Following that, fibroblasts were treated with or without 5 ng/ml of TGF-β1 for 48 h. RNA was extracted from untreated and TGF-β1-treated NOF and was used for specific miRNA cDNA synthesis. The expression of miRNAs relative to RNU48 (reference control) was determined by qRT-PCR in **(A)** NOF1, **(B)** NOF5 and **(C)** NOF804. **(D)** Comparison of the fold changes observed in TLDA and by qRT-PCR. Each reaction was performed in triplicate and data are presented as means ± SEM from three independent experiments for qRT-PCR. Dash lines indicate no data for that miRNA. N=1 for TLDA.

experiments could not be generated for this culture. Thus, NOF804 was mainly used in this study. The validation data showed that miR-424-3p was upregulated in eCAF. Therefore, miR-424-3p was selected for further examination. To gain further insight into the effect of TGF-β1-induced miR-424-3p upregulation in the eCAF, one primary NOF culture (NOF804) was transiently transfected with a synthetic precursor miR-424-3p (pre-miR-424-3p) oligonucleotide for 48 h to overexpress mature miR-424-3p. A non-targeting precursor miRNA was used as a negative control and mock (transfection reagent only) also included in this experiment. The miRNA mimic concentration (50 nM) was selected based on the concentration frequently used in the literature (Liu *et al*., 2012) and previously optimised in the laboratory (Kabir *et al*., 2016). The transfected NOF were serum starved overnight and treated with TGF-β1 or left untreated for 48 h. After the treatment, NOF were harvested for RNA extraction, followed by cDNA synthesis. qRT-PCR was performed on cDNA using primers specific for α-SMA, FN-EDA1, COL1A1 and B2M as a reference gene. B2M was used as the reference gene, as it showed the least variable in CT values between samples, compared to U6 (Appendix 2).

As shown in Figure 4.3, TGF-β1 treatment significantly enhanced α-SMA transcript levels in fibroblasts transfected with mock (36.9±14.1-fold), pre-miR negative control (35.1±10.6-fold) and pre-miR-424-3p (23.5±9.5-fold). Interestingly, overexpression of miR-424-3p caused a significant reduction in TGF-β1-stimulated α-SMA expression by ≈ 69 % (compared to treated-pre-miR negative control) and by ≈ 65 % (compared to treated mock). Next, other myofibroblast differentiation markers were assessed to investigate whether miR-424-3p was able to alter other myofibroblast differentiation markers besides α-SMA. In agreement with data shown in Chapter 3 (section 3.2.2), FN-EDA1 transcript levels were significantly increased in transfected NOF treated with TGF-β1; increases of 24.9±9.8-fold (mock), 27.1±9.1-fold (pre-miR

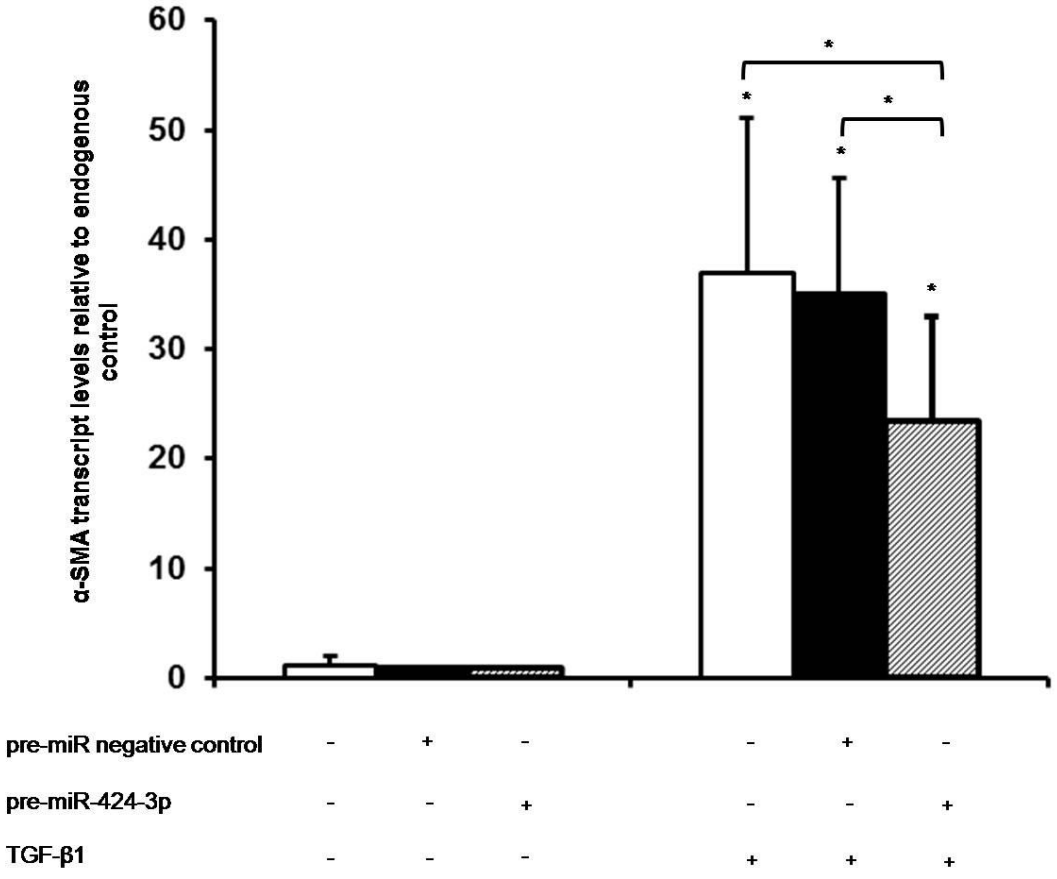

Figure 4.3: **Overexpression of miR-424-3p attenuates TGF-β1 induced α-SMA expression in NOF**

NOF were transiently transfected with pre-miR negative control or pre-miR-424-3p for 48 h. The transfected NOF were serum starved overnight before being treated with or without TGF-β1 for 48 h. Following treatment, NOF were harvested and subjected to RNA extraction and used for cDNA synthesis. The qRT-PCR analysis was done using primers designed to amplify αSMA. B2M was used as a reference gene. Each data represents the mean relative quantification of myofibroblast differentiation markers relative to B2M ± SEM from three independent experiments, for each transfection with or without TGF-β1 compared to untreated pre-miR negative control. Statistical analysis was determined using two-tailed Student T-test with *p <0.05. If not shown by a bar, the significance is compared to the untreated equivalent transfection, or pre-miR negative control, in the case of untreated pre-miR.

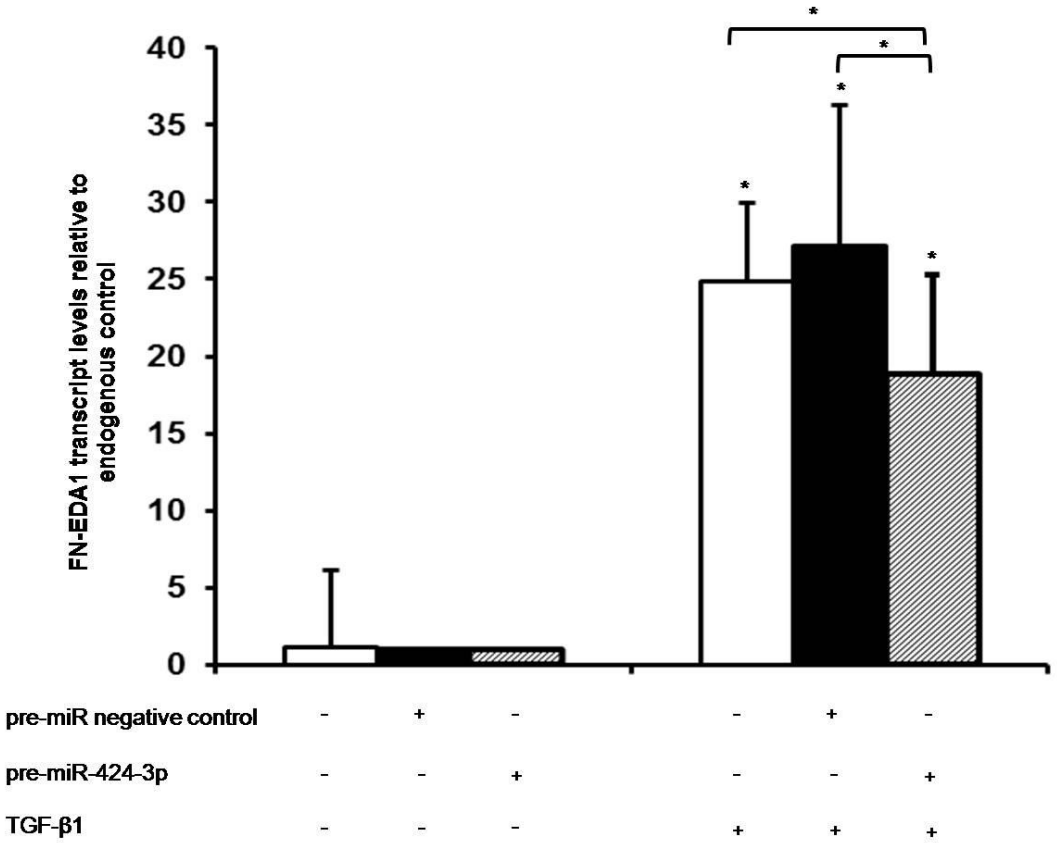

Figure 4.4: **Overexpression of miR-424-3p attenuates TGF-β1 induced FN-EDA1 expression in NOF**

NOF were transiently transfected with pre-miR negative control or pre-miR-424-3p for 48 h. The transfected NOF were serum starved overnight before being treated with or without TGF-β1 for 48 h. Following treatment, NOF were harvested and subjected to RNA extraction and used for cDNA synthesis. The qRT-PCR analysis was done using primers designed to amplify FN-EDA1. B2M was used as a reference gene. Each data represents the mean relative quantification of myofibroblast differentiation markers relative to B2M ± SEM from three independent experiments, for each transfection with or without TGF-β1 compared to untreated pre-miR negative control. Statistical analysis was determined using two-tailed Student T-test with *$p < 0.05$. If not shown by a bar, the significance is compared to the untreated equivalent transfection, or pre-miR negative control, in the case of untreated pre-miR.

negative control) and 18.9±6.5-fold (pre-miR-424-3p) were observed (Figure 4.4). Similar to the effects observed on α-SMA expression, overexpression of miR-424-3p significantly attenuated the TGF-β1-mediated increase in FN-EDA1 expression, 19-fold (compared to ≈27-fold of treated pre-miR negative control) and ≈19-fold (compared to ≈ 25-fold of treated mock). As shown in Figure 4.5, TGF-β1 caused an increase in COL1A1 transcript levels in mock (11.9±12.4-fold), pre-miR negative control (7.9±4.6-fold) and pre-miR 424-3p (9.4±6.6-fold). However, none of these changes reached significance ($p<0.05$). Moreover, overexpression of miR-424-3p did not alter TGF-β1-modulated COL1A1 gene expression in NOF, compared to TGF-β1-treated pre-miR negative control. The data above suggest that miR-424-3p has the ability to modulate α-SMA and FN-EDA1 expression but not COL1A1.

4.2.4 Overexpression of miR-424-3p had no effect on TGF-β1-induced α-SMA protein abundance in NOF

As shown in Chapter 3, TGF-β1 treatment induces α-SMA protein abundance in NOF. To investigate the effect of miR 424-3p on TGF-β1-induced α-SMA protein abundance, NOF were transiently transfected with pre-miR negative control or pre-miR 424-3p for 48 h. NOF were serum starved overnight and treated with TGF-β1 or left untreated for 48 h. Cells were harvested and subjected to protein extraction. The total protein lysates were used for immunoblotting. TGF-β1 caused a small increase in α-SMA protein abundance in mock (1.5 ±0.5-fold), pre-miR negative control (1.3±0.4-fold) and pre-miR-424-3p (1.4±0.2-fold) (Figure 4.6). However, none of these reaches statistical significance ($p<0.05$). Overexpression of miR-424-3p slightly increased TGF-β1-induced α-SMA protein abundance in NOF, compared to treated pre-miR negative control. However, this did not reach significance value tested.

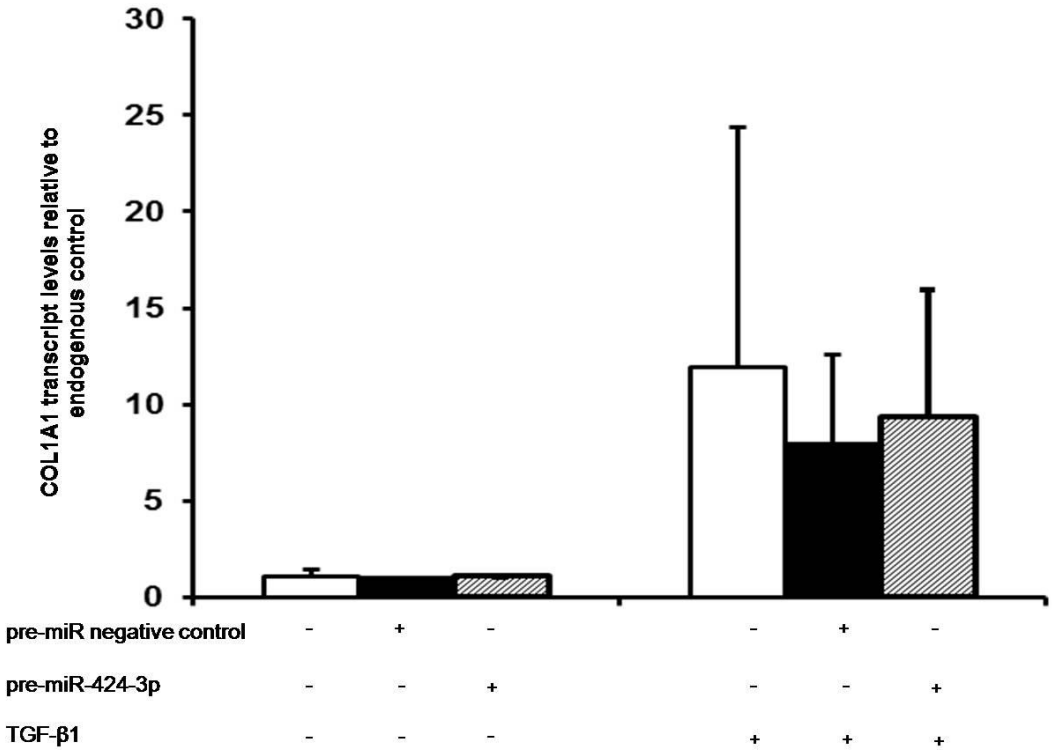

Figure 4.5: **Overexpression of miR-424-3 had no effect on TGF-β1 induced COLIA1 expression in NOF**

NOF were transiently transfected with pre-miR negative control or pre-miR-424-3p for 48 h. Transfected NOF were serum starved overnight before being treated with or without TGF-β1 for 48 h. Following treatment, NOF were harvested and subjected to RNA extraction and used for cDNA synthesis. The qRT-PCR analysis was done using primers designed to amplify COL1A1. B2M was used as a reference gene. Each data represents the mean relative quantification of myofibroblast differentiation markers relative to B2M ± SEM from three independent experiments, for each transfection with or without TGF-β1 compared to untreated pre-miR negative control. Statistical analysis was determined using two-tailed Student T-test, as the significance is compared to the untreated equivalent transfection, or pre-miR negative control, in the case of untreated pre-miR. No significant difference between pre-miR negative control compared to pre-miR 424-3p in TGF-β1-treated NOF.

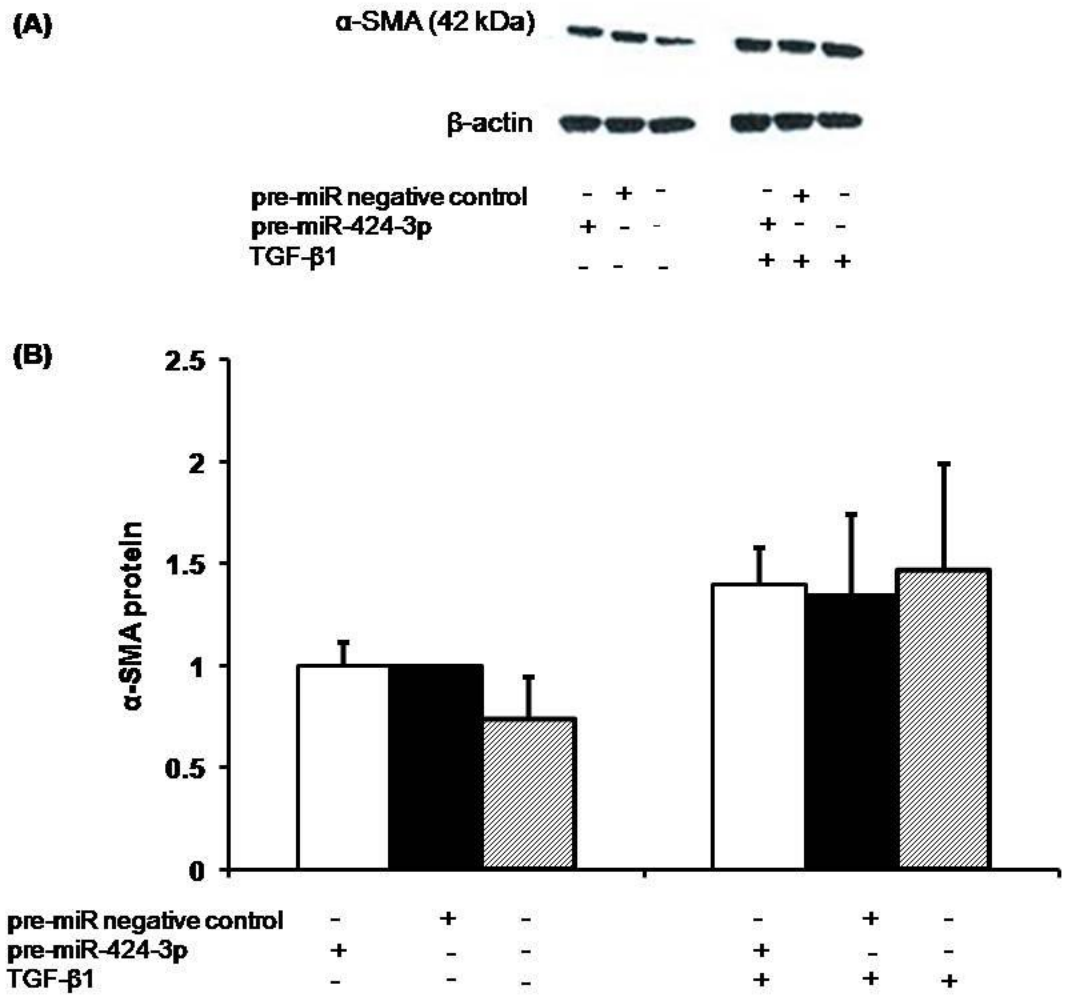

Figure 4.6: Overexpression of miR 424-3p had no effect in TGF-β1-induced α-SMA protein abundance in NOF

NOF were transiently transfected with pre-miR negative control or pre-miR-424-3p for 48 h. Then, NOF were serum starved overnight and treated with or without TGF-β1 for 48 h. NOF were harvested and used for protein extraction. Total protein lysates were used for immunoblotting using antibodies from mouse α-SMA and β-actin as a loading control. **(A)** a representative of protein bands for immunoblot from three independent repeats, **(B)** the quantified amount of protein in each sample using Image J software. Each data represents the mean ± SEM from three independent experiments. Statistical analysis was determined using two-tailed Student T-test, as the significance is compared to the untreated equivalent transfection, or pre-miR negative control, in the case of untreated pre-miR. No significant difference between pre-miR negative control compared to pre-miR 424-3p in TGF-β1-treated NOF.

4.2.5 Overexpression of miR-424-3p had no effect on TGF-β1-induced α-SMA positive stress fibres formation in NOF

In the previous chapter, it was demonstrated that TGF-β1 induces the formation of stress fibres in NOF. To determine the effect of TGF-β1- induced miR-424-3p upregulation on these stress fibre, NOF were seeded onto coverslips and transiently transfected with pre-miR negative control or pre-miR-424-3p for 48 h before being treated with TGF-β1 or left untreated for 48 h. TGF-β1 treatment significantly increased the formation of α-SMA positive stress fibres, by mean relative fluorescence per cell in mock (7.1±1.1-fold), pre-miR negative control (7.0±0.3-fold) and pre-miR-424-3p (5.7±0.7-fold) (Figure 4.7 (B)). Overexpression of miR-424-3p caused no change in the formation of TGF-β1-induced α-SMA positive stress fibres formation, compared to treated pre-miR negative control, but this did not reach statistical significance ($p<0.05$) (Figure 4.7 (A)).

4.2.6 Overexpression of miR-424-3p significantly decreased TGF-β1-induced gel contraction in NOF

To further investigate the role of miR-424-3p in myofibroblast phenotype, a gel collagen contractility assay was performed to examine the effect of overexpression of miR-424-3p on TGF-β1-induced contractility in NOF. NOF were transiently transfected with pre-miR negative control or pre-miR 424-3p for 48 h. Transfected NOF were resuspended in a mixture of rat tail collagen 1 with DMEM (1:1). The mixture was allowed to polymerize, then treated with TGF-β1 or left untreated for 48 h. As shown in Figure 4.8, TGF-β1 significantly induced gel contraction in mock (224±29.5 mm^2), pre-miR negative control (237±29.9 mm^2) and pre-miR-424-3p (286±39.9 mm^2). Interestingly, overexpression of miR-424-3p significantly reduces TGF-β1's ability to induce contraction of gels, indicated by decrease in gels surface area by ≈ 83 %

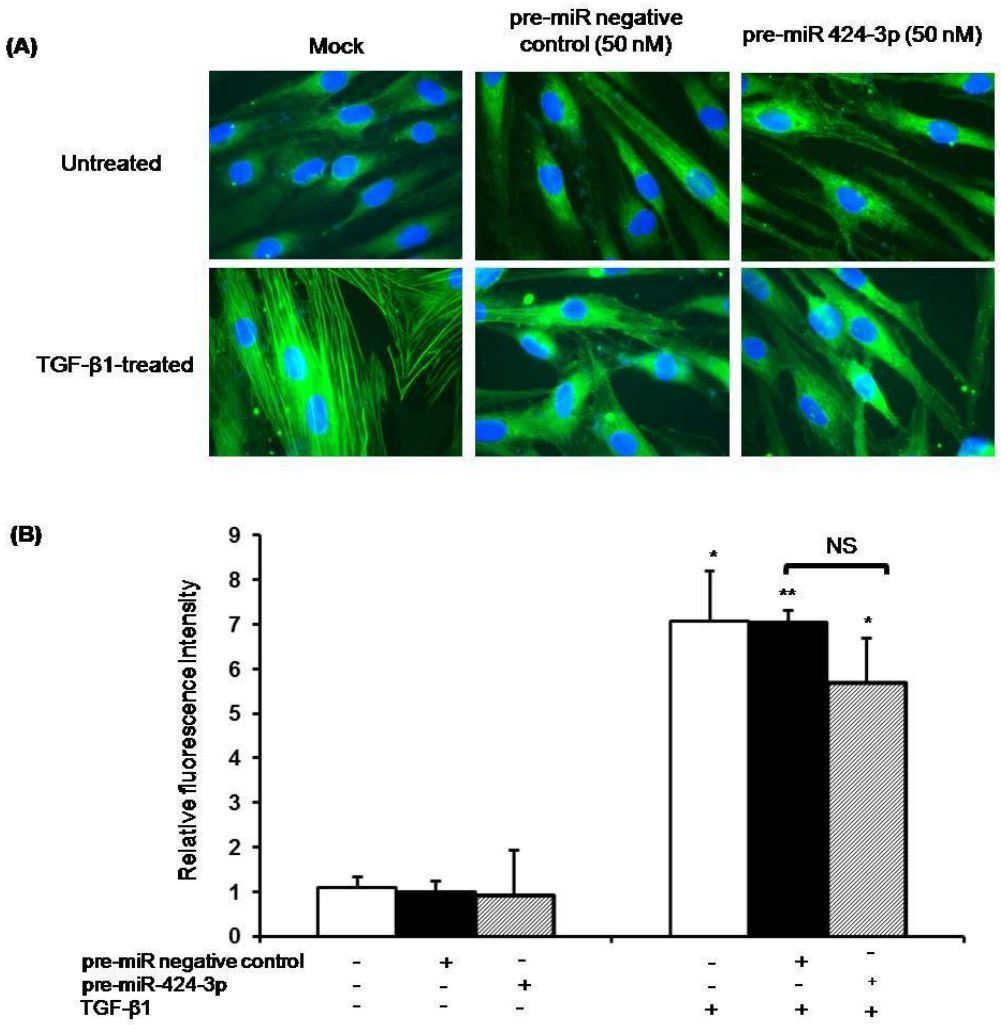

Figure 4.7 Overexpression of miR-424-3p did not prevent the formation of TGF-β1-induced α-SMA positive stress fibres in NOF

NOF were seeded onto coverslips overnight and transiently transfected with pre-miR negative control or pre-miR-424-3p for 48 h. Following that, NOF were serum starved overnight and treated with or without TGF-β1 for 48 h. The coverslips were washed with DPBS prior to fixation with 100 % methanol for 20 min. Then, they were permeabilised in 4 mM sodium deoxycholate for 10 min before being blocked with 2.5 % (w/v) BSA in DPBS for 30 min. The coverslips were incubated with a primary FITC-conjugated α-SMA antibody overnight at 4 ^{0}C. Following incubation, they were washed with DPBS and were mounted with Dapi. The coverslips were viewed under a fluorescence microscope using Pro-Plus 7.0 imaging software at 100x magnification (using oil immersion). **(A)** Representative images of stress fibre formation from three independent repeats. **(B)** The mean fluorescence intensity per cell ± SEM from three independent experiments was quantified using Image J software. Statistical analysis was determined using two-tailed Student T-test with *$p < 0.05$ and **$p < 0.005$. If not shown by a bar, the significance is compared to the untreated equivalent transfection, or pre-miR negative control, in the case of untreated pre-miR.

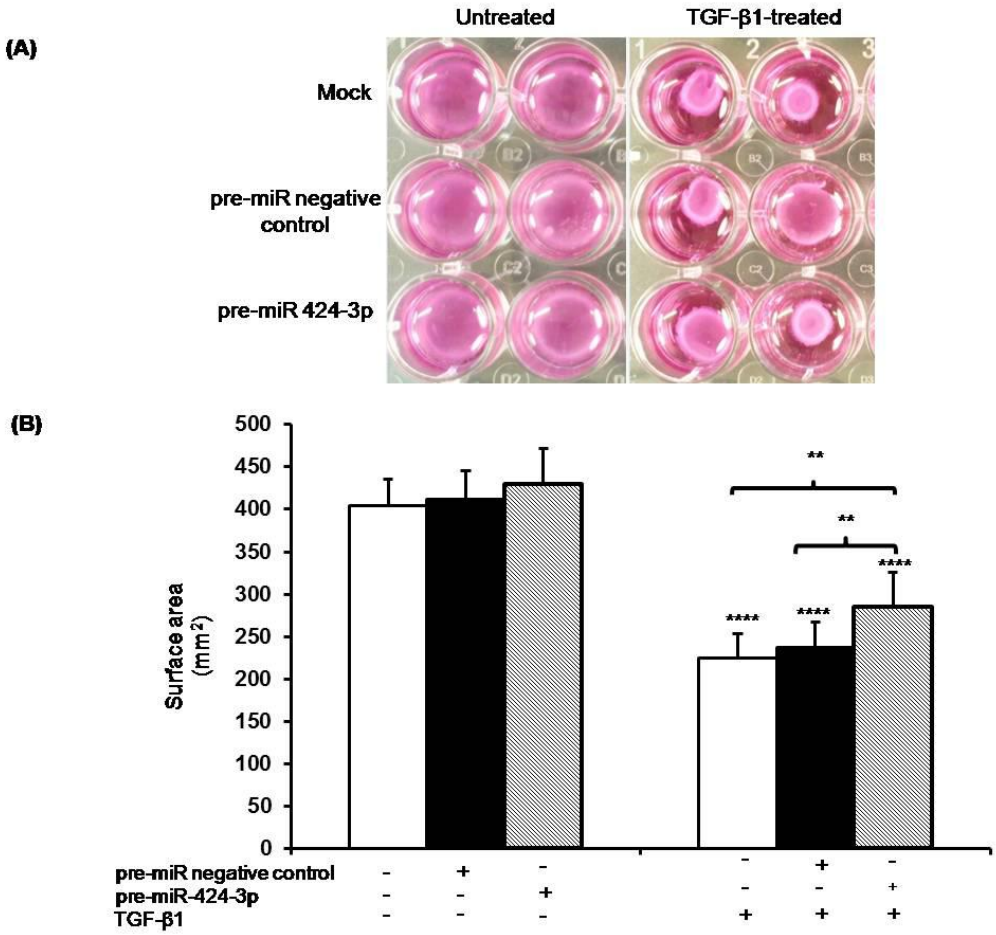

Figure 4.8: Overexpression of miR-424-3p prevents TGF-β1-induced contractility in NOF

NOF were transiently transfected with pre-miR negative control or pre-miR-424-3p for 48 h. Following incubation, the NOF were harvested, counted (2.5 x 10^5 cells/well) and resuspended in a mixture of rat tail collagen 1 (in 0.1 M acetic acid) and DMEM (1:1). The pH was neutralised with 1M NaOH and the mixture was aliquoted into wells (300 µl/well) and left to polymerise in an incubator at 37 ^{0}C with 5 % CO_2. After the gels had polymerised, media were added to each well and incubated for 4 h in the incubator. After that, the media were replaced by serum-free media for overnight. The gels were detached from the sides of the wells with a scalpel and treated with TGF-β1 or left untreated for 48 h. The images were taken at 48 h and the gel contraction was determined by measuring the surface area of the gels with Image J software. **(A)** a representative of gels containing transfected NOF after 48 h of TGF-β1 treatment. **(B)** the quantified of gels contraction, as a surface area (mm^2) compared to untreated pre-miR negative control. Each data represents the mean ± SEM from three independent experiments. Statistical analysis was determined using two-tailed Student T-test with **p < 0.005 and ****p < 0.0001. If not shown by a bar, the significance is compared to the untreated equivalent transfection, or pre-miR negative control, in the case of untreated pre-miR.

(compared to TGF-β1-treated pre-miR negative control) and by ≈ 78 % (compared to treated-mock).

4.2.7 Knockdown of miR-424-3p or miR-145-5p had no effect in TGF-β1-induced fibroblast differentiation markers in NOF

Preliminary study showed that miR-145-5p was downregulated in eCAF. Thus an attempt to inhibit its expression was examined at this section. To investigate further whether inhibition of miR-424-3p and miR-145-5p affected TGF-β1-induced myofibroblast phenotype, one primary NOF culture was transiently transfected with a synthetic miR-424-3p inhibitor or miR-145-5p inhibitor for 48 h. A non-targeting miRNA inhibitor was used as a negative control and mock consisted of transfection reagent only. As stated in Section 4.3, similar concentration of miRNA inhibitors (50 nM) was used in this study. TGF-β1 was added after overnight serum starvation for 48 h. NOF were harvested and used for total RNA extraction, followed by cDNA synthesis using random hexamers. Fibroblast differentiation markers were determined using primers designed to amplify α-SMA, FN-EDA1, COL1A1 and B2M as reference gene by qRT-PCR.

Treatment with TGF-β1 increased α-SMA transcript levels in fibroblasts transfected with mock (64.5±29.8-fold; significant), negative control inhibitor (45.0±8.9-fold; significant), miR-145-5p (50.2±35.2-fold; not significant) and miR-424-3p inhibitor (49.8±14-fold; significant) (Figure 4.9). The α-SMA is slightly increased by 4 fold, not significant ($p<0.05$) when NOF were exposed to the miR-424-3p inhibitor and TGF-β1 in combination, compared to treated negative control inhibitor. Knockdown of miR-145-5p caused a small increase by 5 fold but not significant ($p<0.05$) of TGF-β1-modulated α-SMA gene expression, compared to treated negative inhibitor.

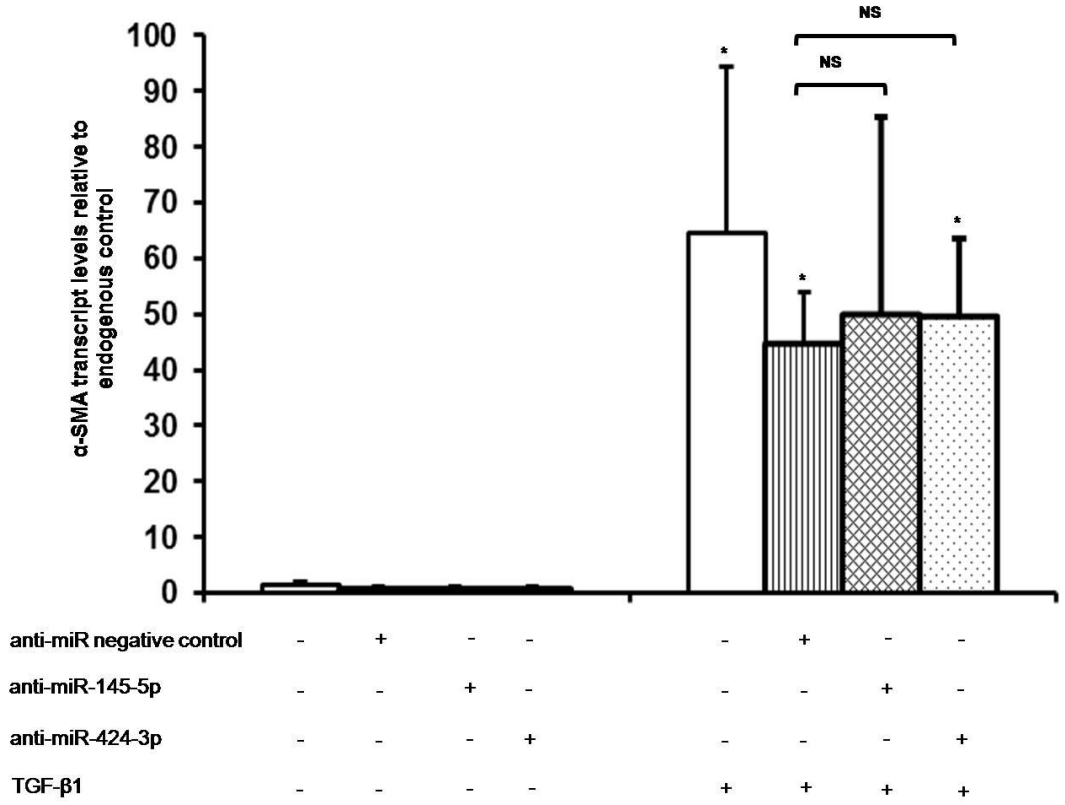

Figure 4.9: Neither inhibition of miR-424-3p nor miR-145-5p had an effect on TGF-β1-induced α-SMA expression in NOF

NOF were transiently transfected with negative control inhibitor, miR-424-3p inhibitor or miR-145-5p for 48 h. The transfected NOF were serum starved overnight before being treated with or without TGF-β1 for 48 h. Following treatment, NOFs were harvested and subjected to RNA extraction and used for cDNA synthesis. The qRT-PCR analysis was done using primers designed to amplify αSMA. B2M was used as a reference gene. Each data represents the mean relative quantification of myofibroblast differentiation markers relative to B2M ± SEM from three independent experiments, for each transfection with or without TGF-β1 compared to untreated negative control inhibitor. Statistical analysis was determined using two-tailed Student T-test with *p <0.05. If not shown by a bar, the significance is compared to the untreated equivalent transfection, or anti-miR negative control, in the case of untreated anti-miRs.

On the other hand, upregulation of FN-EDA1 gene expression was observed in mock (14.1±3.2-fold; significant), negative control inhibitor (11.6±6.3-fold; significant), miR-145-5p (11.3±7.1-fold; not significant) and miR-424-3p (12.2±8.9 -fold; not significant) after TGF-β1 treatment (Figure 4.10). Knockdown of miR-424-3p caused a small increase (not significant) in TGF-β1-induced FN-EDA1 gene expression, compared to treated negative control inhibitor. Meanwhile, inhibition of miR-145-5p had no effect on TGF-β1-induced FN-EDA1 gene expression.

Neither transfection with miR-424-3p inhibitor (7.1±7.0-fold) nor miR-145-5p inhibitor (6.7±5.2-fold) caused a significant increase in TGF-β1-induced COL1A1 transcript levels (Figure 4.11). Similarly, knockdown of these inhibitors does not significantly upregulate TGF-β1-induced COL1A1 gene expression, compared to cells transfected with negative control inhibitor.

4.2.8 Knockdown of miR-424-3p or miR-145-5p did not alter TGF-β1-induced α-SMA protein in NOF

To investigate the effect of miR 424-3p inhibition on TGF-β1-induced α-SMA at the protein level, NOF were transiently transfected with a non-targeting negative control inhibitor or miR-424-3p inhibitor or miR-145-5p inhibitor for 48 h. NOF were serum starved overnight and treated with TGF-β1 or left untreated. NOF were harvested and subjected to protein extraction. The total protein lysates were used for immunoblotting. TGF-β1 caused an increase in α-SMA protein abundance in all conditions, but this did not reach statistical significance ($p<0.05$) (Figure 4.12). Inhibition of miR-424-3p or miR-145-5p had small decreases (not significant) in TGF-β1-induced α-SMA protein abundance, compared to treated negative control inhibitor.

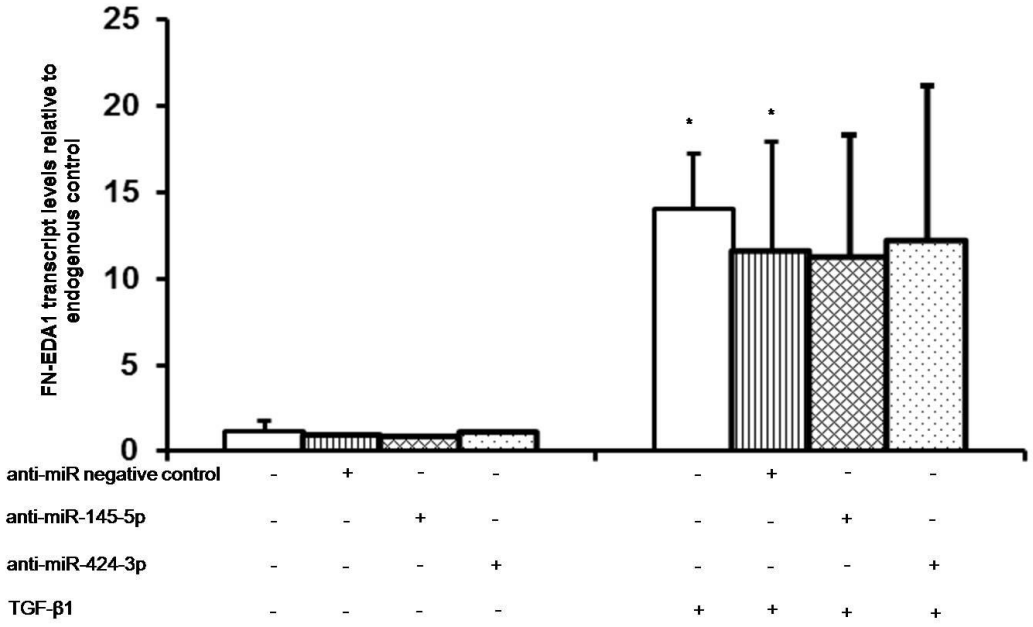

Figure 4.10: Inhibition miR-145-5p or miR-424-3p had no effect on TGF-β1-induced FN-EDA1 expression in NOF

NOF were transiently transfected with negative control inhibitor, miR-424-3p inhibitor or miR-145-5p for 48 h. The transfected NOF were serum starved overnight before being treated with or without TGF-β1 for 48 h. Following treatment, NOF were harvested and subjected to RNA extraction and used for cDNA synthesis. The qRT-PCR analysis was done using primers designed to amplify FN-EDA1. B2M was used as a reference gene. Each data represents the mean relative quantification of myofibroblast differentiation markers relative to B2M ± SEM from three independent experiments, for each transfection with or without TGF-β1 compared to untreated negative control inhibitor. Statistical analysis was determined using two-tailed Student T-test with *p <0.05. The significance is compared to the untreated equivalent transfection, or anti-miR negative control, in the case of untreated anti-miRs. No significant difference between anti-miR negative control compared to anti-miRs in TGF-β1-treated NOF.

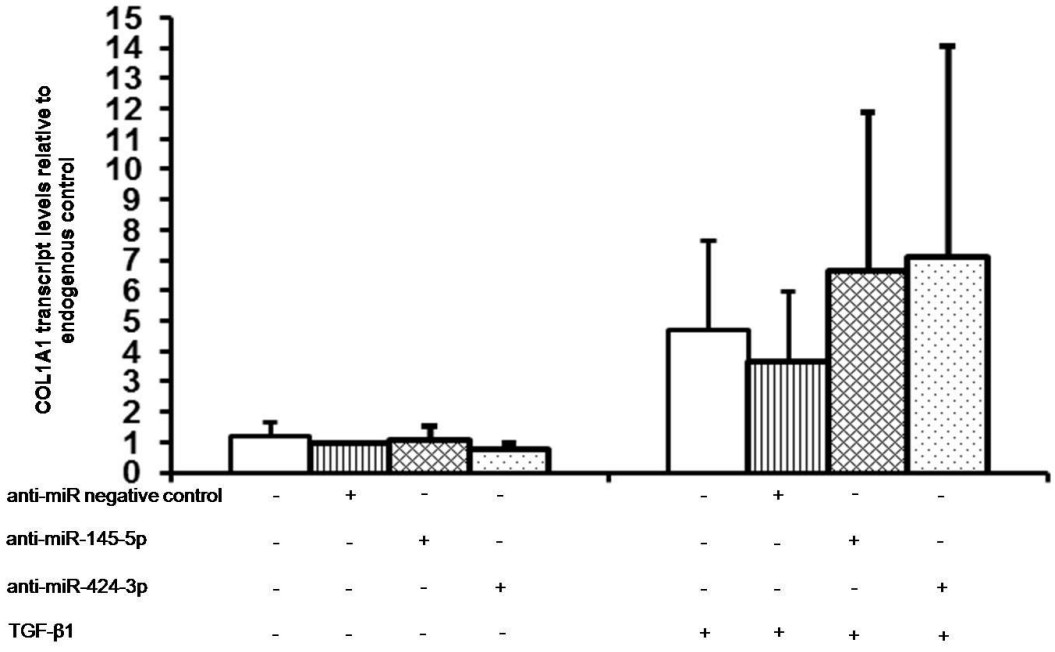

Figure 4.11: Inhibition miR-145-5p or miR-424-3p had no effect on TGF-β1-induced COL1A1 expression in NOF

NOF were transiently transfected with negative control inhibitor, miR-424-3p inhibitor or miR-145-5p for 48 h. The transfected NOF were serum starved overnight before being treated with or without TGF-β1 for 48 h. Following treatment, NOFs were harvested and subjected to RNA extraction and used for cDNA synthesis. The qRT-PCR analysis was done using primers designed to amplify COL1A1. B2M was used as a reference gene. Each data represents the mean relative quantification of myofibroblast differentiation markers relative to B2M ± SEM from three independent experiments, for each transfection with or without TGF-β1 compared to untreated negative control inhibitor. Statistical analysis was determined using two-tailed Student T-test. The significance is compared to the untreated equivalent transfection, or anti-miR negative control, in the case of untreated anti-miRs. No significant difference between anti-miR negative control compared to anti-miRs in TGF-β1-treated NOF.

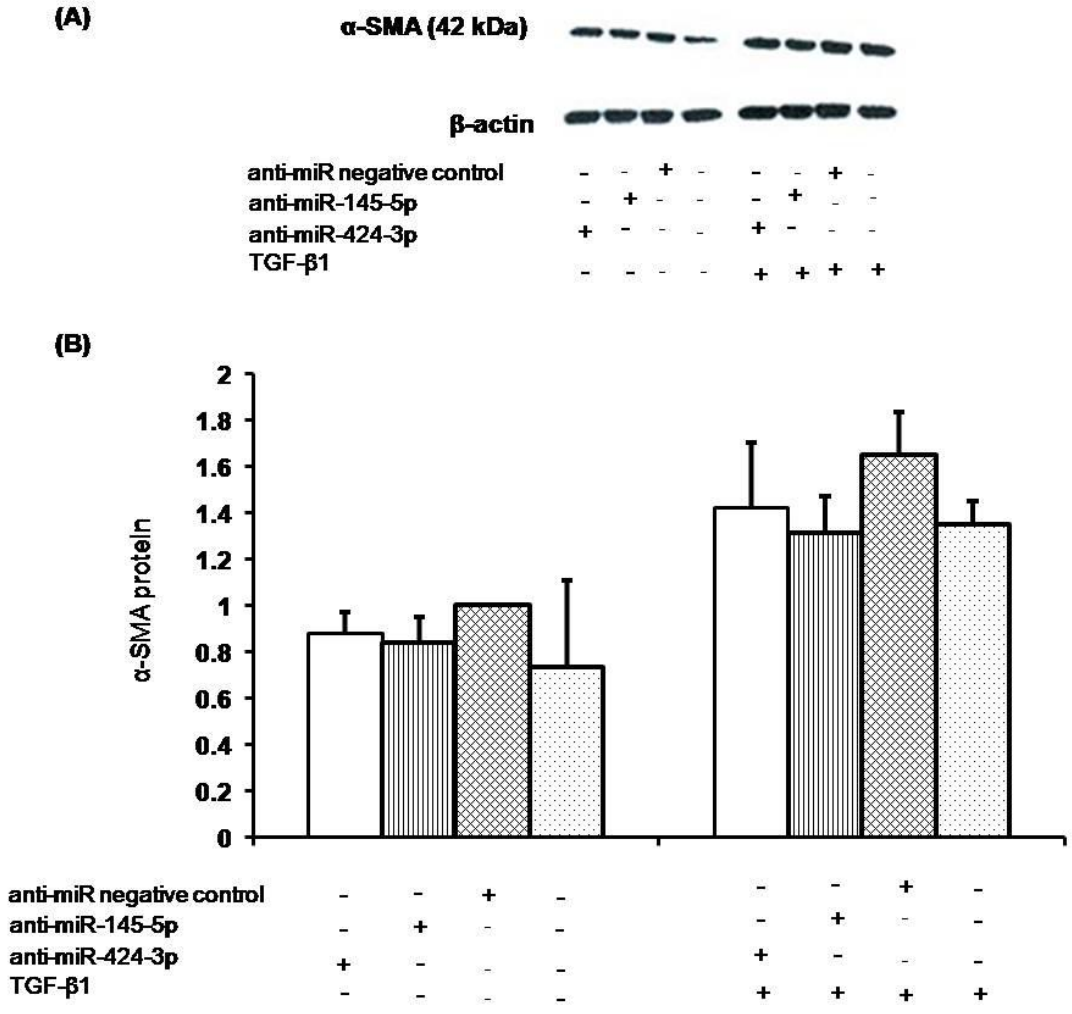

Figure 4.12: Inhibition of miR 424-3p or miR-145-5p did not alter TGF-β1-induced α-SMA protein abundance in NOF

NOF were transiently transfected with negative control inhibitor or miR-424-3p inhibitor or miR-145-5p inhibitor for 48 h. Then, NOF were serum starved overnight and treated with or without TGF-β1 for 48 h. NOF were harvested and used for protein extraction. Total protein lysates were used for immunoblotting using antibodies from mouse α-SMA and β-actin as a loading control. **(A)** a representative of protein bands for immunoblot from three independent repeats, **(B)** the quantified amount of protein in each sample using Image J software. Each data represents the mean ± SEM from three independent experiments. The significance is compared to the untreated equivalent transfection, or anti-miR negative control, in the case of untreated anti-miRs. No significant difference between anti-miR negative control compared to anti-miRs in TGF-β1-treated NOF.

4.2.9 Knockdown of miR-424-3p or miR-145-5p had no effect on TGF-β1-induced α-SMA positive stress fibres formation in NOF

To determine the effect of TGF-β1-induced miR-424-3p upregulation on the formation of stress fibre, NOF were seeded onto coverslips and transiently transfected with negative control inhibitor or miR-424-3p inhibitor or miR-145-5p inhibitor for 48 h before being treated with TGF-β1 or left untreated for 48 h. As shown in Figure 4.13 (A), TGF-β1 promotes α-SMA positive stress fibres formation in NOF transfected with negative control inhibitor (2.1±0.1-fold; significant), miR-424-3p inhibitor (2.7±0.5-fold; significant) or miR-145-5p inhibitor (4.3±1.3-fold; significant), as obviously seen by striking cytoskeletal. The stress fibre was observed much clearer in the TGF-β1-treated mock compared to NOF transfected with other two inhibitors. A small increase in mean relative fluorescence per cell (not significant) was observed when NOF were exposed to the miR-424-3p inhibitor and TGF-β1 in combination, compared to treated negative control inhibitor (Figure 4.13 (B)). Similarly, treatment with TGF-β1 did not significantly increase mean relative fluorescence per cell in miR-145-5p inhibitor-treated NOF, compared to treated negative control inhibitor.

4.2.10 Knockdown of miR-424-3p or miR-145-5p did not alter TGF-β1-induced gel contraction in NOF

A gel collagen contractility assay was done to determine the effect of miR-424-3p on TGF-β1-induced contractility in NOF. NOF were transiently transfected with negative control inhibitor or miR-424-3p inhibitor or miR-145-5p inhibitor for 48 h. Transfected NOF were resuspended in a mixture of rat tail collagen 1 with DMEM (1:1). The mixture was allowed to polymerise, then treated with 5 ng/ml of TGF-β1 or left untreated for 48

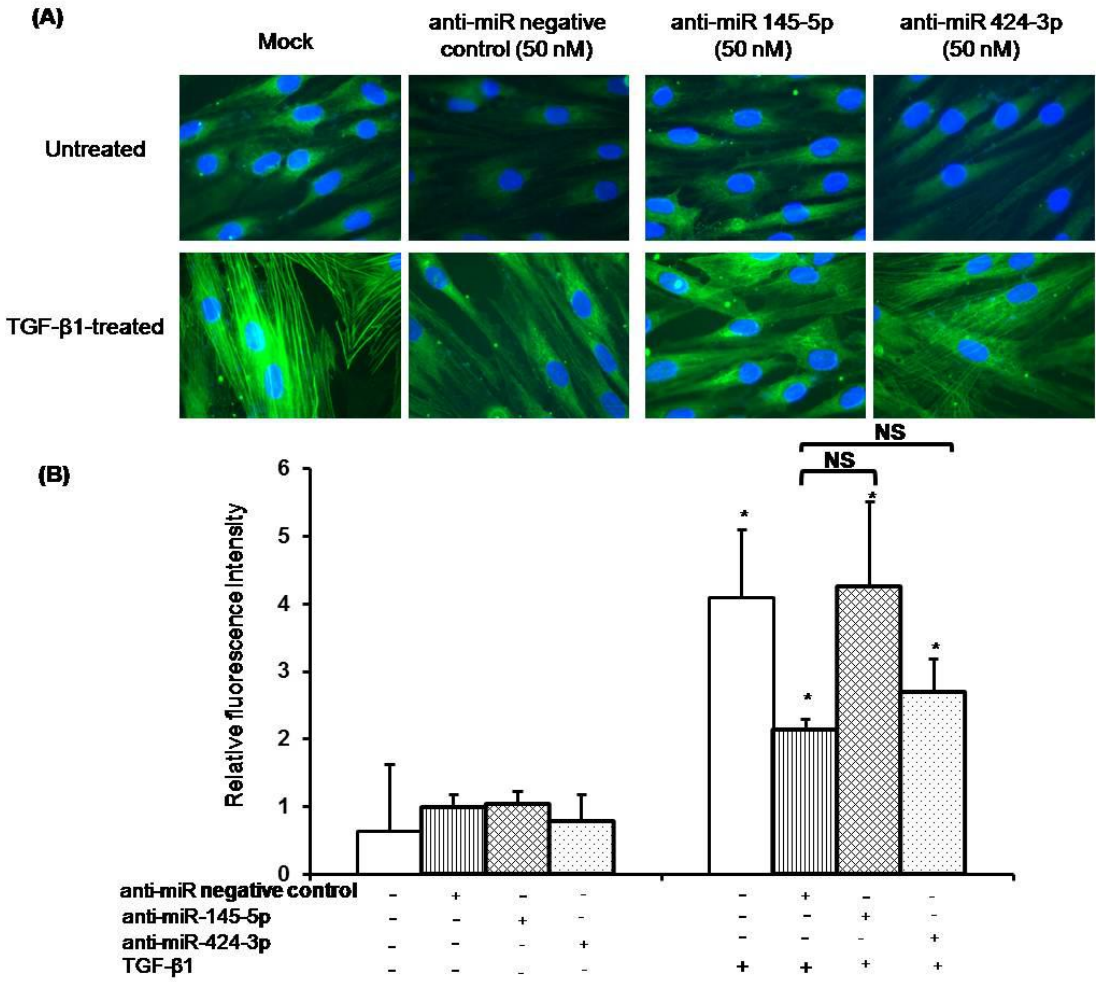

Figure 4.13: Effect of inhibition of miR-424-3p or miR-145-5p on TGF-β1-induced α-SMA positive stress fibres formation in NOF

NOF were seeded onto coverslips overnight and transiently transfected with negative control inhibitor or miR-424-3p inhibitor or miR-145-5p inhibitor for 48 h. Following that, NOF were serum starved overnight and treated with TGF-β1 for 48 h. The coverslips were washed with DPBS prior to fixation with 100 % methanol for 20 min. Then, they were permeabilised in 4 mM sodium deoxycholate for 10 min before being blocked with 2.5 % (w/v) BSA in DPBS for 30 min. The coverslips were incubated with a primary FITC-conjugated α-SMA antibody overnight at 4 ^{0}C. Following incubation, they were washed with DPBS and were mounted with Dapi. The coverslips were viewed under a fluorescence microscope using Pro-Plus 7.0 imaging software at 100x magnification (using oil immersion). **(A)** Representative images of stress fibre formation from three repeats. **(B)** The mean fluorescence intensity per cell ± SEM from three independent experiments was quantified using Image J software. Statistical analysis was determined using two-tailed Student T-test with *$p < 0.05$. If not shown by a bar, the significance is compared to the untreated equivalent transfection, or anti-miR negative control, in the case of untreated anti-miRs.

h. TGF-β1 significantly induced gel contraction in mock (224±29.5 mm^2), negative control inhibitor (284±62.4 mm^2), miR 424-3p inhibitor (295±56.1 mm^2) and miR-145-5p inhibitor (309±50.1 mm^2) (Figure 4.14). However, inhibition of miR-424-3p or miR-145-5p did not alters TGF-β1's ability to induce contraction of gel, compared to treated negative control inhibitor.

4.2.11 miR-424-3p effects on CAF

4.2.11.1 Overexpression of miR-424-3p did not inhibit TGF-β1-induced myofibroblast differentiation markers in CAF

To investigate the involvement of the miR-424-3p in TGF-β1-induced myofibroblast differentiation in CAF, CAF were transiently transfected with precursor negative control or precursor miR-424-3p for 48 h. Following that, CAF were treated with TGF-β1, or left untreated for 48 h and myofibroblast differentiation markers were assessed by qRT-PCR. As shown in Figure 4.15, overexpression of miR-424-3p did not inhibit basal α-SMA expression at mRNA level in CAF. TGF-β1 significantly increases α-SMA transcript levels in CAF transfected with mock (78.0±31.2-fold), pre-miR negative control (48.4±31.3-fold) and pre-miR-424-3p (44.6±19.4-fold). miR-424-3p overexpression in CAF did not significantly decrease TGF-β1-induced α-SMA transcript levels, compared to TGF-β1-treated cells transfected with pre-miR negative control. Similar to α-SMA, overexpression of miR-424-3p did not inhibit basal level of FN-EDA1 transcripts in CAF. TGF-β1 treatment significantly caused increases in FN- EDA1 transcript levels of mock (31.8±15.3-fold), pre-miR negative control (17.0±9-fold) and pre-miR-424-3p (15.8±3.0-fold) (Figure 4.16). Overexpression of miR-424-3p had a small decrease in TGF-β1-induced FN-EDA1 transcript levels, compared to treated pre-miR negative control, this not significant, however. Overexpression of miR-424-3p did not inhibit basal level of COL1A1 transcripts in CAF. Treatment with TGF-β1

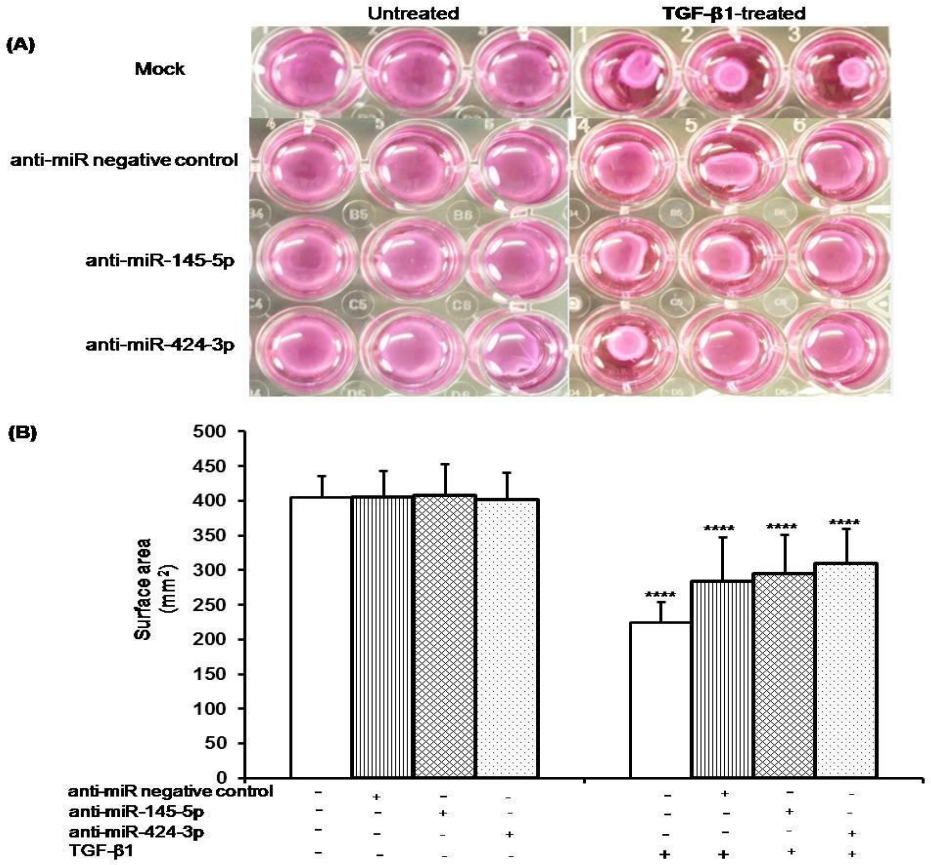

Figure 4.14: Inhibition of miR-424-3p or miR-145-5p did not alter TGF-β1-induced gel contraction in NOF

NOF were transiently transfected with negative control inhibitor or miR-424-3p inhibitor or miR-145-5p inhibitor for 48 h. Following incubation, the NOF were harvested, counted (2.5 x 10^5 cells/well) and resuspended in a mixture of rat tail collagen 1 (in 0.1 M acetic acid) and DMEM (1:1). The pH was neutralised with 1M of NaOH and the mixture was aliquoted into wells (300 µl/well) and left to polymerise in an incubator at 37 ^{0}C with 5 % CO_2. After the gels had polymerised, media were added to each well and incubated for 4 h in the incubator. After that, the media were replaced by serum free media for overnight. The gels were detached from the sided of the wells with a scalpel and treated with TGF-β1 or left untreated for 48 h. The images were taken and the gel contraction was determined by measuring the surface area of the gels with Image J software. **(A)** a representative of gels containing transfected NOF after 48 h of TGF-β1 treatment. **(B)** the quantified of gels contraction, as a mean of surface area (mm^2) ± SEM from three independent experiments, compared to untreated miRNA negative control. Statistical analysis was determined using two-tailed Student T-test with ****$p < 0.0001$. The significance is compared to the untreated equivalent transfection, or anti-miR negative control, in the case of untreated anti-miRs. No significant difference between anti-miR negative control compared to anti-miRs in TGF-β1-treated NOF.

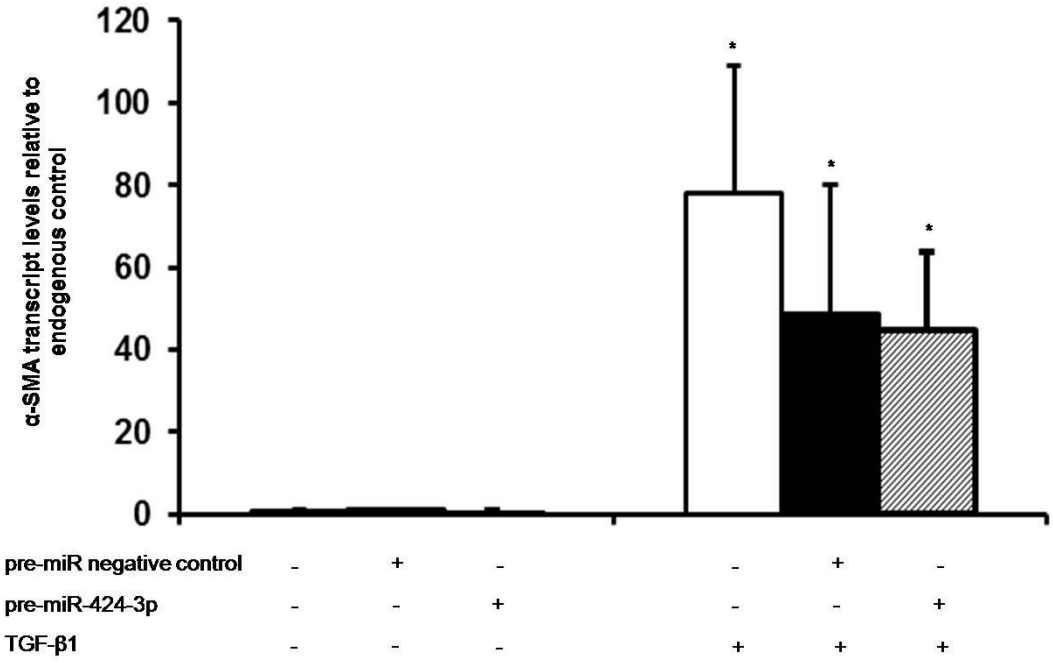

Figure 4.15: Overexpression of miR-424-3p did not inhibit TGF-β1 induced α-SMA expression in CAF

CAF were transiently transfected with pre-miR negative control or pre-miR-424-3p for 48 h. The transfected CAF were serum starved overnight before being treated with or without TGF-β1 for 48 h. Following treatment, CAF were harvested and subjected to RNA extraction and used for cDNA synthesis. The qRT-PCR analysis was done using primers designed to amplify α-SMA. B2M was used as a reference gene. Each data represents the mean relative quantification of myofibroblast differentiation markers relative to B2M ± SEM from three independent experiments, for each transfection with or without TGF-β1 compared to untreated pre-miR negative control. Statistical analysis was determined using two-tailed Student T-test with *p <0.05. The significance is compared to the untreated equivalent transfection, or pre-miR negative control, in the case of untreated pre-miR. No significant difference between pre-miR negative control compared to pre-miR-424-3p in TGF-β1-treated CAF.

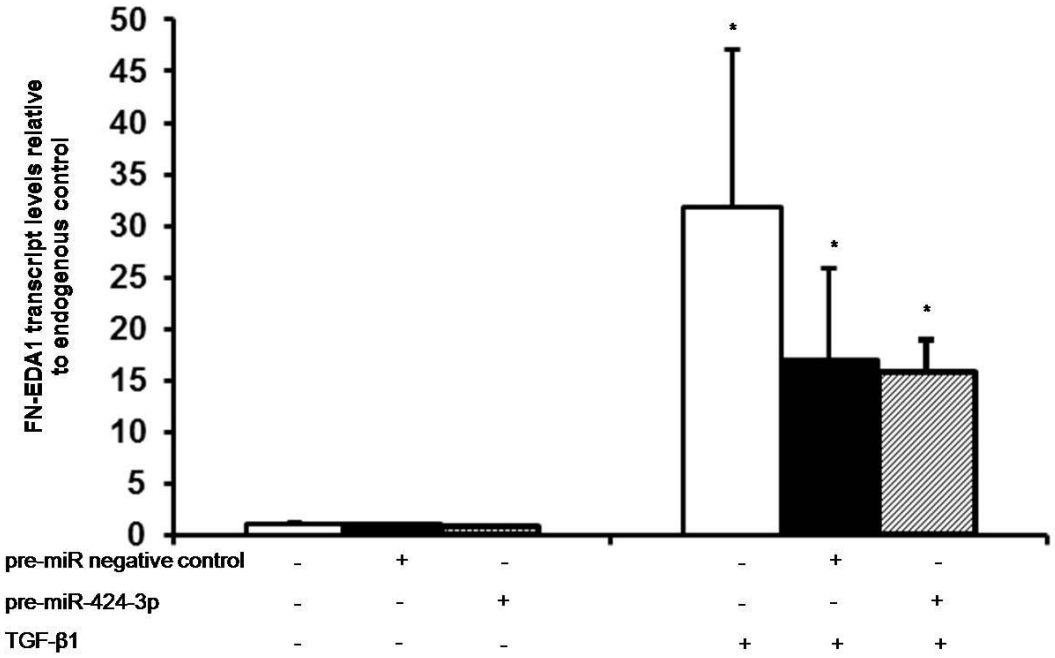

Figure 4.16: Overexpression of miR-424-3p did not inhibit TGF-β1 induced FN-EDA1 expression in CAF

CAF were transiently transfected with pre-miR negative control or pre-miR-424-3p for 48 h. The transfected CAF were serum starved overnight before being treated with or without TGF-β1 for 48 h. Following treatment, CAF were harvested and subjected to RNA extraction and used for cDNA synthesis. The qRT-PCR analysis was done using primers designed to amplify FN-EDA1. B2M was used as a reference gene. Each data represents the mean relative quantification of myofibroblast differentiation markers relative to B2M ± SEM from three independent experiments, for each transfection with or without TGF-β1 compared to untreated pre-miR negative control. Statistical analysis was determined using two-tailed Student T-test with *p <0.05. The significance is compared to the untreated equivalent transfection, or pre-miR negative control, in the case of untreated pre-miR. No significant difference between pre-miR negative control compared to pre-miR-424-3p in TGF-β1-treated CAF.

significantly increased COL1A1 transcript levels in mock (3.4±0.7-fold), pre-miR negative control (3.4±1.6-fold) and pre-miR-424-3p (2.9±1.1-fold). Overexpression of miR-424-3p caused a small decrease (not significant) in TGF-β1-induced COL1A1 gene expression (Figure 4.17).

4.2.11.2 Overexpression of miR-424-3p did not alter TGF-β1-induced α-SMA protein level in CAF

The effect of over-expressing miR-424-3p on α-SMA expression was also investigated at the protein level by measuring α-SMA abundance. CAF were transiently transfected with pre-miR negative control or pre-miR-424-3p for 48 h. Following incubation, they were serum starved overnight and treated with TGF-β1 or left untreated. CAF were harvested and subjected to protein extraction. The total protein lysates were used for western blotting. As shown in Figure 4.18, overexpression of miR-424-3p did not inhibit basal abundance of α-SMA at protein level in CAF. TGF-β1 slightly increased α-SMA protein level in all conditions, however, this not significant ($p<0.05$). Upregulation of miR-424-3p did not alter TGF-β1-induced α-SMA protein abundance, compared to treated pre-miR negative control.

4.2.11.3 Overexpression of miR-424-3p did not prevent the formation of TGF-β1-induced α-SMA positive stress fibres formation in CAF

To assess the effect of miR-424-3p overexpression on stress fibres formation, CAF were transiently transfected with a pre-miR negative control or pre-miR-424-3p for 48 h. TGF-β1 was added for 48 h and α-SMA immunocytochemistry was done to assess the formation of stress fibre in CAF. As shown in Figure 4.19 (A), overexpression of miR-424-3p did not inhibit basal formation of stress fibre in CAF. TGF-β1 promotes the formation of stress fibres, as seen by intense staining of the cytoskeleton in all

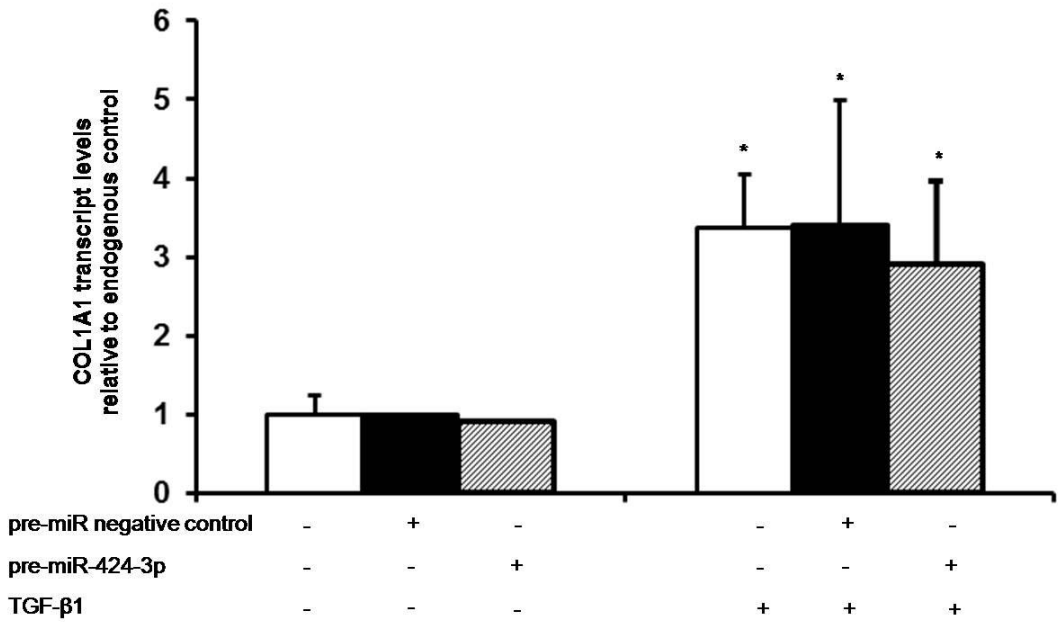

Figure 4.17: Overexpression of miR-424-3p did not inhibit TGF-β1 induced COL1A1 expression in CAF

CAF were transiently transfected with pre-miR negative control or pre-miR-424-3p for 48 h. The transfected CAF were serum starved overnight before being treated with or without TGF-β1 for 48 h. Following treatment, CAF were harvested and subjected to RNA extraction and used for cDNA synthesis. The qRT-PCR analysis was done using primers designed to amplify COL1A1. B2M was used as a reference gene. Each data represents the mean relative quantification of myofibroblast differentiation markers relative to B2M ± SEM from three independent experiments, for each transfection with or without TGF-β1 compared to untreated pre-miR negative control. Statistical analysis was determined using two-tailed Student T-test with *$p < 0.05$. The significance is compared to the untreated equivalent transfection, or pre-miR negative control, in the case of untreated pre-miR. No significant difference between pre-miR negative control compared to pre-miR-424-3p in TGF-β1-treated CAF.

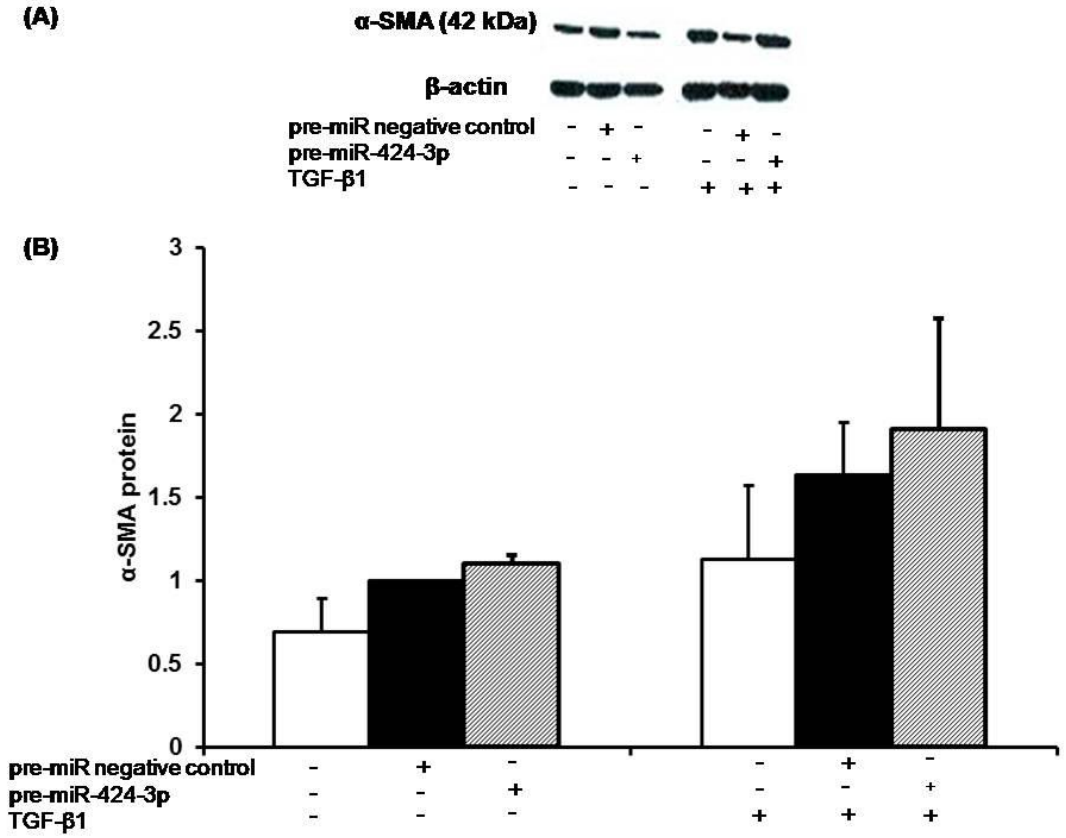

Figure 4.18: Overexpression of miR 424-3p did not alter TGF-β1 response of α-SMA protein abundance in CAF

CAF were transiently transfected with pre-miR negative control or pre-miR-424-3p for 48 h. Then, CAF were serum starved overnight and treated with or without TGF-β1 for 48 h. CAF were harvested and used for protein extraction. Total protein lysates were used for immunoblotting using antibodies from mouse α-SMA and β-actin as a loading control. **(A)** a representative of protein bands for immunoblot from three independent repeats, **(B)** the quantified amount of protein in each sample using Image J software. Each data represents the mean ± SEM from three independent experiments. The significance is compared to the untreated equivalent transfection, or pre-miR negative control, in the case of untreated pre-miR, none of these are significant, however. No significant difference between pre-miR negative control compared to pre-miR-424-3p in TGF-β1-treated CAF.

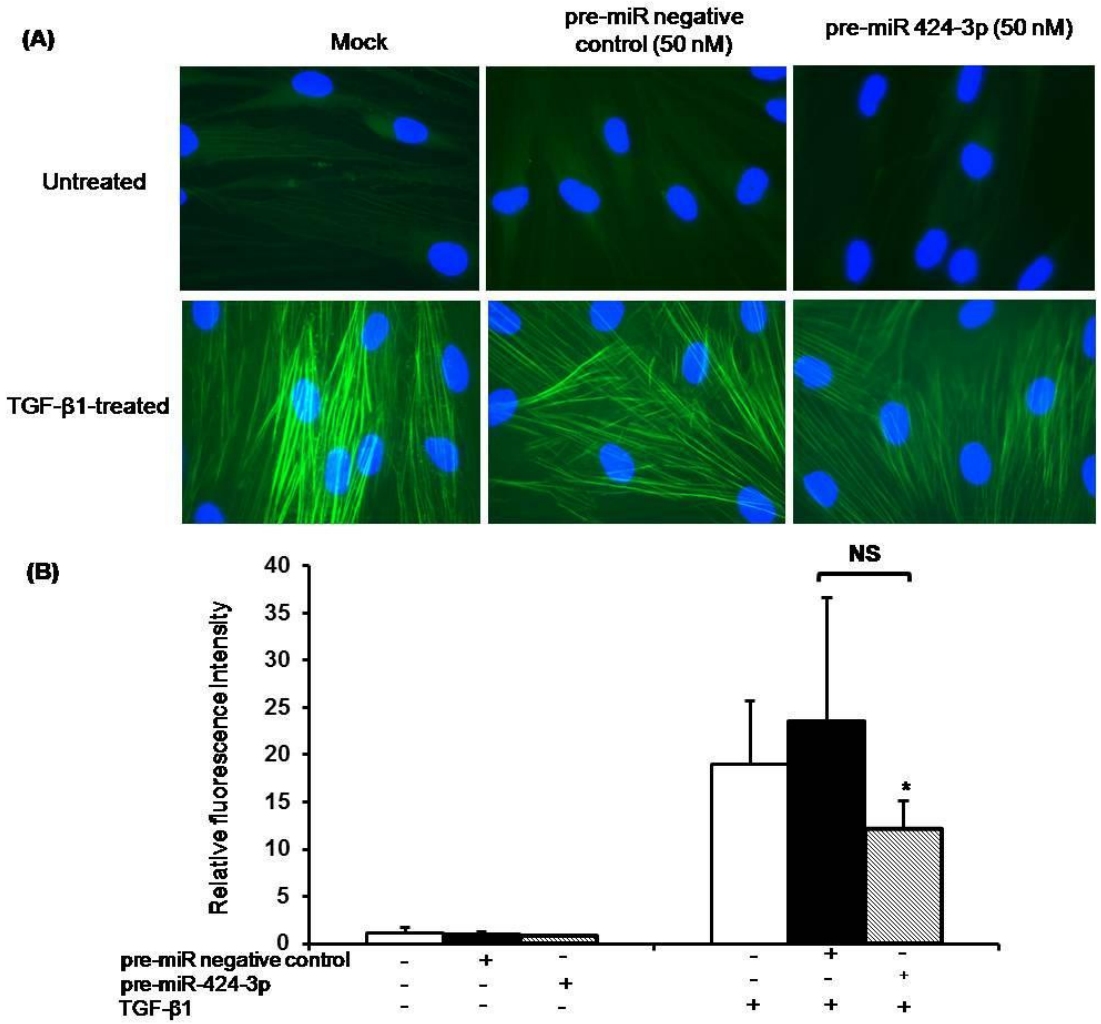

Figure 4.19: Overexpression of miR-424-3p did not prevents the formation of TGF-β1-induced α-SMA positive stress fibres formation in CAF

CAF were seeded onto coverslips overnight and transiently transfected with pre-miR negative control or pre-miR-424-3p for 48 h. Following that, CAF were serum starved overnight and treated with or without TGF-β1 for 48 h. The coverslips were washed with DPBS prior to fixation with 100 % methanol for 20 min. Then, they were permeabilised in 4 mM sodium deoxycholate for 10 min before being blocked with 2.5 % (w/v) BSA in DPBS for 30 min. The coverslips were incubated with a primary FITC-conjugated α-SMA antibody overnight at 4 ^{0}C. Following incubation, they were washed with DPBS and were mounted with Dapi. The coverslips were viewed under a fluorescence microscope using Pro-Plus 7.0 imaging software at 100x magnification (using oil immersion). **(A)** Representative images of stress fibre from three independent repeats. **(B)** The mean fluorescence intensity per cell ± SEM from three independent experiments was quantified using Image J software. Statistical analysis was determined using two-tailed Student T-test with *$p < 0.05$. If not shown by a bar, the significance is compared to the untreated equivalent transfection, or pre-miR negative control, in the case of untreated pre-miR.

conditions, whether transfected with pre-miRs or not. Transfection with pre-miR-424-3p did not significantly alter the response to TGF-β1 compared to either mock or pre-miR negative control. Overexpression of miR-424-3p attenuates TGF-β1–induced α-SMA positive stress fibre formation, however this did not reach significance (Figure 4.19 (B)).

4.2.11.4 Overexpression of miR-424-3p did not alter TGF-β1 response on gel contraction in CAF

To investigate the role of miR-424-3p in regulating TGF-β1-induced gel contraction, CAF were transiently transfected with a pre-miR negative control or a pre-miR-424-3p for 48 h. Transfected CAF were resuspended in a mixture of rat tail collagen 1 with DMEM (1:1). The mixture was allowed to polymerise, then treated with TGF-β1 or left untreated for 48 h. Overexpression of miR-424-3p did not inhibit basal gel contraction in CAF. TGF-β1 promotes gel contraction in CAF transfected with mock (312±26 mm^2), pre-miR negative control (313±62 mm^2) and pre-miR 424-3p (316±53 mm^2) (Figure 4.20). miR-424-3p overexpression had no effect on TGF-β1-induced gel contraction, compared to treated pre-miR negative control.

4.2.11.5 Knockdown of miR-145-5p or miR-424-3p did not alter TGF-β1-induced myofibroblast markers in CAF

An attempt to knockdown the miR-424-3p or miR-145-5p expression was next carried out. CAF were transiently transfected with a miR-424-3p inhibitor or a miR-145-5p inhibitor. A non-targeting inhibitor was used as a negative control and a mock transfection (transfection reagent only) was also included in this experiment. TGF-β1 was added to the culture after 48 h post-transfection. Transfected CAF were harvested for RNA extraction, protein extraction, and immunocytochemistry. Inhibition of miR-424-3p or miR-145-5p did not increase a basal expression of α-SMA and FN-EDA1 at

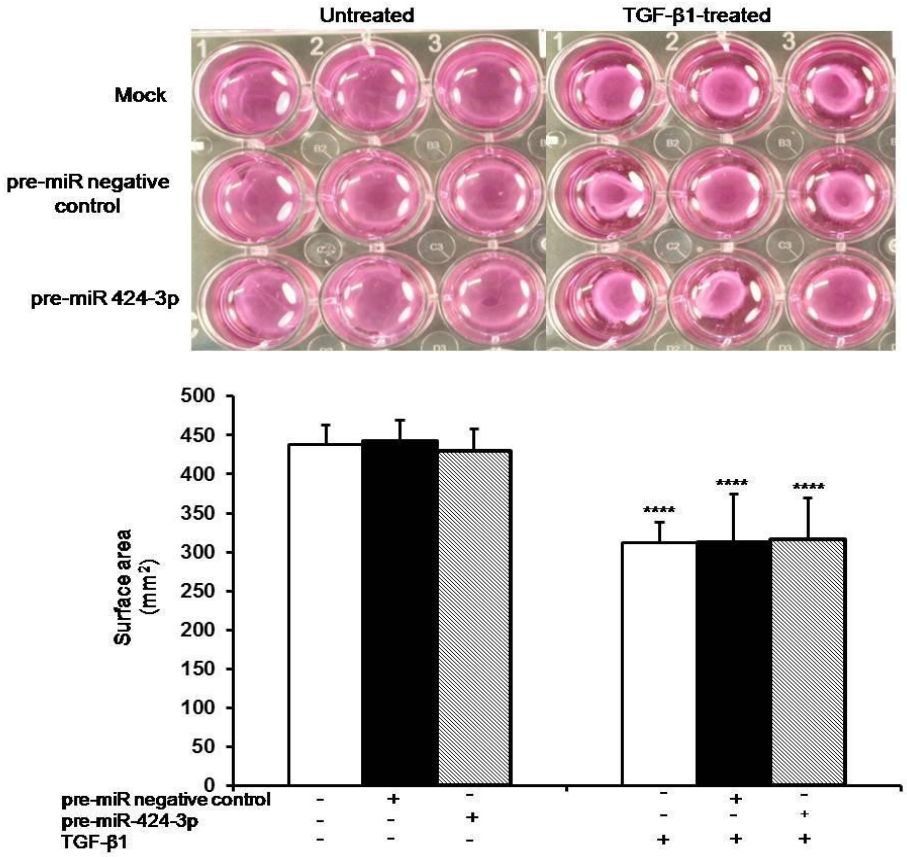

Figure 4.20: Overexpression of miR-424-3p had no effect on TGF-β1-induced gel contraction in CAF

CAF were transiently transfected with pre-miR negative control or pre-miR-424-3p for 48 h. Following incubation, CAF were harvested, counted (2.5 x 10^5 cells/well) and resuspended in a mixture of rat tail collagen 1 (in 0.1 M acetic acid) and DMEM (1:1). The pH was neutralised with 1M of NaOH and the mixture was aliquoted into wells (300 µl/well) and left to polymerise in an incubator at 37 ^{0}C with 5 % CO_2. After the gels had polymerised, media were added to each well and incubated for 4 h in the incubator. After that, the media were replaced by serum-free media for overnight. The gels were detached from the sided of the wells with a scalpel and treated with or without TGF-β1 for 48 h. The images were taken at 48 h and the gel contraction was determined by measuring the surface area of the gels with Image J software. **(A)** a representative of gels containing transfected CAF after 48 h of TGF-β1 treatment. **(B)** the quantified of gels contraction, as a surface area (mm^2) compared to untreated pre-miR negative control. Each data represents the mean ± SEM from three independent experiments. Statistical analysis was determined using two-tailed Student T-test with ****p <0.0001, as the significance is compared to the untreated equivalent transfection, or pre-miR negative control, in the case of untreated pre-miR. No significant difference between pre-miR negative control compared to pre-miR-424-3p in TGF-β1-treated CAF.

transcripts level in CAF. TGF-β1 treatment significantly increased α-SMA transcript levels in all conditions; mock (73.7±33.6-fold), negative control inhibitor (93.6±33.6-fold), anti-miR-145-5p (81.0±50.5-fold) and anti-miR-424-3p (62.4±33.3-fold) (Figure 4.21). Conversely, TGF-β1 treatment did not significantly increase FN-EDA1 transcripts levels in all conditions (Figure 4.22).

Inhibition of miR-424-3p or miR-145-5p did not increase a basal expression of COL1A1 at mRNA level. Meanwhile, treatment of TGF-β1 significantly resulted in increase of COL1A1 transcripts level in mock (3.6±1.4-fold) and anti-miR-424-3p (3.3±1.2-fold) (Figure 4.23). Knockdown of miR-424-3p did not result in increase of TGF-β1-induced myofibroblast differentiation markers, compared to treated negative control inhibitor. On the other hand, inhibition of miR-145-3p caused a small increase (but not significant) in TGF-β1-induced COL1A1 gene expression, compared to treated negative control inhibitor.

4.2.11.6 Knockdown of miR-424-3p or miR-145-5p did not alter TGF-β1-induced α-SMA protein level in CAF

Lastly, inhibition of miR-424-3p or miR-145-5p did not increase a basal abundance of α-SMA at protein level in CAF. TGF-β1 caused a small increase (not significant) in α-SMA at the protein level in mock (0.9±0.3-fold), anti-miR negative control (1.5±0.7-fold), anti-miR-145-5p inhibitor (1.2±0.4-fold) and anti-miR-424-3p (1±0.2-fold) (Figure 4.24). Knockdown of miR-424-3p or miR-145-5p did not alter TGF-β1-induced α-SMA at protein level, compared to treated negative control inhibitor.

4.2.11.7 Knockdown of miR-424-3p, not miR-145-5p, alter TGF-β1 response of positive stress fibres formation in CAF

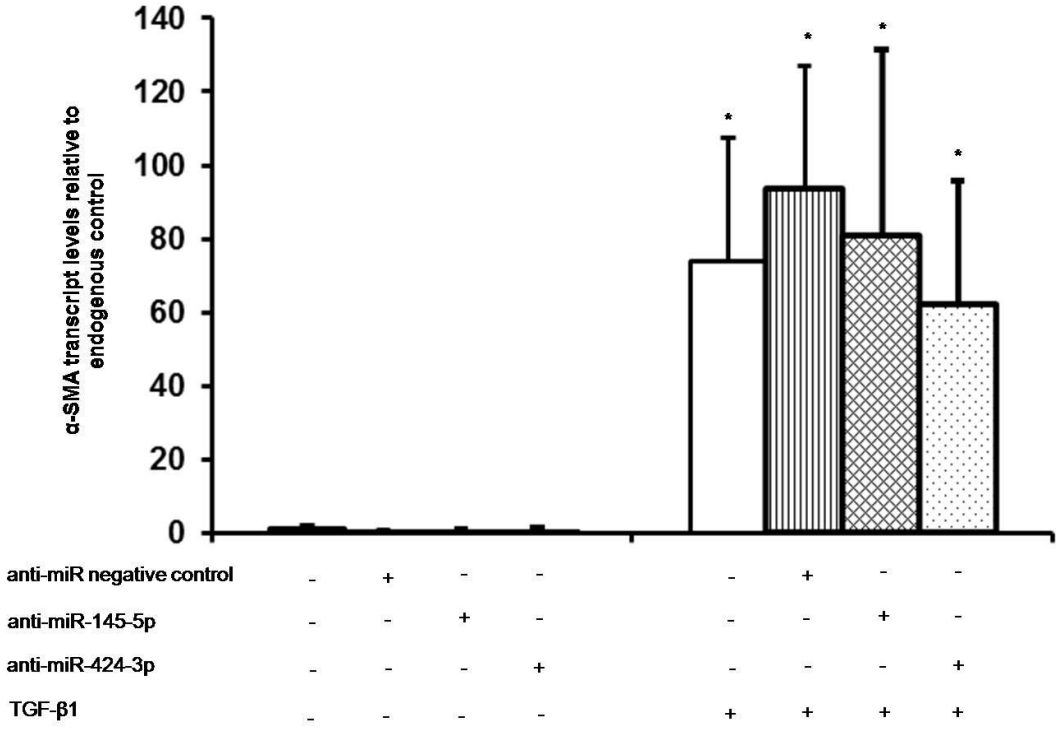

Figure 4.21: Inhibition of miR-424-3p or miR-145-5p did not alter TGF-β1-induced α-SMA expression in CAF

CAF were transiently transfected with negative control inhibitor or miR-424-3p inhibitor or miR 145-5p for 48 h. The transfected CAF were serum starved overnight before being treated with or without TGF-β1 for 48 h. Following treatment, CAF were harvested and subjected to RNA extraction and used for cDNA synthesis. The qRT-PCR analysis was done using primers designed to amplify αSMA. B2M was used as a reference gene. Each data represents the mean relative quantification of myofibroblast differentiation markers relative to B2M ± SEM from three independent experiments, for each transfection with or without TGF-β1 compared to untreated negative control inhibitor. Statistical analysis was determined using two-tailed Student T-test with *p <0.05, as the significance is compared to the untreated equivalent transfection, or anti-miR negative control, in the case of untreated anti-miRs. No significant difference between anti-miR negative control compared to anti-miRs in TGF-β1-treated CAF.

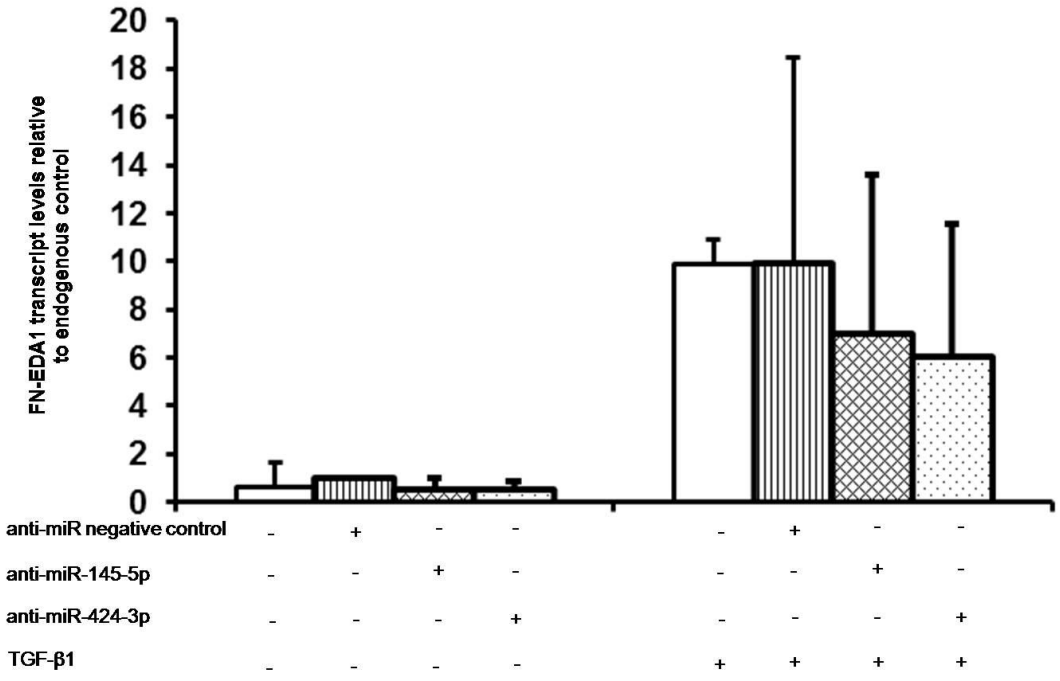

Figure 4.22: Inhibition of miR-424-3p or miR-145-5p did not alter TGF-β1-induced FN-EDA1 expression in CAF

CAF were transiently transfected with negative control inhibitor or miR-424-3p inhibitor or miR 145-5p for 48 h. The transfected CAF were serum starved overnight before being treated with or without TGF-β1 for 48 h. Following treatment, CAF were harvested and subjected to RNA extraction and used for cDNA synthesis. The qRT-PCR analysis was done using primers designed to amplify FN-EDA1. B2M was used as a reference gene. Each data represents the mean relative quantification of myofibroblast differentiation markers relative to B2M ± SEM from three independent experiments, for each transfection with or without TGF-β1 compared to untreated negative control inhibitor. Statistical analysis was determined using two-tailed Student T-test, as the significance is compared to the untreated equivalent transfection, or anti-miR negative control, in the case of untreated anti-miRs, none of these are significant, however. No significant difference between anti-miR negative control compared to anti-miRs in TGF-β1-treated CAF.

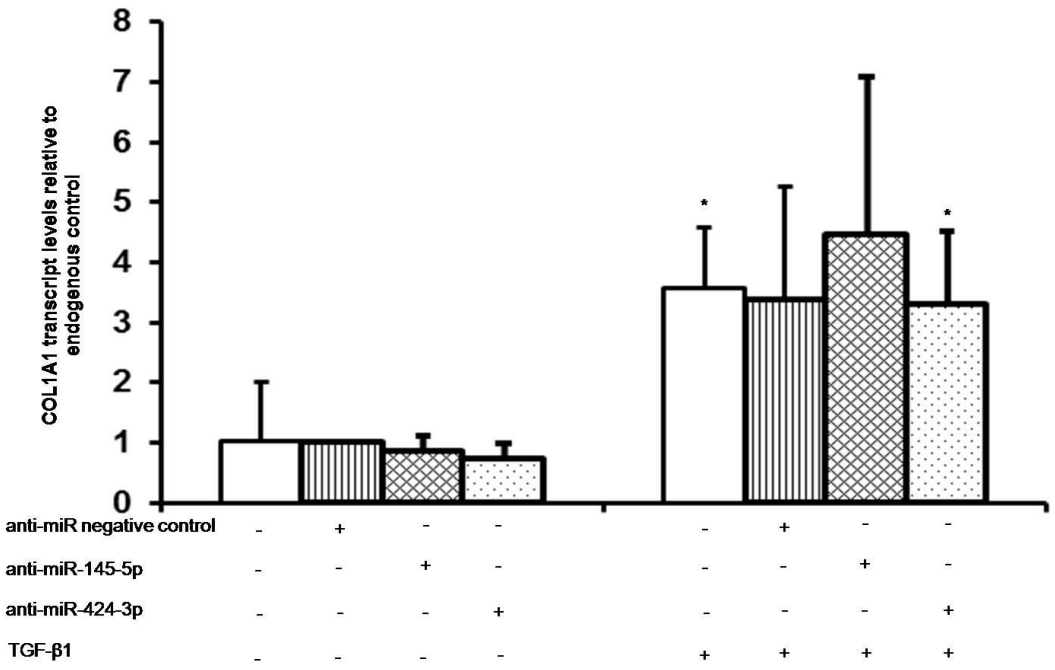

Figure 4.23: Inhibition of miR-424-3p had no effect on TGF-β1-induced COL1A1 expression while knockdown of miR-145-5p did not increases TGF-β1-induced COL1A1 expression in CAF

CAF were transiently transfected with negative control inhibitor or miR-424-3p inhibitor or miR 145-5p for 48 h. The transfected CAF were serum starved overnight before being treated with or without TGF-β1 for 48 h. Following treatment, CAF were harvested and subjected to RNA extraction and used for cDNA synthesis. The qRT-PCR analysis was done using primers designed to amplify COL1A1. B2M was used as a reference gene. Each data represents the mean relative quantification of myofibroblast differentiation markers relative to B2M ± SEM from three independent experiments, for each transfection with or without TGF-β1 compared to untreated negative control inhibitor. Statistical analysis was determined using two-tailed Student T-test with $*p < 0.05$, as the significance is compared to the untreated equivalent transfection, or anti-miR negative control, in the case of untreated anti-miRs. No significant difference between anti-miR negative control compared to anti-miRs in TGF-β1-treated CAF.

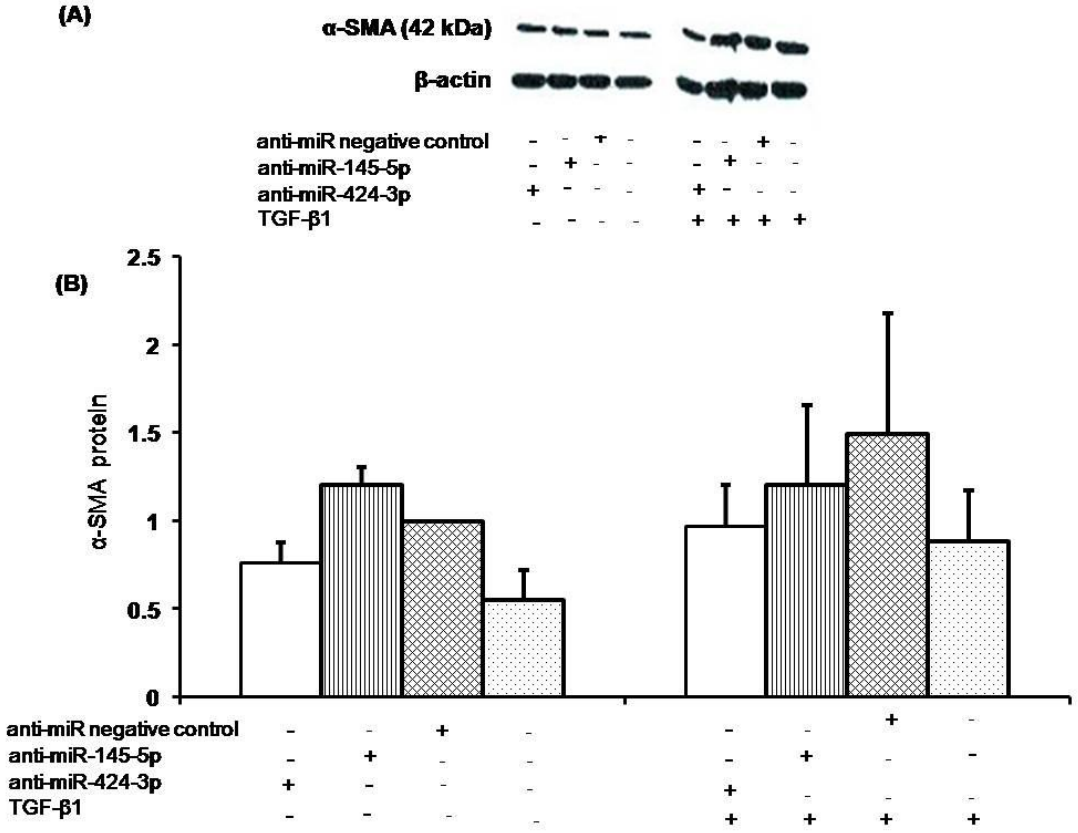

Figure 4.24: Inhibition of miR 424-3p or miR-145-5p did not alter TGF-β1-induced α-SMA protein abundance in CAF

CAF were transiently transfected with negative control inhibitor or miR-424-3p inhibitor or miR-145-5p inhibitor for 48 h. Then, CAF were serum starved overnight and treated with or without TGF-β1 for 48 h. CAF were harvested and used for protein extraction. Total protein lysates were used for immunoblotting using antibodies from mouse α-SMA and β-actin as a loading control. **(A)** a representative of protein bands for immunoblot from three independent repeats, **(B)** the quantified amount of protein in each sample using Image J software. Each data represents the mean ± SEM from three independent experiments. No significant difference between untreated equivalent transfection or anti-miR negative control, in the case of untreated anti-miRs or anti-miR negative control compared to anti-miRs in TGF-β1-treated CAF.

Immunocytochemistry revealed that inhibition of miR-424-3p or miR-145-5p did not increase basal formation of α-SMA positive stress fibre in CAF. TGF-β1 provokes α-SMA positive stress fibre formation in CAF, as seen by the striking increase in cytoskeletal fluorescent staining evident in all conditions following TGF-β1 treatment; mock (35.4±6.7-fold), anti-miR negative control (23.7±3.1-fold), anti-miR-145-5p (22.0±4.1-fold) and anti-miR-424-3p (12.0±0.8-fold) (Figure 4.25 (A)). In this study, the formation of α-SMA positive stress fibres was greater in CAF compared to that in NOF in response to TGF-β1. This is consistent with a previous study (Yang *et al*., 2014) which showed that CAF (from gastric cancer tissue) expressed a high level of α-SMA positive stress fibre, compared to NOF (from normal gastric mucosa). Inhibition of miR-424-3p, not miR-145-5p alter TGF-β1-induced α-SMA positive stress fibre formation, compared to treated negative control inhibitor (Figure 4.25 (B)).

4.2.11.8 Knockdown of miR-424-3p decreases TGF-β1-induced gel contraction; while miR-145-5p increases TGF-β1-induced gel contraction in CAF

As shown in Figure 4.26, Inhibition of miR-424-3p or miR-145-5p did not alter basal gel contraction in CAF. TGF-β1 significantly increased gel contraction in CAF transfected with; mock (312±26 mm2; $p<0.0001$), negative control inhibitor (337±44 mm^2; $p<0.0001$), miR-424-3p inhibitor (388±51 mm^2; not significant) and miR-145-5p inhibitor (304±40 mm^2; $p<0.0001$). Inhibition of miR-424-3p decreases TGF-β1 effects on gel contraction, compared to treated negative control inhibitor while inhibition of miR-145-5p increases TGF-β1-induced gel contraction, compared to treated negative control.

4.3 Discussion

While many studies focused on the important role of CAF in promoting tumour

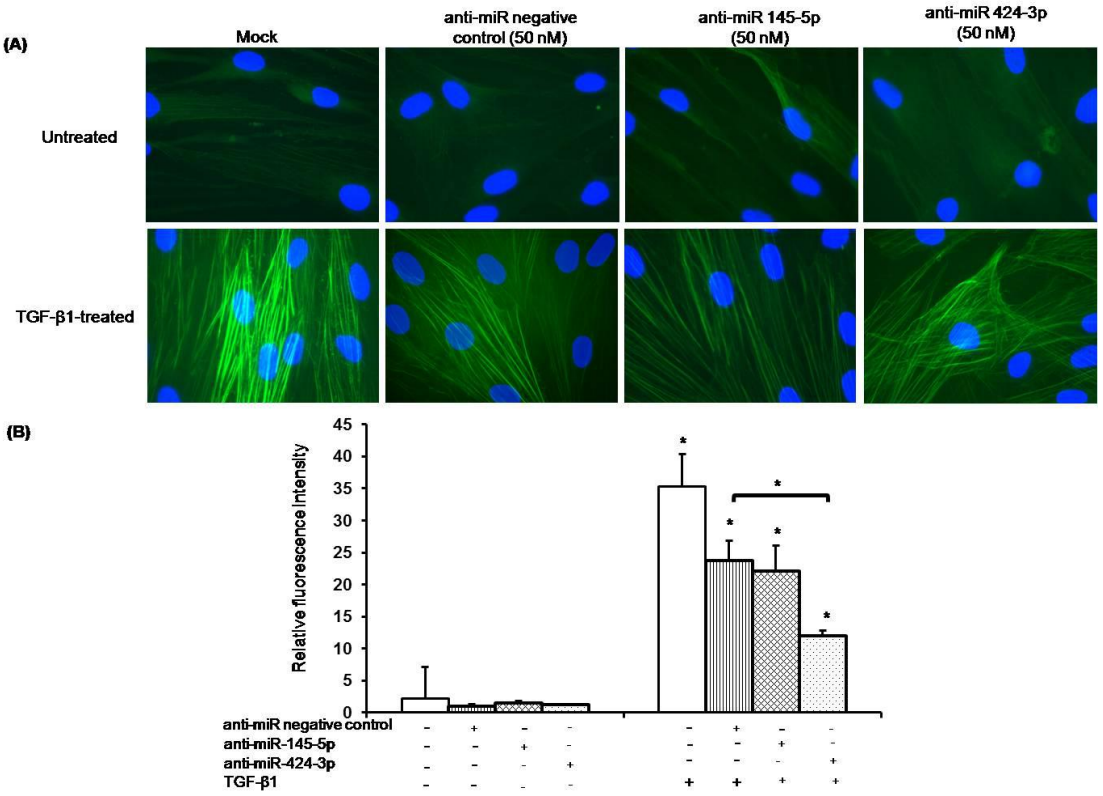

Figure 4.25: Inhibition of miR-424-3p, not miR-145-5p decreases TGF-β1-induced α-SMA positive stress fibres formation in CAF

CAF were seeded onto coverslips overnight and transiently transfected with negative control inhibitor or miR-424-3p inhibitor or miR-145-5p inhibitor for 48 h. Following that, CAF were serum starved overnight and treated with TGF-β1 for 48 h. The coverslips were washed with DPBS prior to fixation with 100 % methanol for 20 min. Then, they were permeabilised in 4 mM sodium deoxycholate for 10 min before being blocked with 2.5 % (w/v) BSA in DPBS for 30 min. The coverslips were incubated with a primary FITC-conjugated α-SMA antibody overnight at 4 ^{0}C. Following incubation, they were washed with DPBS and were mounted with Dapi. The coverslips were viewed under a fluorescence microscope using Pro-Plus 7.0 imaging software at 100x magnification (using oil immersion). **(A)** Representative images of stress fibre from three repeats. **(B)** The mean fluorescence intensity per cell ± SEM from three independent experiments was quantified using Image J software. Statistical analysis was determined using two-tailed Student T-test with *p <0.05. If not shown by a bar, the significance is compared to the untreated equivalent transfection, or anti-miR negative control, in the case of untreated anti-miRs. No significant difference between anti-miR negative control compared to anti-miR-145-5p in TGF-β1-treated CAF.

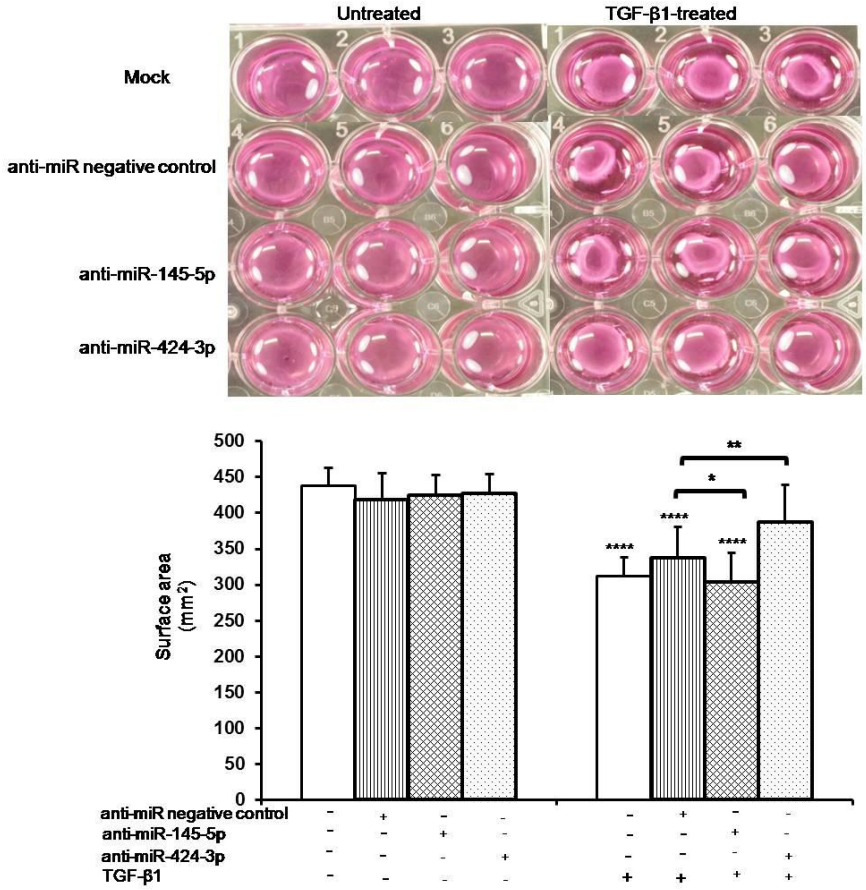

Figure 4.26: Inhibition of miR-424-3p decreases TGF-β1-induced gel contraction; while miR-145-5p increases TGF-β1-induced gel contraction in CAF

CAF were transiently transfected with negative control inhibitor or miR-424-3p inhibitor or miR-145-5p inhibitor for 48 h. Following incubation, the CAF were harvested, counted (2.5 x 10^5 cells/well) and resuspended in a mixture of rat tail collagen 1 (in 0.1 M acetic acid) and DMEM (1:1). The pH was neutralised with 1M of NaOH and the mixture was aliquoted into wells (300 µl/well) and left to polymerise in an incubator at 37 ^{0}C with 5 % CO_2. After the gels had polymerised, media were added to each well and incubated for 4 h in the incubator. After that, the media were replaced by serum-free media for overnight. The gels were detached from the sided of the wells with a scalpel and treated with or without TGF-β1 for 48 h. The images were taken at 48 h and the gel contraction was determined by measuring the surface area of the gels with Image J software. **(A)** a representative of gels containing transfected CAF after 48 h of TGF-β1 treatment. **(B)** the quantified of gels contraction, as a mean of surface area (mm^2) ± SEM from three independent experiments, compared to untreated miRNA negative control. Statistical analysis was determined using two-tailed Student T-test with *p <0.05, **p< 0.005, ****p <0.0001. If not shown by a bar, the significance is compared to the untreated equivalent transfection, or anti-miR negative control, in the case of untreated anti-miRs.

progression, little is known about the role of miRNAs in CAF. As stated in Section 1.10.3, deregulation of miRNAs was observed in CAF from various type of cancer including ovarian cancer (Mitra *et al*., 2012; Tang *et al*., 2016) and breast cancer (Zhao *et al*., 2012). Little is known, however, of the role of miRNA in determining CAF phenotype in oral cancer.

miRNA expression profiling by TLDA here provides evidence that miR-424-5p and miR-145-5p were highly upregulated in two TGF-β1-treated primary oral fibroblasts isolated from healthy subjects, NOF1 and NOF5. Validation by qRT-PCR further supported these findings. Validation of miR-424-3p was done in NOF804, however, the expression of miR-424-3p could not be validated in NOF1 and NOF5. Similar to NOF1 (as mentioned in Chapter 3), NOF5 became slow growing and died. As a result, a newly derived NOF culture, NOF804, was mostly used for the experiments functionally interrogating the role of candidate miRNA throughout this study. The TLDA data showed that miR-424-3p, but not miR-424-5p, is highly upregulated in NOF804 upon TGF-β1 treatment. Validation by qRT-PCR confirmed this finding, although the fold change was lower than that identified by TLDA. However, it still follows the miRNA expression pattern detected in the TLDA. The difference in the fold change between the qPCR and the TLDA screen might reflect the fact that the TLDA screen was carried on one sample, whereas the qPCR validation was carried out in three biological repeats. From the TLDA data, miR-145-5p was found to be downregulated in NOF804 cells, contradicting the findings in the other two NOF cultures (NOF1 and NOF5). This result perhaps indicates the heterogeneity of miRNA expression in NOF cultures derived from slightly different areas in the mouth, or might result from patient-to-patient variability. Given the that miR-145-5p was found to be upregulated by TGF-β1 treatment in two of three cultures, however, and has been reported in other tissues to be involved in

myofibroblast differentiation, this was selected for further functional analyses alongside miR-424-3p.

Two widely employed approaches to study endogenous miRNA function; the introduction to cells of miRNA mimics (gain-of-function) and miRNA inhibitors (loss-of-function) were used in this study. miRNA mimics are chemically modified double-stranded RNA molecules that are processed by cells' endogenous machinery to produce mature miRNAs able to post-transcriptionally repress target genes. Conversely, miRNA inhibitors are chemically modified single-stranded RNA molecules that complementary bind to specific miRNAs (no RISC-like complex association), abrogating their ability to bind to target genes and regulate their expression.

Increasing evidence has recently accumulated about a role for miR-424 in cancers. miR-424-5p expression was decreased in liver cancer tissue compared to normal liver tissue and this downregulation was associated with advanced disease progression in liver cancer patients (Zhang *et al*., 2014). Conversely, Wu and co-workers (2013) demonstrated that miR-424-5p was significantly upregulated in pancreatic cancer. Despite these findings, little is known about the involvement of miR-424 in the tumour microenvironment. Only one study, published in the course of this project, reported that miR-424 potentiates TGF-β-induced myofibroblast differentiation through EMT in human lung epithelial cells (Xiao *et al.*, 2015). Inspection of online databases employing target prediction algorithms, such as TargetScan (http://www.targetscan.org/vert_71/), identified multiple predicted targets of miR-424 in TGF-β signalling. Some of these predicted targets have been verified in the previous studies, including Smurf2 (Xiao *et al*., 2015) and Smad7 (Wang *et al*., 2016). miR-145 has been demonstrated to negatively regulate TGF-β signalling through Smad3 and TGF-βR2 (Megiorni *et al*., 2013; Yang *et al*., 2013). TGF-β1 has been reported to induce miR-143/5 expression, suggesting that

miR-145 could be part of TGF-β pathway (Long and Miano, 2011). miR-145 has been reported in specialised differentiation e.g the gut epithelial and smooth muscle cell maturation (Zeng, Carter, & Childs, 2009). Yang *et al*., (2011) demonstrated that the loss of miR-145 in chondrocyte differentiation, as it directly targets Sox-9, a critical transcription factor in chondrogenesis.

The present study analysed the functional relevance of miR-424-3p or miR-145-5p in TGF-β1-induced eCAF and tumour-derived CAF, with aim of determining whether these miRNAs contribute to the development of the myofibroblast eCAF phenotype decribed in Chapter 3, and by extension the in vivo CAF phenotype. To determine the involvement of these miRNA in reprogramming normal fibroblast into eCAF, NOF and CAF were transfected with miRNA mimic or miRNA inhibitors prior to TGF-β1 treatment. Experiments were then carried out to assess the impact of this on the myofibroblastic phenotypes of eCAF and tumour-derived CAF.

α-SMA is a well-established molecular marker for myofibroblast differentiation. Therefore, α-SMA regulation has been widely studied, particularly at the transcriptional level (Hinz *et al*., 2012). As anticipated, TGF-β1 increased α-SMA expression at both mRNA and protein level in mock transfected NOF. This upregulation was significantly decreased by pretreatment with pre-miR-424-3p at mRNA level. However, overexpression of miR-424-3p did not alter TGF-β1-induced α-SMA protein abundance in NOF; the reasons for this are unclear but perhaps relate to the time-course of this experiment, or perhaps the existence of a compensatory mechanism.

Myofibroblast differentiation requires the combined action of α-SMA, TGF-β1 and FN-EDA1 (Tomasek *et al*., 2002; Gabbiani, 2003; Hinz *et al*., 2007). The early study demonstrated that FN-EDA1 is crucial for the TGF-β1-induced myofibroblastic phenotype (Serini *et al*., 1998). As shown in Section 3.2.2, the increase in FN-EDA1 in

response to TGF-β1 in mock transfected cells is of a similar magnitude as in untransfected NOF, suggesting the transfection procedure did not affect the cell's ability to respond to TGF-β1. Similar to α-SMA, miR-424-3p overexpression significantly attenuates TGF-β1-induced FN-EDA1 transcript levels in NOF. On the other hand, treatment with TGF-β1 did not significantly increase COL1A1 transcript levels in NOF. Moreover, overexpression of miR-424-3p did not inhibit COL1A1 expression in NOF.

The data above suggest that miR-424-3p has the ability to modulate α-SMA and FN-EDA1 expression but not COL1A1. Some studies have identified regulators of α-SMA transcription. Smad3, a major Smad mediator associated with TGF-β signaling, induces α-SMA expression by directly binding to two CAGA motifs of Smad3-binding elements (SBEs), in the promoter of of the α-SMA gene (Hu *et al*., 2003). Fibronectin binds to a large number of growth factors such as TGF-β (Klingberg *et al*., 2013), VEGF (Wijelath *et al*., 2006), HGF (Rahman *et al*., 2005), and PDGF (Smith *et al*., 2009); all of these may contribute to myofibroblast phenotype. Although FN-EDA1 is associated with myofibroblast differentiation, the mechanisms underlying this are poorly understood. Kohan *et al*., (2010) demonstrated that increased FN-EDA1 is sufficient to promote fibroblast differentiation by binding to α4β7 integrin receptor, followed by activation of MAPK/Erk1/2-dependent signalling. *In vivo* (a rat excisional model of wound repair) and *in vitro* (TGFβ1-treated rat fibroblast) studies demonstrated that FN-EDA deposition occurs before α-SMA expression (Serini *et al*., 1998). These findings suggest that FN-EDA deposition occurs through FN-EDA-cell surface receptor interactions that could transmit signals initiated by TGF-β1 and/or synergise with them and act as mediator for the induction of myofibroblast phenotype along with α-SMA expression. Collagen type 1, the native component of ECM, is encoded by two genes; COL1A1 and COL1A2 (Karsenty *et al*., 1991). The synthesis of these two collagens is controlled by TGF-β1

signalling pathway and Smad signalling pathway (Cutroneo *et al*., 2007). TGF-β1 regulates COL1A1 expression by binding directly to TGF-β *cis*-element located between -174 and -84 bp from the transcription start site (Jimenez *et al*., 1994). Taken together, these three genes are regulated by different pathways, therefore, miR-424-3p might target a component of one pathway, but not the other. Furthermore, computational prediction using TargetScan revealed that miR-424-3p is not predicted to directly target α-SMA, FN-EDA1 and COL1A1, suggesting that the regulation of these genes by miR-424-3p may occur via modulation of upstream TGF-β signalling. As seen with untransfected NOF in Chapter 3 (Section 3.2.4), NOF transfected with control, non-targeting oligonucleotides displayed intense cytoskeleton staining associated with elevated α-SMA expression after TGF-β1 treatment, suggesting that the transfection procedure does not alter the cells' ability to respond to TGF-β1. However, the α-SMA positive stress fibres formation was not significantly reduced when NOF were transfected with pre-miR-424-3p and subsequently exposed to TGF-β1.

α-SMA is important in the generation of contractile force in myofibroblasts (Cutroneo *et al*., 2007). Moreover, α-SMA positive myofibroblast contracts more compared to α-SMA negative myofibroblast, as demonstrated using stress-released collagen gels (Hinz *et al*., 2001). How α-SMA regulates the contractility of myofibroblasts remains unclear. However, it was proposed that α-SMA was incorporated into actin stress fibres, thereby increased in contractility of myofibroblasts (Hinz *et al*., 2001). In this study, TGF-β1 significantly increased gel contraction in mock transfected, control transfected and pre-miR-424-3p transfected NOF. Overexpression of miR-424-3p, however, significantly reduced ($p<0.005$) TGF-β1-induced gel contraction, in keeping with the finding that it is able to suppress α-SMA induction.

Collectively, these data demonstrated that miR-424-3p inhibits CAF-like

myofibroblastic phenotype, possibly through a negative feedback loop with TGF-β1. *In silico* pathway analysis indicates that miR-424-3p may target genes related to cell cycle including Cyclin D, CDK2, and CDK6, suggesting that miR-424-3p may play a role in modulating myofibroblast phenotype thtrough a negative feedback loop with TGF-β1. TGF-β induces reorganisation of actin cytoskeleton (a feature of myofibroblast phenotype) through activation of non-Smad pathway, a Rho GTPase signalling (Carthy, 2017). TGF-β induced Rho GTPase in human gingival fibroblasts (Smith *et al*., 2006), human lung fibroblasts (Watts *et al*., 2006) and mouse Swiss3T3 fibroblasts (Vardouli *et al*., 2005), with most studies focused on RhoA (Johnson *et al*., 2014; Manickam *et al*., 2014). The molecular mechanisms underlying TGF-β-induced Rho activation are poorly understood. RhoA/p160ROCK pathway involves in the formation of stress fibre and induction of EMT (Bhowmick *et al*., 2003) and myofibroblast differentiation (Smith *et al*., 2006). However, how TGF-β regulates G1 of cell cycle phase through RhoA/p160ROCK pathway in fibroblasts remains elusive. Bhowmick *et al*., (2003) demonstrated that RhoA and its effector kinase, p160ROCK directly bind and further, prevent the activity of CDC25A to promote cell cycle arrest in TGF-β-treated epithelial cells, but not fibroblasts. Additionally, they demonstrated that TGF-β induces p160ROCK of nuclear translocation in NMuMG epithelial cells and this relocalisation elevates level of phosphorylated CDC25A and inhibits CDC25A phosphatase activity. Interestingly, some miR-16 family including miR-424 targets CDC25A, probably due to its own growth inhibitory effects (Rissland *et al*., 2011). CDC25A activates CDKs, particularly CDK2 (predicted target gene of miR-424-3p) by dephosphorylating threonine and tyrosine phosphor residues on CDK2 (Gu *et al*., 1992). On the other hand, RhoA can regulate Cyclin D (miR-424-3p target gene), a positive regulator of G1 cell cycle phase (Sherr and Roberts, 1999). Cyclin D1 transcripts level is increased in lung fibroblast-derived from idiophatic pulmonary fibrosis, compared to normal lung

fibroblast cell (Watts *et al*., 2006). Interestingly, TGF-β1 further augments Cyclin D1 expression at mRNA and protein level, suggesting that TGF-β1 can mediate Cyclin D expression in fibroblasts. Additionally, inhibition of RhoA using both dominant negative RhoA transfection and simvastat (a pharmacological inhibitor) decreases Cyclin D1 expression in lung fibroblasts. Cyclin D associates with CDK4/6 to promote G1 phase. However, the phosphorylation of this complex can be inhibited by regulation of CDK inhibitors including p15, one of INK4 family members (Sherr and Roberts, 1999). Collectively, these findings contribute to a diverse dimension of TGF-β signalling complexity and subsequent cell cycle arrest. In this study, overexpression of miR-424-3p prevents TGF-β1-induced contraction in NOF and this might reflect a role of miR-424-3p in CAF-like myofibroblast differentiation by regulating one or more pathways related to cell cycle. The proposed signalling pathways (mentioned above) indicating how miR-424-3p may regulates, at least in part, of TGF-β1-induced CAF-like myofibroblastic phenotype (e.g actin cytoskeleton reorganisation) related to cell cycle regulation were illustrated in Figure 4.27.

Members of TGF-β superfamily are implicated in many cellular processes such as differentiation, apoptosis and proliferation (Siegel and Massague, 2003). In normal epithelial cells, TGF-β1 acts as a potent growth inhibitor, however, it has also mitogenic activity in some fibroblasts-derived cell line including NIH 3T3 (Koskinen *et al*., 1991). The anti-proliferative effect of TGF-β involves certain regulators of G1 phase of cell cycle, whose gene expression is mediated by Smad signalling (Massague, 2004). In canonical Smad signalling, the binding of TGF-β receptors by TGF-β superfamily phosphorylates Smad2 and Smad3. Once phosphorylated, Smad2/3 bind to Smad4 (a co-mediator Smad) and in the nucleus, the heteromeric complex together with FoxO, p53 and Sp1 to induce a cell cycle inhibitor, p21 (Pardali *et al*., 2000; Cordenonsi *et al*., 2003;

Seoane *et al*., 2004). p21 directly binds to active Cyclin D-CDK6 and Cyclin E-CDK2 complexes and inhibits their kinase activity, thereby caused cell cycle arrest (Geng and Weinberg, 1993; Koff *et al*., 1993). Taken together, this study suggested that miR-424-3p negatively regulating the pro-tumourigenic properties of stromal fibroblasts by two distinct but interrelated signalling pathways; regulation of Smad activation at the first place, and subsequent regulation of cell cycle by Smads. However, further experimental data are needed to test this hypothesis, particularly testing the effect of miR-424-3p modulation on proliferation.

Given that TGF-β1 upregulates miR-424-3p and miR-145-5p in NOF, an attempt to inhibit miR-424-3p expression or miR-145-5p expression was carried out in NOF. As seen with untransfected NOF in Section 3.2.1 and 3.2.2, mock transfected NOF displayed increased α-SMA, FN-EDA1 and COL1A1 transcript levels when treated with TGF-β1. In addition, TGF-β1 also promoted other expected phenotypic and morphological changes (stress fibre formation, gel contraction and α-SMA protein expression) in mock and control oligonucleotide transfected cells, as expected. However, inhibition of miR-424-3p did not further increase these effects when NOF were exposed to TGF-β1 and miR-424-3p inhibitor in combination for 48 h. Similar results were observed when NOF were exposed to miR-145-5p inhibitor and TGF-β1 in combination. Given that the data previously described indicates that fibroblasts express both of these miRNA, and that overexpression of miR-424-3p suppressed features of myofibroblast differentiation, it was expected that inhibition of this miRNA might increase expression of myofibroblast markers in response to TGF-β1. There are possible reasons that may explain why this result was not obtained. Given that one miRNA regulates many mRNAs and many miRNAs can regulate one mRNA (Zhang *et al*., 2014), the synergistic action of multiple miRNAs may be important for the regulation of target gene. Perhaps, several miRNAs

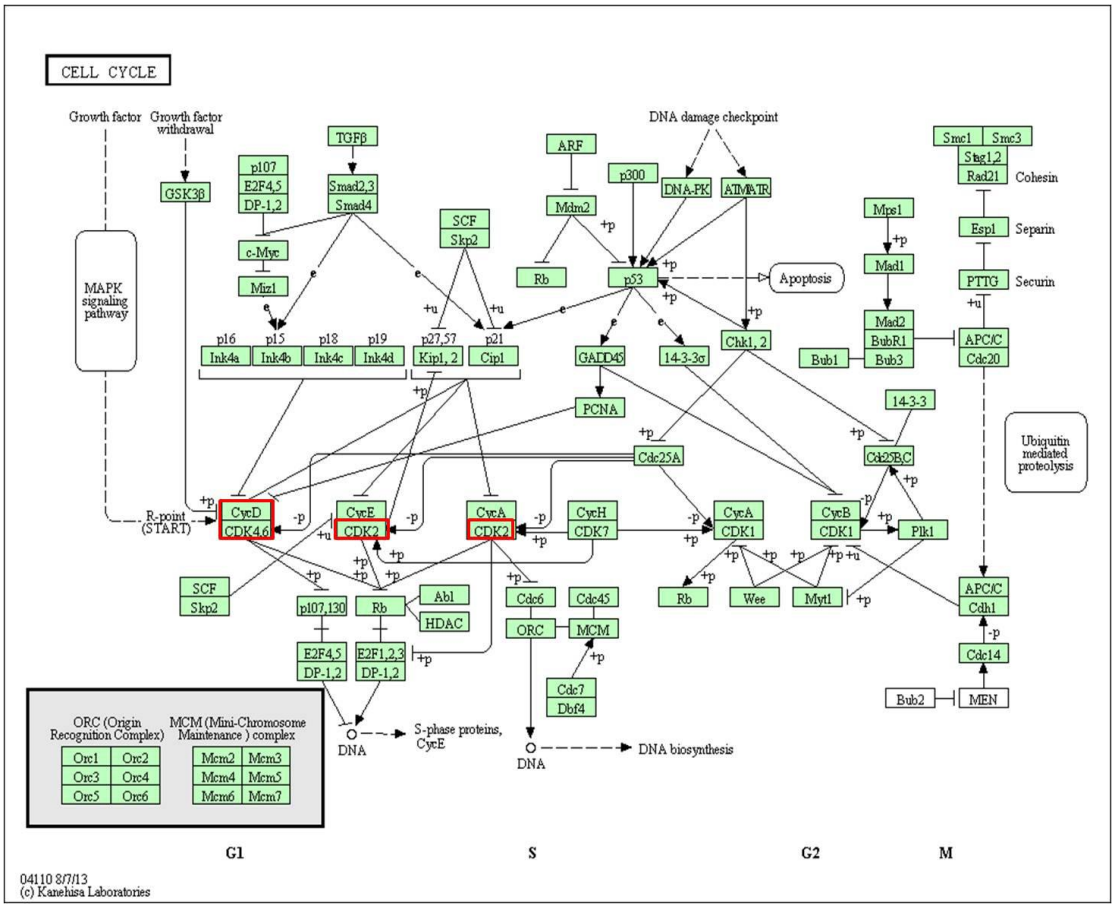

Figure 4.27: miR-424-3p targets genes related to G1 of cell cycle phase

The Kyoto Encyclopedia of genes and genomes (KEGG) pathway analysis of miR-424-3p target genes predicted by miRPath v3.0. miR-424-3p targets genes related to cell cycle; Cyclin D, CDK2, and CDK6. The highlighted red boxes indicate miR-424-3p target genes in G1 of cell cycle phase.

have mild suppressive activities on several different genes, which when combined have an effect on cell phenotype, and therefore just modulating the endogenous expression level of one miRNA in a loss of function assay doesn't have a measurable effect. It is also possible that the response of the fibroblasts to TGF-β1 is maximal under the conditions used, and while it may be inhibited by overexpression of miR-424-3p, inhibition of endogenous activity of this miRNA is unable to further potentiate responses to TGF-β1. A further possibility is that the miRNA inhibitors are not functioning in the conditions used. This was difficult to assess as the inhibitors purchased from Exiqon do not degrade their target miRNAs but sequester them in the form of stable complexes with their target, and may therefore not influence cellular levels of the miRNA, precluding the use of qPCR to interrogate miRNA in inhibitor-transfected cells. Additionally, qPCR does not distinguish between functional miRNAs with non-functional miRNAs (Thomson *et al*., 2013). Perhaps, another reason is inefficient transfection causing an accumulation of oligonucleotides inside vesicles. As a result, the inhibitors and their target are present in different subcellular compartments. This could be experimentally tested, if given sufficient time, with fluorescently labelled anti-miRs and observing the transfected cells under fluorescence microscope.

In this study, the effect of modulating miR-424-3p and miR-145-5p on myofibroblast phenotype in CAF was also investigated. In gain-of-function experiments, TGF-β1 increases α-SMA transcript levels and protein levels, α-SMA positive stress fibre formation and gel contraction in all conditions of transfected CAF including mock. Overexpression of miR-424-3p had no effects in reversing these myofibroblast phenotype in CAF. Given these mixed findings, an attempt to inhibit miR-424-3p expression or miR-145-5p expression in CAF was carried out.

Similar to NOF, TGF-β1 marked increases in myofibroblast differentiation

markers (α-SMA, FN-EDA1 and COL1A1) at mRNA level, α-SMA positive stress fibre formation, gel contraction and α-SMA protein level in all conditions of transfected CAF including mock. However, knockdown of miR-424-3p decreased α-SMA positive stress fibre formation and contractility when CAF were exposed to miR-424-3p inhibitor and TGF-β1 in combination. Inhibition of miR-145 significantly increases TGF-β1-induced gel contraction in CAF. There are possible reasons that contributed to these insignificant findings. First, CAF may express the high endogenous level of miR-424-3p or miR-145-5p, thus the effect of both miRNA inhibitors on myofibroblast phenotype may not be detectable in CAF. Second, inefficient transfection of miRNA inhibitors might have resulted in a small population of cells being transfected and produced the insignificant effects. The effects of pre-miR and anti-miRs on TGF-β1-induced CAF-like myofibroblast in NOF or CAF phenotypes in tumour-derived CAF were summarised in Table 4.1 and Table 4.2.

4.4 Summary

Increasing evidence show that miRNAs are involved in the conversion of fibroblasts into CAF. In this chapter, miRNA expression profile (further validated by qPCR) revealed that miR-424-5p and miR-145-5p were upregulated in TGF-β1 induced myofibroblast differentiation in NOF1 and NOF5. As these two cells died, miRNA profiling was done in new patient-derived NOF, NOF804. From miRNA expression profile, miR-424-3p was upregulated in TGF-β1-treated NOF804. The validation data confirmed this finding. Further, miRNA mimic or miRNA inhibitors were used to examine the role of miR-424-3p in regulating TGF-β1-induced CAF-like myofibroblasts differentiation. The gain-of-function experiments showed that overexpression of miR-424-3p was able to reverse myofibroblastic phenotype associated with TGF-β1 in NOF804. Overexpression of miR-424-3p attenuates TGF-β1 response of α-SMA and

Effect of TGF-β1	NOF	CAF
α-SMA mRNA level	Reduced	No effect
FN-EDA1 mRNA level	Reduced	No effect
COL1A1 mRNA level	No effect	No effect
α-SMA protein level	No effect	No effect
α-SMA positive stress fibre formation	No effect	No effect
Contractility	Decreased	No effect

Table 4.1: Effect of miR-424-3p overexpression in TGF-β1-treated NOF or CAF

Effect of TGF-β1	miR-145-5p		miR-424-3p	
	NOF	CAF	NOF	CAF
α-SMA mRNA level	No effect	No effect	No effect	No effect
FN-EDA1 mRNA level	No effect	No effect	No effect	No effect
COL1A1 mRNA level	No effect	No effect	No effect	No effect
α-SMA protein level	No effect	No effect	No effect	No effect
α-SMA positive stress fibre formation	No effect	No effect	No effect	Decreased
Contractility	No effect	Increased	No effect	Decreased

Table 4.2: Effect of inhibition of anti-miRs in TGF-β1-treated NOF or CAF

FN-EDA1 transcript levels in NOF804. In addition, overexpression of miR-424-3p prevents TGF-β1's ability to induce gel contraction in NOF804. However, overexpression of miR-424-3p did not decrease TGF-β1 associated with α-SMA positive stress fibres formation and α-SMA protein abundance in NOF804. Collectively, these data suggest that miR-424-3p regulates, at least in part, TGF-β1-induced myofibroblast differentiation, and that it might form part of a negative feedback loop to limit the effects of TGF-β1 signalling, as has been described for SMAD7, which is upregulated by TGF-β1 but serves to inhibit downstream phenotypic effects.

Overexpression of miR-424-3p had no effects in reversing TGF-β1-modulated myofibroblastic phenotype in CAF. On the other hand, the loss-of-function experiments of miR-424-3p or miR-145-5p did not work really well in NOF. Inhibition of miR-424-3p decreased TGF-β1-induced α-SMA stress fibre formation in CAF. Inhibition of miR-145-5p increases TGF-β1-induced gel contraction, not other myofibroblast phenotype, in CAF. The functional analysis data presented here were inconclusive, therefore, it might worth to look for other potentially functional miRNA that deregulated in eCAF.

CHAPTER 5: Expression profiling of miRNA during CAF development

5.1 Aim and objectives

The previous chapter provided evidence for the role for miR-424-3p and miR-145-5p in eCAF differentiation, but the variability of the functional changes observed on modulation of these miRNA prompted a fresh, more in depth, analysis to attempt to identify other miRNA which might play a role in eCAF differentiation. Herein, the aim of this chapter was to profile the expression of miRNAs in eCAF using a global miRNA profiling strategy to identify novel miRNA regulators of CAF formation from normal fibroblasts. Additionally, the miRNA expression profile of two subtypes of CAF (isolated from genetically stable OSCC (GS-OSCC) and genetically unstable of OSCC (GU-OSCC)) was determined using the same methodology. To do this, the following objectives were addressed:

1) to determine the differential miRNA expression of eCAF compared to NOF using TLDA, with more repeats and a more sophisticated analysis strategy

2) to determine global miRNA expression of tumour-derived CAF (GS-OSCC and GU-OSCC), compared to NOF using TLDA.

5.2 miRNA expression profiling revealed that novel miRNAs are significantly upregulated in eCAF

Gene expression profiling of stromal cells, predominantly performed in fibroblasts, has been identified as a promising approach to predict markers of disease progression (Finak *et al*., 2008) and therapy response (Farmer *et al*., 2009). Many studies demonstrated differences in gene expression between CAF and normal fibroblasts, particularly identifying differences in the expression of cytokines and ECM molecules (Bauer *et al*., 2010; Utispan *et al*., 2010; Micke *et al*., 2007). Several studies have identified changes in miRNA expression in myofibroblast differentiation, but less is

known about the role of miRNA in CAF development. The expression of miR-21 was reported to be upregulated in MRC-5 fibroblasts (human fetal fibroblast cell line) treated with TGF-β1 or conditioned medium from ovarian cancer cells, compared to untreated fibroblasts or without conditioned medium (Yao *et al*., 2011). While in CAF development, miR-155 was reported to be upregulated in both fibroblasts isolated from ovarian cancer tissue versus fibroblast from the normal ovarian tissue and experimentally induced CAF (Mitra *et al*., 2012). miR-106b is increased in CAF derived from gastric cancer tissues, compared with fibroblasts derived from normal gastric tissue (Yang *et al*., 2014). However, as described in Chapter 4, there have been no reports regarding differential miRNA expression associated with myofibroblast differentiation in the context of OSCC. By using TLDA, this study analysed miRNA expression of eCAF from two primary NOF cultures.

The miRNA expression profiles of eCAF and NOF (as described in Chapter 4) were expanded and re-analysed with the help of a computational biologist, Dr Ryan Pink, from Oxford Brookes University. To increase the statistical power of the data obtained, the TLDA experiments were repeated twice for two primary NOF cultures and the data obtained from the TLDA (two data sets from this experiment and one data set from the previous experiment in Chapter 4) were used for analysis using DataAssist software v2.0. The samples that are used in this analysis were summarised in Table 5.1. Quantitative miRNA expression data were acquired based on ΔCt values of the TLDA results. Normalisation was performed using the mean of all the internal controls on the TLDA cards; small nuclear RNAs (snRNA), RNU44, RNU48 and U6. The False Discovery Rate (FDR) by Benjamini and Hochberg algorithm was applied for analysing corrected p-values from a T-test between sample groups after normalisation. The workflow of the TLDA interrogation of miRNA expression including computational analysis of the data

miRNA cards	NOF5 (n=3)		NOF804 (n=3)	
	Untreated	TGF-β1-treated	Untreated	TGF-β1-treated
Pool A	√	√	√	√
Pool B	√	√	√	√

Table 5.1: NOF cultures that were used in the miRNA expression profiles and the data were analysed using more stringent approach

is illustrated in Figure 5.1.

As shown in Figure 5.2, using this method of analysis, only two miRNAs were significantly upregulated in TGF-β1-treated NOF5; miR-181a (4.2-fold) and Let-7c (2.5-fold), compared to untreated NOF5. No miRNAs were significantly downregulated in TGF-β1-treated NOF5. The other two miRNAs that were focused on earlier in this study (in Chapter 4) were upregulated in TGF-β1-treated NOF5, with miR-145-5p (3.6-fold) and miR-424-3p (230-fold), but these increases did not reach significance using the stringent statistical tests performed here. Only two miRNAs were significantly upregulated in TGF-β1-treated NOF804; miR-503 (28.6-fold) and miR-708 (2.8-fold), but these upregulated miRNAs were different to those upregulated miRNAs identified in NOF5. Unlike NOF5, in which no down-regulated miRNA were identified, miR-1276 was significantly downregulated (0.1-fold) in TGF-β1-treated NOF804 (Figure 5.3). miR-424-3p was upregulated 11.2-fold, however, this did not reach significance. While expression of miR-145-5p was upregulated (not reaching statistical significance) in NOF5, this miRNA was downregulated 1.1-fold (not reaching statistical significance) in TGF-β1-treated NOF804.

5.3 Comparison of miRNA expression profile between CAF and NOF

Lim *et al*., (2011) demonstrated that CAF derived from GU-OSCC had a different transcriptional profile from that of CAF derived from GS-OSCC. This difference possibly involves specific miRNA expression profiles between the two distinct CAF populations as miRNA are one of the regulators of gene expression. Thus, TLDA was used to evaluate the miRNA expression profiles of these distinct CAF populations. CAF from GU-OSCC are predominantly senescent, large and slow growing cells (Lim *et al*., 2011). Three primary NOF isolates from normal oral mucosa (NOF1, NOF2 and NOF5)

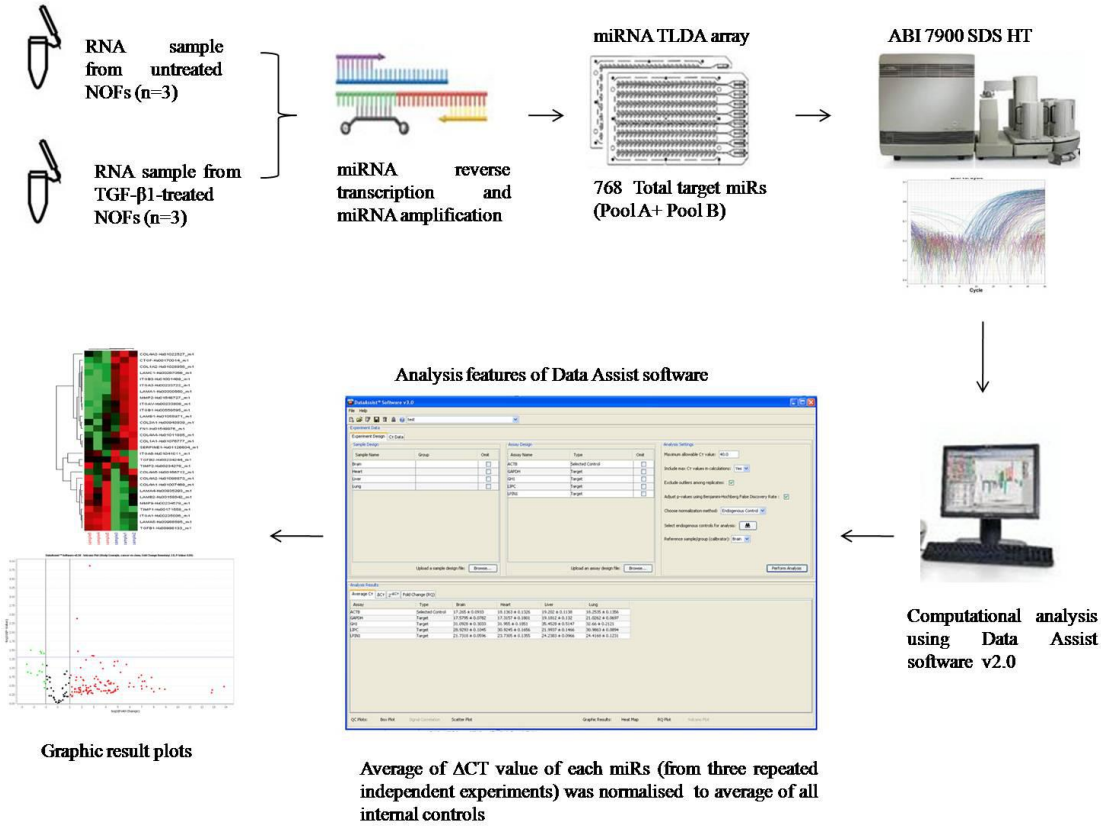

Figure 5.1: Schematic diagram of TLDA including data analysis to determine the miRNA expression profile in NOF stimulated with TGF-β1

NOF cells were incubated with or without 5 ng/ml of TGF-β1 for 48 h. RNA was extracted from fibroblasts and used later for cDNA synthesis. cDNA was amplified and used for TLDA profiling. ΔCt values obtained from qPCR were extracted using RQ manager v1.2.1 and analysed using Data Assist software v2.0. The ΔCt values were normalised to average of internal controls at a Ct cut-off value of 40. Each expressed miRNA was determined as fold change (ΔΔCt values relative to the untreated fibroblasts).

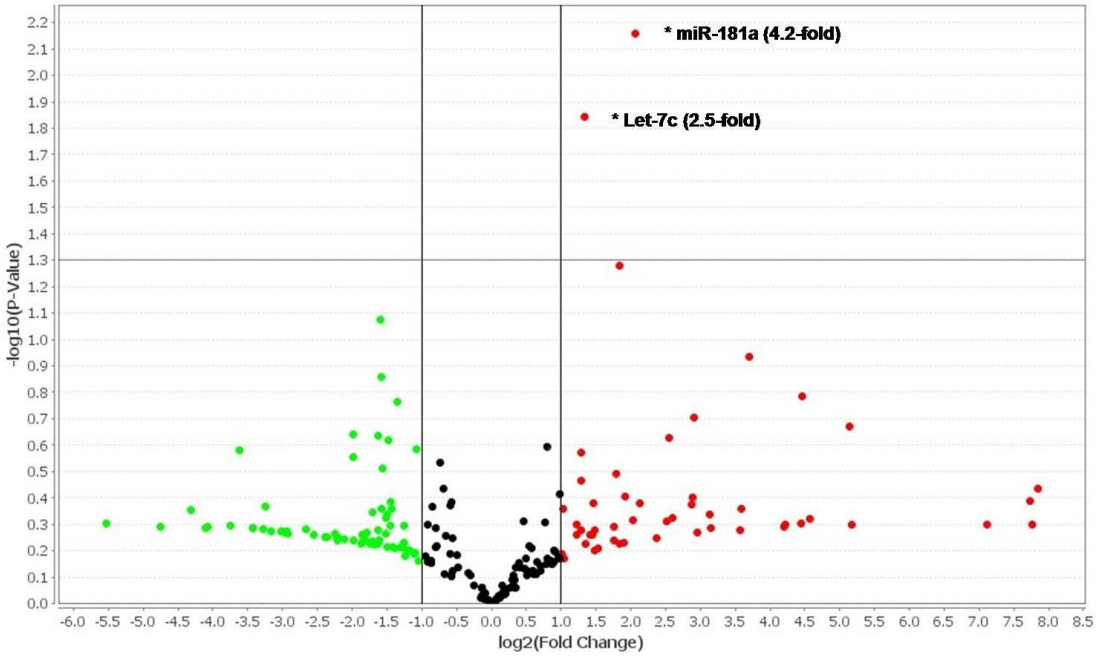

Figure 5.2: A volcano plot of differential miRNA expression in TGF-β1-treated NOF5 compared to untreated NOF5

NOF5 cells were incubated with or without 5 ng/ml of TGF-β1 for 48 h. Fibroblasts were harvested and RNA was extracted for cDNA synthesis. cDNA was amplified and used for TLDA experiment. The volcano plot shows the relationship between fold-change, measured by Log2 (x-axis) and significance, measured by –Log10 (y-axis) between two groups. Each dot represents one miRNA. Only miRNAs above the horizontal line are significant (*$p<0.05$). The green dots denote miRNAs that are downregulated while red dots represent miRNAs that are upregulated. The black dots are either miRNAs that are not significant or below the fold change cut off. miRNAs identified as significant are labelled on the plot. The miRNA expression profiles of NOF5 was produced from three biological repeats.

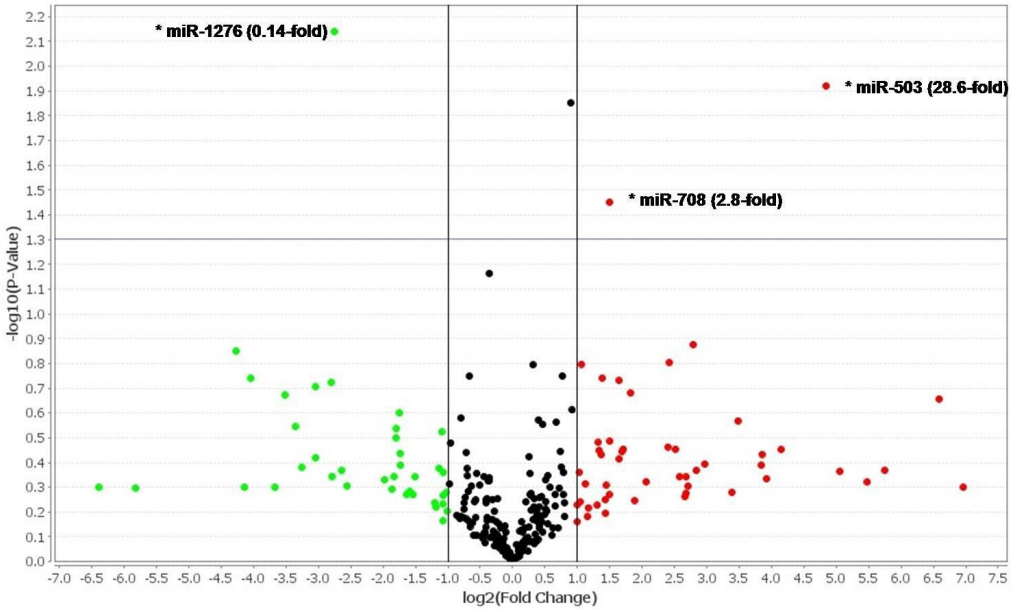

Figure 5.3: A volcano plot of differentially miRNAs expression in TGF-β1-treated NOF804 compared to untreated NOF804

NOF804 cells were incubated with or without 5 ng/ml of TGF-β1 for 48 h. Fibroblasts were harvested and RNA was extracted for cDNA synthesis. cDNA was amplified and used for TLDA experiment. The volcano plot shows the relationship between fold-change, measured by Log2 (x-axis) and significance, measured by –Log10 (y-axis) between two groups. Each dot represents one miRNA. Only miRNAs above the horizontal line are significant (*$p<0.05$). The green dots denote miRNAs that are downregulated while red dots represent miRNAs that are upregulated. The black dots are either miRNAs that are not significant or below the fold change cut off. miRNAs identified as significant are labelled on the plot. The miRNA expression profiles of NOF804 was produced from three biological repeats.

were cultured. RNA was isolated and used to generate cDNA. Pre-amplified cDNA was used as a template for TLDA analysis. Data analysis was performed in collaboration with Dr Ryan Pink (Oxford Brookes University) using miRNA expression data obtained from NOF and CAF of each subtype (generated by Genevieve Melling and Tasnuva Kabir, former PhD students in the Lambert group; this data had not been previously analysed nor included in other PhD theses). The samples that were used in the analysis were summarised in Table. 5.2. Analysis revealed that 281 miRNAs displayed different expression in CAF isolated from GS-OSCC, compared to NOF, where a log 2 of fold change of <1 is considered downregulated and log 2 of fold change >1 is considered upregulated (Figure 5.4 A). Out of these, only 16 miRNAs were significantly upregulated ($p<0.05$) in CAF (GS-OSCC) compared to NOF while none were significantly downregulated in CAF (GS-OSCC). miR-192 was highly upregulated ($p<0.05$) in CAF (GS-OSCC) compared to NOF with a 13.8-fold increase. This was followed by miR-324-5p and miR-484 with 6.1-fold and 5.5-fold increases, respectively. The other miRNAs that were significantly upregulated in CAF (GS-OSCC) are listed in Figure 5.4 (B).

Fourteen miRNAs were significantly upregulated in CAF (GU-OSCC) compared to NOF (Figure 5.5 A). miR-324-5p is highly upregulated in CAF (GU-OSCC) compared to NOF with a 9.3-fold increase. Similar to CAF (GS-OSCC), no miRNA was identified to be significantly downregulated in CAF (GU-OSCC) compared to NOF. Other miRNAs that were significantly upregulated in CAF (GU-OSCC) are listed in Figure 5.5 (B). All the genes or pathways predicted to be targeted by any miRNAs mentioned in this chapter were identified using the online target prediction tool, Diana-miRPath v3.0 (Vlachos *et al*., 2015). Out of 14 significantly altered miRNAs, miR-10a and miR-193b were predicted to target genes encoding ECM components, COL4A3 and COL1A1, respectively. The ECM is remodelled in pathological conditions such cancer and fibrosis.

miRNA cards	Without TGF-β1		
	NOF (NOF1,NOF2, NOF5)	CAF/GS-OSCC (BICR70,BICR73, BICR59)	CAF/GU-OSCC (BICR31,BICR18,BICR3)
Pool A	√	√	√
Pool B	√	√	√

Table 5.2: NOF, CAF (GS-OSCC) and CAF (GU-OSCC) cultures that were used in the miRNA expression profiles and the data were analysed using more stringent approach

(A)

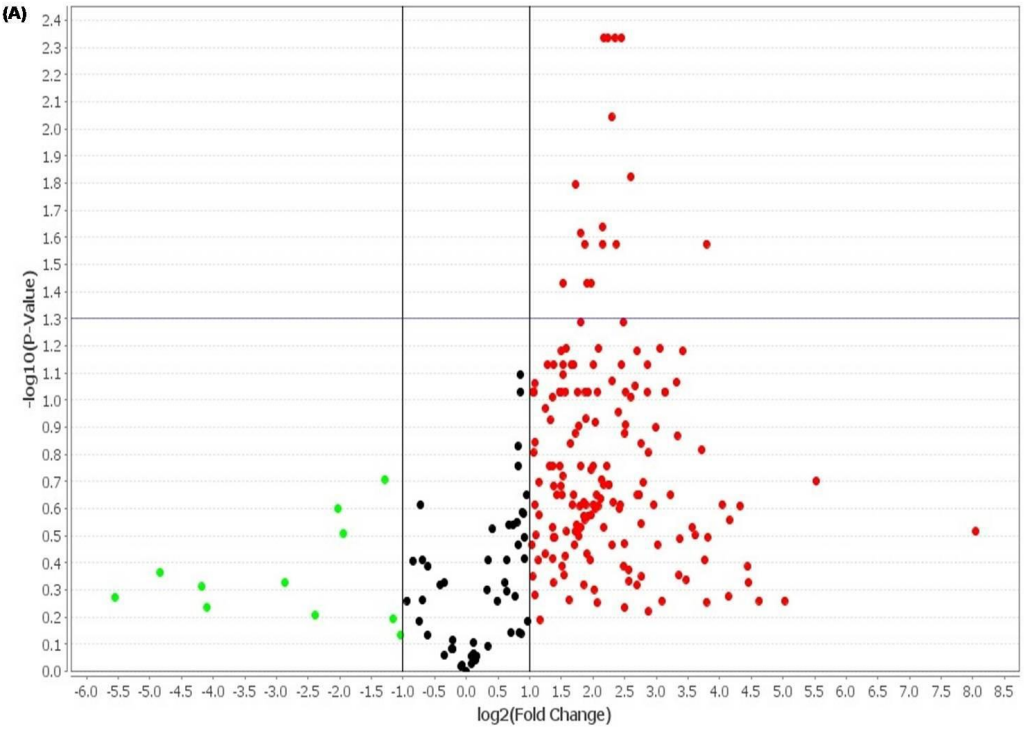

(B)

miRNAs	Fold Change	p-value
Let-7a	3.3	0.016
Let-7d	3.9	0.037
Let-7g	4.7	0.0046
miR-103	4.4	0.023
miR-125a-3p	4.5	0.0046
miR-192	13.8	0.0265
miR-197	4.9	0.0091
miR-199a-3p	5.1	0.0046
miR-28-3p	4.4	0.0265
miR-320	5.2	0.0265
miR-324-5p	6.1	0.015
miR-339-3p	3.7	0.037
miR-376b	3.5	0.0241
miR-454	3.6	0.0265
miR-484	5.5	0.0046
miR-99b	2.9	0.037

Figure 5.4: Differential miRNAs expression in CAF (GS-OSCC) compared to NOF

NOF (NOF1, NOF2 and NOF5) and CAF isolated from genetically stable OSCC (BICR70, BICR73, BICR59) were cultured, RNA was isolated and used for cDNA synthesis. cDNA was amplified and used for TLDA experiment. **(A)** The volcano plot shows the relationship between fold-change, measured by Log2 (x-axis) and significance, measured by –Log10 (y-axis) between two groups. Each dot represents one miRNA. Only miRNAs above the horizontal line are significant (*p<0.05). The green dots denote miRNAs that are downregulated while red dots represent miRNAs that are upregulated. The black dots are either miRNAs that are not significant or below the fold change cut off. **(B)** miRNAs identified as significant are listed below the plot. TLDA experiments were repeated three times.

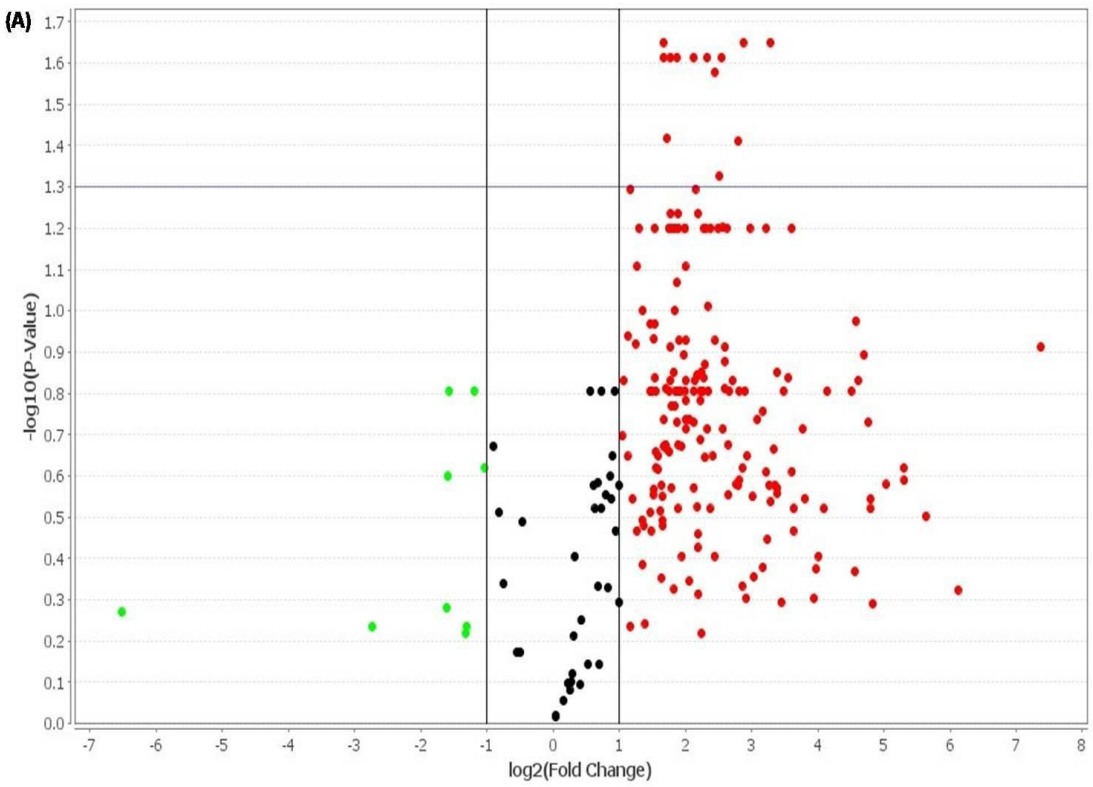

(B)

miRNAs	Fold Change	p-value
miR-10a	5.7	0.0472
miR-128	5.4	0.0264
miR-191	3.7	0.0243
miR-193b	7.3	0.0224
miR-197	3.2	0.0243
miR-30b	4.3	0.0243
miR-320	3.2	0.0224
miR-324-5p	9.7	0.0224
miR-362-5p	5.9	0.0243
miR-376a	5.0	0.0243
miR-376b	3.3	0.0382
miR-494	3.4	0.0243
miR-532-3p	6.9	0.0388

Figure 5.5: Differential miRNA expression in CAF (GU-OSCC) compared to NOF

NOF (NOF1, NOF2 and NOF5) and CAF isolated from genetically unstable OSCC (BICR31, BICR18, BICR3) were cultured, RNA was isolated and used for cDNA synthesis. cDNA was amplified and used for TLDA experiment. **(A)** The volcano plot shows the relationship between fold-change, measured by Log2 (x-axis) and significance, measured by –Log10 (y-axis) between two groups. Each dot represents one miRNA. Only miRNAs above the horizontal line are significant (*$p<0.05$). The green dots denote miRNAs that are downregulated while red dots represent miRNAs that are upregulated. The black dots are either miRNAs that are not significant or below the fold change cut off. **(B)** miRNAs identified as significant are listed below the plot. TLDA experiments were repeated three times.

CAF sustain their major role in ECM remodelling as they are mainly responsible for the synthesis of ECM proteins including collagens. Many cancers, including oral cancers, display desmoplasia, a fibrotic state, characterised by deposition of collagens type I and III and by a degradation of collagen type IV (Kauppila *et al*., 1998; Huijbers *et al*., 2010). Furthermore, CAF are known to generate an abnormal ECM, including aberrant COL1A1 expression, suggesting changes in these miRNA has the potential to modify the CAF phenotype and the ECM of the tumour microenvironment.

miR-362-5p was predicted to target a gene related involved in the Krebs cycle, isocitrate dehydrogenase 1 (IDH1). As mentioned in Section 1.6.3, CAF possibly secrete metabolites (lactate or pyruvate) to fuel the growth of cancer cells. Fiaschi *et al*., (2012) demonstrated that CAF secreted lactate and ketone bodies, later utilised by cancer cells for oxidative phosphorylation. Additionally, β-hydroxybutyrate (a ketone body) increased cancer cell proliferation by 3-fold, compared to control group, while lactate promoted angiogenesis in a tumour model. A recent study showed that isocitrate dehydrogenase 3α (IDH3α) downregulation causes metabolic reprogramming of oxidative phosphorylation to glycolysis in CAF (Zhang *et al*., 2015). This study found that IDH3α inhibition increased glucose uptake, lactate production and reduce oxygen consumption in CAF. In contrast, overexpression of IDH3α inhibited TGF-β1-induced lactate production in CAF. This data suggests these miRNAs have the potential to regulate the metabolome of CAF and thereby influence their behaviour and that of nearby cancer cells.

5.4 Comparison of miRNA expression profile between CAF isolated from GS-OSCC and CAF isolated from GU-OSCC

The results described in Section 5.3 showed that both CAF from GS-OSCC and GU-OSCC display distinct miRNA expression profiles compared to NOF. Out of these,

the only miRNAs upregulated in both CAF (GS-OSCC) and CAF (GU-OSCC) are indicated in a Venn diagram (Figure 5.6 A). This diagram was generated using the online tool Data Overlapping and Area-Proportional Venn Diagram, obtained from http://bioinforx.com/bxarrays/overlap.php. Only four miRNAs were highly expressed in both subtypes of CAF when compared to NOF; miR-197, miR-320, miR-324-5p and miR-376b. The fold change and statistical value for both subtypes of CAF are outlined in Figure 5.6 (B).

5.5 Discussion

miRNA can regulate many biological processes and have shown promise as biomarkers for various diseases (Ling *et al*., 2016; Iorio and Croce, 2009). miRNAprofiling may be used to classify subgroups of tumours, especially for poorly differentiated tumours that are difficult to distinguish by histological analysis (Dai *et al*., 2014). miRNAs have attractive features for translation as biomarkers from the bench to clinical practice; these include simple extraction (the principles of miRNA isolation is the same as RNA extraction, except miRNA isolation was slightly modified to retain small RNA fraction (Accerbi *et al*., 2010)), miRNA profiling by qRT-PCR and other analytical methods, and resistance to degradation (Kwan *et al*., 2016). qRT-PCR provides absolute miRNA quantification with dynamic range, low cost and greatest sensitivity compared to other methods including RNA-seq (Pritchard *et al*., 2016). miRNA have been demonstrated to be more stable than mRNAs in various specimen types including blood plasma/serum (Arroyo *et al*., 2011) and formalin-fixed tissue blocks (Doleshal *et al*., 2008).

The functional analysis data from Chapter 4 were inconclusive. Therefore, the TLDA data were re-analysed using more samples and a more stringent analytical approach to look for other potentially functional miRNA. The results from the second

(A)

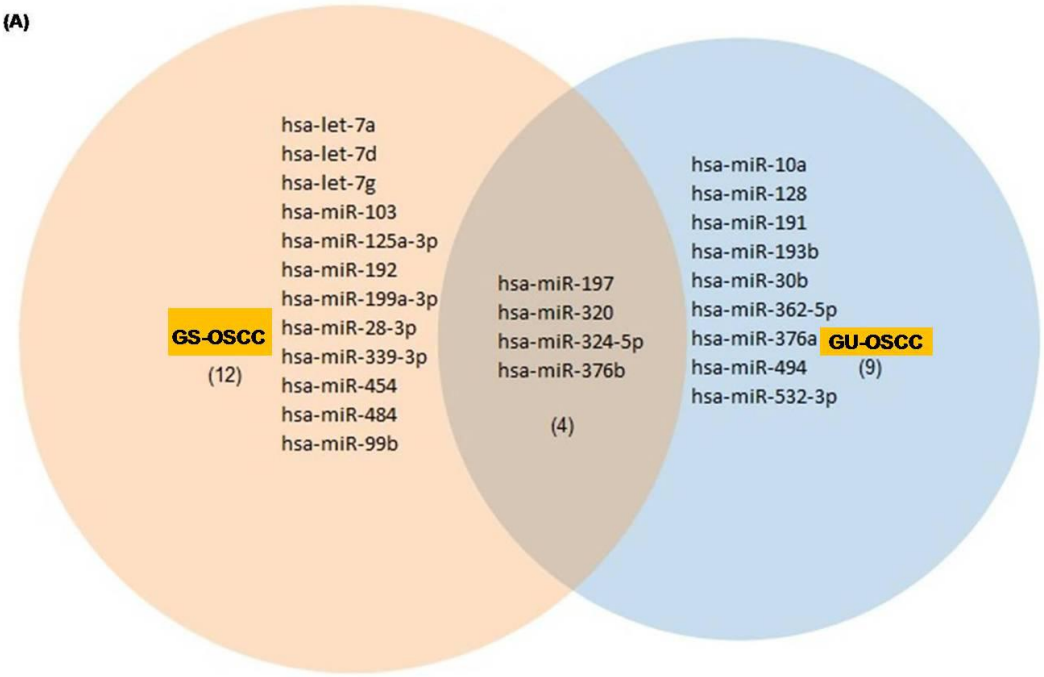

(B)

miRNA	CAFs (GS-OSCC)		CAFs (GU-OSCC)	
	Fold change	p-value	Fold change	p-value
miR-197	4.9	0.0091	3.2	0.0243
miR-320	5.2	0.0265	3.2	0.0224
miR-324-5p	6.1	0.0150	9.7	0.0224
miR-376b	3.5	0.0241	3.3	0.0382

Figure 5.6: Commonly altered miRNAs in both CAF derived from GS-OSCC and GU-OSCC compared to NOF

NOF and CAF (GS-OSCC and GU-OSCC) were grown, RNA was isolated and used for cDNA synthesis. cDNA was amplified and used for TLDA experiment. **(A)** Venn diagram shows that miRNAs that significantly upregulated in CAF (GS-OSCC), CAF (GU-OSCC) and in both **(B)** Listed miRNAs that overlapped between two different data sets.

method of analysis revealed that miR-181a and Let-7c were significantly upregulated in NOF5 cells after TGF-β1 treatment. Surprisingly, whilst miR-424-5p was upregulated, in keeping with the findings in Chapter 4, miR-145-5p was downregulated (but not reaching significance ($p<0.05$)) in TGF-β1-treated NOF5 cells in this analysis. Therefore, these findings might explain the inconclusive results obtained from the functional analysis experiments in Chapter 4, and suggest caution should be employed when interpreting the findings of TLDA miRNA screening approaches. miR-181a, one of two miRNA identified as altered in this reanalysis, belongs to the miR-181 family which includes miR-181a, miR-181b, miR-181c and miR-181d (Giordano and Columbano, 2013). This family of miRNA has been implicated in many cellular processes such as cell proliferation, apoptosis, invasion and as a tumour suppressor (Shi *et al*., 2008; Chen *et al*., 2013; Jianwei *et al*., 2013). miR-181a was overexpressed in cirrhosis and hepatocellular carcinoma (Brockhausen *et al*., 2015). In OSCC, miR-181a was reported to be frequently downregulated and overexpression of miR-181a decreased K-ras protein level (Shin *et al*., 2011). Previous studies demonstrated that TGF-β regulates the expression of miR-181b in hepatocytes by targeting TIMP3 (Wang *et al*., 2010) and p27 (Wang *et al*., 2012). miR-181a promotes TGF-β-mediated EMT by suppressing Smad7 in ovarian cancer cells (Parikh *et al*., 2014). TGF-β upregulates miR-181a expression to promote EMT of breast cancer cells (Taylor *et al*., 2013). Taken together, these findings indicate TGF-β may be a regulator of the expression of miR-181 family members. In agreement with this, TGF-β1 caused upregulation of miR-181a expression in NOF5 and was predicted to target Smad7, a negative regulator of TGF-β signalling. TGF-β activates Smad2 and Smad3 proteins (receptor-activated Smad) by reducing the association of Smad2/3 with Smad7 (one of the inhibitory Smads). However, no evidence of miR-181a involvement in myofibroblast differentiation or fibrosis of OSCC has been reported to date, and further functional assays are required to confirm this.

The human Let-7 family consists of 10 miRNAs, located on different chromosomes; Let-7a, Let-7b, Let-7c, Let-7d, Let-7e, Let-7f, Let-7g, Let-7i, miR-98 and miR-202. The Let-7 family has been demonstrated to be involved in the control of cellular processes; embryogenesis (R. Maller Schulman *et al*., 2008), tumour suppressive functions (Zhang *et al*., 2007) and regulation of cell proliferation (Johnson *et al*., 2007). Let-7 is commonly viewed as a tumour suppressor miRNA; increasing evidence demonstrates that Let-7 is downregulated in various types of cancer including colon cancer (Akao *et al*., 2006), gastric cancer (Zhang *et al*., 2007), breast cancer (Huang *et al*., 2015) and lung cancer (Takamizawa *et al*., 2004). However, upregulation of certain Let-7 family members has been observed in some types of human cancers such as upregulation of Let-7b and Let-7i in lymphoma (Lawrie *et al*., 2009). This implies that Let-7 family does not play as tumour suppressor role under all circumstances or in all tissues. Only one study reported a high level of Let 7c expression in cardiac fibroblast during EndMT (Ghosh *et al*., 2012). To date, no evidence of Let-7c involvement in myofibroblast differentiation or CAF development has been reported. Interestingly, Let-7c is predicted to target COL1A1, a key component of the ECM and one of the markers of myofibroblast phenotype, suggesting it has the potential to modulate CAF and myofibroblast differentiation.

miR-503 and miR-708 were highly upregulated in TGF-β1-treated NOF804 cells, compared to unstimulated cells. The miRNA changes in response to TGF-β1 are different between the two NOF cultures. This might be due to experimental variation including passage number of the NOF used. Perhaps, the response could also be altered by site specific differences where NOF are from different parts of buccal mucosa and health status of the patient (e.g oral bacterial infection). miR-424-3p was upregulated while miR-145-5p was downregulated in TGF-β1-treated NOF804 cells. However, these two

miRNAs did not reach statistical significance ($p<0.05$).

miR-503 possesses the same seed sequence and genomic organisation of the miR-16 family which includes miR-424 (Caporali and Emanueli, 2011). Thus, miR-503 is considered as a part of the miR-16 family. Moreover, miR-503 promotes fibrosis in cardiac cells (Zhou *et al*., 2016). In addition, miR-503 is important in myoblast differentiation as well as myogenesis (Wang *et al*., 2009; Caporali *et al*., 2011). miR-503 is predicted to target genes related to TGF-β signaling pathway, Smad7 and Smurf1 (a negative regulator of BMP signalling). Controlled proteolysis by Smad ubiquitination regulatory factors (Smurfs) plays an important role in regulating cellular responses of TGF-β signaling pathway. Smurf1 facilitates myogenic differentiation of TGF-β-treated mouse C2C12 cells, compared to untreated cells (Ying *et al*., 2003). Smurf1 has been demonstrated to interact with Smad7 (one of the inhibitory Smads), inducing the ubiquitination-mediated degradation of the activated TGF-β receptors (Ebisawa *et al*., 2001). Thus, it is possible that miR-503 may be involved functionally in myofibroblastic differentiation.

miR-708 is located at the chromosomal locus 11q14.1 (Saini *et al*., 2011) and is one of the more recently discovered miRNA to play role in cancer. miR-708 expression is reported to be decreased in renal cancer cells and restoration of miR-708 expression promotes apoptosis in renal cancer cells (Saini *et al*., 2011). However, it is unknown whether miR-708 has any effect in tumour-stroma interaction. In this study, expression of miR-708 was highly upregulated in eCAF. miR-708 is predicted to target genes related to TGF-β signaling, including Smad2 (a positive regulator of TGF-β signaling) and COL1A1. It is well accepted that Smad2/3 activation is crucial for Smad4-dependent transcription regulation, suggesting a potential role for this miRNA is regulating responses of fibroblasts to TGF-β1.

In the present study, a differential miRNAs expression profile from two subtypes of CAF (GS-OSCC and GU-OSCC) compared to NOF was determined. These two CAF were fully characterised by Hassona and co-workers (2013). The TLDA data showed that there were 16 miRNAs significantly deregulated in CAF (GS-OSCC). Among of these, miR-192 is highly upregulated in CAF (GS-OSCC), compared to NOF. miR-192 was reported to be highly expressed in mesangial cells upon TGF-β1 treatment and was associated with elevated expression of COL1A2B by downregulating ZEB2 expression (Kato *et al*., 2007). Recently, miR-192 was demonstrated to take part in cell cycle control (Braun *et al*., 2008; Georges *et al*., 2008). miR-192 was predicted to target gene related to cell cycle (specifically DNA damage checkpoint) by regulating CDK1. CAF (GU-OSCC) have significantly more ROS production compared to CAF (GS-OSCC) (Hassona *et al*., 2013). In agreement with this, DNA damage elicits cell cycle arrest in CAF (GS-OSCC; wild-type TP53/p16^{INK4A}), by regulating transcription factor p53 (G1 phase). Activated p53 is stabilised through protection from MDM2, later transactivates the expression of genes including p21. The activated p21 inhibits G1 CDKs, resulting in DNA repair (Barnum and O'Connell, 2014), suggesting that miR-192-mediated regulation of CDK1 might play a role in determining the phenotype of these cells; further experimental testing of this hypothesis is required, however.

Fourteen miRNAs were significantly upregulated in CAF (GU-OSCC), compared to NOF with miR-324-5p showing the highest differential expression. In cancer, miR-324-5p was found to repress transcription factor Gli-1, promoting differentiation of medulloblastoma cells (Ferretti *et al*., 2008), but little else is known of its roles. miR-324-5p is predicted to target a gene involved in glycosaminoglycan biosynthesis (specifically heparan sulphate/heparin), exostosin glycosyltransferase 2 (EXT2). Heparan sulphate proteoglycans are macromolecules that served as a scaffold

for the attachment of various ECM components including collagen, laminin and fibronectin (Vlodavsky *et al*., 1996). In this study, three miRNAs were identified to be involved in p53 signaling by targeting different genes in cell cycle checkpoints; miR-30b (G1 arrest; Cyclin D, Cyclin E and CDK6), miR-376a (p53 negative feedback; MDM2) and miR-532-3p (G1 arrest; Cyclin D and p53 negative feedback; MDM2). CAF (GU-OSCC) is characterised by loss of TP53/p16^{INK4A} (Hassona *et al*., 2013), therefore, when DNA damage occurred in this cell, the ability to induce cell cycle arrest at specific points in the cell cycle, particularly DNA repair mechanism was impaired, leading cells to senesce. Furthermore, CAF (GU-OSCC) are enlarged cells, slow growing cells, expressed genes associated with cellular senescence, and expressed more SA β-Gal enzyme activity (marker of senescence) compared to normal oral mucosa and CAF (GS-OSCC) (Lim *et al*., 2011; Hassona *et al*., 2013). Additionally, CAF (GU-OSCC) accumulated with oxidative DNA damage, the number of 8-oxo-dG -positive cells was increased in this CAF subset relative to CAF (GS-OSCC). The role of MDM2, an ubiquitin ligase is to maintain the low level of p53 expression in unstressed cells (Kubbutat *et al*., 1997). The expression of MDM2 induced by p53 caused p53 degradation, thus, MDM2-p53 serves as a negative feedback loop (Moll and Petrenko, 2003). Perhaps, the MDM2-p53 negative feedback loop acts the same manner to maintain the status level of p53 in CAF (GU-OSCC). In this study, the miRNA expression profile of CAF (GU-OSCC) is distinctly different from than that observed in fibroblasts treated with cisplatin (Kabir *et al*., 2016), suggesting a difference between senescent CAF and fibroblasts artificially induced to senesce. Additionally, miR-335 was upregulated in cisplatin-treated normal fibroblasts and a miR-335/COX2/PTEN axis able to modulate an inflammatory SASP of CAF, thus promoting tumour-supportive microenvironment. Using the method of analysis employed here, miR-335 was not found to be significantly up-regulated in senescent CAF.

There were four miRNAs highly expressed in both CAF (GS-OSCC) and CAF (GU-OSCC); miR-197, miR-320, miR-324-5p and miR-376b. miR-197 is located at the chromosome 1p13.3 and little is known about the role of miR-197 in cancer. miR-197 is secreted into the extracellular environment via cancer-related exosomes and is involved in regulation of cell proliferation (Grange *et al*., 2011). High expression of miR-197 is correlated with reduced Fus1 (a tumour suppressor) expression in NSCLC tumour specimens (Du *et al*., 2009). Similar to miR-324-5p, miR-197 was predicted to target gene related to glycosaminoglycan biosynthesis (specifically heparan sulphate/heparin), exostosin glycosyltransferase 2 (EXT2). miR-320, another miRNA highly expressed in both subtypes of CAF, is reported to be present in extracellular vesicles derived from cancer and normal tissue (Skog *et al*., 2008; Guduric-Fuchs *et al*., 2012). miR-320-Pten-Ets2 axis in stromal fibroblasts can modulate cancer-stroma communications and plays a role in human breast cancer (Bronisz *et al*., 2012). miR-320 was predicted to be involved in TGF-β signaling by targeting Smad3 (a positive regulator of TGF-β signaling). Activated Smad3 is important for Smad4-dependent transcription regulation. The Smad3-Smad4 complex was transported into the nucleus and this complexes activate specific genes. Little is known about the involvement of miR-376b in cancer. One study demonstrated that miR-376b was downregulated in rapamycin-induced autophagy in MCF-7 cell and both genes related to autophagy, ATG4C and BECN1 are downstream targets of miR-376b (Korkmaz *et al*., 2012). None of genes were predicted to target any pathway related to any CAF biology, suggesting that cell-cell interactions might regulate miR-376b expression to reflect a protective response in cellular homeostasis or a detrimental effect in disease condition but again, this requires experimental validation.

Given that hundreds of miRNA were differentially expressed in CAF from two subtypes of OSCC, it is not unsure whether the experiments carried out are measuring

different miRNA expression or measuring similar miRNA expression across various conditions. The principle component analysis (PCA), therefore, provide simplified analysis to clearly determine the variables (samples) from the big data set that may explain the difference in the observation (miRNA expression). Comparison between miRNA expression using PCA will reveal distint clusters across the CAF (two suvtypes of OSCC) and NOF. A comparison of miRNA expression profiles between CAF (GS-OSCC) with CAF (GU-OSCC) could also be done in this experiment to compare miRNA differentially expressed within two distinct subpopulations of CAF derived from OSCCs.

5.6 Summary

In this chapter, miR-424-5p and miR-145-5p were not significantly upregulated in eCAF derived from NOF5, in contrast to the results of the analysis presented in Chapter 4. Likewise, miR-424-3p was not significantly upregulated in the TGF-β1-treated NOF804. miR-145-5p also appears to be downregulated but not significant ($p<0.05$) in the TGF-β1-treated NOF804. These findings might explain the variable results obtained from the functional analysis experiments in Chapter 4. Other potentially functional miRNAs obtained from the analyses might emerge as interesting candidates to control myofibroblast differentiation or CAF development. Furthermore, this study had identified distinct miRNAs expression profile between CAF (GS-OSCC) with CAF (GU-OSCC). This study provides information several miRNA candidates in senescent CAF, a subpopulation of CAF that contribute to cancer progression through modulation of secretome, termed the senescence-associated secretory phenotype (SASP) (Laberge *et al*., 2015). Furthermore, the SASP comprises of elevated levels of cytokines, growth factors, ECM proteins and other factors, which helps to create a pro-tumourigenic extracellular milieu. The molecular mechanisms underlying the pro-tumourigenic of SASP is poorly understood. Therefore, elucidating the mechanisms responsible for the SASP production

(including the involvement of miRNA) could provide a new approach in therapy since stromal fibroblasts are thought to be genetically stable (Loeffler *et al*., 2006) and may therefore add to the repertoire of currently available treatments alongside those targeting genetically unstable or drug-resistant tumour cells.

CHAPTER 6: Discussion

6.1 General discussion

The close relationship between cancer cells and stromal cells in the tumour microenvironment is believed to promote cancer growth and progression. The tumour microenvironmental milieu consists of multiple cells, including cancer associated fibroblasts (CAF), and generates an altered extracellular matrix (ECM), cytokines, chemokines, and pro-angiogenic factors, collectively creating a more permissive microenvironment to encourage tumour proliferation (Pietras and Ostman, 2010) and metastasis (Liao *et al*., 2009). Fibroblasts found in the tumour microenvironment are referred to by a variety of names, but most commonly as CAF. CAF have been demonstrated to be involved in many aspects of cancer development; invasion and metastasis (Duda *et al*., 2010), ECM remodeling (Gaggioli *et al*., 2007), angiogenesis (Gerber *et al*., 2009) and resistance to therapy. In OSCC, stromal CAF facilitate tumour growth and progression by altering the proliferation, invasion, and metastasis of cancer cells (Thode *et al*., 2011). Therefore, CAF may represent potential therapeutic targets for anticancer therapy; this potential is amplified by their genetic stability which makes them unlikely to develop resistance to therapy as seen with cancer cell-targeted treatments.

Myofibroblasts are generally considered not to be exactly the same as CAF but share a number of characteristics. Myofibroblasts are found in healing wounds and have fibroblast and smooth muscle cell characteristics. Thus, myofibroblasts express α-SMA and are able to generate contractile force to promote wound closure (Tomasek *et al*., 2002). Upon completion of wound repair, the α-SMA expression decreases, the contractile activity of myofibroblasts is terminated and myofibroblasts undergo programmed cell death (apoptosis) (Desmouliere *et al*., 1995). However, in pathological situations resembling a healing wound such as cancer, myofibroblastic fibroblasts remain activated, neither reverting back to normal phenotype nor being removed by apoptosis

(Li *et al*., 2007). Myofibroblasts in a neoplastic stroma have been shown to be a predictive marker of poor prognoses in various cancer including OSCC (Desmouliere *et al*., 2004; Sobral *et al*., 2011; De-assis *et al*., 2012; Dourado *et al*., 2017).

CAF represent heterogeneous phenotypes; they exist as a varied population of myofibroblastic cells mixed with other fibroblastic phenotypes that do not express α-SMA but may be tumour promoting nevertheless (Desmouliere *et al*., 2004; Micke and Ostman, 2004). Sugimoto *et al*., (2006) demonstrated that CAF comprise mixed populations of activated fibroblasts; one subset was FSP1 positive but lacked expression of α-SMA, whereas the other FSP1 negative subset co-expressed α-SMA. These subpopulations of CAF might have distinct role in cancer progression. Two CAF phenotypes were identified in genetically stable or genetically unstable OSCC; GS-OSCC and GU-OSCC. Lim *et al* (2011) characterised OSCC based on the presence of inactivating mutations/chromosomal deletions of TP53/$p16^{INK4A}$. They found that fibroblasts derived from genetically unstable OSCC (GU-OSCC; loss of TP53/$p16^{INK4A}$) were senescent and differ in transcriptional profile to fibroblasts derived from genetically stable OSCC (GS-OSCC; wild-type TP53/$p16^{INK4A}$). The development of senescent CAF was induced by ROS associated with TGF-β1 and TGF-β2 from GU-OSCC keratinocytes (Hassona *et al*., 2012). However, in this model not all the CAF are senescent, further suggesting the presence of heterogeneity. Therefore, it is impossible to fully model the transition to a mixed CAF phenotype *in vitro*, but this study at least represents a subtype (myofibroblastic) associated with disease progression.

CAF originate from multiple origins including resident fibroblast undergoing mesenchymal-mesenchymal transition (MMT) (Radisky *et al*., 2007). Morphologically, fibroblasts are elongated cells with a spindle-like shape. Fibroblasts are the non-epithelial, non-vascular and non-inflammatory cells of connective tissue (Tarin and Croft, 1969).

Fibroblasts reside within the ECM and are one of the most abundant cell type in connective tissue.

In this study, NOF extracted from human buccal mucosa were used as an *in vitro* model to examine the molecular mechanisms underlying myofibroblast-like CAF transition. It is well-known that cancer cells secrete high levels of TGF-β1 along with other growth factors such as PDGF (Massague, 2008). These paracrine secretions are believed to trigger a transition of resting fibroblasts to CAF phenotype with myofibroblastic features in various cancers including OSCC (Lewis *et al*., 2004).

The molecular mechanisms by which TGF-β1- mediates the conversion of oral fibroblasts to a myofibroblastic, CAF-like phenotype remain unclear. Here, it was hypothesised that specific miRNA regulate the development of the myofibroblastic CAF phenotype. In order to test this hypothesis, TGF-β1 was first used to differentiate NOF into an experimentally-derived CAF phenotype (eCAF) in culture. Dose and time course experiments were performed to optimise the appropriate TGF-β1 concentration and treatment time needed for maximal induction of CAF-like myofibroblast differentiation, within the physiological range of TGF-β1. TGF-β1 concentrations (0.05-5 ng/ml) were chosen based on a previous study (Walker *et al*., 2004). In this study, 5 ng/ml was used as the optimal concentration of TGF-β1 and 48 h as optimal time course for fibroblast activation to a CAF-like myofibroblastic eCAF phenotype, as determined by increased expression of α-SMA at mRNA and protein level. There was a biological variability observed in all primary NOF cultures in response to TGF-β1 throughout this study, however the majority of cultures showed at least some response, albeit of varying magnitude. NOF5 showed greater response to TGF-β1 among other NOF as assessed by increased α-SMA expression. The differences observed are perhaps due to the freshness of TGF-β1 and also the condition of NOF such as the passage number (previous data

accrued in the lab indicates that NOF cultures do not senesce within the range of passages used, but it is impossible to exclude other phenotypic variations that may have been induced by culture). Additionally, patient-to-patient variability contributes to these differences such as age, smoking status and health status (e.g oral infection).

Another myofibroblast and CAF marker, FN-EDA1, was also used as CAF marker to monitor eCAF development in this study. Unlike α-SMA, this marker is not fully characterised in myofibroblast differentiation. FN-EDA1 has been demonstrated to be re-expressed in various pathological processes including wound healing and liver fibrosis (Ffrench-Constant *et al*., 1989; Jamagin *et al*., 1994). Serini and co-workers (1999) demonstrated that FN-EDA1 plays an important role in TGF-β1-induced myofibroblast differentiation in cultured rat subcutaneous, lung and dermis fibroblasts. TGF-β1 induced differentiation into myofibroblasts with increased FN-EDA1 production in cultured colonic lamina propria fibroblasts (Brenmoehl *et al*., 2009). Taken together, TGF-β1 has been shown to increase FN-EDA1 production and is becoming an established myofibroblast differentiation marker, and was hence used in this study. Here, it was shown, for the first time to our knowledge, that TGF-β1 robustly induces FN-EDA1 expression in oral fibroblast cultures. However, how FN-EDA1 regulates, or participates in, myofibroblast differentiation remains unknown. In this study, similar to α-SMA, NOF5 demonstrated the highest increase in FN-EDA1 expression in response to TGF-β1 at mRNA level compared to the other NOF cultures.

Actin stress fibres are comprised of bundles of polymerized actin filaments connected to modified focal adhesion complexes, thus providing the transmembrane link to components of ECM (Goldman *et al*., 1975). CAF have cytoplasmic β-actin and γ-actin isoforms which participate in actin stress fibre formation (Sandbo *et al*., 2011). As mentioned above, α-SMA expression is induced in NOF under stimulation with TGF-β1.

α-SMA is rapidly incorporated into actin stress fibre, thereby increasing the contractility of fibroblasts (Serini and Gabbiani, 1999). In keeping with this, in this study, TGF-β1 not only increase gene expression of α-SMA but also promoted the development of α-SMA positive stress fibres. Fluorescence microscopic analysis showed that TGF-β1 increased α-SMA positive staining cells compared to untreated cells, in all NOF cultures. This result is consistent with a highly contractile phenotype of eCAF under TGF-β1 stimulation, as assessed by collagen contraction assays. The appearance of actin stress fibres is closely related to the generation of contractile force, particularly in intact granulation tissue (Hinz *et al*., 2001). Stress fibre contraction is controlled by the Rho-dependent regulation of non-muscle myosin together with the stress fibre (Pellegrin and Mellor, 2007). In keeping with the findings reported here, TGF-β1 induces myofibroblast differentiation of human gingival fibroblasts by increasing α-SMA expression and α-SMA positive stress fibres formation, compared to untreated cells (Lewis *et al*., 2004). In another study, flow cytometric analysis showed that treatment of human buccal fibroblasts with TGF-β1 increased α-SMA production compared to unstimulated cells (Kellermann *et al*., 2007). In summary, the findings reported here are in keeping with, and add to, existing understanding of the ability of TGF-β1 to induce a myofibroblastic CAF-like phenotype in oral fibroblasts *in vitro*, giving confidence that this optimised model of CAF differentiation could be used for subsequent analysis of underlying molecular mechanisms.

Little is known about the role of miRNAs in the tumour microenvironment, especially in stromal cells of OSCC. Evidence in the literature suggests miRNAs are likely to play a role in TGF-β1 signaling; most members of the TGF-β1 pathway are known or predicted to be targeted by one or more miRNAs (Butz *et al*., 2012). Furthermore, TGF-β1 directly regulates the biogenesis of miRNAs through Smads

(Zhong *et al*., 2010). The expression of miR-21 was upregulated in TGF-β1-treated fibroblast isolated from normal lung tissue, compared to untreated fibroblasts (Yao *et al*., 2011). The expression of miR-31 and miR-214 were downregulated in CAF from ovarian tumours (Mitra *et al*., 2012). Here it was hypothesised, therefore, that miRNA play a role in the development of a myofibroblastic CAF. To begin to test this hypothesis, the expression profile of miRNAs during the differentiation of normal fibroblasts to eCAF was studied. The data presented in this study demonstrated that eCAF exhibit distinct miRNAs expression profiles compared to corresponding NOF. A preliminary analysis of the tiling low density array (TLDA) data accrued indicated that hundreds of miRNAs were deregulated in TGF-β1-treated NOF culture, compared to unstimulated NOF. Out of these, miR-424-5p and miR-145-5p were highly upregulated in eCAF from NOF1 and NOF5 cultures while miR-424-3p was highly upregulated in eCAF from NOF804 culture. Conversely, the miR-145-5p was downregulated in eCAF from NOF804 culture. Thus, these three miRNAs were selected for further validation by qRT-PCR. The qRT-PCR data generally correlated with the TLDA data, although different magnitudes of changes were observed in some cases between the two techniques used.

To gain a further insight on how these miRNAs regulate TGF-β1-induced CAF-like myofibroblast differentiation, both the loss-of-function and the gain-of-function experiments were carried out. miR-145 is a miRNA previously identified to play a role in fibroblast differentiation in different contexts. Wang and colleagues (2014) demonstrated that miR-145 induces conversion of cardiac fibroblasts into myofibroblast. Additionally, miR-145 plays an important role in lung myofibroblast differentiation (Yang *et al*., 2013). Relatively, little is known about miR-424 in the tumour-stroma interactions; miR-424 was demonstrated to regulate myofibroblast differentiation in human lung epithelial through EMT (Xiao *et al*., 2015) but otherwise its role in this context is little documented.

In this study, the role of miR-424-5p and miR-145-5p could not be investigated further in NOF1 and NOF5 cultures (used for the TLDA profiling) due to problems with their culture which arose after the profiling had been carried out. Therefore, a newly-derived NOF culture, NOF804 was mainly used throughout this study to investigate the role of miR-424-3p and miR-145-5p in TGF-β1-induced CAF-like myofibroblast differentiation.

The present study revealed that miR-424-3p is able to modulate, at least in part, TGF-β1-induced myofibroblast differentiation in NOF804. Overexpression of miR-424-3p attenuated the expression of TGF-β1-induced myofibroblast markers, with pronounced effects on α-SMA and FN-EDA1 transcript levels. In line with this finding, overexpression of miR-424-3p prevented TGF-β1-induced contractility in NOF804. However, overexpression of miR-424-3p had only a small effect on TGF-β1-induced α-SMA abundance at protein level and TGF-β1-induced stress fibre formation. An attempt to inhibit miR-424-3p and miR-145-5p (loss-of-function assays) in NOF did not work well as the functional analysis showed unconvincing data for both inhibitors. There was some variability in response to inhibition of miR-424-3p and miR-145-5p between biological repeats in NOF, as indicated by large standard errors of the mean generated from the data. These possibly due to the efficiency of individual transfections or of variations in the NOF themselves (e.g passage number and confluency). Further investigations would be required to determine the reasons for the variation observed, such as transfecting fluorescently tagged inhibitors to examine transfection efficiency.

Given the changes in expression and the functional data observed in eCAF in this study, the function of miR-424-3p and miR-145-5p in tumour-derived CAF from OSCC was also investigated. Overexpression of miR-424-3p did not inhibit basal myofibroblast phenotype or further TGF-β1-induced myofibroblast differentiation in CAF. Neither inhibition of miR-424-3p nor miR-145-5p increase basal myofibroblast phenotype in

CAF. Inhibition of miR-434-3p decreased TGF-β1-induced positive stress fibre formation and collagen contractility in CAF. Inhibition of miR-145-5p significantly increases TGF-β1's ability to induced gel contraction, but not other markers of the myofibroblast phenotype, in CAF.

As some of the functional data obtained were somewhat inconclusive (particularly with regards to miR-145), and the original NOF cultures became unusable, NOF804 cells were used to generate three repeats and the data re-analysed using a more sophisticated approach. The TLDA data revealed that miR-424-3p and miR-145-5p were not differentially expressed in eCAF from NOF804. Additionally, the re-analysed TLDA data revealed other potential miRNA candidates differentially expressed in eCAF from NOF804 culture; miR-503 and miR-708. miR-503 is predicted to target Smad7 and Smurf1 (a negative regulator of TGF-β or BMP signaling pathway), while miR-708 is predicted to target Smad2 (a positive regulator of TGF-β signaling) and COL1A1 (a component of ECM).

This study also demonstrated the miRNA signature of CAF derived from two subtypes of OSCC. CAF (GU-OSCC) were large, slow growing and associated with cellular senescence (Lim *et al*., 2011). Furthermore, this type of CAF exhibited high SA β-Gal expression and upregulation of $p16^{INK4A}$ (Hassona *et al*., 2013). CAF (GS-OSCC) are wild-type TP53/$p16^{INK4A}$. The present study revealed that 16 miRNAs were significantly deregulated in CAF (GS-OSCC), with miR-192 highly upregulated in CAF (GS-OSCC), compared to NOF. Fourteen miRNAs were significantly upregulated in CAF (GU-OSCC), compared to NOF with miR-324-5p showed the highest expression among the other miRNAs. Out of the 14 altered miRNAs, three miRNAs are predicted to target genes related to G1 cell cycle or p53 negative feedback; miR-30b (Cyclin D, Cyclin E and CDK6), miR-376a (MDM2) and miR-532-3p (Cyclin D and MDM2). All

of these genes might be involved in maintaining the phenotype of CAF (GU-OSCC) which are predominantly senescent and slow growing in culture. Both types of CAF share common miRNAs expression changes; miR-197, miR-320, miR-324-5p and miR-376b. miR-197, miR-320 and miR-376b are predicted to target different genes related to CAF biology (e.g TGF-β signaling, ECM component) or regulation of autophagy. Thus, targeting these miRNAs might have translational benefits in clinical therapy of either genetically stable or unstable tumours of OSCC.

6.2 Limitations of the study

The present study optimised the generation of eCAF by assessing two molecular markers of myofibroblast differentiation; α-SMA and FN-EDA1, as well as stress fibre formation and fibroblast contractility. Although these findings are sufficient to confirm the cells are CAF-like cells but within the same type of tissue, CAF markers are not uniquely expressed on these cells, suggesting distinct CAF subpopulations exist. Sugimoto and co-workers (2006) demonstrated that one CAF-subtype characterized by co-expression of α-SMA, PDGFRβ, and NG2, while another subtype expressed FSP-1. Furthermore, FSP-1-positive fibroblast was identified as being mostly non-myofibroblast-rich cell populations of CAF and was demonstrated to accelerate tumourigenesis *in vivo* and human tumour xenograft model (Trimboli *et al*., 2009; Erez *et al*., 2010; O'Connell *et al*., 2011). Collectively, it would be interesting to examine other myofibroblast markers, to confirm the faithfulness of the phenotype observed in this study to CAF *in vivo*. For example, FAP, which is reported to be highly expressed by CAF in various human epithelial cancers such as breast, ovarian and lung cancers (Cheng *et al*., 2005), could have been analysed if more time had been available.

Immunocytochemistry of stress fibre formation can be improved by including a red Phalloidin antibody that stained F-actin. This could highlight the cytoplasm and

fibroblasts, relative to α-SMA expression.

The gel collagen contraction assay demonstrated that the cells assessed in this study were CAF-like cells. Giving that CAF exist from various fibroblast populations, this method is limited as it only gives quantitative contraction for populations of cells, not individual cells. In addition, matrix tension alone is unable to complete myofibroblast differentiation. The matrix tension transferred to fibroblast is modulated by integrins, found in focal adhesion complex (Arora *et al*., 1999) and these focal adhesions could be assessed by scanning electron microscopy. Furthermore, matrix tension is important to generate the intermediate cells that are thought to transform into differentiated myofibroblasts, termed proto-myofibroblasts (Tomasek *et al*., 2002).

In this study, NOF cultures seem to be quite heterogenous in their level of α-SMA expression in response to TGF-β1. This could be explained by demonstrating whether the NOF cultures used in this study respond to canonical TGF-β signaling e.g Smad7 gene expression by qRT-PCR. Other approach, a single cell RNA-seq might be useful to look for the heterogeneity within NOF cultures.

qPCR is a commonly used method for studying miRNA function upon transfection with miRNA mimics or miRNA inhibitors. However, this method does not accurately determine the level of miRNA. In theory, for a miRNA to be functional, miRNA must be incorporated into RISC complex. Thus, qPCR does not distinguish between functional miRNA or non-functional miRNA. In addition, miRNA inhibitors can give a false positive result because, after cell lysis, most of the inhibitors released from cellular vesicles can directly interfere with the PCR reaction (Thomson *et al*., 2013). Better approaches to measure the effectiveness of transfection are the use of miRNA reporter assay or measurement of miRNA level by Argonaute immunoprecipitation (a key component of the RISC complex).

CAF are possibly derived from various origins with specific transitions. CAF might arise from resident fibroblasts through MMT while epithelial cells acquire EMT to become CAF (Cirri and Chiarugi, 2011). In this study, it is unsure whether CAF from OSCC originate from resident fibroblasts or cancer cells. A karyotypic analysis should be done to exclude CAF that originate from cancer cells through EMT. CAF have a stable diploid karyotype while cancer cells are polyploid (Aprelikova *et al*., 2010). Therefore, the role of miR-424-3p in TGF-β1-induced myofibroblast differentiation can be fairly compared between eCAF with real CAF.

6.3 Future work

The findings obtained from this study have raised many questions in the context of myofibroblast differentiation or CAF development. As mentioned in Section 6.2, some of the experiments could be carried out to further characterise eCAF.

Although miR-424-3p was partially involved in TGF-β1-induced CAF-like myofibroblast differentiation, its pro-tumorigenic roles in the cancer progression should be investigated in various aspects including hypoxia and angiogenesis. miR-424 is a hypoxia-induced miRNA and targets HIFs, transcription factors that regulate tumour cell survival and angiogenesis (Ghosh *et al*., 2010). Moreover, miR-424 regulates tumour metabolism by upregulation of glycolysis through regulation of IDH3α during TGF-β1-induced CAF formation (Zhang *et al*., 2015).

The significantly upregulated miRNAs (re-analysed TLDA data) in eCAF from NOF804 should be validated by qRT-PCR. The roles of selected miRNAs could be studied by both gain-of-function and loss-of-function experiment. For the loss-of-function study, another method should be implemented such as miRNA sponges. This method uses plasmid constructs either transiently or stably transfected into the cells

containing multiple miRNA binding sites for a selected miRNA. Once the functional role of miRNAs was established, downstream cytokines, chemokines and growth factors can be predicted using target prediction tools such as TargetScan and Diana-microT.

The role of selected miRNAs could be studied in the context of tumour-stroma interactions. This can be achieved by 3D models of co-culturing cancer cells with CAF or fibroblasts stably transfected with miRNA mimics or miRNA inhibitors, to see the effects of those miRNAs in cancer progression such as invasion and angiogenesis. Giving that TGF-β1 regulates myofibroblast differentiation, a study could be carried out to assess whether the selected miRNAs are downstream of TGF-β signaling.

Certain exosome-secreted miRNAs can be transferred from stromal cells to cancer cells. Vanpoucke and co-workers (2004) demonstrated that miR-223 is highly expressed in IL-4-induced TAMs, not in breast cancer cells. This miRNA can be transmitted from TAMs to cancer cells and inhibits Myocyte-specific enhancer factor 2C (Mef2C), a transcription factor that promotes cell migration. Therefore, a study could be conducted to determine the transmission of selected miRNAs between associated stromal cells with oral cancer cells and examining the tumour promoting effects of these selected miRNAs.

6.4 Conclusions and clinical significance

This study identified miR-424-3p as a regulator, at least in part, of TGF-β1-induced CAF-like myofibroblast differentiation. miR-424-3p overexpression was able to prevent TGF-β1-induced CAF-like myofibroblastic phenotype. However, more in-depth investigations are needed to better understand the exact mechanisms and the tumour-promoting role of miR-424-3p in oral stroma-cancer interactions.

This study emphasised the exciting potential of other miRNA candidates that

differentially expressed in eCAF and these miRNAs might reverse the myofibroblastic phenotype in the fibrosis and in the tumour microenvironment. Additionally, this study has highlighted the miRNA signatures of CAF from two subtypes of OSCC. These miRNA signatures have valuable indicators in clinical diagnosis, prognosis and therapeutic targets in OSCC. Cancer cells and CAF have different biological characteristics, thus the same miRNAs might play different roles in them. Although there is distinct miRNAs expression profile in CAF from some type of cancer, some miRNAs are shown to have a common role in CAF from different cancers. miR-21 is highly upregulated in the CAF from various cancer tissues and this indicates poor prognoses (Bullock *et al*., 2013; Li *et al*., 2013; Nielsen *et al*., 2011). The ability to manipulate miRNA expression currently predominantly involves the use of miRNA inhibitors or miRNA mimic. However, the successful delivery *in vivo* is still challenging. The nature of naked miRNAs; hydrophilicity, polyanionic nature and high molecular weight, makes them unable to cross the cell membrane (Wang *et al*., 2010). Furthermore, administration of miRNAs by intravenous resulted in poor tissue distribution due to renal bypass. All of these technical challenges need to be overcome before translating the mechanistic insight gained in studies such as this to a clinical setting.

REFERENCES

Accerbi, M., Schmidt, S.A., De Paoli, E., Park, S., Jeong, D.H. and Green, P.J. Methods for isolation of total RNA to recover miRNAs and other small RNAs from diverse species. *Plant MicroRNAs: Methods and Protocols* 2010; 31-50.

Akao, Y., Nakagawa, Y. and Naoe, T. let-7 microRNA functions as a potential growth suppressor in human colon cancer cells. *Biological and Pharmaceutical Bulletin* 2006; 29(5): 903-906.

Akhmetshina, A., Palumbo, K., Dees, C., Bergmann, C., Venalis, P., Zerr, P., Horn, A., Kireva, T., Beyer, C., Zwerina, J. and Schneider, H. Activation of canonical Wnt signalling is required for TGF-β-mediated fibrosis. *Nature communications* 2012; (*3*): 735.

Akhurst, R. J. TGF-β antagonists: why suppress atumor suppressor? *J. Clin. Invest.* 2002; 109: 1533–1536.

Allinen, M., Beroukhim, R., Cai, L., Brennan, C., Lahti-Domenici, J., Huang, H., Porter, D., Hu, M., Chin, L., Richardson, A. and Schnitt, S. Molecular characterization of the tumor microenvironment in breast cancer. *Cancer cell* 2004; 6(1): 17-32.

Ambros, V. The functions of animal microRNAs. *Nature* 2004; 431(7006): 350-355.

American Cancer Society. Cancer Facts & Figures 2011. Atlanta: American Cancer Society; 2011.

Annes, J.P., Munger, J.S. and Rifkin, D.B. Making sense of latent TGFβ activation. *Journal of cell science* 2003; 116(2): 217-224.

Aprelikova, O., Yu, X., Palla, J., Wei, B.R., John, S., Yi, M., Stephens, R., Simpson, R.M., Risinger, J.I., Jazaeri, A. and Niederhuber, J. The role of miR-31 and its target gene SATB2 in cancer-associated fibroblasts. *Cell Cycle* 2010; 9(21): 4387-4398.

Aprelikova, Olga and Jeffrey, E. Green MicroRNA regulation in cancerassociated fibroblasts. *Cancer Immunol. Immunother* 2012; 61, 231–237.

Argiris A. Induction chemotherapy for head and neck cancer: will history repeat itself? *J Natl Compr Canc Netw* 2005; 3: 393–403.

Argiris A, Karamouzis MV, Raben D, Ferris RL. Head and neck cancer. *Lancet* 2008; 371:1695–709.

Arora, P.D. and McCulloch, C.A. Dependence of collagen remodelling on α-smooth muscle actin expression by fibroblasts. *Journal of cellular physiology* 1994; 159(1): 161-175.

Arora, P.D., Narani, N. and McCulloch, C.A. The compliance of collagen gels regulates transforming growth factor-β induction of α-smooth muscle actin in fibroblasts. *The American journal of pathology* 1999; 154(3): 871-882.

Arroyo, J.D., Chevillet, J.R., Kroh, E.M., Ruf, I.K., Pritchard, C.C., Gibson, D.F., Mitchell, P.S., Bennett, C.F., Pogosova-Agadjanyan, E.L., Stirewalt, D.L. and Tait, J.F. Argonaute2 complexes carry a population of circulating microRNAs independent of vesicles in human plasma. *Proceedings of the National Academy of Sciences* 2011; 108(12): 5003-5008.

Ask, K., Bonniaud, P., Maass, K., Eickelberg, O., Margetts, P.J., Warburton, D., Groffen, J., Gauldie, J. and Kolb, M. Progressive pulmonary fibrosis is mediated by TGF-β isoform 1 but not TGF-β3. *The international journal of biochemistry & cell biology* 2008; 40(3):484-495.

Assoian R.K., Fleurdelys B.E., Stevenson H.C., Miller P.J., Madtes D.K., Raines E.W., Ross R., Sporn M.B., Expression and secretion of type beta transforming growth factor by activated human macrophages. *Proc. Natl. Acad. Sci. USA*1987; 84: 6020–6024.

Attisano, L. and Wrana, J.L. Signal transduction by the TGF-β superfamily. *Science* 2002; 296(5573): 1646-1647.

Baglole, C.J., Ray, D.M., Bernstein, S.H., Feldon, S.E., Smith, T.J., Sime, P.J. and Phipps, R.P. More than structural cells, fibroblasts create and orchestrate the tumor microenvironment. *Immunological investigations* 2006; *35*(3-4): 297-325.

Balz V, Scheckenbach K, Gotte K, Bockmuhl U, Petersen I, Bier H. Is the p53 inactivation frequency in squamous cell carcinomas of the head and neck underestimated? Analysis of p53 exons 2-11 and human papillomavirus 16/18 E6 transcripts in 123 unselected tumor specimens. *Cancer Res* 2003; 63: 1188–91.

Banyard, J., Chung, I., Wilson, A.M., Vetter, G., Le Béchec, A., Bielenberg, D.R. and Zetter, B.R. Regulation of epithelial plasticity by miR-424 and miR-200 in a new prostate cancer metastasis model. *Scientific reports* 2013; 3.

Barca-Mayo, O. and Lu, Q.R. Fine-tuning oligodendrocyte development by microRNAs. *Frontiers in neuroscience* 2012; 6.

Barh, D., Malhotra, R., Ravi, B. and Sindhurani, P. MicroRNA let-7: an emerging next-generation cancer therapeutic. *Current oncology* 2010; 17(1): 70.

Barlev, N.A., Sayan, B.S., Candi, E. and Okorokov, A.L. The microRNA and p53 families join forces against cancer. *Cell death and differentiation* 2010; 17(2): 373.

Barnum, K.J. and O'Connell, M.J. Cell cycle regulation by checkpoints. *Cell Cycle Control: Mechanisms and Protocols* 2014; 29-40.

Bartel, D. P. MicroRNAs: target recognition and regulatory functions. *Cell* 2009;136 (2): 215-233.

Bauer, M., Su, G., Casper, C., He, R., Rehrauer, W. and Friedl, A. Heterogeneity of gene expression in stromal fibroblasts of human breast carcinomas and normal breast. *Oncogene* 2010; 29(12): 1732.

Beauséjour, C.M., Krtolica, A., Galimi, F., Narita, M., Lowe, S.W., Yaswen, P. and Campisi, J. Reversal of human cellular senescence: roles of the p53 and p16 pathways. *The EMBO journal* 2003; 22(16): 4212-4222.

Bell, E., Ivarsson, B. and Merrill, C. Production of a tissue-like structure by contraction of collagen lattices by human fibroblasts of different proliferative potential in vitro. *Proceedings of the National Academy of Sciences* 1979; 76(3): 1274-1278.

Bergfeld, S.A. and DeClerck, Y.A. Bone marrow-derived mesenchymal stem cells and the tumor microenvironment. *Cancer and Metastasis Reviews* 2010; *29*(2): 249-261.

Bhowmick, N.A., Ghiassi, M., Aakre, M., Brown, K., Singh, V. and Moses, H.L. TGF-β-induced RhoA and p160ROCK activation is involved in the inhibition of Cdc25A with resultant cell-cycle arrest. *Proceedings of the National Academy of Sciences* 2003; 100(26): 15548-15553.

Bishop, J.F. Cancer facts: a concise oncology text: Bishop, J.F. (ed). Harwood academic publishers 1999; 3-4.

Bochaton-Piallat, M.L., Kapetanios, A.D., Donati, G., Redard, M., Gabbiani, G., & Pournaras, C.J. TGF—β1, TGF-β receptor II and ED-A fibronectin expression in myofibroblast of vitreoretinopathy. *Investigation Ophthalmology & Visual Science* 2000; 41 (8): 2336-2342, 1552-5783.

Bogatkevich, G.S., Tourkina, E., Silver, R.M. and Ludwicka-Bradley, A. Thrombin differentiates normal lung fibroblasts to a myofibroblast phenotype via the

proteolytically activated receptor-1 and a protein kinase C-dependent pathway. *Journal of Biological Chemistry* 2001; 276(48): 45184-45192.

Bowen, T., Jenkins, R.H. and Fraser, D.J. MicroRNAs, transforming growth factor beta-1, and tissue fibrosis. *The Journal of pathology* 2013; 229(2): 274-285.

Braig, M. and Schmitt, C.A. Oncogene-induced senescence: putting the brakes on tumor development. *Cancer research* 2006; 66(6): 2881-2884.

Braun, C.J., Zhang, X., Savelyeva, I., Wolff, S., Moll, U.M., Schepeler, T., Ørntoft, T.F., Andersen, C.L. and Dobbelstein, M. p53-Responsive micrornas 192 and 215 are capable of inducing cell cycle arrest. *Cancer research* 2008; 68(24): 10094-10104.

Brenmoehl J, Miller SN, Hofmann C, Vogl D, Falk W, Schölmerich J, Rogler G. Transforming growth factor-β1 induces intestinal myofibroblast differentiation and modulates their migration. *World J Gastroenterol* 2009; 15(12): 1431-1442.

Breving, K. and Esquela-Kerscher, A. The complexities of microRNA regulation: mirandering around the rules. *The international journal of biochemistry & cell biology* 2010; 42(8): 1316-1329.

Brockhausen, J., Tay, S.S., Grzelak, C.A., Bertolino, P., Bowen, D.G., d'Avigdor, W.M., Teoh, N., Pok, S., Shackel, N., Gamble, J.R. and Vadas, M. miR-181a mediates TGF-β-induced hepatocyte EMT and is dysregulated in cirrhosis and hepatocellular cancer. *Liver International* 2015; 35(1): 240-253.

Bronisz, A., Godlewski, J., Wallace, J.A., Merchant, A.S., Nowicki, M.O., Mathsyaraja, H., Srinivasan, R., Trimboli, A.J., Martin, C.K., Li, F. and Yu, L. Reprogramming of the tumor microenvironment by stromal PTEN-regulated miR-320. *Nature cell biology* 2012; 14(2): 159.

Bronisz, A., Wang, Y., Nowicki, M.O., Peruzzi, P., Ansari, K.I., Ogawa, D., Balaj, L., De Rienzo, G., Mineo, M., Nakano, I. and Ostrowski, M.C. Extracellular vesicles modulate the glioblastoma microenvironment via a tumor suppression signaling network directed by miR-1. *Cancer research* 2014; 74(3): 738-750.

Brosius, F.C III. New insights into the mechanisms of fibrosis and sclerosis in diabetic nephropathy. *Rev Endocr Metab Disord* 2008; 9:245–254.

Brown, R.A., Prajapati, R., McGrouther, D.A., Yannas, IV., Eastwood, M. Tensional homeostasis in dermal fibroblasts: mechanical responses to mechanical loading in three-dimensional substrates. *J Cell Physiol* 1998; 175:323–332.

Bujak, M., Ren, G., Kweon, H.J., Dobaczewski, M., Reddy, A., Taffet, G., Wang, X.F. and Frangogiannis, N.G. Essential role of Smad3 in infarct healing and in the pathogenesis of cardiac remodeling. *Circulation* 2007; 116(19): 2127-2138.

Bullock, M.D., Pickard, K.M., Nielsen, B.S., Sayan, A.E., Jenei, V., Mellone, M., Mitter, R., Primrose, J.N., Thomas, G.J., Packham, G.K. and Mirenzami, A.H. Pleiotropic actions of miR-21 highlight the critical role of deregulated stromal microRNAs during colorectal cancer progression. *Cell death & disease* 2013; 4(6): 684.

Burk, U., Schubert, J., Wellner, U., Schmalhofer, O., Vincan, E., Spaderna, S. and Brabletz, T. A reciprocal repression between ZEB1 and members of the miR-200 family promotes EMT and invasion in cancer cells. *EMBO reports* 2008; 9(6): 582-589.

Bussard, K.M., Mutkus, L., Stumpf, K., Gomez-Manzano, C. and Marini, F.C. Tumor-associated stromal cells as key contributors to the tumor microenvironment. *Breast Cancer Research* 2016; 18(1): 84.

Butler, J.P., Tolić-Nørrelykke, I.M., Fabry, B. and Fredberg, J.J. Traction fields, moments, and strain energy that cells exert on their surroundings. *American Journal of Physiology-Cell Physiology 2002;* 282(3): 595-605.

Butz, Henriett; Rácz, Károly; Hunyady, László; Patócs, Attila. Crosstalk between TGF-β signaling and the microRNA machinery. *Trends in pharmacological sciences* 2012; 33 (7): 382-93.

Calin GA, Dumitru CD, Shimizu M, et al. Frequent deletions and down-regulation of micro-RNA genes miR15 and miR16 at 13q14 in chronic lymphocytic leukemia. *Proc Natl Acad Sci USA* 2002; 99:15524–9.

Campisi, J., Kim, S.H., Lim, C.S. and Rubio, M. Cellular senescence, cancer and aging: the telomere connection. *Experimental gerontology* 2001; 36(10): 1619-1637.

Campisi, J. Cellular senescence as a tumor-suppressor mechanism. *Trends in cell biology* 2001; 11: 27-31.

Camps, J.L., Chang, S.M., Hsu, T.C., Freeman, M.R., Hong, S.J., Zhau, H.E., von Eschenbach, A.C. and Chung, L.W. Fibroblast-mediated acceleration of human epithelial tumor growth in vivo. *Proceedings of the National Academy of Sciences* 1990; *87*(1): 75-79.

Camps, C., Buffa, F.M., Colella, S., Moore, J., Sotiriou, C., Sheldon, H., Harris, A.L., Gleadle, J.M. and Ragoussis, J. hsa-miR-210 Is induced by hypoxia and is an

independent prognostic factor in breast cancer. *Clinical cancer research* 2008; 14(5): 1340-1348.

Capaccio, P., Pruneri, G., Carboni, N., Pagliari, A.V., Quatela, M., Cesana, B.M. and Pignataro, L. Cyclin D1 expression is predictive of occult metastases in head and neck cancer patients with clinically negative cervical lymph nodes. *Head & neck* 2000; *22*(3): 234-240.

Caporali, A. and Emanueli, C. MicroRNA-503 and the extended microRNA-16 family in angiogenesis. *Trends in cardiovascular medicine* 2011; 21(6): 162-166.

Carthy, J.M., Luo, Z. and McManus, B.M. WNT3A induces a contractile and secretory phenotype in cultured vascular smooth muscle cells that is associated with increased gap junction communication. *Laboratory Investigation* 2012; 92(2): 246.

Carthy, J.M., Sundqvist, A., Heldin, A., Van Dam, H., Kletsas, D., Heldin, C.H. and Moustakas, A. Tamoxifen Inhibits TGF-β-Mediated Activation of Myofibroblasts by Blocking Non-Smad Signaling Through ERK1/2. *Journal of cellular physiology* 2015; 230(12): 3084-3092.

Casey, T.M., Eneman, J., Crocker, A., White, J., Tessitore, J., Stanley, M., Harlow, S., Bunn, J.Y., Weaver, D., Muss, H. and Plaut, K. Cancer associated fibroblasts stimulated by transforming growth factor beta1 (TGF-β1) increase invasion rate of tumor cells: a population study. *Breast cancer research and treatment* 2008; 110(1): 39-49.

Catto, J.W., Alcaraz, A., Bjartell, A.S., White, R.D.V., Evans, C.P., Fussel, S., Hamdy, F.C., Kallioniemi, O., Mengual, L., Schlomm, T. and Visakorpi, T. MicroRNA in prostate, bladder, and kidney cancer: a systematic review. *European urology* 2011; 59(5): 671-681.

Chamorro-Jorganes, A., Araldi, E., Penalva, L.O., Sandhu, D., Fernández-Hernando, C. and Suárez, Y. MicroRNA-16 and microRNA-424 regulate cell-autonomous angiogenic functions in endothelial cells via targeting vascular endothelial growth factor receptor-2 and fibroblast growth factor receptor-1. *Arteriosclerosis, thrombosis, and vascular biology* 2011; 31(11): 2595-2606.

Chan, J.A., Krichevsky, A.M., Kosik, K.S. MicroRNA-21 is an antiapoptotic factor in human glioblastoma cells. *Cancer Res* 2005; 65:6029–33.

Chang, C.J., Hsu, C.C., Chang, C.H., Tsai, L.L., Chang, Y.C., Lu, S.W., Yu, C.H., Huang, H.S., Wang, J.J., Tsai, C.H. and Chou, M.Y. Let-7d functions as novel

regulator of epithelial-mesenchymal transition and chemoresistant property in oral cancer. *Oncology reports* 2011; 26(4): 1003-1010.

Chang, H.Y., Chi, J.T., Dudoit, S., Bondre, C., van de Rijn, M., Botstein, D. and Brown, P.O. Diversity, topographic differentiation, and positional memory in human fibroblasts. *Proceedings of the National Academy of Sciences* 2002; 99(20): 12877-12882.

Chen, C.Z. MicroRNAs as oncogenes and tumor suppressors. *N Engl J Med* 2005; 353:1768–71.

Chen, G., Shen, Z.L., Wang, L., Lv, C.Y., Huang, X.E. and Zhou, R.P. Hsa-miR-181a-5p expression and effects on cell proliferation in gastric cancer. *Asian Pacific Journal of Cancer Prevention* 2013; 14(6): 3871-3875.

Chen, J.H., Chen, W.L.K., Sider, K.L., Yip, C.Y.Y. and Simmons, C.A. β-catenin mediates mechanically regulated, transforming growth factor-β1–induced myofibroblast differentiation of aortic valve interstitial cells. *Arteriosclerosis, thrombosis, and vascular biology* 2011; 31(3): 590-597.

Chen, Z., Li, Y., Zhang, H., Huang, P. and Luthra, R. Hypoxia-regulated microRNA-210 modulates mitochondrial function and decreases ISCU and COX10 expression. *Oncogene* 2010; 29(30): 4362.

Cheng, H., Zhang, L., Cogdell, D.E., Zheng, H., Schetter, A.J., Nykter, M., Harris, C.C., Chen, K., Hamilton, S.R. and Zhang, W. Circulating plasma MiR-141 is a novel biomarker for metastatic colon cancer and predicts poor prognosis. *PloS one* 2011; 6(3): 17745.

Cheng, J.D., Valianou, M., Canutescu, A.A., Jaffe, E.K., Lee, H.O., Wang, H., Lai, J.H., Bachovchin, W.W. and Weiner, L.M. Abrogation of fibroblast activation protein enzymatic activity attenuates tumor growth. *Molecular cancer therapeutics* 2005; 4(3):351-360.

Chou, J., Lin, J.H., Brenot, A., Kim, J.W., Provot, S. and Werb, Z. GATA3 suppresses metastasis and modulates the tumour microenvironment by regulating microRNA-29b expression. *Nature cell biology* 2013; 15(2): 201.

Cimmino, A., Calin, G.A., Fabbri., M, et al. miR-15 and miR-16 induce apoptosis by targeting BCL2. *Proc Natl Acad Sci USA* 2005; 102:13944–9.

Cirri P, Chiarugi P. Cancer associated fibroblasts: the dark side of the coin. *Am J Cancer Res* 2011; 1: 482–497.

Clevers, H. and Nusse, R. Wnt/β-catenin signaling and disease. *Cell* 2012; 149(6): 1192-1205.

Cohen, E.E., Lingen, M.W, Vokes, E.E. The expanding role of systemic therapy in head and neck cancer. *J Clin Oncol* 2004; 22: 1743–52.

Colevas AD. Chemotherapy options for patients with metastatic or recurrent squamous cell carcinoma of the head and neck. *J Clin Oncol* 2006; 24: 2644–52.

Cordenonsi, M., Dupont, S., Maretto, S., Insinga, A., Imbriano, C. and Piccolo, S. Links between tumor suppressors: p53 is required for TGF-β gene responses by cooperating with Smads. *Cell* 2003; 113(3): 301-314.

Cordes, K.R., Sheehy, N.T., White, M., Berry, E., Morton, S.U., Muth, A.N., Lee, T.H., Miano, J.M., Ivey, K.N. and Srivastava, D. miR-145 and miR-143 regulate smooth muscle cell fate decisions. *Nature* 2009; 460(7256): 705.

Corsten, M.F., Miranda, R., Kasmieh, R., Krichevsky, A.M., Weissleder, R. and Shah, K. MicroRNA-21 knockdown disrupts glioma growth in vivo and displays synergistic cytotoxicity with neural precursor cell–delivered S-TRAIL in human gliomas. *Cancer research* 2007; 67(19): 8994-9000.

Critchley, D.R. Focal adhesions–the cytoskeletal connection. *Current opinion in cell biology* 2000; 12(1): 133-139.

Cukierman, E., Bassi, D.E. The mesenchymal tumor microenvironment: a drugresistant niche. *Cell Adh Migr* 2012; 6:285–96.

Cunha, G.R., Hayward, S.W. and Wang, Y.Z. Role of stroma in carcinogenesis of the prostate. *Differentiation* 2002; 70(9-10): 473-485.

Curado MP, Edwards B, Shin HR, Storm H, Ferlay J, Heanue M, et al. Cancer Incidence in Five Continents, vol. IX. IARC Scientific Publication No. 160. In: Curado MP, Edwards B, Shin HR, Storm H, Ferlay J, Heanue M, Boyle P, editors. Lyon: International Agency for Research on Cancer, 2007.

Cutroneo, K.R. TGF-β–induced fibrosis and SMAD signaling: oligo decoys as natural therapeutics for inhibition of tissue fibrosis and scarring. *Wound Repair and Regeneration* 2007; 15(s1).

Czauderna, F., Fechtner, M., Dames, S., Aygün, H., Klippel, A., Pronk, G.J., Giese, K. and Kaufmann, J. Structural variations and stabilising modifications of synthetic siRNAs in mammalian cells. *Nucleic acids research* 2003; 31(11): 2705-2716.

Dai, X., Chen, A. and Bai, Z. Integrative investigation on breast cancer in ER, PR and HER2-defined subgroups using mRNA and miRNA expression profiling. *Scientific reports* 2014:4.

Darby, I., Skalli, O. and Gabbiani, G. a-Smooth muscle actin is transiently expressed by myofibroblasts during experimental wound healing. *Lab Invest* 1990 ; 63(1): 21-29.

De Andres L, Brunet J, Lopez-Pousa A, et al. Randomized trial of neoadjuvant cisplatin and fl uorouracil versus carboplatin and fluorouracil in patients with stage IV-M0 head and neck cancer. *J Clin Oncol* 1995; 13: 1493–500.

de-Assis, E.M., Pimenta, L.G., Costa-e-Silva, E., Souza, P.E. and Horta, M.C. Stromal myofibroblasts in oral leukoplakia and oral squamous cell carcinoma. *Medicina oral, patologia oral y cirugia bucal* 2012; 17(5): 733.

Dembo, M. and Wang, Y.L. Stresses at the cell-to-substrate interface during locomotion of fibroblasts. *Biophysical journal* 1999*;* 76(4): 2307-2316.

Derynck, R., Akhurst, R. J. & Balmain, A. TGF-β signaling in tumor suppression and cancer progression. *Nature Genet* 2001; 29: 117–129.

Desmouliere A, Redard M, Darby I, and Gabbiani G. Apoptosis mediates the decrease in cellularity during the transition between granulation tissue and scar. *Am J Pathol* 1995; 146: 56-66.

Desmouliere, A., Guyot, C. and Gabbiani, G. The stroma reaction myofibroblast: a key player in the control of tumor cell behavior. *International Journal of Developmental Biology* 2004; 48(5-6): 509-517.

De Veirman, K., Rao, L., De Bruyne, E., Menu, E., Van Valckenborgh, E., Van Riet, I., Frassanito, M.A., Di Marzo, L., Vacca, A. and Vanderkerken, K. Cancer associated fibroblasts and tumor growth: focus on multiple myeloma. *Cancers* 2014: 6(3): 1363-1381.

DeWever, O., Mareel, M. Role of tissue stroma in cancer cell invasion. *J Pathol* 2003; 200: 429–47.

DeWever, O., Westbroek, W., Verloes, A., Bloemen, N., Bracke, M., Gespach, C., Bruyneel, E. and Mareel, M. Critical role of N-cadherin in myofibroblast invasion and migration in vitro stimulated by colon-cancer-cell-derived TGF-β or wounding. *Journal of cell science* 2004; 117(20): 4691-4703.

Dhanda, J., Triantafyllou, A., Liloglou, T., Kalirai, H., Lloyd, B., Hanlon, R., Shaw, R.J., Sibson, D.R. and Risk, J.M. SERPINE1 and SMA expression at the invasive front predict extracapsular spread and survival in oral squamous cell carcinoma. *British journal of cancer* 2014; 111(11): 2114.

Diez, J. Do microRNAs regulate myocardial fibrosis? *Nat Clin Pract Cardiovasc Med* 2009; 6:88– 89.

Dimri, G.P., Lee, X., Basile, G., Acosta, M., Scott, G., Roskelley, C., Medrano, E.E., Linskens, M., Rubelj, I. and Pereira-Smith, O. A biomarker that identifies senescent human cells in culture and in aging skin in vivo. *Proceedings of the National Academy of Sciences* 1995; *92*(20): 9363-9367.

Ding, M., Newman, F., Raben, D. New radiation therapy techniques for the treatment of head and neck cancer. *Otolaryngol ClinNorth Am* 2005; 38: 371–95.

Direkze, N.C., Hodivala-Dilke, K., Jeffery, R., Hunt, T., Poulsom, R., Oukrif, D., Alison, M.R. and Wright, N.A. Bone marrow contribution to tumor-associated myofibroblasts and fibroblasts. *Cancer research* 2004; 64(23): 8492-8495.

Direkze, N.C. and Alison, M.R. Bone marrow and tumour stroma: an intimate relationship. *Hematological oncology* 2006; *24*(4): 189-195.

Doleshal, M., Magotra, A.A., Choudhury, B., Cannon, B.D., Labourier, E. and Szafranska, A.E. Evaluation and validation of total RNA extraction methods for microRNA expression analyses in formalin-fixed, paraffin-embedded tissues. *The Journal of Molecular Diagnostics* 2008; 10(3): 203-211.

Dominici, M.L.B.K., Le Blanc, K., Mueller, I., Slaper-Cortenbach, I., Marini, F.C., Krause, D.S., Deans, R.J., Keating, A., Prockop, D.J. and Horwitz, E.M. Minimal criteria for defining multipotent mesenchymal stromal cells. The International Society for Cellular Therapy position statement. *Cytotherapy* 2006; 8(4): 315-317.

Dourado, M.R., Guerra, E.N., Salo, T., Lambert, D.W. and Coletta, R.D. Prognostic value of the immunohistochemical detection of cancer-associated fibroblasts in oral cancer: a systematic review and meta-analysis. *Journal of Oral Pathology & Medicine* 2017.

Du, L., Schageman, J.J., Subauste, M.C., Saber, B., Hammond, S.M., Prudkin, L., Wistuba, I.I., Ji, L., Roth, J.A., Minna, J.D. and Pertsemlidis, A. miR-93, miR-98, and miR-197 regulate expression of tumor suppressor gene FUS1. *Molecular Cancer Research* 2009; 7(8): 1234-1243.

Duan, W.J., Yu, X., Huang, X.R., Yu, J.W. and Lan, H.Y. Opposing roles for Smad2 and Smad3 in peritoneal fibrosis *in vivo* and *in vitro*. *The American journal of pathology* 2014; 184(8): 2275-2284.

du Bois, R.M. Strategies for treating idiopathic pulmonary fibrosis. *Nat Rev Drug Discov* 2010.

Duda, D.G., Duyverman, A.M., Kohno, M., Snuderl, M., Steller, E.J., Fukumura, D. and Jain, R.K. Malignant cells facilitate lung metastasis by bringing their own soil. *Proceedings of the National Academy of Sciences* 2010; 107(50): 21677-21682.

Dugina, V., Alexandrova, A., Chaponnier, C., Vasiliev, J. and Gabbiani, G. Rat fibroblasts cultured from various organs exhibit differences in α-smooth muscle actin expression, cytoskeletal pattern, and adhesive structure organization. *Experimental cell research* 1998; 238(2): 481-490.

Dumont, N., Arteaga, C.L. Transforming growth factor-beta and breast cancer: Tumor promoting effects of transforming growth factor-beta. *Breast Cancer Res* 2000; 2:125–32.

D'souza, G., Kreimer, A.R., Viscidi, R., Pawlita, M., Fakhry, C., Koch, W.M., Westra, W.H. and Gillison, M.L. Case–control study of human papillomavirus and oropharyngeal cancer. *New England Journal of Medicine* 2007; 356(19): 1944-1956.

D'Souza-Schorey, C., Boshans, R.L., McDonough, M., Stahl, P.D. and Van Aelst, L. A role for POR1, a Rac1-interacting protein, in ARF6-mediated cytoskeletal rearrangements. *The EMBO Journal* 1997; 16(17): 5445-5454.

Ebisawa, T., Fukuchi, M., Murakami, G., Chiba, T., Tanaka, K., Imamura, T. and Miyazono, K. Smurf1 interacts with transforming growth factor-β type I receptor through Smad7 and induces receptor degradation. *Journal of Biological Chemistry* 2001; 276(16): 12477-12480.

Edlund, S., Landström, M., Heldin, C.H. and Aspenström, P. Transforming growth factor-β–induced mobilization of actin cytoskeleton requires signaling by small GTPases Cdc42 and RhoA. *Molecular biology of the cell* 2002; 13(3): 902-914.

Egeblad, M., Werb, Z. New functions for the matrix metalloproteinases in cancer progression. *Nat Rev Cancer* 2002; 2:161-74.

Elia, L., Quintavalle, M., Zhang, J., Contu, R., Cossu, L., Latronico, M.V., Peterson, K.L., Indolfi, C., Catalucci, D., Chen, J. and Courtneidge, S.A. The knockout of

miR-143 and-145 alters smooth muscle cell maintenance and vascular homeostasis in mice: correlates with human disease. *Cell death and differentiation 2009*; 16(12): 1590.

Enkelmann, A., Heinzelmann, J., von Eggeling, F., Walter, M., Berndt, A., Wunderlich, H. and Junker, K. Specific protein and miRNA patterns characterise tumour-associated fibroblasts in bladder cancer. *Journal of cancer research and clinical oncology* 2011; 137(5): 751-759.

Erez, N., Truitt, M., Olson, P. and Hanahan, D. Cancer-associated fibroblasts are activated in incipient neoplasia to orchestrate tumor-promoting inflammation in an NF-κB-dependent manner. *Cancer cell* 2010; 17(2): 135-147.

Evans, R.A., Tian, Y.C., Steadman, R. and Phillips, A.O. TGF-β1-mediated fibroblast–myofibroblast terminal differentiation—the role of smad proteins. *Experimental cell research* 2003; 282(2): 90-100.

Eyden, B. The myofibroblast: phenotypic characterization as a prerequisite to understanding its functions in translational medicine. *Journal of cellular and molecular medicine* 2008; 12(1): 22-37.

Fan, L., Wu, Q., Xing, X., Wei, Y. and Shao, Z. MicroRNA-145 targets vascular endothelial growth factor and inhibits invasion and metastasis of osteosarcoma cells. *Acta Biochim Biophys Sin* 2012; 44(5): 407-414.

Fanucchi, M., Khuri, F.R., Shin, D., Johnstone, PAS., Chen, A. Update in the management of head and neck cancer. *Update Cancer Ther* 2006; 1: 211-9.

Farmer, P., Bonnefoi, H., Anderle, P., Cameron, D., Wirapati, P., Becette, V., André, S., Piccart, M., Campone, M., Brain, E. and MacGrogan, G. A stroma-related gene signature predicts resistance to neoadjuvant chemotherapy in breast cancer. *Nature medicine* 2009; 15(1): 68-74.

Farsi, J. and Aubin, J.E. Microfilament rearrangements during fibroblast-induced contraction of three-dimensional hydrated collagen gels. *Cytoskeleton* 1984; *4*(1): 29-40.

Ferretti, E., De Smaele, E., Miele, E., Laneve, P., Po, A., Pelloni, M., Paganelli, A., Di Marcotullio, L., Caffarelli, E., Screpanti, I. and Bozzoni, I. Concerted microRNA control of Hedgehog signalling in cerebellar neuronal progenitor and tumour cells. *The EMBO journal* 2008; 27(19): 2616-2627.

Ffrench-Constant, C., Van, W.L., Dvorak, H.F., & Hynes, R.O. Reappearance of an embryonic pattern of fibronectin splicing during wound healing in the adult rat. *The Journal of Cell Biology* 1989; 109: 903-914, 0021-9525

Fiaschi, T., Marini, A., Giannoni, E., Taddei, M.L., Gandellini, P., De Donatis, A., Lanciotti, M., Serni, S., Cirri, P. and Chiarugi, P. Reciprocal metabolic reprogramming through lactate shuttle coordinately influences tumor-stroma interplay. *Cancer research* 2012; 72(19): 5130-5140.

Finak, G., Bertos, N., Pepin, F., Sadekova, S., Souleimanova, M., Zhao, H., Chen, H., Omeroglu, G., Meterissian, S., Omeroglu, A. and Hallett, M. Stromal gene expression predicts clinical outcome in breast cancer. *Nature medicine* 2008; 14(5): 518-527.

Flanders, K.C., Sullivan, C.D., Fujii, M., Sowers, A., Anzano, M.A., Arabshahi, A., Major, C., Deng, C., Russo, A., Mitchell, J.B. and Roberts, A.B. Mice lacking Smad3 are protected against cutaneous injury induced by ionizing radiation. *The American journal of pathology* 2002; 160(3): 1057-1068.

Flavell, S.J., Hou, T.Z., Lax, S., Filer, A.D., Salmon, M. and Buckley, C.D. Fibroblasts as novel therapeutic targets in chronic inflammation. *British journal of pharmacology* 2008; 153(S1).

Fleming, Y.M., Ferguson, G.J., Spender, L.C., Larsson, J., Karlsson, S., Ozanne, B.W., Grosse, R. and Inman, G.J. TGF-[beta]-mediated activation of RhoA signalling is required for efficient V12HaRas and V600EBRAF transformation. *Oncogene*, 2009; 28(7): 983.

Folini, M., Gandellini, P., Longoni, N., Profumo, V., Callari, M., Pennati, M., Colecchia, M., Supino, R., Veneroni, S., Salvioni, R. and Valdagni, R. miR-21: an oncomir on strike in prostate cancer. *Molecular cancer* 2010; 9(1): 12.

Forino, M., Torregrossa, R., Ceol, M., Murer, L., Vella, M.D., Prete, D.D., D'angelo, A. and Anglani, F. TGFβ1 induces epithelial–mesenchymal transition, but not myofibroblast transdifferentiation of human kidney tubular epithelial cells in primary culture. *International journal of experimental pathology* 2006; 87(3): 197-208.

Forrest, A.R., Kanamori-Katayama, M., Tomaru, Y., Lassmann, T., Ninomiya, N., Takahashi, Y., de Hoon, M.J., Kubosaki, A., Kaiho, A., Suzuki, M. and Yasuda, J. Induction of microRNAs, mir-155, mir-222, mir-424 and mir-503, promotes monocytic differentiation through combinatorial regulation.2010; *arXiv preprint arXiv:1007.2689*.

Frangogiannis, N.G., Michael, L.H. and Entman, M.L. Myofibroblasts in reperfused myocardial infarcts express the embryonic form of smooth muscle myosin heavy chain (SMemb). *Cardiovascular research* 2000; 48(1): 89-100.

Friess H, Yamanaka Y, Buchler M, et al. Enhancedexpression of transforming growth factor beta isoformsin pancreatic cancer correlates with decreased survival. *Gastroenterology* 1993; 105:1846–56.

Fujii, N., Shomori, K., Shiomi, T., Nakabayashi, M., Takeda, C., Ryoke, K. and Ito, H. Cancer-associated fibroblasts and CD163-positive macrophages in oral squamous cell carcinoma: their clinicopathological and prognostic significance. *Journal of oral pathology & medicine* 2012; 41(6): 444-451.

Fukino, K., Shen, L., Matsumoto, S., Morrison, C.D., Mutter, G.L. and Eng, C. Combined total genome loss of heterozygosity scan of breast cancer stroma and epithelium reveals multiplicity of stromal targets. *Cancer Research* 2004; 64(20): 7231-7236.

Fuse, M., Nohata, N., Kojima, S., Sakamoto, S., Chiyomaru, T., Kawakami, K., Enokida, H., Nakagawa, M., Naya, Y., Ichikawa, T. and Seki, N. Restoration of miR-145 expression suppresses cell proliferation, migration and invasion in prostate cancer by targeting FSCN1. *International journal of oncology* 2011; 38(4): 1093-1101.

Gabbiani, G., Ryan, G. B. and Majno, G. Presence of modified fibroblast in granulation tissue and their possible role in wound contraction. *Experientia* 1971; 27, 549551.

Gabbiani, G. The myofibroblast in wound healing and fibrocontractive diseases. *J. Pathol.* 2003; 200: 500–503.

Gabriely, G., Wurdinger, T., Kesari, S., Esau, C.C., Burchard, J., Linsley, P.S. and Krichevsky, A.M. MicroRNA 21 promotes glioma invasion by targeting matrix metalloproteinase regulators. *Molecular and cellular biology* 2008; 28(17): 5369-5380.

Gaggioli, C., Hooper, S., Hidalgo-Carcedo, C., Grosse, R., Marshall, J.F., Harrington, K. and Sahai, E. Fibroblast-led collective invasion of carcinoma cells with differing roles for RhoGTPases in leading and following cells. *Nature cell biology* 2007; 9(12): 1392.

Garin-Chesa P, Old LJ, Rettig WJ. Cell surface glycoprotein of reactive stromal fibroblasts as a potential antibody target in human epithelial cancers. *Proc Natl Acad Sci U S A*. 1990; 87:7235– 7239.

Geng, Y. and Weinberg, R.A. Transforming growth factor beta effects on expression of G1 cyclins and cyclin-dependent protein kinases. *Proceedings of the National Academy of Sciences* 1993; 90(21): 10315-10319.

Georges, S.A., Biery, M.C., Kim, S.Y., Schelter, J.M., Guo, J., Chang, A.N., Jackson, A.L., Carleton, M.O., Linsley, P.S., Cleary, M.A. and Chau, B.N. Coordinated regulation of cell cycle transcripts by p53-Inducible microRNAs, miR-192 and miR-215. *Cancer research* 2008; 68(24): 10105-10112.

Gerber, P.A., Hippe, A., Buhren, B.A., Müller, A. and Homey, B. Chemokines in tumor-associated angiogenesis. *Biological chemistry* 2009; 390(12): 1213-1223.

Gerrard, L.C.C., Halimah, Y, Rampal, S. Cancer incidence in peninsular Malaysia, 2003-2005 [online], 2008. Available from World Wide Web: http://www.radiologymalaysia.org

Ghosh, A.K., Nagpal, V., Covington, J.W., Michaels, M.A. and Vaughan, D.E. Molecular basis of cardiac endothelial-to-mesenchymal transition (EndMT): differential expression of microRNAs during EndMT. *Cellular signalling* 2012; 24(5): 1031-1036.

Ghosh, G., Subramanian, I.V., Adhikari, N., Zhang, X., Joshi, H.P., Basi, D., Chandrashekhar, Y.S., Hall, J.L., Roy, S., Zeng, Y. and Ramakrishnan, S. Hypoxia-induced microRNA-424 expression in human endothelial cells regulates HIF-α isoforms and promotes angiogenesis. *The Journal of clinical investigation* 2010; 120(11): 4141.

Giannakakis, A., Sandaltzopoulos, R., Greshock, J., Liang, S., Huang, J., Hasegawa, K., Li, C., O'Brien-Jenkins, A., Katsaros, D., Weber, B.L. and Simon, C. miR-210 links hypoxia with cell cycle regulation and is deleted in human epithelial ovarian cancer. *Cancer biology & therapy* 2008; 7(2): 255-264.

Giannoni, E., Bianchini, F., Masieri, L., Serni, S., Torre, E., Calorini, L., and Chiarugi, P. Reciprocal activation of prostate cancer cells and cancerassociated fibroblasts stimulates epithelialmesenchymal transition and cancer stemness. *Cancer Res* 2010; 70: 6945-6956.

Gil, J. and Peters, G. Regulation of the INK4b-ARF-INK4a tumour suppressor locus: all for one or one for all. *Nature reviews. Molecular cell biology* 2006; 7(9): 667.

Giordano, S. and Columbano, A. MicroRNAs: new tools for diagnosis, prognosis, and therapy in hepatocellular carcinoma? *Hepatology* 2013; 57(2): 840-847.

Giry, M., Popoff, M.R., von Eichel-Streiber, C.H.R.I.S.T.O.P.H. and Boquet, P. 1995. Transient expression of RhoA, -B, and-C GTPases in HeLa cells potentiates resistance to Clostridium difficile toxins A and B but not to Clostridium sordellii lethal toxin. *Infection and immunity* 1995; 63(10): 4063-4071.

Goicoechea, S.M., Garcia-Mata, R., Staub, J., Valdivia, A., Sharek, L., McCulloch, C.G., Hwang, R.F., Urrutia, R., Yeh, J.J., Kim, H.J. and Otey, C.A. Palladin promotes invasion of pancreatic cancer cells by enhancing invadopodia formation in cancer-associated fibroblasts. *Oncogene*2014; 33(10): 1265.

Goldman, R.D., Lazarides, E., Pollack, R., Weber, K. The distribution of actin in non-muscle cells. The use of actin antibody in the localization of actin within the microfilament bundles of mouse 3T3 cells. *Exp Cell Res* 1975; 90:333–44.

Goh, P.P., Sze, D.M, Roufogalis, B.D. Molecular and cellular regulators of cancer angiogenesis. *Curr Cancer Drug Targets* 2007; 7:743–758.

Gonda, T.A., Varro, A., Wang, T.C. and Tycko, B. Molecular biology of cancer-associated fibroblasts: can these cells be targeted in anti-cancer therapy? In *Seminars in cell & developmental biology* 2010; 21(1): 2-10). Academic Press.

Goubran, H.A., Kotb, R.R., Stakiw, J., Emara, M.E. and Burnouf, T. Regulation of tumor growth and metastasis: the role of tumor microenvironment. *Cancer growth and metastasis* 2014; *7*: 9.

Grange, C., Tapparo, M., Collino, F., Vitillo, L., Damasco, C., Deregibus, M.C., Tetta, C., Bussolati, B. and Camussi, G. Microvesicles released from human renal cancer stem cells stimulate angiogenesis and formation of lung premetastatic niche. *Cancer research* 2011; 71(15): 5346-5356.

Grannas, K., Arngården, L., Lönn, P., Mazurkiewicz, M., Blokzijl, A., Zieba, A. and Söderberg, O. Crosstalk between Hippo and TGFβ: subcellular localization of YAP/TAZ/Smad complexes. *Journal of molecular biology* 2015; 427(21): 3407-3415.

Gras, C., Ratuszny, D., Hadamitzky, C., Zhang, H., Blasczyk, R. and Figueiredo, C. miR-145 contributes to hypertrophic scarring of the skin by inducing myofibroblast activity. *Molecular Medicine* 2015; 21(1): 296.

Gregory, P.A., Bert, A.G., Paterson, E.L., Barry, S.C., Tsykin, A., Farshid, G., Vadas, M.A., Khew-Goodall, Y. and Goodall, G.J. The miR-200 family and miR-205 regulate epithelial to mesenchymal transition by targeting ZEB1 and SIP1. *Nature cell biology* 2008; 10(5): 593-601.

Grubisha MJ, Cifuentes ME, Hammes SR, Defranco DB. A local paracrine and endocrinenetwork involving TGFbeta: Cox-2, ROS, and estrogenreceptor beta influences reactive stromal cell regulation of prostate cancer cell motility. *Mol Endocrinol* 2012; 26(6): 940–54.

Grum-Schwensen B, Klingelhofer J, Berg CH, El-Naaman C, Grigorian M, Lukanidin E, Ambartsumian N. Suppression of tumor development and metastasis formation in mice lacking the S100A4(mts1) gene. *Cancer Res* 2005; 65:3772–3780.

Gu, Y, Rosenblatt, J. and Morgan, D.O. Cell cycle regulation of CDK2 activity by phosphorylation of Thr160 and Tyr15. *The EMBO journal* 1992; 11(11): 3995.

Guduric-Fuchs, J., O'Connor, A., Camp, B., O'Neill, C.L., Medina, R.J. and Simpson, D.A. Selective extracellular vesicle-mediated export of an overlapping set of microRNAs from multiple cell types. *BMC genomics* 2012; 13(1): 357.

Gupta, G.P. and Massagué, J. Cancer metastasis: building a framework. *Cell* 2006; 127(4): 679-695.

Hall, B., Andreeff, M., and Marini, F. The participation of mesenchymal stem cells in tumor stroma formation and their application as targeted-gene delivery vehicles. *Handb Exp Pharmacol* 2007; 263-283.

Hanahan, D., Weinberg, R.A. The hallmark of cancer: The next generation. *Cell* 2011; 144: 646-674.

Hao, S., He, W., Li, Y., Ding, H., Hou, Y., Nie, J., Hou, F.F., Kahn, M. and Liu, Y. Targeted inhibition of β-catenin/CBP signaling ameliorates renal interstitial fibrosis. *Journal of the American Society of Nephrology* 2011; 22(9): 1642-1653.

Hashibe, M., Brennan, P., Chuang, S.C., Boccia, S., Castellsague, X., Chen, C., Curado, M.P., Dal Maso, L., Daudt, A.W., Fabianova, E. and Fernandez, L. Interaction between tobacco and alcohol use and the risk of head and neck cancer: pooled analysis in the International Head and Neck Cancer Epidemiology Consortium. *Cancer Epidemiology and Prevention Biomarkers* 2009; 18(2): 541-550.

Hassona, Y., Cirillo, N., Lim, K.P., Herman, A., Mellone, M., Thomas, G.J., Pitiyage, G.N., Parkinson, E.K. and Prime, S.S. Progression of genotype-specific oral cancer leads to senescence of cancer-associated fibroblasts and is mediated by oxidative stress and TGF-β. *Carcinogenesis* 2013; 34(6): 1286-1295.

Hay, E.D. An overview of epithelio-mesenchymal transformation. *Cells Tissues Organs* 1995; *154*(1): 8-20.

Hayflick, L. The limited in vitro lifetime of human diploid cell strains. *Experimental cell research* 1965; 37(3): 614-636.

Henderson, W.R., Chi, E.Y., Ye, X., Nguyen, C., Tien, Y.T., Zhou, B., Borok, Z., Knight, D.A. and Kahn, M. Inhibition of Wnt/β-catenin/CREB binding protein (CBP) signaling reverses pulmonary fibrosis. *Proceedings of the National Academy of Sciences* 2010; 107(32): 14309-14314.

Herbig, U., Jobling, W.A., Chen, B.P., Chen, D.J. and Sedivy, J.M. Telomere shortening triggers senescence of human cells through a pathway involving ATM, p53, and p21 CIP1, but not p16 INK4a. *Molecular cell* 2004; 14(4): 501-513.

Hermeking, H. p53 enters the microRNA world. *Cancer cell* 2007; 12(5): 414-418.

Hinz, B., Mastrangelo D, Iselin CE, Chaponnier C, Gabbiani G. Mechanical tension controls granulation tissue contractile activity and myofibroblast differentiation. *Am J Pathol* 2001(a);159: 1009–20.

Hinz, B., Celetta, G., Tomasek, J.J., Gabbiani, G. and Chaponnier, C. Alpha-smooth muscle actin expression upregulates fibroblast contractile activity. *Molecular biology of the cell* 2001(b); 12(9): 2730-2741.

Hinz, B. Formation and function of the myofibroblast during tissue repair. *Journal of Investigative Dermatology* 2007; 127(3): 526-537.

Hinz, B., Phan, S.H., Thannickal, V.J., Prunotto, M., Desmoulière, A., Varga, J., De Wever, O., Mareel, M. and Gabbiani, G. Recent developments in myofibroblast biology: paradigms for connective tissue remodeling. *The American journal of pathology* 2012; 180(4): 1340-1355.

Ho, A.S., Huang, X., Cao, H., Christman-Skieller, C., Bennewith, K., Le, Q.T. and Koong, A.C. Circulating miR-210 as a novel hypoxia marker in pancreatic cancer. *Translational oncology* 2010; 3(2): 109-113.

Honda, E., Yoshida, K. and Munakata, H. Transforming growth factor-β upregulates the expression of integrin and related proteins in MRC-5 human myofibroblasts. *The Tohoku journal of experimental medicine* 2010; 220(4): 319-327.

Htwe, S.S., Cha, B.H., Yue, K., Khademhosseini, A., Knox, A.J. and Ghaemmaghami, A.M. Role of ROCK isoforms in regulation of stiffness induced myofibroblast differentiation in lung fibrosis. *American Journal of Respiratory Cell and Molecular Biology* 2017 (ja).

Hu, B., Wu, Z. and Phan, S.H. Smad3 mediates transforming growth factor-β–induced α-smooth muscle actin expression. *American journal of respiratory cell and molecular biology* 2003; 29(3): 397-404.

Hu, J., Guo, H., Li, H., Liu, Y., Liu, J., Chen, L., Zhang, J. and Zhang, N. MiR-145 regulates epithelial to mesenchymal transition of breast cancer cells by targeting Oct4. *PloS one* 2012; 7(9): 45965.

Huang, X., Yang, Y., Guo, Y., Cao, Z.L., Cui, Z.W., Hu, T.C. and Gao, L.B. Association of a let-7 KRAS rs712 polymorphism with the risk of breast cancer. *Genet Mol Res* 2015; 14: 16913-16920.

Huang, Z., Huang, D., Ni, S., Peng, Z., Sheng, W. and Du, X. Plasma microRNAs are promising novel biomarkers for early detection of colorectal cancer. *International journal of cancer* 2010; 127(1): 118-126.

Huijbers, I.J., Iravani, M., Popov, S., Robertson, D., Al-Sarraj, S., Jones, C. and Isacke, C.M. A role for fibrillar collagen deposition and the collagen internalization receptor endo180 in glioma invasion. *PloS one* 2010; *5*(3): 9808.

Hunt, T.K. The physiology of wound healing. *Ann Emerg Med* 1998; 17: 1265 – 1273.

Hunt, S., Jones, A.V., Hinsley, E.E., Whawell, S.A. and Lambert, D.W. MicroRNA-124 suppresses oral squamous cell carcinoma motility by targeting ITGB1. *FEBS letters* 2011; 585(1):187-192.

Hynes, R. O. (1990) In *Fibronectins* (1st Ed.) (Rich, A., Editor), Springer-Verlag, New York, New York, USA

Hynes, R.O. Integrins: bidirectional, allosteric signaling machines. *Cell* 2002; 110:673–87.

Hyrup, B. and Nielsen, P.E. Peptide nucleic acids (PNA): synthesis, properties and potential applications. *Bioorganic & medicinal chemistry* 1996; 4(1): 5-23.

Ichimi, T., Enokida, H., Okuno, Y., Kunimoto, R., Chiyomaru, T., Kawamoto, K., Kawahara, K., Toki, K., Kawakami, K., Nishiyama, K. and Tsujimoto, G. Identification of novel microRNA targets based on microRNA signatures in bladder cancer. *International journal of cancer* 2009; 125(2): 345-352.

Ina, K., Kitamura, H., Tatsukawa, S. and Fujikura, Y. The Contribution of Fibronectin ED-A Expression to Myofibroblast Transdifferentiation in Diabetic Renal Fibrosis. In *Diabetic Nephropathy* 2012; InTech.

Iorio, M.V. and Croce, C.M. MicroRNAs in cancer: small molecules with a huge impact. *Journal of clinical oncology* 2009; 27(34): 5848-5856.

Itahana, K., Zou, Y., Itahana, Y., Martinez, J.L., Beausejour, C., Jacobs, J.J., Van Lohuizen, M., Band, V., Campisi, J. and Dimri, G.P. Control of the replicative life span of human fibroblasts by p16 and the polycomb protein Bmi-1. *Molecular and cellular biology* 2003; 23(1): 389-401.

Iwano, M., Plieth, D., Danoff, T.M., Xue, C., Okada, H. and Neilson, E.G. Evidence that fibroblasts derive from epithelium during tissue fibrosis. *The Journal of clinical investigation*, 2002; 110(3): 341.

Jamagin, W.R., Rockey, D.C., Koteliansky, V.E., Wang, S.S., & Bissel, D.M. Expression of variant fibronectins in wound healing: Cellular source and biological activity of the ElllA segment in rat hepatic fibrogenesis. *The Journal of Cell Biology,* 1994; 127: 2037-2048, 0021-9525.

Jiang, J., Lee, E.J., Gusev, Y., Schmittgen, T.D. Real-time expression profiling of microRNA precursors in human cancer cell lines. *Nucleic Acids Res* 2005; 33:5394–403

Jianwei, Z., Fan, L., Xiancheng, L., Enzhong, B., Shuai, L. and Can, L. MicroRNA 181a improves proliferation and invasion, suppresses apoptosis of osteosarcoma cell. *Tumor Biology* 2013; 34(6): 3331-3337.

Jimenez, S.A., Varga, J., Olsen, A., Li, L., Diaz, A., Herhal, J. and Koch, J. Functional analysis of human alpha 1 (I) procollagen gene promoter. Differential activity in collagen-producing and-nonproducing cells and response to transforming growth factor beta 1. *Journal of Biological Chemistry* 1994; 269(17): 12684-12691.

Johansson, A.C., Ansell, A., Jerhammar, F., Lindh, M.B., Grénman, R., Munck-Wikland, E., Östman, A. and Roberg, K. Cancer-Associated Fibroblasts Induce Matrix Metalloproteinase–Mediated Cetuximab Resistance in Head and Neck Squamous Cell Carcinoma Cells. *Molecular Cancer Research* 2012; 10(9): 1158-1168.

Johnson, L.A., Rodansky, E.S., Haak, A.J., Larsen, S.D., Neubig, R.R. and Higgins, P.D. Novel Rho/MRTF/SRF Inhibitors Block Matrix-stiffness and TGF-β–Induced Fibrogenesis in Human Colonic Myofibroblasts. *Inflammatory bowel diseases* 2014; 20(1):154.

Johnson, S.M., Grosshans, H., Shingara, J., Byrom, M., Jarvis, R., Cheng, A., Labourier, E., Reinert, K.L., Brown, D. and Slack, F.J. RAS is regulated by the let-7 microRNA family. *Cell* 2005; 120(5): 635-647.

Jones, R.G and Thompson CB. Tumor suppressors and cell metabolism: a recipe for cancer growth. *Genes Dev* 2009; 23: 537-548.

Joyce, J.A., Pollard J.W. Microenvironmental regulation of metastasis. *Nat Rev Cancer* 2009; 9:239-52.

Kabir, T.D., Leigh, R.J., Tasena, H., Mellone, M., Coletta, R.D., Parkinson, E.K., Prime, S.S., Thomas, G.J., Paterson, I.C., Zhou, D. and McCall, J. A miR-335/COX-2/PTEN axis regulates the secretory phenotype of senescent cancer-associated fibroblasts. *Aging (Albany NY)* 2016; 8(8): 1608.

Kadera, B.E., Li, L., Toste, P.A., Wu, N., Adams, C., Dawson, D.W. and Donahue, T.R. MicroRNA-21 in pancreatic ductal adenocarcinoma tumor-associated fibroblasts promotes metastasis. *PloS one* 2013; 8(8): 71978.

Kalluri, R. and M. Zeisberg."Fibroblasts in cancer." *Nat Rev Cancer* 2006; 6(5): 392-401.

Kalluri R. EMT: when epithelial cells decide to become mesenchymal-like cells. *J Clin Invest* 2009; 119: 1417-1419

Kalluri, R. The biology and function of fibroblasts in cancer. *Nature reviews Cancer* 2016; 16(9): 582-598.

Karamouzis, M.V, Grandis J.R, Argiris A. Therapies directed against epidermal growth factor receptor in aerodigestive carcinomas. *JAMA* 2007; 298: 70–82.

Karnoub, A.E., Dash, A.B., Vo, A.P., Sullivan, A., Brooks, M.W., Bell, G.W., Richardson, A.L., Polyak, K., Tubo, R. and Weinberg, R.A. Mesenchymal stem cells within tumour stroma promote breast cancer metastasis. *Nature* 2007; 449(7162): 557.

Karsenty, G. and de Crombrugghe, B. Conservation of binding sites for regulatory factors in the coordinately expressed α1 (I) and α2 (I) collagen promoters. *Biochemical and biophysical research communications* 1991; *177*(1): 538-544.

Kato, M., Zhang, J., Wang, M., Lanting, L., Yuan, H., Rossi, J.J. and Natarajan, R. MicroRNA-192 in diabetic kidney glomeruli and its function in TGF-β-induced collagen expression via inhibition of E-box repressors. *Proceedings of the National Academy of Sciences* 2007; 104(9): 3432-3437.

Kauppila, S., Stenbäck, F., Risteli, J., Jukkola, A. and Risteli, L. Aberrant type I and type III collagen gene expression in human breast cancer in vivo. *The Journal of pathology* 1998; 186(3): 262-268.

Kawaguchi, T., Komatsu, S., Ichikawa, D., Morimura, R., Tsujiura, M., Konishi, H., Takeshita, H., Nagata, H., Arita, T., Hirajima, S. and Shiozaki, A. Clinical impact of circulating miR-221 in plasma of patients with pancreatic cancer. *British journal of cancer* 2013; 108(2): 361.

Kellermann, M.G., Sobral, L.M., Da Silva, S.D., Zecchin, K.G., Graner, E., Lopes, M.A., Nishimoto, I., Kowalski, L.P. and Coletta, R.D. Myofibroblasts in the stroma of oral squamous cell carcinoma are associated with poor prognosis. *Histopathology* 2007; 51(6): 849-853.

Kharaziha, P., De Raeve, H., Fristedt, C., Li, Q., Gruber, A., Johnsson, P., Kokaraki, G., Panzar, M., Laane, E., Österborg, A. and Zhivotovsky, B. Sorafenib has potent antitumor activity against multiple myeloma in vitro, ex vivo, and in vivo in the 5T33MM mouse model. *Cancer research* 2012; 72(20): 5348-5362

Kim, J., Kang, Y., Kojima, Y., Lighthouse, J.K., Hu, X., Aldred, M.A., McLean, D.L., Park, H., Comhair, S.A., Greif, D.M. and Erzurum, S.C. An endothelial apelin-FGF link mediated by miR-424 and miR-503 is disrupted in pulmonary arterial hypertension. *Nature medicine* 2013; 19(1): 74-82.

Kim, N.H., Kim, H.S., Li, X.Y., Lee, I., Choi, H.S., Kang, S.E., Cha, S.Y., Ryu, J.K., Yoon, D., Fearon, E.R. and Rowe, R.G. A p53/miRNA-34 axis regulates Snail1-dependent cancer cell epithelial–mesenchymal transition. *J Cell Biol* 2011; 195(3): 417-433.

Kinoshita, H., Hirata, Y., Nakagawa, H., Sakamoto, K., Hayakawa, Y., Takahashi, R., Nakata, W., Sakitani, K., Serizawa, T., Hikiba, Y. and Akanuma, M. Interleukin-6 mediates epithelial–stromal interactions and promotes gastric tumorigenesis. *PloS one* 2013; 8(4): 60914.

Klingberg, F., Hinz, B. and White, E.S. The myofibroblast matrix: implications for tissue repair and fibrosis. *The Journal of pathology* 2013; 229; (2): 298-309.

Koff, A., Ohtsuki, M., Polyak, K., Roberts, J.M. and Massagué, J. Negative regulation of G1 in mammalian cells: inhibition of cyclin E-dependent kinase by TGF-β. *Science* 1993; 536-539.

Kohan, M., Muro, A.F., White, E.S. and Berkman, N. EDA-containing cellular fibronectin induces fibroblast differentiation through binding to α4β7 integrin

receptor and MAPK/Erk 1/2-dependent signaling. *The FASEB Journal* 2010; 24(11): 4503-4512.

Kojima Y, Acar A, Eaton EN, Mellody KT, Scheel C, Ben-Porath I, Onder TT, Wang ZC, Richardson AL, Weinberg RA, and Orimo A. Autocrine TGF-beta and stromal cell-derived factor-1 (SDF-1) signaling drives the evolution of tumor-promoting mammary stromal myofibroblasts. *Proc Natl Acad Sci U S A* 2010; 107: 20009-20014.

Koppenol, W.H, P.L. Bounds, C.V. Dang, Otto Warburg's contributions to current concepts of cancer metabolism, *Nat. Rev. Cancer* 2011; 115:325–337.

Korkmaz, G., Le Sage, C., Tekirdag, K.A., Agami, R. and Gozuacik, D. miR-376b controls starvation and mTOR inhibition-related autophagy by targeting ATG4C and BECN1. *Autophagy* 2012; 8(2): 165-176.

Kornblihtt, A.R., Pesce, C.G., Alonso, C.R., Cramer, P., Srebrow, A., Werbajh, S. and Muro, A.F. The fibronectin gene as a model for splicing and transcription studies. *The FASEB Journal* 1996; 10(2): 248-257.

Korpal, M., Lee, E.S., Hu, G. and Kang, Y. The miR-200 family inhibits epithelial-mesenchymal transition and cancer cell migration by direct targeting of E-cadherin transcriptional repressors ZEB1 and ZEB2. *Journal of Biological Chemistry* 2008 283(22): 14910-14914.

Kosaka, N. and Ochiya, T. Unraveling the mystery of cancer by secretory microRNA: horizontal microRNA transfers between living cells. *Frontiers in genetics* 2011; 2.

Kosaka, N., Yoshioka, Y., Hagiwara, K., Tominaga, N., Katsuda, T. and Ochiya, T. Trash or Treasure: extracellular microRNAs and cell-to-cell communication. *Frontiers in genetics* 2013; 4.

Koskinen, P.J., Sistonen, L., Bravo, R. and Alitalo, K. Immediate Early Gene Responses of NIH 3T3 Fibroblasts and NMuMG Epithelial Cells to TGFβ-1. *Growth Factors* 1991; 5(4): 283-293.

Koukourakis, M.I., Giatromanolaki, A., Harris, A.L. and Sivridis, E. Comparison of metabolic pathways between cancer cells and stromal cells in colorectal carcinomas: a metabolic survival role for tumor-associated stroma. *Cancer research* 2006; *66*(2): 632-637.

Kreimer AR, Cliff ord GM, Boyle P, Franceschi S. Human papillomavirus types in head and neck squamous cell carcinomas worldwide: a systematic review. *Cancer Epidemiol Biomarkers Prev* 2005; 14: 467–75.

Krishnamurthy, J., Ramsey, M.R., Ligon, K.L., Torrice, C., Koh, A., Bonner-Weir, S. and Sharpless, N.E. p16INK4a induces an age-dependent decline in islet regenerative potential. *Nature* 2006; 443(7110): 453.

Kubbutat, M.H., Jones, S.N. and Vousden, K.H. Regulation of p53 stability by Mdm2. *Nature* 1997; 387(6630): 299.

Kuninty, P.R., Schnittert, J., Storm, G. and Prakash, J. MicroRNA targeting to modulate tumor microenvironment. *Frontiers in oncology* 2016; *6*.

Kuperwasser, C., Chavarria, T., Wu, M., Magrane, G., Gray, J.W., Carey, L., Richardson, A., Weinberg, R.A. Reconstruction of functionally normal and malignant human breast tissues in mice. *Proc Natl Acad Sci U S A*. 2004; 101:4966–4971.

Kurkinen, M., Vaheri, A.N.T.T.I., Roberts, P.J. and Stenman, S. Sequential appearance of fibronectin and collagen in experimental granulation tissue. *Laboratory investigation; a journal of technical methods and pathology* 1980; 43(1): 47-51.

Kurose, K., Hoshaw-Woodard, S., Adeyinka, A., Lemeshow, S., H. Watson, P. and Eng, C. Genetic model of multi-step breast carcinogenesis involving the epithelium and stroma: clues to tumour–microenvironment interactions. *Human molecular genetics* 2001; 10(18): 1907-1913.

Kwan, J.Y., Psarianos, P., Bruce, J.P., Yip, K.W. and Liu, F.F. The complexity of microRNAs in human cancer. *Journal of radiation research* 2016; *57*(S1): 106-111.

Laberge, R.M., Sun, Y., Orjalo, A.V., Patil, C.K., Freund, A., Zhou, L., Curran, S.C., Davalos, A.R., Wilson-Edell, K.A., Liu, S. and Limbad, C. MTOR regulates the pro-tumorigenic senescence-associated secretory phenotype by promoting IL1A translation. *Nature cell biology* 2015; *17*(8): 1049.

Lakomy, R., Sana, J., Hankeova, S., Fadrus, P., Kren, L., Lzicarova, E., Svoboda, M., Dolezelova, H., Smrcka, M., Vyzula, R. and Michalek, J. MiR-195, miR-196b, miR-181c, miR-21 expression levels and O-6-methylguanine-DNA methyltransferase methylation status are associated with clinical outcome in glioblastoma patients. *Cancer science* 2011; 102(12): 2186-2190.

Lawrie, C.H., Chi, J., Taylor, S., Tramonti, D., Ballabio, E., Palazzo, S., Saunders, N.J., Pezzella, F., Boultwood, J., Wainscoat, J.S. and Hatton, C.S. Expression of

microRNAs in diffuse large B cell lymphoma is associated with immunophenotype, survival and transformation from follicular lymphoma. *Journal of cellular and molecular medicine* 2009; 13(7): 1248-1260.

Le Beau, M.M., Lemons, R.S., Larson, R.A., Arai, N. and Rowley, J.D. Interleukin-4 and interleukin-5 map to human chromosome 5 in a region encoding growth factors and receptors and are deleted in myeloid leukemias with a del (5q). *Blood* 1989; 73(3): 647-650.

Lee, P.Y., Li, Z. and Huang, L. Thermosensitive hydrogel as a Tgf-β1 gene delivery vehicle enhances diabetic wound healing. *Pharmaceutical research* 2003; 20(12): 1995-2000.

Lee, Y.S. and Dutta, A. MicroRNAs: Small but potent oncogenes or tumor suppressors. *Curr. Opin. Investig. Drugs* 2006; 7: 560–564.

Lefebvre, J.L. Laryngeal preservation in head and neck cancer: multidisciplinary approach. *Lancet Oncol* 2006; 7: 747–55.

Lewis, M.P., Lygoe, K.A., Nystrom, M.L., Anderson, W.P., Speight, P.M., Marshall, J.F. and Thomas, G.J. Tumour-derived TGF-β1 modulates myofibroblast differentiation and promotes HGF/SF-dependent invasion of squamous carcinoma cells. *British journal of cancer* 2004; 90(4): 822.

Li, B., Han, Q., Zhu, Y., Yu, Y., Wang, J. and Jiang, X. Down-regulation of miR-214 contributes to intrahepatic cholangiocarcinoma metastasis by targeting Twist. *The FEBS journal* 2012; 279(13): 2393-2398.

Li, D., Zhao, Y., Liu, C., Chen, X., Qi, Y., Jiang, Y., Zou, C., Zhang, X., Liu, S., Wang, X. and Zhao, D. Analysis of MiR-195 and MiR-497 expression, regulation and role in breast cancer. *Clinical cancer research* 2011; 17(7): 1722-1730.

Li, G, Satyamoorthy K, Meier F, Berking C, Bogenrieder T, Herlyn M. Function and regulation of melanoma-stromal fibroblast interactions: when seeds meet soil. *Oncogene.* 2003; 22:3162–3171.

Li, J., Chen, J. and Kirsner, R. Pathophysiology of acute wound healing. *Clinics in dermatology* 2007; 25(1): 9-18.

Li, Q., Zhang, D., Wang, Y., Sun, P., Hou, X., Larner, J., Xiong, W. and Mi, J. MiR-21/Smad 7 signaling determines TGF-β1-induced CAF formation. *Scientific reports* 2013; 3: 2038.

Liao, D., Luo, Y., Markowitz, D., Xiang, R. and Reisfeld, R.A. Cancer associated fibroblasts promote tumor growth and metastasis by modulating the tumor immune microenvironment in a 4T1 murine breast cancer model. *PloS one* 2009; 4(11): 7965.

Lim, K.P., Cirillo, N., Hassona, Y., Wei, W., Thurlow, J.K., Cheong, S.C., Pitiyage, G., Parkinson, E.K. and Prime, S.S. Fibroblast gene expression profile reflects the stage of tumour progression in oral squamous cell carcinoma. *The Journal of pathology* 2011; 223(4): 459-469.

Lin, E.Y. and Pollard, J.W. Tumor-associated macrophages press the angiogenic switch in breast cancer. *Cancer Research* 2007; 67(11): 5064-5066.

Ling, H., Krassnig, L., Bullock, M.D. and Pichler, M. MicroRNAs in testicular cancer diagnosis and prognosis. *Urologic Clinics of North America* 2016; 43(1): 127-134.

Linsley, P.S., Schelter, J., Burchard, J., Kibukawa, M., Martin, M.M., Bartz, S.R., Johnson, J.M., Cummins, J.M., Raymond, C.K., Dai, H. and Chau, N. Transcripts targeted by the microRNA-16 family cooperatively regulate cell cycle progression. *Molecular and cellular biology* 2007; 27(6): 2240-2252.

Lippmani, S. and Hong, W.H.S.W.K. Frequent microsatellite alterations at chromosomes 9p21 and 3p14 in oral premalignant lesions and their value in cancer risk assessment. *Nature medicine* 1996; *2*(6).

Littlepage, L.E., Egeblad, M. and Werb, Z. Coevolution of cancer and stromal cellular responses. *Cancer cell* 2005; *7*(6): 499-500.

Liu, F., Lagares, D., Choi, K.M., Stopfer, L., Marinković, A., Vrbanac, V., Probst, C.K., Hiemer, S.E., Sisson, T.H., Horowitz, J.C. and Rosas, I.O. Mechanosignaling through YAP and TAZ drives fibroblast activation and fibrosis. *American Journal of Physiology-Lung Cellular and Molecular Physiology* 2015; *308*(4): L344-L357.

Liu, Q., Fu, H., Sun, F., Zhang, H., Tie, Y., Zhu, J., Xing, R., Sun, Z. and Zheng, X. miR-16 family induces cell cycle arrest by regulating multiple cell cycle genes. *Nucleic acids research* 2008; 36(16): 5391-5404.

Liu, S., Kumar, S.M., Lu, H., Liu, A., Yang, R., Pushparajan, A., Guo, W. and Xu, X. MicroRNA-9 up-regulates E-cadherin through inhibition of NF-κB1–Snail1 pathway in melanoma. *The Journal of pathology* 2012; 226(1): 61-72.

Liu, X., Wang, C., Chen, Z., Jin, Y., Wang, Y., Kolokythas, A., Dai, Y. and Zhou, X. MicroRNA-138 suppresses epithelial–mesenchymal transition in squamous cell carcinoma cell lines. *Biochemical Journal* 2011; 440(1): 23-31.

Livak, K.J. and Schmittgen, T.D. Analysis of relative gene expression data using real-time quantitative PCR and the 2− ΔΔCT method. *Methods* 2001; 25(4): 402-408.

Loeffler, M., Krüger, J.A., Niethammer, A.G. and Reisfeld, R.A. Targeting tumor-associated fibroblasts improves cancer chemotherapy by increasing intratumoral drug uptake. *Journal of Clinical Investigation* 2006; 116(7): 1955.

Lohr M, Schmidt C, Ringel J, Kluth M, Muller P, Nizze H, and Jesnowski R. Transforming growth factor-beta1 induces desmoplasia in an experimental model of human pancreatic carcinoma. *Cancer Res 2001*; 61: 550-555.

Long, X. and Miano, J.M. Transforming growth factor-β1 (TGF-β1) utilizes distinct pathways for the transcriptional activation of microRNA 143/145 in human coronary artery smooth muscle cells. *Journal of Biological Chemistry* 2011; 286(34): 30119-30129.

Lu, R. and O. Barca."Fine-tuning oligodendrocyte development by miRNAs." Frontiers in Neuroscience 2012; 6.

Mackenzie J, Ah-See K, Thakker N, Sloan P, Maran AG, Birch J, et al. Increasing incidence of oral cancer amongst young persons: what is the aetiology? *Oral Oncol* 2000; 36:387–9.

Madden, J. W., and Smith, H. C. The rate of collagen synthesis and deposition in dehisced and resutured wounds. *Surg. Gynecol. Obstet* 1970; 130: 487.

Mani, S.A., Guo, W., Liao, M.J., Eaton, E.N., Ayyanan, A., Zhou, A.Y., Brooks, M., Reinhard, F., Zhang, C.C., Shipitsin, M. and Campbell, L.L. The epithelial-mesenchymal transition generates cells with properties of stem cells. *Cell* 2008; 133(4): 704-715.

Manickam, N., Patel, M., Griendling, K.K., Gorin, Y. and Barnes, J.L. RhoA/Rho kinase mediates TGF-β 1-induced kidney myofibroblast activation through Poldip2/Nox4-derived reactive oxygen species. *American Journal of Physiology-Renal Physiology* 2014; 307(2): F159-F171.

Marsh, D., Suchak, K., Moutasim, K.A., Vallath, S., Hopper, C., Jerjes, W., Upile, T., Kalavrezos, N., Violette, S.M., Weinreb, P.H. and Chester, K.A. Stromal features are predictive of disease mortality in oral cancer patients. *The Journal of pathology* 2011; 223(4): 470-481.

Martinez-Outschoorn, Ubaldo E., Renee M. Balliet, Dayana Rivadeneira, Barbara Chiavarina, Stephanos Pavlides, Chenguang Wang, Diana Whitaker-Menezes et al. "Oxidative stress in cancer associated fibroblasts drives tumor-stroma co-evolution: A new paradigm for understanding tumor metabolism, the field effect and genomic instability in cancer cells." *Cell cycle* 2010; 9(16): 3276-3296.

Martinez-Outschoorn, U.E., Lin, Z., Trimmer, C., Flomenberg, N., Wang, C., Pavlides, S., Pestell, R.G., Howell, A., Sotgia, F. and Lisanti, M.P. Cancer cells metabolically" fertilize" the tumor microenvironment with hydrogen peroxide, driving the Warburg effect: implications for PET imaging of human tumors. *Cell cycle* 2011; *10*(15): 2504-2520.

Massagué, J. G1 cell-cycle control and cancer. *Nature* 2004; *432* (7015): 298.

Massagué, J. TGFβ in cancer. *Cell* 2008; 134(2): 215-230.

Mbeunkui, F. and Johann, D.J. Cancer and the tumor microenvironment: a review of an essential relationship. *Cancer chemotherapy and pharmacology* 2009; *63*(4): 571-582.

McAnulty, R.J. Fibroblasts and myofibroblasts: their source, function and role in disease. *Int J Biochem Cell Biol* 2007; 39: 666-671.

McCaul, J.A, Gordon K.E, Clark .LJ, Parkinson E.K. Telomeraseinhibition and the future management of head-and-neck cancer. *Lancet Oncol* 2002; 3: 280–88.

McCawley, L.J, Matrisian L.M. Matrix metalloproteinases: multifunctional contributors to tumor progression. *Mol Med Today* 2000; 6:149–56.

Medici, D, Hay ED, and Olsen BR. Snail andSlug promote epithelial-mesenchymal transition through Beta-Catenin-T-cell factor-4- dependent expression of transforming growth factor-beta3. *Mol Biol Cell* 2008; 19: 4875- 4887.

Melling, G (2015). The role of MicroRNA-145 in the tumour microenvironment. The University of Sheffield, UK.

Meltzer, P.S. Cancer genomics: small RNAs with big impacts. *Nature* 2005; 435(7043): 745-746.

Megiorni, F., Cialfi, S., Cimino, G., De Biase, R.V., Dominici, C., Quattrucci, S. and Pizzuti, A. Elevated levels of miR-145 correlate with SMAD3 down-regulation in cystic fibrosis patients. *Journal of Cystic Fibrosis* 2013; 12(6): 797-802.

Mei, M., Ren, Y., Zhou, X., Yuan, X.B., Han, L., Wang, G.X., Jia, Z., Pu, P.Y., Kang, C.S. and Yao, Z. Downregulation of miR-21 enhances chemotherapeutic effect of taxol in breast carcinoma cells. *Technology in cancer research & treatment* 2010; 9(1): 77-86.

Meltzer, P.S. Cancer genomics: small RNAs with big impacts. *Nature* 2005; 435:7.

Meng, F., Henson, R., Wehbe–Janek, H., Ghoshal, K., Jacob, S.T. and Patel, T. MicroRNA-21 regulates expression of the PTEN tumor suppressor gene in human hepatocellular cancer. *Gastroenterology* 2007; 133(2): 647-658.

Meyer-ter-Vehn, T., Gebhardt, S., Sebald, W., Buttmann, M., Grehn, F., Schlunck, G. and Knaus, P. p38 inhibitors prevent TGF-β–induced myofibroblast transdifferentiation in human Tenon fibroblasts. *Investigative ophthalmology & visual science* 2006; 47(4): 1500-1509.

Micke, P., and Ostman, A. Tumour-stroma interaction: cancer-associated fibroblasts as novel targets in anti-cancer therapy? *Lung Cancer* 2004; 45 (2), 163–175.

Micke, P., Kappert, K., Ohshima, M., Sundquist, C., Scheidl, S., Lindahl, P., Heldin, C.H., Botling, J., Ponten, F. and Östman, A. In situ identification of genes regulated specifically in fibroblasts of human basal cell carcinoma. *Journal of Investigative Dermatology* 2007; 127(6): 1516-1523.

Miles, G.D., Seiler, M., Rodriguez, L., Rajagopal, G. and Bhanot, G. Identifying microRNA/mRNA dysregulations in ovarian cancer. *BMC research notes* 2012; 5(1): 164.

Mirastschijski, U., Haaksma, C.J., Tomasek, J.J. and Ågren, M.S., 2004. Matrix metalloproteinase inhibitor GM 6001 attenuates keratinocyte migration, contraction and myofibroblast formation in skin wounds. *Experimental cell research*, *299*(2), pp.465-475.

Mishra, P.K., Tyagi, N., Kumar, M., Tyagi, S.C. MicroRNAs as a therapeutic target for cardiovascular diseases. *J Cell Mol Med* 2009; 13:778–789

Mitra, A.K., Zillhardt, M., Hua, Y., Tiwari, P., Murmann, A.E., Peter, M.E. and Lengyel, E. MicroRNAs reprogram normal fibroblasts into cancer-associated fibroblasts in ovarian cancer. *Cancer discovery* 2012; 2(12): 1100-1108.

Moll, U.M. and Petrenko, O. The MDM2-p53 interaction. *Molecular cancer research* 2003; 1(14): 1001-1008.

Motoyama, K., Inoue, H., Nakamura, Y., Uetake, H., Sugihara, K. and Mori, M. Clinical significance of high mobility group A2 in human gastric cancer and its relationship to let-7 microRNA family. *Clinical cancer research* 2008; 14(8): 2334-2340.

Munger K, Howley PM. Human papillomavirus immortalization and transformation functions. *Virus Res* 2002; 89: 213–28.

Muro, A.F., Chauhan, A.K., Gajovic, S., Iaconcig, A., Porro, F., Stanta, G. and Baralle, F.E. Regulated splicing of the fibronectin EDA exon is essential for proper skin wound healing and normal lifespan. *The Journal of cell biology* 2003; 162(1): 149-160.

Myers EN, Wagner RL, Johnson JT. Microlaryngoscopic surgery for T1 glottic lesions: a cost-eff ective option. *Ann Otol Rhinol Laryngol* 1994; 103: 28–30.

Nairismägi, M.L., Vislovukh, A., Meng, Q., Kratassiouk, G., Beldiman, C., Petretich, M., Groisman, R., Füchtbauer, E.M., Harel-Bellan, A. and Groisman, I. Translational control of TWIST1 expression in MCF-10A cell lines recapitulating breast cancer progression. *Oncogene* 2012; 31(47): 4960.

Nam, J.W., Rissland, O.S., Koppstein, D., Abreu-Goodger, C., Jan, C.H., Agarwal, V., Yildirim, M.A., Rodriguez, A. and Bartel, D.P., 2014. Global analyses of the effect of different cellular contexts on microRNA targeting. *Molecular cell*, *53*(6), pp.1031-1043.

Narimatsu, M., Samavarchi-Tehrani, P., Varelas, X. and Wrana, J.L. Distinct polarity cues direct Taz/Yap and TGFβ receptor localization to differentially control TGFβ-induced Smad signaling. *Developmental cell* 2015; 32(5): 652-656.

National Cancer Institute. 2015. Head and neck cancers. [ONLINE] Available at http://www.cancer.gov. [Accessed 29 March 2017].

Ni, J., Dong, Z., Han, W., Kondrikov, D. and Su, Y. The role of RhoA and cytoskeleton in myofibroblast transformation in hyperoxic lung fibrosis. *Free Radical Biology and Medicine* 2013; 61: 26-39.

Nielsen, B.S., Jørgensen, S., Fog, J.U., Søkilde, R., Christensen, I.J., Hansen, U., Brünner, N., Baker, A., Møller, S. and Nielsen, H.J. High levels of microRNA-21 in the stroma of colorectal cancers predict short disease-free survival in stage II colon cancer patients. *Clinical & experimental metastasis* 2011; 28(1): 27-38.

Nithiananthan, S., Crawford, A., Knock, J.C., Lambert, D.W. and Whawell, S.A. Physiological Fluid Flow Moderates Fibroblast Responses to TGF-β1. *Journal of cellular biochemistry* 2017; 118(4): 878-890.

Noh, J.H., Chang, Y.G., Kim, M.G., Jung, K.H., Kim, J.K., Bae, H.J., Eun, J.W., Shen, Q., Kim, S.J., Kwon, S.H. and Park, W.S. MiR-145 functions as a tumor suppressor by directly targeting histone deacetylase 2 in liver cancer. *Cancer letters* 2013; 335(2): 455-462.

Noseda, M., Fu, Y., Niessen, K., Wong, F., Chang, L., McLean, G. and Karsan, A. Smooth muscle α-actin is a direct target of Notch/CSL. *Circulation research* 2006; *98*(12): 1468-1470.

O'Connell, J.T., Sugimoto, H., Cooke, V.G., MacDonald, B.A., Mehta, A.I., LeBleu, V.S., Dewar, R., Rocha, R.M., Brentani, R.R., Resnick, M.B. and Neilson, E.G. VEGF-A and Tenascin-C produced by S100A4+ stromal cells are important for metastatic colonization. *Proceedings of the National Academy of Sciences* 2011; 108(38): 16002-16007.

Oda, D., Gown, A.M., Berg, J.S.V. and Stern, R. The fibroblast-like nature of myofibroblast. *Experimental and molecular pathology* 1988; 49(3): 316-329.

Overall, C.M. and Kleifeld, O. Tumour microenvironment--opinion: validating matrix metalloproteinases as drug targets and anti-targets for cancer therapy. *Nature reviews. Cancer*, 2006; 6(3): 227.

Owens, D.M., Wei, S., Smart, R.C. A multihit, multistage model of chemical carcinogenesis. *Carcinogenesis* 1999; 20: 1837-1844.

Paget, S. The distribution of secondary growths in cancer of the breast. Lancet 1889; 1:571–572

Pal, A., Melling, G., Hinsley, E.E., Kabir, T.D., Colley, H.E., Murdoch, C. and Lambert, D.W. Cigarette smoke condensate promotes pro-tumourigenic stromal–epithelial interactions by suppressing miR-145. *Journal of Oral Pathology & Medicine* 2013; 42(4): 309-314.

Pan, X., Chen, Z., Huang, R., Yao, Y. and Ma, G. Transforming growth factor β1 induces the expression of collagen type I by DNA methylation in cardiac fibroblasts. *PloS one* 2013; 8(4): 60335.

Pardali, K., Kurisaki, A., Morén, A., Ten Dijke, P., Kardassis, D. and Moustakas, A. Role of Smad proteins and transcription factor Sp1 in p21Waf1/Cip1 regulation

by transforming growth factor-β. *Journal of Biological Chemistry* 2000; 275(38): 29244-29256.

Parikh, A., Lee, C., Joseph, P., Marchini, S., Baccarini, A., Kolev, V., Romualdi, C., Fruscio, R., Shah, H., Wang, F. and Mullokandov, G. microRNA-181a has a critical role in ovarian cancer progression through the regulation of the epithelial–mesenchymal transition. *Nature communications* 2014 ; *5*: 2977.

Park, S.M, Gaur, A.B, Lengyel, E, Peter M.E. The miR-200 family determines the epithelial phenotype of cancer cells by targeting the E-cadherin repressors ZEB1 and ZEB2. *Genes Dev* 2008; 22: 894–907.

Parkin, D.M, Bray, F, Ferlay, J, Pisani, P. Global cancer statistics, 2002. *CA Cancer J Clin* 2005; **55:** 74–108.

Parsonage, G., Filer, A.D., Haworth, O., Nash, G.B., Rainger, G.E., Salmon, M. and Buckley, C.D. A stromal address code defined by fibroblasts. *Trends in immunology* 2005; *26*(3): 150-156.

Pavlides, S., Whitaker-Menezes, D., Castello-Cros, R., Flomenberg, N., Witkiewicz, A.K., Frank, P.G., Casimiro, M.C., Wang, C., Fortina, P., Addya, S. and Pestell, R.G. The reverse Warburg effect: aerobic glycolysis in cancer associated fibroblasts and the tumor stroma. *Cell cycle* 2009; 8(23): 3984-4001.

Pellegrin S, Mellor H. Actin stress fibres. *J Cell Sci* 2007; 120: 3491–9.

Peña, C., Céspedes, M.V., Lindh, M.B., Kiflemariam, S., Mezheyeuski, A., Edqvist, P.H., Hägglöf, C., Birgisson, H., Bojmar, L., Jirström, K. and Sandström, P. STC1 expression by cancer-associated fibroblasts drives metastasis of colorectal cancer. *Cancer research* 2013; 73(4):1287-1297.

Perez-Ordonez, B, Beauchemin, M, Jordan, R.C. Molecular biology of squamous cell carcinoma of the head and neck. *J Clin Pathol* 2006; 59: 445–53.

Petersen, O.W., Nielsen, H.L., Gudjonsson, T., Villadsen, R., Rank, F., Niebuhr, E., Bissell, M.J. and Rønnov-Jessen, L. Epithelial to mesenchymal transition in human breast cancer can provide a nonmalignant stroma. *The American journal of pathology* 2003; 162(2): 391-402.

Piersma, B., de Rond, S., Werker, P.M., Boo, S., Hinz, B., van Beuge, M.M. and Bank, R.A. YAP1 is a driver of myofibroblast differentiation in normal and diseased fibroblasts. *The American journal of pathology* 2015; 185(12): 3326-3337.

Pietras, K, Ostman, A. Hallmarks of cancer: interactions with the tumor stroma. *Exp Cell Res*. 2010; 316:1324-1331.

Pignataro, L., Pruneri, G., Carboni, N., Capaccio, P., Cesana, B.M., Neri, A. and Buffa, R. Clinical relevance of cyclin D1 protein overexpression in laryngeal squamous cell carcinoma. *Journal of clinical oncology* 1998; 16(9): 3069-3077.

Poola, I., DeWitty, R.L., Marshalleck, J.J., Bhatnagar, R., Abraham, J. and Leffall, L.D. Identification of MMP-1 as a putative breast cancer predictive marker by global gene expression analysis. *Nature medicine* 2005; 11(5): 481.

Potenta, S., Zeisberg, E. and Kalluri, R. The role of endothelial-to-mesenchymal transition in cancer progression. *British journal of cancer* 2008; 99(9): 1375.

Pottier, N., Maurin, T., Chevalier, B., Puissegur, M.P., Lebrigand, K., Robbe-Sermesant K., Bertero, T., Lino Cardenas, C.L., Courcot, E., Rios, G., Fourre, S., Lo-Guidice, J.M., Marcet, B., Cardinaud, B., Barbry, P., Mari, B. Identification of keratinocyte growth factor as a target of microRNA-155 in lungfibroblasts: implication in epithelial-mesenchymal interactions. *PLoS ONE* 2009; 4:6718.

Powell, D.W., Mifflin, R.C., Valentich, J.D., Crowe, S.E., Saada, J.I. and West, A.B. Myofibroblasts. I. Paracrine cells important in health and disease. *American Journal of Physiology-Cell Physiology* 1999; *277*(1): C1-C19.

Pritchard, C.C., Cheng, H.H. and Tewari, M. MicroRNA profiling: approaches and considerations. *Nature reviews. Genetics* 2012; 13(5):358.

Qiu, P., Ritchie, R.P., Fu, Z., Cao, D., Cumming, J., Miano, J.M., Wang, D.Z., Li, H.J. and Li, L. Myocardin enhances Smad3-mediated transforming growth factor-β1 signaling in a CArG box-independent manner. *Circulation research* 2005; 97(10): 983-991.

R. Maller Schulman, B., Liang, X., Stahlhut, C., DelConte, C., Stefani, G. and Slack, F.J. The let-7 microRNA target gene, Mlin41/Trim71 is required for mouse embryonic survival and neural tube closure. *Cell cycle* 2008; 7(24): 3935-3942.

Radisky, D.C, Kenny PA, and Bissell MJ. Fibrosis and cancer: do myofibroblasts come also from epithelial cells via EMT? *J Cell Biochem* 2007; 101: 830-839.

Rahman, S., Patel, Y., Murray, J., Patel, K.V., Sumathipala, R., Sobel, M. and Wijelath, E.S. Novel hepatocyte growth factor (HGF) binding domains on fibronectin and vitronectin coordinate a distinct and amplified Met-integrin induced signalling pathway in endothelial cells. *BMC cell biology* 2005; 6(1): 8.

Ramirez, A.M., Shen, Z., Ritzenthaler, J.D. and Roman, J. Myofibroblast Transdifferentiation in Obliterative Bronchiolitis: TGF-β Signaling Through

Smad3-Dependent and-Independent Pathways. *American journal of transplantation* 2006; 6(9):2080-2088.

Rasanen, K and Vaheri, A. Activation of fibroblasts in cancer stroma. *Exp Cell Res* 2010; 316: 2713-2722.

Raz, Y. and Erez, N. An inflammatory vicious cycle: Fibroblasts and immune cell recruitment in cancer. *Experimental cell research* 2013; 319(11): 1596-1603.

Reardon, D.A., Akabani, G., Coleman, R.E., Friedman, A.H., Friedman, H.S., Herndon, J.E., McLendon, R.E., Pegram, C.N., Provenzale, J.M., Quinn, J.A. and Rich, J.N. Salvage Radioimmunotherapy with Murine Iodine-131–Labeled Antitenascin Monoclonal Antibody 81C6 for Patients with Recurrent Primary and Metastatic Malignant Brain Tumors: Phase II Study Results. *Journal of clinical oncology* 2006; 24(1): 115-122.

Reddel, R.R. The role of senescence and immortalization in carcinogenesis. *Carcinogenesis* 2000; 21(3): 477-484.

Ridley, A.J. and Hall, A. The small GTP-binding protein rho regulates the assembly of focal adhesions and actin stress fibers in response to growth factors. *Cell* 1992; 70(3): 389-399.

Rifkin, D.B. Latent transforming growth factor-β (TGF-β) binding proteins: orchestrators of TGF-β availability. *J. Biol. Chem* 2005; 280: 7409–7412.

Rissland, O.S., Hong, S.J. and Bartel, D.P. MicroRNA destabilization enables dynamic regulation of the miR-16 family in response to cell-cycle changes. *Molecular cell* 2011; *43*(6): 993-1004.

Roberts, A.B, Wakefield, L.M. The two faces of transforming growth factor beta in carcinogenesis. *Proc Natl Acad Sci USA* 2003;100 (15): 8621–3.

Rocco, J.W, Sidransky D. p16(MTS-1/CDKN2/INK4a) in cancer progression. *Exp Cell Res* 2001; 264**:** 42–55.

Rodemann, H. P. & Muller, G. A. Characterization of human renal fibroblasts in health and disease: II. *In vitro* growth, differentiation, and collagen synthesis of fibroblasts from kidneys with interstitial fibrosis. *Am. J. Kidney Dis* 1991; 17, 684–686.

Rodriguez, T., Altieri, A., Chatenoud, L., Gallus, S., Bosetti, C., Negri, E., Franceschi, S., Levi, F., Talamini, R. and La Vecchia, C. Risk factors for oral and pharyngeal cancer in young adults. *Oral oncology* 2004; *40*(2): 207-213.

Rong, G., Kang, H., Wang, Y., Hai T., Sun, H. Candidate Markers That Associate with Chemotherapy Resistance in Breast Cancer through the Study on Taxotere-Induced Damage to Tumor Microenvironment and Gene Expression Profiling of Carcinoma-Associated Fibroblasts (CAFs). PLoS ONE 2013 8(8): 70960.

Ronnov-Jessen L, Petersen O.W. Induction of alpha-smooth muscle actin by transforming growth factor-beta 1 in quiescent human breast gland fibroblasts. Implications for myofibroblast generation in breast neoplasia. *Lab Invest* 1993; 68: 696–707.

Ronnov-Jessen, L., Peterson, O.W., Bissell, M.J. Cellular changes involved in converson of normal to malignant breast: importance of the stromal reaction. *Physiol Rev* 1996; 76: 69 – 125.

Rosa, A., Ballarino, M., Sorrentino, A., Sthandier, O., De Angelis, F.G., Marchioni, M., Masella, B., Guarini, A., Fatica, A., Peschle, C. and Bozzoni, I. The interplay between the master transcription factor PU. 1 and miR-424 regulates human monocyte/macrophage differentiation. *Proceedings of the National Academy of Sciences* 2007; 104(50): 19849-19854.

Roth, C., Rack, B., Müller, V., Janni, W., Pantel, K. and Schwarzenbach, H. Circulating microRNAs as blood-based markers for patients with primary and metastatic breast cancer. *Breast Cancer Research* 2010; 12(6): R90.

Rowley, D.R. What might a stromal response mean to prostate cancer progression? *Cancer Metast Rev* 1998; 17: 411 – 419.

Roy, S.G., Nozaki, Y. and Phan, S.H. Regulation of α-smooth muscle actin gene expression in myofibroblast differentiation from rat lung fibroblasts. *The international journal of biochemistry & cell biology* 2011; 33(7): 723-734.

Ruwali, M., Pant, M.C, Shah P.P, Mishr, a B.N, Parmar D. Polymorphism in cytochrome P450 2A6 and glutathione S-transferase P1 modifies head and neck cancer risk and treatment outcome. *Mutat Res* 2009.

Ruzicka, D.L. and Schwartz, R.J. Sequential activation of alpha-actin genes during avian cardiogenesis: vascular smooth muscle alpha-actin gene transcripts mark the onset of cardiomyocyte differentiation. *The Journal of cell biology* 1988; 107(6): 2575-2586.

Sachdeva, M., Zhu, S., Wu, F., Wu, H., Walia, V., Kumar, S., Elble, R., Watabe, K. and Mo, Y.Y. p53 represses c-Myc through induction of the tumor suppressor miR-145. *Proceedings of the National Academy of Sciences* 2009; 106(9): 3207-3212.

Saini, S., Yamamura, S., Majid, S., Shahryari, V., Hirata, H., Tanaka, Y. and Dahiya, R. MicroRNA-708 induces apoptosis and suppresses tumorigenicity in renal cancer cells. *Cancer research* 2011; *71*(19): 6208-6219.

Sandbo, N. and N. Dulin. "Actin cytoskeleton in myofibroblast differentiation: ultrastructure defining form and driving function." *Transl Res* 2011; 158(4): 181-196.

Sandbo, N., Lau, A., Kach, J., Ngam, C., Yau, D. and Dulin, N.O. Delayed stress fiber formation mediates pulmonary myofibroblast differentiation in response to TGF-β. *American Journal of Physiology-Lung Cellular and Molecular Physiology*, 2011; 301(5): L656-L666.

Scaria, V., Hariharan, M., Pillai, B., Maiti, S. and Brahmachari, S.K. Host–virus genome interactions: macro roles for microRNAs. *Cellular microbiology* 2007; 9(12): 2784-2794.

Schaaij-Visser, Tieneke B.M.; Brakenhoff, Ruud H.; Leemans, C. René; Heck, Albert J.R. Protein biomarker discovery for head and neck cancer *Journal of Proteomics* 2012; 73 (10): 1790-180.

Schepeler, T., Reinert, J.T., Ostenfeld, M.S., Christensen, L.L., Silahtaroglu, A.N., Dyrskjøt, L., Wiuf, C., Sørensen, F.J., Kruhøffer, M., Laurberg, S. and Kauppinen, S. Diagnostic and prognostic microRNAs in stage II colon cancer. *Cancer research* 2008; 68(15): 6416-6424.

Schickel, R., Boyerinas, B., Park, S.M & Peter, M.E. MicroRNAs: key players in the immune system, differentiation, tumorigenesis and cell death. *Oncogene* 2008; 27 5959–5974.

Schilling, J. Wound healing. *Surg. Clin. North Am* 1976; 56: 859.

Schoen, F.J. Aortic valve structure-function correlations: role of elastic fibers no longer a stretch of the imagination. *J Heart Valve Dis* 1997; 6:1–6.

Schurch, W., Seemayer, T.A, Hinz, B., Gabbiani, G. Myofibroblast. Mills SE, editor. Philadelphia: Lippincott-Williams & Wilkins Publishers, Histology for Pathologists. 2007:123–164.

Scott, A.M., Wiseman, G., Welt, S., Adjei, A., Lee, F.T., Hopkins, W., Divgi, C.R., Hanson, L.H., Mitchell, P., Gansen, D.N. and Larson, S.M. A Phase I dose-escalation study of sibrotuzumab in patients with advanced or metastatic fibroblast activation protein-positive cancer. *Clinical cancer research* 2003; 9(5): 1639-1647.

Sebens, S., Schafer, H: The tumor stroma as mediator of drug resistance–a potential target to improve cancer therapy? *Curr Pharm Biotechnol* 2012, 13(11): 2259–2272.

Semenza, G.L. Hypoxia-inducible factors in physiology and medicine. *Cell* 2012; 148(3): 399-408.

Sempere, L.F., Christensen, M., Silahtaroglu, A., Bak, M., Heath, C.V., Schwartz, G., Wells, W., Kauppinen, S. and Cole, C.N. Altered MicroRNA expression confined to specific epithelial cell subpopulations in breast cancer. *Cancer research* 2007; 67(24): 11612-11620.

Serini, G., Bochaton-Piallat, M.L., Ropraz, P., Geinoz, A., Borsi, L., Zardi, L., & Gabbiani, G. The fibronectin domain ED-A is crucial for myofibroblastic phenotype induction by transforming growth factor-β1. *The Journal of Cell Biology* 1998; 142, (3): 873-881, 0021-9525.

Serini, G., Gabbiani G. Mechanisms of myofibroblast activity and phenotypic modulation. *Exp Cell Res* 1999; 250:273–83.

Seoane, J., Le, H.V., Shen, L., Anderson, S.A. and Massagué, J. Integration of Smad and forkhead pathways in the control of neuroepithelial and glioblastoma cell proliferation. *Cell* 2004; 117(2): 211-223.

Shafer, S.L. and Towler, D.A. Transcriptional regulation of SM22α by Wnt3a: convergence with TGFβ 1/Smad signaling at a novel regulatory element. *Journal of molecular and cellular cardiology*, 2009; 46(5): 621-635.

Shen, H., Yu, X., Yang, F., Zhang, Z., Shen, J., Sun, J., Choksi, S., Jitkaew, S. and Shu, Y. Reprogramming of Normal Fibroblasts into Cancer-Associated Fibroblasts by miRNAs-Mediated CCL2/VEGFA Signaling. *PLoS genetics* 2016; 12(8): 1006244.

Sherr, C.J. and McCormick, F. The RB and p53 pathways in cancer. *Cancer cell* 2002; *2*(2): 103-112.

Sherr, C.J. and Roberts, J.M. CDK inhibitors: positive and negative regulators of G1-phase progression. *Genes & development* 1999; *13*(12): 1501-1512.

Shi, L., Cheng, Z., Zhang, J., Li, R., Zhao, P., Fu, Z. and You, Y. hsa-mir-181a and hsa-mir-181b function as tumor suppressors in human glioma cells. *Brain research* 2008; 1236: 185-193.

Shin, K.H., Bae, S.D., Hong, H.S., Kim, R.H., Kang, M.K. and Park, N.H. miR-181a shows tumor suppressive effect against oral squamous cell carcinoma cells by downregulating K-ras. *Biochemical and biophysical research communications* 2011; 404(4): 896-902.

Siegel, P. M. & Massague, J. Cytostatic and apoptotic actions of TGF-β in homeostasis and cancer. *Nature Rev. Cancer* 2003; 3: 807–821.

Siegel, R., and Jemal, A. Cancer facts and figures 2011. [Online] Avilable at world wide web: http://www.cancer.org.

Simian, M., Hirai, Y., Navre, M., Werb, Z., Lochter, A. and Bissell, M.J. The interplay of matrix metalloproteinases, morphogens and growth factors is necessary for branching of mammary epithelial cells. *Development* 2001; 128(16): 3117-3131.

Skalli, O. and Gabbiani, G. The biology of the myofibroblast relationship to wound contraction and fibrocontractive diseases. In *The molecular and cellular biology of wound repair* 1988; 373-402: Springer US.

Skog, J., Wurdinger, T., Van Rijn, S., Meijer, D., Gainche, L., Sena-Esteves, M., Curry Jr, W.T., Carter, R.S., Krichevsky, A.M. and Breakefield, X.O. Glioblastoma microvesicles transport RNA and protein that promote tumor growth and provide diagnostic biomarkers. *Nature cell biology* 2008; 10(12): 1470.

Smith, B.D., Smith, G.L., Carter, D., Sasaki, C.T., Haffty, B.G. Prognostic signifi cance of vascular endothelial growth factor protein levels in oral and oropharyngeal squamous cell carcinoma. *J Clin Oncol* 2000; 18: 2046–52.

Smith, E.M., Mitsi, M., Nugent, M.A. and Symes, K. PDGF-A interactions with fibronectin reveal a critical role for heparan sulfate in directed cell migration during Xenopus gastrulation. *Proceedings of the National Academy of Sciences* 2009; 106(51): 21683-21688.

Smith, P.C., Cáceres, M. and Martinez, J. Induction of the myofibroblastic phenotype in human gingival fibroblasts by transforming growth factor-β1: role of RhoA-ROCK and c-Jun N-terminal kinase signaling pathways. *Journal of periodontal research* 2006; 41(5): 418-425.

Sobral, L.M., Zecchin, K.G., Nascimento de Aquino, S., Lopes, M.A., Graner, E. and Coletta, R.D. Isolation and characterization of myofibroblast cell lines from oral squamous cell carcinoma. *Oncology reports* 2011; 25 (4): 1013-1020.

Souders, C.A, Bowers, S.L, Baudino, T.A. Cardiac fibroblast: the renaissance cell. *Circ Res* 2009; 105:1164–1176.

Spaeth, E., Klopp, A., Dembinski, J., Andreeff, M., and Marini, F. Inflammation and tumor microenvironments: defining the migratory itinerary of mesenchymal stem cells. *Gene Ther* 2008; 15: 730-738.

Spaeth, E.L., Dembinski, J.L., Sasser, A.K., Watson, K., Klopp, A., Hall, B., Andreeff, M. and Marini, F. Mesenchymal stem cell transition to tumor-associated fibroblasts contributes to fibrovascular network expansion and tumor progression. *PloS one* 2009; 4(4): 4992.

Straussman, R., Morikawa, T., Shee, K., Barzily-Rokni, M., Qian, Z.R., Du, J., Davis, A., Mongare, M.M., Gould, J., Frederick, D.T. and Cooper, Z.A. Tumour micro-environment elicits innate resistance to RAF inhibitors through HGF secretion. *Nature* 2012; 487(7408): 500-504.

Strutz, F., Okada, H., Lo, C.W., Danoff, T., Carone, R.L., Tomaszewski, J.E. and Neilson, E.G. Identification and characterization of a fibroblast marker: FSP1. *The Journal of cell biology* 1995; 130(2): pp.393-405.

Suarez, C.., Rodrigo, J.P, Ferlito, A., Cabanillas, R., Shaha, A.R., Rinaldo, A. Tumours of familial origin in the head and neck. *Oral Oncol* 2006; 42:965–78.

Sugimoto, H., Munde, l T.M, Kieran, M.W, Kalluri, R: Identification of fibroblast heterogeneity in the tumor microenvironment. *Cancer Biol Ther* 2006, 5:1640-1646.

Suh, S.O., Chen, Y., Zaman, M.S., Hirata, H., Yamamura, S., Shahryari, V., Liu, J., Tabatabai, Z.L., Kakar, S., Deng, G. and Tanaka, Y. MicroRNA-145 is regulated by DNA methylation and p53 gene mutation in prostate cancer. *Carcinogenesis* 2011; 32(5): 772-778.

Szeto, S.G., Narimatsu, M., Lu, M., He, X., Sidiqi, A.M., Tolosa, M.F., Chan, L., De Freitas, K., Bialik, J.F., Majumder, S. and Boo, S. YAP/TAZ are mechanoregulators of TGF-β-Smad signaling and renal fibrogenesis. *Journal of the American Society of Nephrology* 2016; pp.ASN-2015050499.

Takahashi, M., Fukami, S., Iwata, N., Inoue, K., Itohara, S., Itoh, H., Haraoka, J., Saido T. In vivo glioma growth requires host-derived matrix metalloproteinase 2 for maintenance of angioarchitecture. *Pharmacol Resn* 2002; 46:155–163.

Takamizawa, J., Konishi, H., Yanagisawa, K., Tomida, S., Osada, H., Endoh, H., Harano, T., Yatabe, Y., Nagino, M., Nimura, Y. and Mitsudomi, T. Reduced expression

of the let-7 microRNAs in human lung cancers in association with shortened postoperative survival. *Cancer research* 2004; 64(11): 3753-3756.

Tang, X., Hou, Y., Yang, G., Wang, X., Tang, S., Du, Y.E., Yang, L., Yu, T., Zhang, H., Zhou, M. and Wen, S. Stromal miR-200s contribute to breast cancer cell invasion through CAF activation and ECM remodeling. *Cell death and differentiation* 2016; 23(1): 132.

Tarin, D. and C. B. Croft. "Ultrastructural features of wound healing in mouse skin." J Anat 1969; 105 (1): 189-190.

Tavares-Valente, D., Baltazar, F., Moreira, R. and Queirós, O. Cancer cell bioenergetics and pH regulation influence breast cancer cell resistance to paclitaxel and doxorubicin. *Journal of bioenergetics and biomembranes* 2013; 45(5): 467-475.

Taylor, M.A., Sossey-Alaoui, K., Thompson, C.L., Danielpour, D. and Schiemann, W.P., 2013. TGF-β upregulates miR-181a expression to promote breast cancer metastasis. *The Journal of clinical investigation*, *123*(1), p.150.

Tlsty, T.D, Hein, P.W. Know thy neighbor: stromal cells can contribute oncogenic signals 2001; *Curr Opin Genet Dev* 11: 54 – 59.

Thiery, J.P., Acloque, H., Huang, R.Y. and Nieto, M.A. Epithelial-mesenchymal transitions in development and disease. *Cell* 2009; 139(5): 871-890.

Thode, C., Jørgensen, T.G., Dabelsteen, E., Mackenzie, I. and Dabelsteen, S. Significance of myofibroblasts in oral squamous cell carcinoma. *Journal of Oral Pathology & Medicine* 2011; 40(3): 201-207.

Thomasset, N., Lochter, A., Sympson, C.J., Lund, L.R., Williams, D.R., Behrendtsen, O., Werb, Z., Bissell, M.J. Expression of autoactivated stromelysin-1 in mammary glands of transgenic mice leads to a reactive stroma during early development. *Am J Pathol* 1998; 153:457–467.

Thomson, D.W., Bracken, C.P., Szubert, J.M. and Goodall, G.J. On measuring miRNAs after transient transfection of mimics or antisense inhibitors. *PloS one* 2013; 8(1): 55214.

Thum, T., Gross, C., Fiedler, J., Fischer, T., Kissler, S., Bussen, M., Galuppo, P., Just, S., Rottbauer, W., Frantz, S., Castoldi, M., Soutschek, J., Koteliansky, V., Rosenwald, A., Basson, M.A., Licht, J.D., Pena, J.T, Rouhanifard, S.H, Muckenthaler, M.U., Tuschl, T., Martin, G.R., Bauersachs, J., Engelhardt, S. MicroRNA-21 contributes to myocardial disease by stimulating MAP kinase signalling in fibroblasts. *Nature* 2008; 456:980–984.

Tomasek, J. J., Gabbiani, G., Hinz, B., Chaponnier, C. & Brown, R. A. Myofibroblasts and mechanoregulation of connective tissue remodelling. *Nature Rev. Mol. Cell Biol* 2002; 3, 349–363.

Tran, N., McLean, T., Zhang, X., Zhao, C.J., Thomson, J.M., O'Brien, C. and Rose, B. MicroRNA expression profiles in head and neck cancer cell lines. *Biochemical and biophysical research communications* 2007; 358(1): 12-17.

Trang, P., Medina, P.P., Wiggins, J.F., Ruffino, L., Kelnar, K., Omotola, M., Homer, R., Brown, D., Bader, A.G., Weidhaas, J.B. and Slack, F.J. Regression of murine lung tumors by the let-7 microRNA. *Oncogene* 2010; 29(11): 1580.

Trang, P., Wiggins, J.F., Daige, C.L., Cho, C., Omotola, M., Brown, D., Weidhaas, J.B., Bader, A.G. and Slack, F.J. Systemic delivery of tumor suppressor microRNA mimics using a neutral lipid emulsion inhibits lung tumors in mice. *Molecular Therapy* 2011; 19(6): 1116-1122.

Trimboli, A.J., Cantemir-Stone, C.Z., Li, F., Wallace, J.A., Merchant, A., Creasap, N., Thompson, J.C., Caserta, E., Wang, H., Chong, J.L. and Naidu, S. Pten in stromal fibroblasts suppresses mammary epithelial tumors. *Nature* 2008; 461(7267): 1084.

Tsellou, E. and Kiaris, H. Fibroblast independency in tumors: implications in cancer therapy. *Future Medicine* 2008; 427-432.

Tsuyada, A., Chow, A., Wu, J., Somlo, G., Chu, P., Loera, S., Luu, T., Li, A.X., Wu, X., Ye, W. and Chen, S. CCL2 mediates cross-talk between cancer cells and stromal fibroblasts that regulates breast cancer stem cells. *Cancer research* 2012; 72(11): 2768-2779.

Tuxhorn, J.A., McAlhany, S.J., Yang, F., Dang, T.D. and Rowley, D.R. Inhibition of transforming growth factor-β activity decreases angiogenesis in a human prostate cancer-reactive stroma xenograft model. *Cancer research* 2002; 62(21): 6021-6025.

Utispan, K., Thuwajit, P., Abiko, Y., Charngkaew, K., Paupairoj, A., Chau-in, S. and Thuwajit, C. Gene expression profiling of cholangiocarcinoma-derived fibroblast reveals alterations related to tumor progression and indicates periostin as a poor prognostic marker. *Molecular cancer* 2010; 9(1): 13.

Valadi, H., Ekström, K., Bossios, A., Sjöstrand, M., Lee, J.J. and Lötvall, J.O. Exosome-mediated transfer of mRNAs and microRNAs is a novel mechanism of genetic exchange between cells. *Nature cell biology* 2007; 9(6): 654.

Van Aelst, L. and D'Souza-Schorey, C. Rho GTPases and signaling networks. *Genes & development* 1997; 11(18): 2295-2322.

Vanpoucke, G., Goossens, S., De Craene, B., Gilbert, B., Van Roy, F. and Berx, G. GATA-4 and MEF2C transcription factors control the tissue-specific expression of the αT-catenin gene CTNNA3. *Nucleic acids research* 2004; 32(14): 4155-4165.

van Rooij, E., Sutherland, L.B., Thatcher, J.E., DiMaio, J.M., Naseem, RH., Marshall, W.S., Hill, J.A., Olson, E.N. Dysregulation of microRNAs after myocardial infarction reveals a role of miR-29 in cardiac fibrosis. *Proc Natl Acad Sci U S A* 2008; 105:13027–13032.

van Zijl, F., Krupitza, G., Mikulits, W. Initial steps of metastasis: cell invasion and endothelial transmigration. *Mutat Res* 2011; 728:23-34.

Varelas, X., Sakuma, R., Samavarchi-Tehrani, P., Peerani, R., Rao, B.M., Dembowy, J., Yaffe, M.B., Zandstra, P.W. and Wrana, J.L. TAZ controls Smad nucleocytoplasmic shuttling and regulates human embryonic stem-cell self-renewal. *Nature cell biology* 2008; 10(7): 837.

Vardouli, L., Moustakas, A. and Stournaras, C. LIM-kinase 2 and cofilin phosphorylation mediate actin cytoskeleton reorganization induced by transforming growth factor-β. *Journal of Biological Chemistr 2005;* 280(12): 11448-11457.

Vartio, T., Laitinen, L., Narvanen, O., Cutolo, M., Thornell, L.E., Zardi, L. and Virtanen, I. Differential expression of the ED sequence-containing form of cellular fibronectin in embryonic and adult human tissues. *Journal of cell science* 1987; 88(4) 419-430.

Vaughan, M.B, Howard, E.W., Tomasek, J.J. Transforming growth factor-beta1 promotes the morphological and functional differentiation of the myofibroblast. *Exp Cell Res* 2000; 257:180–9.

Vermeulen, L., Felipe De Sousa, E.M., Van Der Heijden, M., Cameron, K., De Jong, J.H., Borovski, T., Tuynman, J.B., Todaro, M., Merz, C., Rodermond, H. and Sprick, M.R. Wnt activity defines colon cancer stem cells and is regulated by the microenvironment. *Nature cell biology* 2010; 12(5): 468.

Vlachos, I.S., Zagganas, K., Paraskevopoulou, M.D., Georgakilas, G., Karagkouni, D., Vergoulis, T., Dalamagas, T. and Hatzigeorgiou, A.G., 2015. DIANA-miRPath v3. 0: deciphering microRNA function with experimental support. *Nucleic acids research*, *43*(W1), pp. W460-W466.

Vlodavsky, I., Miao, H.Q., Medalion, B., Danagher, P. and Ron, D. Involvement of heparan sulfate and related molecules in sequestration and growth promoting activity of fibroblast growth factor. *Cancer and Metastasis Reviews* 1996; 15(2): 177-186.

Volinia, S., Calin, G.A., Liu, C.G., Ambs, S., Cimmino, A., Petrocca, F., Visone, R., Iorio, M., Roldo, C., Ferracin, M. and Prueitt, R.L. A microRNA expression signature of human solid tumors defines cancer gene targets. *Proceedings of the National academy of Sciences of the United States of America* 2006; 103(7): 62257-2261.

Wahlestedt, C., Salmi, P., Good, L., Kela, J., Johnsson, T., Hökfelt, T., Broberger, C., Porreca, F., Lai, J., Ren, K. and Ossipov, M. Potent and nontoxic antisense oligonucleotides containing locked nucleic acids. *Proceedings of the National Academy of Sciences* 2000; 97(10): 5633-5638.

Waldrip, W.R., Bikoff, E.K., Hoodless, P.A., Wrana, J.L. and Robertson, E.J. Smad2 signaling in extraembryonic tissues determines anterior-posterior polarity of the early mouse embryo. *Cell* 1998; 92(6): 797-808.

Walker, G.A., Masters, K.S., Shah, D.N., Anseth, K.S. and Leinwand, L.A. Valvular myofibroblast activation by transforming growth factor-β. *Circulation research* 2004; *95*(3): 253-260.

Walter, K., Omura, N., Hong, S.M., Griffith, M. and Goggins, M. Pancreatic cancer associated fibroblasts display normal allelotypes. *Cancer biology & therapy* 2008; 7(6): 882-888.

Wang, B., Hsu, S.H., Majumder, S., Kutay, H., Huang, W., Jacob, S.T. and Ghoshal, K. TGFβ mediated upregulation of hepatic miR-181b promotes hepatocarcinogenesis by targeting TIMP3. *Oncogene* 2010; 29(12): 1787.

Wang, B., Li, W., Guo, K., Xiao, Y., Wang, Y. and Fan, J. miR-181b promotes hepatic stellate cells proliferation by targeting p27 and is elevated in the serum of cirrhosis patients. *Biochemical and biophysical research communications* 2012; 421(1): 4-8.

Wang, F., Wang, J., Yang, X., Chen, D. and Wang, L. MiR-424-5p participates in esophageal squamous cell carcinoma invasion and metastasis via SMAD7 pathway mediated EMT. *Diagnostic pathology* 2016; 11(1): 88.

Wang, F., Zhao, X.Q., Liu, J.N., Wang, Z.H., Wang, X.L., Hou, X.Y., Liu, R., Gao, F., Zhang, M.X., Zhang, Y. and Bu, P.L. Antagonist of microRNA-21 improves balloon injury-induced rat iliac artery remodeling by regulating proliferation and

apoptosis of adventitial fibroblasts and myofibroblasts. *Journal of cellular biochemistry* 2012; 113(9): 2989-3001.

Wang, F.E., Zhang, C., Maminishkis, A., Dong, L., Zhi, C., Li, R., Zhao, J., Majerciak, V., Gaur, A.B., Chen, S. and Miller, S.S. MicroRNA-204/211 alters epithelial physiology. *The FASEB Journal* 2010; 24(5): 1552-1571.

Wang, Q., Tang, H., Yin, S. and Dong, C. Downregulation of microRNA-138 enhances the proliferation, migration and invasion of cholangiocarcinoma cells through the upregulation of RhoC/p-ERK/MMP-2/MMP-9. *Oncology reports* 2013; 29(5): 2046-2052.

Wang, Q., Wang, Y., Minto, A.W., Wang, J., Shi, Q., Li, X., Quigg, R.J. MicroRNA-377 is up-regulated and can lead to increased fibronectin production in diabetic nephropathy. *FASEB J* 2008; 22:4126–4135.

Wang, X.H., Qian, R.Z., Zhang, W., Chen, S.F., Jin, H.M. and Hu, R.M. MicroRNA-320 expression in myocardial microvascular endothelial cells and its relationship with insulin-like growth factor-1 in type 2 diabetic rats. *Clinical and Experimental Pharmacology and Physiology* 2009; 36(2): 181-188.

Wang, Y.S., Li, S.H., Guo, J., Mihic, A., Wu, J., Sun, L., Davis, K., Weisel, R.D. and Li, R.K. Role of miR-145 in cardiac myofibroblast differentiation. *Journal of molecular and cellular cardiology* 2014; *66*: 94-105.

Watts, K.L., Cottrell, E., Hoban, P.R. and Spiteri, M.A. RhoA signaling modulates cyclin D1 expression in human lung fibroblasts; implications for idiopathic pulmonary fibrosis. *Respiratory research* 2006; 7(1): 88.

Weber, F., Shen, L., Fukino, K., Patocs, A., Mutter, G.L., Caldes, T. and Eng, C. Total-genome analysis of BRCA1/2-related invasive carcinomas of the breast identifies tumor stroma as potential landscaper for neoplastic initiation. *The American Journal of Human Genetics* 2006; 78(6): 961-972.

Wijelath, E.S., Rahman, S., Namekata, M., Murray, J., Nishimura, T., Mostafavi-Pour, Z., Patel, Y., Suda, Y., Humphries, M.J. and Sobel, M. Heparin-II domain of fibronectin is a vascular endothelial growth factor-binding domain. *Circulation research* 2006; 99(8): 853-860.

Wikström, P., Stattin, P., Franck-Lissbrant, I., Damber, J.E. and Bergh, A. Transforming growth factor β1 is associated with angiogenesis, metastasis, and poor clinical outcome in prostate cancer. *The Prostate* 1998; 37(1): 9-29.

Witte, M.B. and Barbul, A. General principles of wound healing. *Surgical Clinics of North America* 1997; 77(3): 509-528.

White, N.M.A., Khella, H.W.Z., Grigull, J., Adzovic, S., Youssef, Y.M., Honey, R.J., Stewart, R., Pace, K.T., Bjarnason, G.A., Jewett, M.A.S. and Evans, A.J. miRNA profiling in metastatic renal cell carcinoma reveals a tumour-suppressor effect for miR-215. *British journal of cancer* 2011; 105(11): 1741.

Woodcock-Mitchell, J., Mitchell, J.J., Low, R.B., Kieny, M., Sengel, P., Rubbia, L., Skalli, O., Jackson, B. and Gabbiani, G. α-Smooth muscle actin is transiently expressed in embryonic rat cardiac and skeletal muscles. *Differentiation* 1988; 39(3): 161-166.

Wu, K., Hu, G., He, X., Zhou, P., Li, J., He, B. and Sun, W. MicroRNA-424-5p suppresses the expression of SOCS6 in pancreatic cancer. *Pathology & Oncology Research* 2013; 19(4): 739-748.

Xia, H., Cheung, W.K., Ng, S.S., Jiang, X., Jiang, S., Sze, J., Leung, G.K., Lu, G., Chan, D.T., Bian, X.W. and Kung, H.F. Loss of brain-enriched miR-124 microRNA enhances stem-like traits and invasiveness of glioma cells. *Journal of Biological Chemistry* 2012; 287(13): 9962-9971.

Xiao, X., Huang, C., Zhao, C., Gou, X., Senavirathna, L.K., Hinsdale, M., Lloyd, P. and Liu, L. Regulation of myofibroblast differentiation by miR-424 during epithelial-to-mesenchymal transition. *Archives of biochemistry and biophysics* 2015; 566: 49-57.

Xing, F., Saidou, J. and Watabe, K. Cancer associated fibroblasts (CAFs) in tumor microenvironment. *Frontiers in bioscience: a journal and virtual library* 2010; 15: 166.

Xu, G., Redard, M., Gabbiani, G. and Neuville, P. Cellular retinol-binding protein-1 is transiently expressed in granulation tissue fibroblasts and differentially expressed in fibroblasts cultured from different organs. *The American journal of pathology* 1997; 151(6): 1741.

Xu, J., Li, Y., Wang, F., Wang, X., Cheng, B., Ye, F., Xie, X., Zhou, C. and Lu, W. Suppressed miR-424 expression via upregulation of target gene Chk1 contributes to the progression of cervical cancer. *Oncogene* 2013; 32(8): 976.

Xu, N., Papagiannakopoulos, T., Pan, G., Thomson, J.A. and Kosik, K.S. MicroRNA-145 regulates OCT4, SOX2, and KLF4 and represses pluripotency in human embryonic stem cells. *Cell* 2009; 137(4): 647-658.

Yagi, K., Goto, D., Hamamoto, T., Takenoshita, S., Kato, M. and Miyazono, K. Alternatively Spliced Variant of Smad2 Lacking Exon 3 comparison with wild-type Smad2 and Smad3. *Journal of Biological Chemistry* 1999; *274*(2): 703-709.

Yanaihara, N., Caplen, N., Bowman, E., Seike, M., Kumamoto, K., Yi, M., Stephens, R.M., Okamoto, A., Yokota, J., Tanaka, T. and Calin, G.A. Unique microRNA molecular profiles in lung cancer diagnosis and prognosis. *Cancer cell* 2006; 9(3): 189-198.

Yang, F., Tuxhorn, J.A., Ressler, S.J., McAlhany, S.J., Dang, T.D. and Rowley, D.R. Stromal expression of connective tissue growth factor promotes angiogenesis and prostate cancer tumorigenesis. *Cancer research* 2005; 65(19): 8887-8895.

Yang, M., Chen, J., Su, F., Yu, B., Su, F., Lin, L., Liu, Y., Huang, J.D. and Song, E. Microvesicles secreted by macrophages shuttle invasion-potentiating microRNAs into breast cancer cells. *Molecular cancer* 2011; 10(1): 117.

Yang, S., Cui, H., Xie, N., Icyuz, M., Banerjee, S., Antony, V.B., Abraham, E., Thannickal, V.J. and Liu, G. miR-145 regulates myofibroblast differentiation and lung fibrosis. *The FASEB Journal* 2013; 27(6): 2382-2391.

Yang, T.H., Thoreson, A.R., Gingery, A., Larson, D.R., Passe, S.M., An, K.N., Zhao, C. and Amadio, P.C. Collagen gel contraction as a measure of fibroblast function in an animal model of subsynovial connective tissue fibrosis. *Journal of Orthopaedic Research* 2015; 33(5): 668-674.

Yang, T.S., Yang, X.H., Chen, X., Wang, X.D., Hua, J., Zhou, D.L., Zhou, B. and Song, Z.S. MicroRNA-106b in cancer-associated fibroblasts from gastric cancer promotes cell migration and invasion by targeting PTEN. *FEBS letters* 2014; 588(13): 2162-2169.

Yao, Q., Cao, S., Li, C., Mengesha, A., Kong, B. and Wei, M. Micro-RNA-21 regulates TGF-β-induced myofibroblast differentiation by targeting PDCD4 in tumor-stroma interaction. *International journal of cancer* 2011; 128(8): 1783-1792.

Yin, J..J, Selander, K., Chirgwin, J.M, et al. TGF-beta signaling blockade inhibits PTHrP secretion by breast cancer cells and bone metastases development. *J Clin Invest* 1999;103: 197–206.

Ying, S.X., Hussain, Z.J. and Zhang, Y.E. Smurf1 facilitates myogenic differentiation and antagonizes the bone morphogenetic protein-2-induced osteoblast conversion by targeting Smad5 for degradation. *Journal of Biological Chemistry* 2003; 278(40): 39029-39036.

Yoo, B.H., Bochkareva, E., Bochkarev, A., Mou, T.C. and Gray, D.M. 2′-O-methyl-modified phosphorothioate antisense oligonucleotides have reduced non-specific effects in vitro. *Nucleic acids research* 2004; 32(6): 2008-2016.

Yuan, G.C., Cai, L., Elowitz, M., Enver, T., Fan, G., Guo, G., Irizarry, R., Kharchenko, P., Kim, J., Orkin, S. and Quackenbush, J. Challenges and emerging directions in single-cell analysis. *Genome biology* 2017; *18*(1): 84.

Zahran, F., Ghalwash, D., Shaker, O., Al-Johani, K. and Scully, C. Salivary microRNAs in oral cancer. *Oral diseases* 2015; 21(6): 739-747.

Zeisberg, E.M., Potenta, S., Xie, L., Zeisberg, M., and Kalluri, R. Discovery of endothelial to mesenchymal transition as a source for carcinoma associated fibroblasts. *Cancer Res* 2007; 67: 10123-10128.

Zeng, L., Carter, A.D. and Childs, S.J. miR-145 directs intestinal maturation in zebrafish. *Proceedings of the National Academy of Sciences* 2009; 106(42): 17793-17798.

Zhang, C. MicroRNA-145 in vascular smooth muscle cell biology: a new therapeutic target for vascular disease. *Cell Cycle* 2009; 8(21): 3469-3473.

Zhang, D., Wang, Y., Shi, Z., Liu, J., Sun, P., Hou, X., Zhang, J., Zhao, S., Zhou, B.P. and Mi, J. Metabolic reprogramming of cancer-associated fibroblasts by IDH3α downregulation. *Cell reports* 2015; 10(8): 1335-1348.

Zhang, H.F., Xu, L.Y. and Li, E.M. A family of pleiotropically acting microRNAs in cancer progression, miR-200: potential cancer therapeutic targets. *Current pharmaceutical design* 2014; 20 (11): 1896-1903.

Zhang, H.H., Wang, X.J., Li, G.X., Yang, E. and Yang, N.M. Detection of let-7a microRNA by real-time PCR in gastric carcinoma. *World journal of gastroenterology: WJG* 2007; *13*(20): 2883.

Zhang, J., Fan, G., Zhao, H., Wang, Z., Li, F., Zhang, P., Zhang, J., Wang, X. and Wang, W. Targeted inhibition of focal adhesion kinase attenuates cardiac fibrosis and preserves heart function in adverse cardiac remodeling. *Scientific Reports* 2017; *7*.

Zhang, Y., Li, T., Guo, P., Kang, J., Wei, Q., Jia, X., Zhao, W., Huai, W., Qiu, Y., Sun, L. and Han, L. MiR-424-5p reversed epithelial-mesenchymal transition of

anchorage-independent HCC cells by directly targeting ICAT and suppressed HCC progression. *Scientific reports* 2014; 4.

Zhang, Y., Wang, Z. and Gemeinhart, R.A. Progress in microRNA delivery. *Journal of Controlled Release* 2013; 172(3): 962-974.

Zhang, Y.E. Non-smad signaling pathways of the TGF-β family. *Cold Spring Harbor perspectives in biology* 2017; 9(2): 022129.

Zhang, Z., Sun, H., Dai, H., Walsh, R., Imakura, M., Schelter, J., Burchard, J., Dai, X., Chang, A.N., Diaz, R.L. and Marszalek, J.R. MicroRNA miR-210 modulates cellular response to hypoxia through the MYC antagonist MNT. *Cell cycle* 2009; *8*(17): 2756-2768.

Zhang, Z., Zhang, B., Li, W., Fu, L., Fu, L., Zhu, Z. and Dong, J.T. Epigenetic silencing of miR-203 upregulates SNAI2 and contributes to the invasiveness of malignant breast cancer cells. *Genes & cancer* 2011; 2(8): 782-791.

Zhao, J., Shi, W., Wang, Y.L., Chen, H., Bringas, P., Datto, M.B., Frederick, J.P., Wang, X.F. and Warburton, D. Smad3 deficiency attenuates bleomycin-induced pulmonary fibrosis in mice. *American Journal of Physiology-Lung Cellular and Molecular Physiology* 2002; 282(3): 585-593.

Zhao, L., Sun, Y., Hou, Y., Peng, Q., Wang, L., Luo, H., Tang, X., Zeng, Z & Liu, M. MiRNA expression analysis of cancer-associated fibroblasts and normal fibroblasts in breast cancer. *Int J Biochem Cell Biol* 2012; 44: 2051-2059.

Zhong, H., Wang, H.R., Yang, S., Zhong, J.H., Wang, T., Wang, C. and Chen, F.Y. Targeting Smad4 links microRNA-146a to the TGF-β pathway during retinoid acid induction in acute promyelocytic leukemia cell line. *International journal of hematology* 2010; 92(1): 129-135.

Zhou, B.B., Fridman, J.S., Liu, X., Friedman, S.M., Newton, R.C, Scherle, P.A. ADAM proteases, ErbB pathways and cancer. *Expert Opin Investig Drugs* 2005; 14:591-606.

Zhou, Y., Deng, L., Zhao, D., Chen, L., Yao, Z., Guo, X., Liu, X., Lv, L., Leng, B., Xu, W. and Qiao, G. MicroRNA-503 promotes angiotensin II-induced cardiac fibrosis by targeting Apelin-13. *Journal of cellular and molecular medicine* 2016; 20(3): 495-505.

Zhu, Y., Richardson, J.A., Parada, L.F. and Graff, J.M. Smad3 mutant mice develop metastatic colorectal cancer. *Cell* 1998; 94(6): 703-714.

Zou, C., Xu, Q., Mao, F., Li, D., Bian, C., Liu, L.Z., Jiang, Y., Chen, X., Qi, Y., Zhang, X. and Wang, X. MiR-145 inhibits tumor angiogenesis and growth by N-RAS and VEGF. *Cell Cycle* 2012; 11(11): 2137-2145.

APPENDICES

Appendix 1: miRNAs were differentially expressed in TGF-β1-treated NOF5 and NOF804, compared to unstimulated cells

	NOF5		
	POOL A		POOL B
miRNA	Fold change relative to endogenous control	miRNA	Fold change relative to endogenous control
ath-miR159a-4373390	23.5205	ath-miR159a-000338	693379.4241
has-miR-155-4395459	39.3471	dme-miR-7-000268	1355.7923
hsa-let-7a-4373169	0.8503	hsa-let-7a#-002307	767.943
hsa-let-7b-4395446	13.9199	hsa-let-7b#-002404	556.2827
hsa-let-7c-4373167	7.9977	hsa-let-7c#-002405	412.044
hsa-let-7d-4395394	3.1351	hsa-let-7e#-002407	286.1412
hsa-let-7e-4395517	11.1247	hsa-let-7f-1#-002417	270.8893
hsa-let-7f-4373164	0.8015	hsa-let-7f-2#-002418	166.4621
hsa-let-7g-4395393	3.672	hsa-let-7g#-002118	151.9676
hsa-miR-100-4373160	9.6295	hsa-let-7i#-002172	149.7065
hsa-miR-101-4395364	4.8569	hsa-miR-100#-002142	139.7136
hsa-miR-103-4373158	10.0458	hsa-miR-101#-002143	133.549
hsa-miR-105-4395278	23.5205	hsa-miR-105#-002168	122.1013
hsa-miR-106a-4395280	8.5705	hsa-miR-106a#-002170	121.1873
hsa-miR-106b-4373155	42.3921	hsa-miR-106b#-002380	118.8496
hsa-miR-107-4373154	51.3527	hsa-miR-10a#-002288	108.9179
hsa-miR-10a-4373153	40.3904	hsa-miR-10b#-002315	105.6101
hsa-miR-10b-4395329	23.5205	hsa-miR-1178-002777	102.0158
hsa-miR-122-4395356	47.5434	hsa-miR-1179-002776	99.5907
hsa-miR-124-4373295	190.9864	hsa-miR-1180-002847	98.5417
hsa-miR-125a-3p-4395310	30.3056	hsa-miR-1182-002830	80.0651
hsa-miR-125a-5p-4395309	18.7463	hsa-miR-1183-002841	64.6361

hsa-miR-125b-4373148	18.4361	hsa-miR-1184-002842	59.5174
hsa-miR-126-4395339	0.9604	hsa-miR-1197-002810	58.781
hsa-miR-127-3p-4373147	12.5434	hsa-miR-1200-002829	55.6967
hsa-miR-127-5p-4395340	0.2717	hsa-miR-1201-002781	51.9416
hsa-miR-128-4395327	17.9875	hsa-miR-1203-002877	48.4198
hsa-miR-129-3p-4373297	4.3416	hsa-miR-1204-002872	47.5712
hsa-miR-129-5p-4373171	23.5205	hsa-miR-1205-002778	40.4702
hsa-miR-130a-4373145	10.1969	hsa-miR-1206-002878	37.9526
hsa-miR-130b-4373144	12.5966	hsa-miR-1208-002880	33.418
hsa-miR-132-4373143	1.1433	hsa-miR-122#-002130	29.7438
hsa-miR-133a-4395357	23.5205	hsa-miR-1224-3P-002752	29.4284
hsa-miR-133b-4395358	23.5205	hsa-miR-1225-3P-002766	28.731
hsa-miR-134-4373299	14.5511	hsa-miR-1226#-002758	26.8033
hsa-miR-135a-4373140	23.5205	hsa-miR-1227-002769	25.0383
hsa-miR-135b-4395372	23.5205	hsa-miR-1228#-002763	24.2924
hsa-miR-136-4373173	23.5205	hsa-miR-1233-002768	24.2065
hsa-miR-137-4373301	8.8141	hsa-miR-1236-002761	23.4883
hsa-miR-138-4395395	4.1264	hsa-miR-1238-002927	23.359
hsa-miR-139-3p-4395424	23.5205	hsa-miR-124#-002197	23.1468
hsa-miR-139-5p-4395400	23.5205	hsa-miR-1243-002854	21.8261
hsa-miR-140-3p-4395345	23.5205	hsa-miR-1244-002791	21.7244
hsa-miR-140-5p-4373374	6.6558	hsa-miR-1245-002823	21.5804
hsa-miR-141-4373137	23.5205	hsa-miR-1247-002893	21.4227
hsa-miR-142-3p-4373136	23.5205	hsa-miR-1248-002870	18.818
hsa-miR-142-5p-4395359	23.5205	hsa-miR-1249-002868	17.5877
hsa-miR-143-4395360	11.8463	hsa-miR-1250-002887	17.5877
hsa-miR-1-4395333	4.6237	hsa-miR-1251-002820	17.5877

hsa-miR-145-4395389	15.882	hsa-miR-1252-002860	17.5877
hsa-miR-146a-4373132	3.4807	hsa-miR-1253-002894	17.5877
hsa-miR-146b-3p-4395472	23.5205	hsa-miR-1254-002818	17.5877
hsa-miR-146b-5p-4373178	4.7002	hsa-miR-1255A-002805	17.5877
hsa-miR-147-4373131	80.0484	hsa-miR-1255B-002801	17.5877
hsa-miR-147b-4395373	0.9086	hsa-miR-1256-002850	17.5877
hsa-miR-148a-4373130	7.6001	hsa-miR-1257-002910	17.5877
hsa-miR-148b-4373129	23.5205	hsa-miR-1259-002796	17.5877
hsa-miR-149-4395366	2.6512	hsa-miR-125b-1#-002378	17.5877
hsa-miR-150-4373127	5.4383	hsa-miR-125b-2#-002158	17.5877
hsa-miR-152-4395170	7.4918	hsa-miR-126#-000451	17.5877
hsa-miR-153-4373305	0.4288	hsa-miR-1260-002896	17.5877
hsa-miR-154-4373270	23.5205	hsa-miR-1262-002852	17.5877
hsa-miR-15a-4373123	21.6382	hsa-miR-1263-002784	17.5877
hsa-miR-15b-4373122	6.0544	hsa-miR-1264-002799	17.5877
hsa-miR-16-4373121	3.7566	hsa-miR-1265-002790	17.5877
hsa-miR-17-4395419	7.6342	hsa-miR-1267-002885	17.5877
hsa-miR-181a-4373117	9.1514	hsa-miR-1269-002789	17.5877
hsa-miR-181c-4373115	23.5205	hsa-miR-1270-002807	17.5877
hsa-miR-182-4395445	23.5205	hsa-miR-1271-002779	17.5877
hsa-miR-183-4395380	23.5205	hsa-miR-1272-002845	17.5877
hsa-miR-184-4373113	23.5205	hsa-miR-1274A-002883	17.5877
hsa-miR-185-4395382	12.071	hsa-miR-1274B-002884	17.5877
hsa-miR-186-4395396	122.5838	hsa-miR-1275-002840	17.5877
hsa-miR-187-4373307	23.5205	hsa-miR-1276-002843	17.5877
hsa-miR-188-3p-4395217	23.5205	hsa-miR-1278-002851	17.5877
hsa-miR-18a-4395533	4.4586	hsa-miR-1282-002803	17.5877

hsa-miR-18b-4395328	8.1728	hsa-miR-1283-002890	17.5877
hsa-miR-190-4373110	23.5205	hsa-miR-1284-002903	17.5877
hsa-miR-191-4395410	4.9801	hsa-miR-1285-002822	17.5877
hsa-miR-192-4373108	185.8343	hsa-miR-1286-002773	17.5877
hsa-miR-193a-3p-4395361	2.7188	hsa-miR-1288-002832	17.5877
hsa-miR-193a-5p-4395392	15.4677	hsa-miR-1289-002871	17.5877
hsa-miR-193b-4395478	7.3966	hsa-miR-129#-002298	17.5877
hsa-miR-194-4373106	121.7636	hsa-miR-1290-002863	17.5877
hsa-miR-195-4373105	0.7559	hsa-miR-1291-002838	17.5877
hsa-miR-196b-4395326	23.5205	hsa-miR-1292-002824	17.5877
hsa-miR-197-4373102	15.1103	hsa-miR-1293-002905	17.5877
hsa-miR-198-4395384	247.8456	hsa-miR-1294-002785	17.5877
hsa-miR-199a-3p-4395415	4.3626	hsa-miR-1296-002908	17.5877
hsa-miR-199a-5p-4373272	46.254	hsa-miR-1298-002861	17.5877
hsa-miR-199b-5p-4373100	19.5191	hsa-miR-1300-002902	17.5877
hsa-miR-19a-4373099	7.2889	hsa-miR-1301-002827	17.5877
hsa-miR-19b-4373098	8.1775	hsa-miR-1302-002901	17.5877
hsa-miR-200a-4378069	23.5205	hsa-miR-1303-002792	17.5877
hsa-miR-200b-4395362	14.1055	hsa-miR-1304-002874	17.5877
hsa-miR-200c-4395411	206.7585	hsa-miR-1305-002867	17.5877
hsa-miR-202-4395474	148.5199	hsa-miR-130a#-002131	17.5877
hsa-miR-203-4373095	13.9715	hsa-miR-130b#-002114	17.5877
hsa-miR-204-4373094	1.44	hsa-miR-132#-002132	17.5877
hsa-miR-205-4373093	23.5205	hsa-miR-1324-002815	17.5877
hsa-miR-208-4373091	23.5205	hsa-miR-135b#-002159	17.5877
hsa-miR-208b-4395401	23.5205	hsa-miR-136#-002100	17.5877
hsa-miR-20a-4373286	5.418	hsa-miR-138-2#-002144	17.5877

hsa-miR-20b-4373263	8.4131	hsa-miR-141#-002145	17.5877
hsa-miR-210-4373089	6.3306	hsa-miR-143#-002146	17.5877
hsa-miR-211-4373088	23.5205	hsa-miR-144#-002148	17.5877
hsa-miR-212-4373087	5.4215	hsa-miR-144-002676	17.5877
hsa-miR-21-4373090	14.67	hsa-miR-145#-002149	17.5877
hsa-miR-214-4395417	12.8408	hsa-miR-146a#-002163	17.5877
hsa-miR-215-4373084	23.5205	hsa-miR-148a#-002134	17.5877
hsa-miR-216a-4395331	23.5205	hsa-miR-148b#-002160	17.5877
hsa-miR-216b-4395437	23.5205	hsa-miR-149#-002164	17.5877
hsa-miR-217-4395448	23.5205	hsa-miR-151-3p-002254	17.5877
hsa-miR-218-4373081	2.2986	hsa-miR-151-5P-002642	17.5877
hsa-miR-219-1-3p-4395206	23.5205	hsa-miR-154#-000478	17.5877
hsa-miR-219-2-3p-4395501	23.5205	hsa-miR-155#-002287	17.5877
hsa-miR-219-5p-4373080	23.5205	hsa-miR-15a#-002419	17.5877
hsa-miR-220-4373078	23.5205	hsa-miR-15b#-002173	17.5877
hsa-miR-220b-4395317	23.5205	hsa-miR-16-1#-002420	17.5877
hsa-miR-220c-4395322	23.5205	hsa-miR-16-2#-002171	17.5877
hsa-miR-221-4373077	6.8815	hsa-miR-17#-002421	17.5877
hsa-miR-222-4395387	4.8118	hsa-miR-181a-2#-002317	17.5877
hsa-miR-223-4395406	1.0642	hsa-miR-181c#-002333	17.5877
hsa-miR-22-4373079	4.6465	hsa-miR-182#-000483	17.5877
hsa-miR-224-4395210	8.7645	hsa-miR-1825-002907	17.5877
hsa-miR-23a-4373074	18.9632	hsa-miR-1826-002873	17.5877
hsa-miR-23b-4373073	5.5586	hsa-miR-183#-002270	17.5877
hsa-miR-24-4373072	4.0199	hsa-miR-185#-002104	17.5877
hsa-miR-25-4373071	15.2134	hsa-miR-186#-002105	17.5877
hsa-miR-26a-4395166	3.1261	hsa-miR-18a#-002423	17.5877

hsa-miR-26b-4395167	3.0542	hsa-miR-18b#-002310	17.5877
hsa-miR-27a-4373287	12.2575	hsa-miR-190b-002263	17.5877
hsa-miR-27b-4373068	16.2697	hsa-miR-191#-002678	17.5877
hsa-miR-28-3p-4395557	5.4701	hsa-miR-192#-002272	17.5877
hsa-miR-28-5p-4373067	9.3106	hsa-miR-193b#-002366	17.5877
hsa-miR-296-3p-4395212	23.5205	hsa-miR-194#-002379	17.5877
hsa-miR-296-5p-4373066	6.238	hsa-miR-195#-002107	17.5877
hsa-miR-298-4395301	23.5205	hsa-miR-196a#-002336	17.5877
hsa-miR-299-3p-4373189	68.7081	hsa-miR-19a#-002424	17.5877
hsa-miR-299-5p-4373188	23.5205	hsa-miR-19b-1#-002425	17.5877
hsa-miR-29a-4395223	4.1143	hsa-miR-200a#-001011	17.5877
hsa-miR-29b-4373288	7.5818	hsa-miR-200b#-002274	17.5877
hsa-miR-29c-4395171	24.8781	hsa-miR-200c#-002286	17.5877
hsa-miR-301a-4373064	9.8173	hsa-miR-202#-002362	17.5877
hsa-miR-301b-4395503	8.7546	hsa-miR-206-000510	17.5877
hsa-miR-302a-4378070	38.7632	hsa-miR-20a#-002437	17.5877
hsa-miR-302b-4378071	23.5205	hsa-miR-20b#-002311	17.5877
hsa-miR-302c-4378072	35.131	hsa-miR-21#-002438	17.5877
hsa-miR-30b-4373290	1.9462	hsa-miR-213-000516	17.5877
hsa-miR-30c-4373060	1.624	hsa-miR-214#-002293	17.5877
hsa-miR-31-4395390	6.3657	hsa-miR-218-1#-002094	17.5877
hsa-miR-320-4395388	9.0689	hsa-miR-218-2#-002294	17.5877
hsa-miR-323-3p-4395338	1.6552	hsa-miR-22#-002301	17.5877
hsa-miR-32-4395220	11.4333	hsa-miR-221#-002096	17.5877
hsa-miR-324-3p-4395272	16.3936	hsa-miR-222#-002097	17.5877
hsa-miR-324-5p-4373052	28.1596	hsa-miR-223#-002098	17.5877
hsa-miR-325-4373051	23.5205	hsa-miR-23a#-002439	17.5877

hsa-miR-326-4373050	23.5205	hsa-miR-23b#-002126	17.5877
hsa-miR-328-4373049	4.0228	hsa-miR-24-1#-002440	17.5877
hsa-miR-329-4373191	23.5205	hsa-miR-24-2#-002441	17.5877
hsa-miR-330-3p-4373047	46.239	hsa-miR-25#-002442	17.5877
hsa-miR-330-5p-4395341	36.2309	hsa-miR-26a-1#-002443	17.5877
hsa-miR-331-3p-4373046	0.3498	hsa-miR-26a-2#-002115	17.5877
hsa-miR-331-5p-4395344	23.5205	hsa-miR-26b#-002444	17.5877
hsa-miR-335-4373045	7.634	hsa-miR-27a#-002445	17.5877
hsa-miR-337-5p-4395267	5.467	hsa-miR-27b#-002174	17.5877
hsa-miR-338-3p-4395363	23.5205	hsa-miR-29a#-002447	17.5877
hsa-miR-339-3p-4395295	16.8844	hsa-miR-29b-1#-002165	17.5877
hsa-miR-339-5p-4395368	17.9011	hsa-miR-29b-2#-002166	17.5877
hsa-miR-33b-4395196	0.0394	hsa-miR-302a#-002381	17.5877
hsa-miR-340-4395369	19.3061	hsa-miR-302b#-002119	17.5877
hsa-miR-342-3p-4395371	0.1507	hsa-miR-302c#-000534	17.5877
hsa-miR-342-5p-4395258	23.5205	hsa-miR-302d#-002120	17.5877
hsa-miR-345-4395297	5.256	hsa-miR-302d-000535	17.5877
hsa-miR-346-4373038	23.5205	hsa-miR-30a-3p-000416	17.5877
hsa-miR-34a-4395168	11.4531	hsa-miR-30a-5p-000417	17.5877
hsa-miR-34c-5p-4373036	7.9793	hsa-miR-30b#-002129	17.5877
hsa-miR-361-5p-4373035	47.7995	hsa-miR-30c-1#-002108	17.5877
hsa-miR-362-3p-4395228	23.5205	hsa-miR-30c-2#-002110	17.5877
hsa-miR-362-5p-4378092	4.1255	hsa-miR-30d#-002305	17.5877
hsa-miR-363-4378090	61.2089	hsa-miR-30d-000420	17.5877
hsa-miR-365-4373194	2.508	hsa-miR-30e-3p-000422	17.5877
hsa-miR-367-4373034	562.7276	hsa-miR-31#-002113	17.5877
hsa-miR-369-3p-4373032	23.5205	hsa-miR-32#-002111	17.5877

hsa-miR-369-5p-4373195	23.5205	hsa-miR-320B-002844	17.5877
hsa-miR-370-4395386	10.0491	hsa-miR-335#-002185	17.5877
hsa-miR-371-3p-4395235	23.5205	hsa-miR-337-3p-002157	17.5877
hsa-miR-372-4373029	93.103	hsa-miR-338-5P-002658	17.5877
hsa-miR-373-4378073	23.5205	hsa-miR-33a#-002136	17.5877
hsa-miR-374a-4373028	3.0311	hsa-miR-33a-002135	17.5877
hsa-miR-374b-4381045	0.1215	hsa-miR-340#-002259	17.5877
hsa-miR-375-4373027	23.5205	hsa-miR-34a#-002316	17.5877
hsa-miR-376a-4373026	11.2752	hsa-miR-34b-000427	17.5877
hsa-miR-376b-4373196	6.9329	hsa-miR-34b-002102	17.5877
hsa-miR-376c-4395233	4.78	hsa-miR-361-3p-002116	17.5877
hsa-miR-377-4373025	20.4803	hsa-miR-363#-001283	17.5877
hsa-miR-379-4373349	8.0854	hsa-miR-367#-002121	17.5877
hsa-miR-380-4373022	23.5205	hsa-miR-374a#-002125	17.5877
hsa-miR-381-4373020	169.2748	hsa-miR-374b#-002391	17.5877
hsa-miR-382-4373019	7.8411	hsa-miR-376a#-002127	17.5877
hsa-miR-383-4373018	1.2196	hsa-miR-377#-002128	17.5877
hsa-miR-384-4373017	23.5205	hsa-miR-378-000567	17.5877
hsa-miR-409-5p-4395442	44.4965	hsa-miR-378-002243	17.5877
hsa-miR-410-4378093	5.0206	hsa-miR-380-5p-000570	17.5877
hsa-miR-411-4381013	5.3804	hsa-miR-409-3p-002332	17.5877
hsa-miR-412-4373199	23.5205	hsa-miR-411#-002238	17.5877
hsa-miR-422a-4395408	102.4424	hsa-miR-424#-002309	17.5877
hsa-miR-423-5p-4395451	24.8356	hsa-miR-425#-002302	17.5877
hsa-miR-424-5p-4373201	158.4425	hsa-miR-431#-002312	17.5877
hsa-miR-425-4380926	7.0499	hsa-miR-432#-001027	17.5877
hsa-miR-429-4373203	23.5205	hsa-miR-432-001026	17.5877

hsa-miR-431-4395173	23.5205	hsa-miR-452#-002330	17.5877
hsa-miR-433-4373205	8.0084	hsa-miR-454#-001996	17.5877
hsa-miR-448-4373206	23.5205	hsa-miR-483-3p-002339	17.5877
hsa-miR-449a-4373207	23.5205	hsa-miR-488-001106	17.5877
hsa-miR-449b-4381011	23.5205	hsa-miR-497#-002368	17.5877
hsa-miR-450a-4395414	9.6866	hsa-miR-497-001043	17.5877
hsa-miR-450b-3p-4395319	1.2294	hsa-miR-500-001046	17.5877
hsa-miR-450b-5p-4395318	23.5205	hsa-miR-505#-002087	17.5877
hsa-miR-451-4373360	23.5205	hsa-miR-513B-002757	17.5877
hsa-miR-452-4395440	30.3581	hsa-miR-513C-002756	17.5877
hsa-miR-453-4395429	23.5205	hsa-miR-516-3p-001149	17.5877
hsa-miR-454-4395434	5.5653	hsa-miR-517#-001113	17.5877
hsa-miR-455-3p-4395355	4.1149	hsa-miR-518c#-001158	17.5877
hsa-miR-455-5p-4378098	14.5077	hsa-miR-518e#-002371	17.5877
hsa-miR-483-5p-4395449	36.766	hsa-miR-518f#-002387	17.5877
hsa-miR-484-4381032	6.2973	hsa-miR-519b-3p-002384	17.5877
hsa-miR-485-3p-4378095	7.0485	hsa-miR-519e#-001166	17.5877
hsa-miR-485-5p-4373212	23.5205	hsa-miR-520c-3p-002400	17.5877
hsa-miR-486-3p-4395204	4.6161	hsa-miR-520D-3P-002743	17.5877
hsa-miR-486-5p-4378096	17.4468	hsa-miR-520h-001170	17.5877
hsa-miR-487a-4378097	46.6	hsa-miR-524-001173	17.5877
hsa-miR-487b-4378102	5.687	hsa-miR-541#-002200	17.5877
hsa-miR-488-4395468	23.5205	hsa-miR-543-002376	17.5877
hsa-miR-489-4395469	500.201	hsa-miR-545#-002266	17.5877
hsa-miR-490-3p-4373215	1.8807	hsa-miR-548E-002881	17.5877
hsa-miR-491-3p-4395471	23.5205	hsa-miR-548G-002879	17.5877
hsa-miR-491-5p-4381053	5.0725	hsa-miR-548H-002816	17.5877

hsa-miR-492-4373217	23.5205	hsa-miR-548I-002909	17.5877
hsa-miR-493-4395475	10.7538	hsa-miR-548J-002783	17.5877
hsa-miR-494-4395476	38.4501	hsa-miR-548K-002819	17.5877
hsa-miR-495-4381078	3.4779	hsa-miR-548L-002904	17.5877
hsa-miR-496-4386771	23.5205	hsa-miR-548M-002775	17.5877
hsa-miR-499-3p-4395538	23.5205	hsa-miR-548N-002888	17.5877
hsa-miR-499-5p-4381047	23.5205	hsa-miR-548P-002798	17.5877
hsa-miR-500-4395539	11.233	hsa-miR-549-001511	17.5877
hsa-miR-501-3p-4395546	23.5205	hsa-miR-550-001544	17.5877
hsa-miR-501-5p-4373226	23.5205	hsa-miR-550-002410	17.5877
hsa-miR-502-3p-4395194	23.5205	hsa-miR-551a-001519	17.5877
hsa-miR-502-5p-4373227	23.5205	hsa-miR-551b#-002346	17.5877
hsa-miR-503-4373228	1.4747	hsa-miR-552-001520	17.5877
hsa-miR-504-4395195	23.5205	hsa-miR-553-001521	17.5877
hsa-miR-505-4395200	11.5745	hsa-miR-554-001522	17.5877
hsa-miR-506-4373231	23.5205	hsa-miR-555-001523	17.5877
hsa-miR-507-4373232	23.5205	hsa-miR-557-001525	17.5877
hsa-miR-508-3p-4373233	23.5205	hsa-miR-558-001526	17.5877
hsa-miR-508-5p-4395203	23.5205	hsa-miR-559-001527	17.5877
hsa-miR-509-3-5p-4395266	23.5205	hsa-miR-562-001529	17.5877
hsa-miR-509-5p-4395346	270.9502	hsa-miR-563-001530	17.5877
hsa-miR-510-4395352	23.5205	hsa-miR-564-001531	17.5877
hsa-miR-511-4373236	23.5205	hsa-miR-566-001533	17.5877
hsa-miR-512-3p-4381034	23.5205	hsa-miR-567-001534	17.5877
hsa-miR-512-5p-4373238	23.5205	hsa-miR-569-001536	17.5877
hsa-miR-513-5p-4395201	23.5205	hsa-miR-571-001613	17.5877
hsa-miR-515-3p-4395480	23.5205	hsa-miR-572-001614	17.5877

hsa-miR-515-5p-4373242	23.5205	hsa-miR-573-001615	17.5877
hsa-miR-516a-5p-4395527	23.5205	hsa-miR-575-001617	17.5877
hsa-miR-516b-4395172	23.5205	hsa-miR-577-002675	17.5877
hsa-miR-517a-4395513	23.5205	hsa-miR-578-001619	17.5877
hsa-miR-517b-4373244	23.5205	hsa-miR-580-001621	17.5877
hsa-miR-517c-4373264	3.5539	hsa-miR-581-001622	17.5877
hsa-miR-518a-3p-4395508	23.5205	hsa-miR-583-001623	17.5877
hsa-miR-518a-5p-4395507	23.5205	hsa-miR-584-001624	17.5877
hsa-miR-518b-4373246	65.5054	hsa-miR-585-001625	17.5877
hsa-miR-518c-4395512	23.5205	hsa-miR-586-001539	17.5877
hsa-miR-518d-3p-4373248	47.8956	hsa-miR-587-001540	17.5877
hsa-miR-518d-5p-4395500	23.5205	hsa-miR-588-001542	17.5877
hsa-miR-518e-4395506	23.5205	hsa-miR-589-001543	17.5877
hsa-miR-518f-4395499	31.8641	hsa-miR-590-3P-002677	17.5877
hsa-miR-519a-4395526	211.2811	hsa-miR-591-001545	17.5877
hsa-miR-519c-3p-4373251	23.5205	hsa-miR-592-001546	17.5877
hsa-miR-519d-4395514	23.5205	hsa-miR-593-001547	17.5877
hsa-miR-519e-4395481	23.5205	hsa-miR-593-002411	17.5877
hsa-miR-520a-3p-4373268	35.2142	hsa-miR-595-001987	17.5877
hsa-miR-520a-5p-4378085	23.5205	hsa-miR-596-001550	17.5877
hsa-miR-520b-4373252	23.5205	hsa-miR-599-001554	17.5877
hsa-miR-520d-5p-4395504	23.5205	hsa-miR-600-001556	17.5877
hsa-miR-520e-4373255	23.5205	hsa-miR-601-001558	17.5877
hsa-miR-520f-4373256	23.5205	hsa-miR-603-001566	17.5877
hsa-miR-520g-4373257	23.5205	hsa-miR-604-001567	17.5877
hsa-miR-521-4373259	1864.6731	hsa-miR-605-001568	17.5877
hsa-miR-522-4395524	23.5205	hsa-miR-606-001569	17.5877

hsa-miR-523-4395497	806.6315	hsa-miR-607-001570	17.5877
hsa-miR-524-5p-4395174	23.5205	hsa-miR-608-001571	17.5877
hsa-miR-525-3p-4395496	23.5205	hsa-miR-609-001573	17.5877
hsa-miR-525-5p-4378088	23.5205	hsa-miR-613-001586	17.5877
hsa-miR-526b-4395493	23.5205	hsa-miR-614-001587	17.5877
hsa-miR-532-3p-4395466	3.4478	hsa-miR-616-001589	17.5877
hsa-miR-532-5p-4380928	3.0169	hsa-miR-617-001591	17.5877
hsa-miR-539-4378103	1.1272	hsa-miR-620-002672	17.5877
hsa-miR-541-4395312	23.5205	hsa-miR-621-001598	17.5877
hsa-miR-542-3p-4378101	307.2191	hsa-miR-622-001553	17.5877
hsa-miR-542-5p-4395351	100.6068	hsa-miR-623-001555	17.5877
hsa-miR-544-4395376	23.5205	hsa-miR-624-001557	17.5877
hsa-miR-545-4395378	23.5205	hsa-miR-625#-002432	17.5877
hsa-miR-548a-3p-4380948	14.2504	hsa-miR-626-001559	17.5877
hsa-miR-548a-5p-4395523	23.5205	hsa-miR-628-3p-002434	17.5877
hsa-miR-548b-3p-4380951	23.5205	hsa-miR-629-001562	16.9567
hsa-miR-548b-5p-4395519	23.5205	hsa-miR-630-001563	16.7116
hsa-miR-548c-3p-4380993	33.458	hsa-miR-631-001564	15.6464
hsa-miR-548c-5p-4395540	23.5205	hsa-miR-633-001574	15.1656
hsa-miR-548d-3p-4381008	23.5205	hsa-miR-634-001576	13.3539
hsa-miR-548d-5p-4395348	29.4464	hsa-miR-635-001578	13.1963
hsa-miR-551b-4380945	23.5205	hsa-miR-637-001581	13.1451
hsa-miR-556-3p-4395456	23.5205	hsa-miR-638-001582	13.0142
hsa-miR-556-5p-4395455	23.5205	hsa-miR-639-001583	12.9851
hsa-miR-561-4380938	5.7754	hsa-miR-640-001584	12.1378
hsa-miR-570-4395458	23.5205	hsa-miR-641-001585	12.0803
hsa-miR-574-3p-4395460	4.3002	hsa-miR-643-001594	11.3221

hsa-miR-576-3p-4395462	7.6028	hsa-miR-644-001596	10.8864
hsa-miR-576-5p-4395461	23.5205	hsa-miR-645-001597	10.7479
hsa-miR-579-4395509	3.8765	hsa-miR-646-001599	10.4608
hsa-miR-582-3p-4395510	23.5205	hsa-miR-647-001600	10.1779
hsa-miR-582-5p-4395175	23.5205	hsa-miR-648-001601	9.9725
hsa-miR-589-4395520	23.5205	hsa-miR-649-001602	9.8514
hsa-miR-590-5p-4395176	4.8888	hsa-miR-650-001603	9.6578
hsa-miR-597-4380960	8.8643	hsa-miR-656-001510	9.3012
hsa-miR-598-4395179	6.9868	hsa-miR-657-001512	8.9936
hsa-miR-615-3p-4386777	23.5205	hsa-miR-658-001513	8.6393
hsa-miR-615-5p-4395464	23.5205	hsa-miR-659-001514	8.3493
hsa-miR-616-4395525	23.5205	hsa-miR-661-001606	8.2315
hsa-miR-618-4380996	36.1117	hsa-miR-662-001607	8.0731
hsa-miR-624-4395541	23.5205	hsa-miR-663B-002857	7.9636
hsa-miR-625-4395542	23.5205	hsa-miR-664-002897	7.2388
hsa-miR-627-4380967	23.5205	hsa-miR-665-002681	6.7298
hsa-miR-628-5p-4395544	31.848	hsa-miR-668-001992	6.1211
hsa-miR-629-4395547	23.5205	hsa-miR-675-002005	6.0426
hsa-miR-636-4395199	21.4634	hsa-miR-7-2#-002314	6.0367
hsa-miR-642-4380995	1.2197	hsa-miR-708#-002342	5.9833
hsa-miR-651-4381007	23.5205	hsa-miR-720-002895	5.7528
hsa-miR-652-4395463	23.5205	hsa-miR-744#-002325	5.5783
hsa-miR-653-4395403	23.5205	hsa-miR-765-002643	5.4235
hsa-miR-654-3p-4395350	23.5205	hsa-miR-766-001986	5.4105
hsa-miR-654-5p-4381014	23.5205	hsa-miR-767-3p-001995	5.4043
hsa-miR-655-4381015	5.9068	hsa-miR-767-5p-001993	5.3756
hsa-miR-660-4380925	6.1259	hsa-miR-769-3p-002003	5.1785

hsa-miR-671-3p-4395433	8.4804	hsa-miR-769-5p-001998	5.0678
hsa-miR-672-4395438	23.5205	hsa-miR-770-5p-002002	4.9669
hsa-miR-674-4395193	23.5205	hsa-miR-802-002004	4.767
hsa-miR-708-4395452	45.8284	hsa-miR-875-5p-002203	4.7057
hsa-miR-744-4395435	16.7737	hsa-miR-888#-002213	4.3947
hsa-miR-758-4395180	6.7678	hsa-miR-892b-002214	4.2836
hsa-miR-871-4395465	0.6495	hsa-miR-9#-002231	4.1696
hsa-miR-872-4395375	23.5205	hsa-miR-920-002150	4.0391
hsa-miR-873-4395467	23.5205	hsa-miR-921-002151	4.0108
hsa-miR-874-4395379	23.5205	hsa-miR-922-002152	3.7473
hsa-miR-875-3p-4395315	23.5205	hsa-miR-924-002154	3.6158
hsa-miR-876-3p-4395336	139.3249	hsa-miR-92a-1#-002137	3.3763
hsa-miR-876-5p-4395316	2.1509	hsa-miR-92a-2#-002138	3.2164
hsa-miR-885-3p-4395483	23.5205	hsa-miR-92b#-002343	3.1413
hsa-miR-885-5p-4395407	13.3061	hsa-miR-93#-002139	3.0077
hsa-miR-886-3p-4395305	93.4103	hsa-miR-933-002176	2.9857
hsa-miR-886-5p-4395304	119.6733	hsa-miR-934-002177	2.7396
hsa-miR-887-4395485	23.5205	hsa-miR-935-002178	2.6577
hsa-miR-888-4395323	0.24	hsa-miR-936-002179	2.5506
hsa-miR-889-4395313	1.8714	hsa-miR-937-002180	2.3409
hsa-miR-890-4395320	23.5205	hsa-miR-938-002181	2.2432
hsa-miR-891a-4395302	23.5205	hsa-miR-939-002182	1.7178
hsa-miR-891b-4395321	23.5205	hsa-miR-941-002183	1.6038
hsa-miR-892a-4395306	23.5205	hsa-miR-942-002187	1.4808
hsa-miR-92a-4395169	9.1218	hsa-miR-943-002188	1.2127
hsa-miR-93-4373302	7.9923	hsa-miR-944-002189	1.1105
hsa-miR-9-4373285	2.8102	hsa-miR-96#-002140	1.0071

hsa-miR-95-4373011	23.5205	hsa-miR-99b#-002196	0.8998
hsa-miR-96-4373372	23.5205	mmu-let-7d#-001178	0.7703
hsa-miR-98-4373009	23.5205	rno-miR-29c#-001818	0.5758
hsa-miR-99a-4373008	8.5819	rno-miR-7#-001338	0.5347

NOF804			
	POOL A		**POOL B**
miRNA	**Fold change relative to endogenous control**	**miRNA**	**Fold change relative to endogenous control**
ath-miR159a-000338	0.6997	ath-miR159a-000338	1.6749
hsa-let-7a-000377	1.5291	dme-miR-7-000268	1.6749
hsa-let-7b-002619	0.8121	hsa-let-7a#-002307	1.6749
hsa-let-7c-000379	0.7327	hsa-let-7b#-002404	1.6749
hsa-let-7d-002283	0.8825	hsa-let-7c#-002405	1.6749
hsa-let-7e-002406	1.3711	hsa-let-7e#-002407	1.6749
hsa-let-7f-000382	1.0097	hsa-let-7f-1#-002417	1.6749
hsa-let-7g-002282	0.7353	hsa-let-7f-2#-002418	1.6749
hsa-miR-100-000437	1.0874	hsa-let-7g#-002118	1.6749
hsa-miR-1-002222	0.6997	hsa-let-7i#-002172	1.6749
hsa-miR-101-002253	2.8332	hsa-miR-100#-002142	1.6749
hsa-miR-103-000439	0.5841	hsa-miR-101#-002143	1.6749
hsa-miR-105-002167	0.6997	hsa-miR-105#-002168	1.6749
hsa-miR-106a-002169	0.7933	hsa-miR-106a#-002170	1.6749
hsa-miR-106b-000442	1.118	hsa-miR-106b#-002380	1.4418
hsa-miR-107-000443	0.6997	hsa-miR-10a#-002288	1.6749
hsa-miR-10a-000387	6.0443	hsa-miR-10b#-002315	1.6749
hsa-miR-10b-002218	0.6997	hsa-miR-1179-002776	1.6749
hsa-miR-122-002245	0.6997	hsa-miR-1180-002847	1.7378
hsa-miR-125a-	1.4514	hsa-miR-1182-	1.6749

3p-002199		002830	
hsa-miR-125a-5p-002198	0.4159	hsa-miR-1183-002841	0.601
hsa-miR-125b-000449	0.6847	hsa-miR-1184-002842	1.6749
hsa-miR-126-002228	0.5668	hsa-miR-1197-002810	1.6749
hsa-miR-127-000452	0.4637	hsa-miR-1200-002829	1.6749
hsa-miR-127-5p-002229	6.6082	hsa-miR-1201-002781	1.276
hsa-miR-128a-002216	0.5219	hsa-miR-1203-002877	1.6749
hsa-miR-129-000590	0.6997	hsa-miR-1204-002872	1.6749
hsa-miR-130a-000454	0.7438	hsa-miR-1205-002778	1.6749
hsa-miR-130b-000456	0.3083	hsa-miR-1206-002878	1.6749
hsa-miR-132-000457	0.5206	hsa-miR-1208-002880	1.5875
hsa-miR-133a-002246	0.8089	hsa-miR-122#-002130	1.6749
hsa-miR-133b-002247	0.6997	hsa-miR-1224-3P-002752	1.6749
hsa-miR-135a-000460	0.6997	hsa-miR-1225-3P-002766	1.6749
hsa-miR-135b-002261	1.3636	hsa-miR-1226#-002758	1.6749
hsa-miR-136-000592	0.6997	hsa-miR-1227-002769	1.6749
hsa-miR-138-002284	0.5721	hsa-miR-1228#-002763	1.6749
hsa-miR-139-3p-002313	0.6997	hsa-miR-1233-002768	0.7897
hsa-miR-139-5p-002289	0.6025	hsa-miR-1236-002761	1.6749
hsa-miR-140-3p-002234	0.6721	hsa-miR-1238-002927	1.6749
hsa-miR-141-000463	0.6997	hsa-miR-124#-002197	1.6749
hsa-miR-142-3p-000464	0.6997	hsa-miR-1243-002854	0.0233
hsa-miR-142-5p-002248	0.6835	hsa-miR-1244-002791	1.6749
hsa-miR-143-002249	0.5008	hsa-miR-1245-002823	1.6749
hsa-miR-145-002278	0.8488	hsa-miR-1247-002893	0.6303
hsa-miR-146a-000468	0.2853	hsa-miR-1248-002870	1.6749
hsa-miR-146b-001097	0.2396	hsa-miR-1249-002868	3.0697
hsa-miR-146b-3p-002361	1.0784	hsa-miR-1250-002887	1.6749

hsa-miR-147-000469	0.6997	hsa-miR-1251-002820	1.6749
hsa-miR-147b-002262	0.6997	hsa-miR-1252-002860	0.8318
hsa-miR-148a-000470	2.3594	hsa-miR-1253-002894	1.6749
hsa-miR-148b-000471	0.6997	hsa-miR-1254-002818	2.4443
hsa-miR-149-002255	0.4322	hsa-miR-1255A-002805	1.6749
hsa-miR-150-000473	2.4744	hsa-miR-1255B-002801	1.4136
hsa-miR-152-000475	0.6534	hsa-miR-1256-002850	1.6749
hsa-miR-154-000477	0.6997	hsa-miR-1257-002910	1.6749
hsa-miR-155-002623	0.4708	hsa-miR-1259-002796	1.6749
hsa-miR-15a-000389	9.5846	hsa-miR-125b-1#-002378	3.3217
hsa-miR-15b-000390	1.3393	hsa-miR-125b-2#-002158	1.6749
hsa-miR-16-000391	0.7199	hsa-miR-126#-000451	0.3467
hsa-miR-17-002308	0.7947	hsa-miR-1260-002896	1.8033
hsa-miR-181a-000480	0.7446	hsa-miR-1262-002852	0.6785
hsa-miR-181c-000482	0.6997	hsa-miR-1263-002784	1.6749
hsa-miR-182-002334	0.6997	hsa-miR-1264-002799	1.6749
hsa-miR-183-002269	0.6997	hsa-miR-1265-002790	1.6749
hsa-miR-184-000485	0.1677	hsa-miR-1267-002885	1.6749
hsa-miR-185-002271	0.2892	hsa-miR-1269-002789	1.6749
hsa-miR-186-002285	0.4078	hsa-miR-1270-002807	0.4201
hsa-miR-188-3p-002106	0.0067	hsa-miR-1271-002779	2.2591
hsa-miR-18a-002422	0.0875	hsa-miR-1272-002845	1.6749
hsa-miR-18b-002217	0.6997	hsa-miR-1274A-002883	0.7443
hsa-miR-190-000489	0.6997	hsa-miR-1274B-002884	2.5995
hsa-miR-191-002299	0.4024	hsa-miR-1275-002840	1.77
hsa-miR-192-000491	0.6997	hsa-miR-1276-002843	0.9254
hsa-miR-193a-3p-002250	1.447	hsa-miR-1278-002851	1.6749

hsa-miR-193a-5p-002281	0.8241	hsa-miR-1282-002803	3.6572
hsa-miR-193b-002367	0.8436	hsa-miR-1283-002890	1.6749
hsa-miR-194-000493	2.562	hsa-miR-1284-002903	1.6749
hsa-miR-195-000494	0.8325	hsa-miR-1285-002822	1.8009
hsa-miR-196b-002215	0.6997	hsa-miR-1286-002773	1.6749
hsa-miR-197-000497	0.7679	hsa-miR-1288-002832	1.6749
hsa-miR-198-002273	2.4384	hsa-miR-1289-002871	1.6749
hsa-miR-199a-000498	0.5757	hsa-miR-129#-002298	1.6749
hsa-miR-199a-3p-002304	1.8781	hsa-miR-1290-002863	0.6104
hsa-miR-199b-000500	0.6997	hsa-miR-1291-002838	0.2716
hsa-miR-19a-000395	0.3332	hsa-miR-1292-002824	1.6749
hsa-miR-19b-000396	0.5962	hsa-miR-1293-002905	1.6749
hsa-miR-200a-000502	0.6997	hsa-miR-1294-002785	1.6749
hsa-miR-200b-002251	0.6997	hsa-miR-1296-002908	1.6749
hsa-miR-200c-002300	0.6997	hsa-miR-1298-002861	10.1843
hsa-miR-202-002363	3.1571	hsa-miR-1300-002902	0.5826
hsa-miR-203-000507	0.6997	hsa-miR-1301-002827	1.6749
hsa-miR-204-000508	0.4223	hsa-miR-1302-002901	1.6749
hsa-miR-205-000509	0.6997	hsa-miR-1303-002792	1.6749
hsa-miR-208-000511	0.6997	hsa-miR-1304-002874	1.6749
hsa-miR-208b-002290	0.6997	hsa-miR-1305-002867	2.0474
hsa-miR-20a-000580	0.9346	hsa-miR-130a#-002131	1.6749
hsa-miR-20b-001014	1.504	hsa-miR-130b#-002114	1.6749
hsa-miR-210-000512	1.2569	hsa-miR-132#-002132	1.6749
hsa-miR-21-000397	2.1622	hsa-miR-1324-002815	1.6749
hsa-miR-211-000514	0.6997	hsa-miR-135b#-002159	1.6749
hsa-miR-212-000515	0.7791	hsa-miR-136#-002100	1.062

hsa-miR-214-002306	0.7622	hsa-miR-138-2#-002144	1.6749
hsa-miR-215-000518	0.6997	hsa-miR-141#-002145	1.6749
hsa-miR-216a-002220	0.6997	hsa-miR-143#-002146	1.6749
hsa-miR-216b-002326	0.6997	hsa-miR-144#-002148	1.6749
hsa-miR-217-002337	0.6997	hsa-miR-144-002676	1.6749
hsa-miR-218-000521	0.5959	hsa-miR-145#-002149	0.2771
hsa-miR-219-000522	0.0499	hsa-miR-146a#-002163	1.6749
hsa-miR-219-1-3p-002095	0.6997	hsa-miR-148a#-002134	1.6749
hsa-miR-219-2-3p-002390	0.6997	hsa-miR-148b#-002160	1.6749
hsa-miR-220-000523	0.6997	hsa-miR-149#-002164	0.499
hsa-miR-22-000398	0.6997	hsa-miR-151-3p-002254	1.7156
hsa-miR-220b-002206	0.6997	hsa-miR-151-5P-002642	1.066
hsa-miR-220c-002211	0.6997	hsa-miR-154#-000478	1.6749
hsa-miR-221-000524	0.4726	hsa-miR-155#-002287	1.6749
hsa-miR-222-002276	0.5334	hsa-miR-15a#-002419	1.6749
hsa-miR-223-002295	0.6997	hsa-miR-15b#-002173	1.6749
hsa-miR-224-002099	0.8512	hsa-miR-16-1#-002420	1.6749
hsa-miR-23a-000399	0.6997	hsa-miR-16-2#-002171	1.6749
hsa-miR-23b-000400	0.6264	hsa-miR-17#-002421	1.6749
hsa-miR-24-000402	0.7368	hsa-miR-181a-2#-002317	2.8195
hsa-miR-25-000403	0.5669	hsa-miR-181c#-002333	1.6749
hsa-miR-26a-000405	0.5968	hsa-miR-182#-000483	1.6749
hsa-miR-26b-000407	0.6235	hsa-miR-1825-002907	11.2466
hsa-miR-27a-000408	0.9981	hsa-miR-1826-002873	0
hsa-miR-27b-000409	1.0066	hsa-miR-183#-002270	1.6749
hsa-miR-28-000411	0.591	hsa-miR-185#-002104	1.6749
hsa-miR-28-3p-002446	0.7206	hsa-miR-186#-002105	1.6749

hsa-miR-296-000527	0.8984	hsa-miR-18a#-002423	2.117
hsa-miR-296-3p-002101	1.5573	hsa-miR-18b#-002310	1.6749
hsa-miR-298-002190	0.6997	hsa-miR-190b-002263	0.2706
hsa-miR-299-3p-001015	0.6997	hsa-miR-191#-002678	1.1866
hsa-miR-299-5p-000600	0.6997	hsa-miR-192#-002272	2.2811
hsa-miR-29a-002112	0.5384	hsa-miR-193b#-002366	4.6207
hsa-miR-29b-000413	0.1487	hsa-miR-194#-002379	1.6749
hsa-miR-29c-000587	0.4146	hsa-miR-195#-002107	1.6749
hsa-miR-301-000528	3.7665	hsa-miR-196a#-002336	1.6749
hsa-miR-301b-002392	0.6997	hsa-miR-19a#-002424	1.6749
hsa-miR-302a-000529	3.3068	hsa-miR-19b-1#-002425	6.1045
hsa-miR-302b-000531	0.6997	hsa-miR-200a#-001011	1.6749
hsa-miR-302c-000533	0.6997	hsa-miR-200b#-002274	1.6749
hsa-miR-30b-000602	0.7406	hsa-miR-200c#-002286	1.6749
hsa-miR-30c-000419	1.5614	hsa-miR-202#-002362	1.6749
hsa-miR-31-002279	0.7296	hsa-miR-206-000510	3.123
hsa-miR-320-002277	0.6453	hsa-miR-20a#-002437	1.6749
hsa-miR-32-002109	0.6997	hsa-miR-20b#-002311	1.6749
hsa-miR-323-3p-002227	0.2792	hsa-miR-21#-002438	1.6749
hsa-miR-324-3p-002161	0.7198	hsa-miR-213-000516	1.6749
hsa-miR-324-5p-000539	0.6015	hsa-miR-214#-002293	1.497
hsa-miR-325-000540	0.6997	hsa-miR-218-1#-002094	1.6749
hsa-miR-326-000542	0.6997	hsa-miR-218-2#-002294	1.6749
hsa-miR-328-000543	0.7301	hsa-miR-22#-002301	1.4548
hsa-miR-329-001101	0.6997	hsa-miR-221#-002096	1.6749
hsa-miR-330-000544	0.9414	hsa-miR-222#-002097	1.6749
hsa-miR-330-5p-002230	0.6997	hsa-miR-223#-002098	1.6749

hsa-miR-331-000545	1.7596	hsa-miR-23a#-002439	1.6749
hsa-miR-331-5p-002233	0.6997	hsa-miR-23b#-002126	1.6749
hsa-miR-335-000546	0.6997	hsa-miR-24-1#-002440	1.6749
hsa-miR-337-5p-002156	0.5613	hsa-miR-24-2#-002441	1.6749
hsa-miR-338-3p-002252	0.6997	hsa-miR-25#-002442	0.5825
hsa-miR-339-3p-002184	0.5215	hsa-miR-26a-1#-002443	1.6749
hsa-miR-339-5p-002257	0.6568	hsa-miR-26a-2#-002115	1.6749
hsa-miR-33b-002085	0.6997	hsa-miR-26b#-002444	1.2274
hsa-miR-340-002258	0.6997	hsa-miR-27a#-002445	3.3541
hsa-miR-342-3p-002260	0.5818	hsa-miR-27b#-002174	2.5356
hsa-miR-342-5p-002147	0.6997	hsa-miR-29a#-002447	1.6749
hsa-miR-345-002186	0.3677	hsa-miR-29b-1#-002165	1.6749
hsa-miR-346-000553	0.6997	hsa-miR-29b-2#-002166	1.6749
hsa-miR-34a-000426	0.9894	hsa-miR-302a#-002381	1.6749
hsa-miR-34c-000428	0.2774	hsa-miR-302b#-002119	1.6749
hsa-miR-361-000554	2.5859	hsa-miR-302c#-000534	1.6749
hsa-miR-362-001273	1.5385	hsa-miR-302d#-002120	1.6749
hsa-miR-362-3p-002117	0.6997	hsa-miR-302d-000535	1.6749
hsa-miR-363-001271	0.8406	hsa-miR-30a-3p-000416	1.0249
hsa-miR-365-001020	0.7871	hsa-miR-30a-5p-000417	1.7889
hsa-miR-367-000555	0.6997	hsa-miR-30b#-002129	1.6749
hsa-miR-369-3p-000557	11.3433	hsa-miR-30c-1#-002108	1.6749
hsa-miR-369-5p-001021	0.6997	hsa-miR-30c-2#-002110	1.6749
hsa-miR-370-002275	0.1519	hsa-miR-30d#-002305	1.6749
hsa-miR-371-3p-002124	0.6997	hsa-miR-30d-000420	2.115
hsa-miR-372-000560	0.6997	hsa-miR-30e-3p-000422	0.5474
hsa-miR-373-000561	0.6997	hsa-miR-31#-002113	2.5438

hsa-miR-374-000563	0.2971	hsa-miR-32#-002111	1.6749
hsa-miR-375-000564	0.6997	hsa-miR-320B-002844	2.1975
hsa-miR-376a-000565	0.7629	hsa-miR-335#-002185	1.6749
hsa-miR-376b-001102	0.6997	hsa-miR-337-3p-002157	1.6749
hsa-miR-376c-002122	0.8157	hsa-miR-338-5P-002658	1.747
hsa-miR-377-000566	0.6997	hsa-miR-33a#-002136	1.6749
hsa-miR-380-3p-000569	0.6997	hsa-miR-33a-002135	1.6749
hsa-miR-381-000571	0.3631	hsa-miR-340#-002259	0.5812
hsa-miR-382-000572	0.9969	hsa-miR-34a#-002316	0.575
hsa-miR-383-000573	0.6997	hsa-miR-34b-000427	1.6749
hsa-miR-384-000574	0.6997	hsa-miR-34b-002102	0.9085
hsa-miR-409-5p-002331	0.6997	hsa-miR-361-3p-002116	1.6749
hsa-miR-410-001274	0.5501	hsa-miR-363#-001283	1.6749
hsa-miR-411-001610	0.1462	hsa-miR-367#-002121	1.6749
hsa-miR-412-001023	0.6997	hsa-miR-374a#-002125	1.6749
hsa-miR-422a-002297	0.6997	hsa-miR-374b#-002391	1.6749
hsa-miR-423-5p-002340	0.3625	hsa-miR-376a#-002127	1.6749
hsa-miR-424-5p-000604	2.2683	hsa-miR-377#-002128	1.6964
hsa-miR-425-5p-001516	0.8478	hsa-miR-378-000567	1.6749
hsa-miR-429-001024	0.6997	hsa-miR-378-002243	4.0845
hsa-miR-431-001979	0.6997	hsa-miR-380-5p-000570	1.6749
hsa-miR-433-001028	0.5603	hsa-miR-409-3p-002332	0.8199
hsa-miR-448-001029	0.6997	hsa-miR-411#-002238	1.6749
hsa-miR-449-001030	1.9075	hsa-miR-424#-002309	77.692
hsa-miR-449b-001608	0.6997	hsa-miR-425#-002302	1.1146
hsa-miR-450a-002303	8.2843	hsa-miR-431#-002312	1.6749
hsa-miR-450b-3p-002208	0.6997	hsa-miR-432#-001027	0.2326

hsa-miR-450b-5p-002207	0.6997	hsa-miR-432-001026	1.1377
hsa-miR-452-002329	0.7628	hsa-miR-452#-002330	1.6749
hsa-miR-453-002318	0.6997	hsa-miR-454#-001996	1.6749
hsa-miR-454-002323	0.5841	hsa-miR-483-3p-002339	1.0858
hsa-miR-455-001280	0.5855	hsa-miR-488-001106	1.6749
hsa-miR-455-3p-002244	0.956	hsa-miR-497#-002368	1.6749
hsa-miR-483-5p-002338	0.5919	hsa-miR-497-001043	1.6749
hsa-miR-484-001821	0.613	hsa-miR-500-001046	0.5512
hsa-miR-485-3p-001277	0.7478	hsa-miR-505#-002087	2.4169
hsa-miR-485-5p-001036	0.2511	hsa-miR-513B-002757	1.6749
hsa-miR-486-001278	0.7229	hsa-miR-513C-002756	1.6749
hsa-miR-486-3p-002093	0.6997	hsa-miR-516-3p-001149	0.5444
hsa-miR-487a-001279	0.6997	hsa-miR-517#-001113	1.6749
hsa-miR-487b-001285	0.6337	hsa-miR-518c#-001158	1.6749
hsa-miR-488-002357	0.6997	hsa-miR-518e#-002371	1.6749
hsa-miR-489-002358	0.6997	hsa-miR-518f#-002387	1.6749
hsa-miR-490-001037	0.1556	hsa-miR-519b-3p-002384	1.6749
hsa-miR-491-3p-002360	0.6997	hsa-miR-519e#-001166	1.6749
hsa-miR-492-001039	0.6997	hsa-miR-520c-3p-002400	0.7957
hsa-miR-493-002364	0.6001	hsa-miR-520D-3P-002743	1.4857
hsa-miR-494-002365	0.6051	hsa-miR-520h-001170	1.6749
hsa-miR-499-3p-002427	0.6997	hsa-miR-524-001173	1.6749
hsa-miR-500-002428	0.0883	hsa-miR-541#-002200	1.6749
hsa-miR-501-001047	10.8236	hsa-miR-543-002376	1.2367
hsa-miR-501-3p-002435	0.6997	hsa-miR-545#-002266	1.6749
hsa-miR-502-001109	0.6997	hsa-miR-548E-002881	1.6749
hsa-miR-502-3p-002083	0.6997	hsa-miR-548G-002879	1.6749

hsa-miR-503-001048	10.2227	hsa-miR-548H-002816	1.6749
hsa-miR-504-002084	0.6997	hsa-miR-548I-002909	1.6749
hsa-miR-505-002089	0.6997	hsa-miR-548J-002783	1.6749
hsa-miR-506-001050	0.6997	hsa-miR-548K-002819	1.6749
hsa-miR-507-001051	0.6997	hsa-miR-548L-002904	1.6749
hsa-miR-508-001052	0.6997	hsa-miR-548M-002775	1.6749
hsa-miR-508-5p-002092	0.6997	hsa-miR-548N-002888	1.6749
hsa-miR-509-3-5p-002155	0.6997	hsa-miR-548P-002798	1.6749
hsa-miR-509-5p-002235	0.6997	hsa-miR-549-001511	1.6749
hsa-miR-510-002241	0.6997	hsa-miR-550-001544	1.6749
hsa-miR-511-001111	0.6997	hsa-miR-550-002410	1.3621
hsa-miR-512-3p-001823	0.6997	hsa-miR-551a-001519	1.6749
hsa-miR-512-5p-001145	0.6997	hsa-miR-551b#-002346	1.6749
hsa-miR-513-5p-002090	0.6997	hsa-miR-552-001520	1.6749
hsa-miR-515-3p-002369	0.6997	hsa-miR-553-001521	1.6749
hsa-miR-515-5p-001112	0.6997	hsa-miR-554-001522	1.6749
hsa-miR-516a-5p-002416	0.6997	hsa-miR-555-001523	1.6749
hsa-miR-516b-001150	0.6997	hsa-miR-557-001525	1.6749
hsa-miR-517a-002402	13.928	hsa-miR-558-001526	1.6749
hsa-miR-517b-001152	1.1642	hsa-miR-559-001527	1.6749
hsa-miR-517c-001153	0.6997	hsa-miR-562-001529	1.6749
hsa-miR-518a-3p-002397	0.6997	hsa-miR-563-001530	1.6749
hsa-miR-518a-5p-002396	0.6997	hsa-miR-564-001531	0.5713
hsa-miR-518b-001156	0.6997	hsa-miR-566-001533	1.6749
hsa-miR-518c-002401	0.6997	hsa-miR-567-001534	1.6749
hsa-miR-518d-001159	1.3102	hsa-miR-569-001536	1.6749
hsa-miR-518d-5p-002389	0.6997	hsa-miR-571-001613	0.1488

hsa-miR-518e-002395	0.6997	hsa-miR-572-001614	1.6749
hsa-miR-518f-002388	0.6997	hsa-miR-573-001615	0.354
hsa-miR-519a-002415	1.7681	hsa-miR-575-001617	1.6749
hsa-miR-519c-001163	0.6997	hsa-miR-577-002675	1.6749
hsa-miR-519d-002403	0.6997	hsa-miR-578-001619	1.6749
hsa-miR-519e-002370	0.6997	hsa-miR-580-001621	1.6749
hsa-miR-520a#-001168	0.6997	hsa-miR-581-001622	1.6749
hsa-miR-520a-001167	0.6997	hsa-miR-583-001623	1.6749
hsa-miR-520b-001116	0.6997	hsa-miR-584-001624	1.6749
hsa-miR-520d-5p-002393	0.6997	hsa-miR-585-001625	0.3207
hsa-miR-520e-001119	0.6997	hsa-miR-586-001539	1.6749
hsa-miR-520f-001120	0.6997	hsa-miR-587-001540	1.6749
hsa-miR-520g-001121	1.2846	hsa-miR-588-001542	1.6749
hsa-miR-521-001122	4.9327	hsa-miR-589-001543	1.6749
hsa-miR-522-002413	0.6997	hsa-miR-590-3P-002677	1.6749
hsa-miR-523-002386	0.1598	hsa-miR-591-001545	0.0322
hsa-miR-524-5p-001982	0.6997	hsa-miR-592-001546	0.5099
hsa-miR-525-001174	0.6997	hsa-miR-593-001547	1.6749
hsa-miR-525-3p-002385	0.6997	hsa-miR-593-002411	1.6749
hsa-miR-526b-002382	0.6997	hsa-miR-595-001987	1.6749
hsa-miR-532-001518	0.7981	hsa-miR-596-001550	1.2906
hsa-miR-532-3p-002355	0.549	hsa-miR-599-001554	1.6749
hsa-miR-539-001286	1.308	hsa-miR-600-001556	1.6749
hsa-miR-541-002201	0.6997	hsa-miR-601-001558	2.1635
hsa-miR-542-3p-001284	0.6997	hsa-miR-603-001566	0.5978
hsa-miR-542-5p-002240	4.0347	hsa-miR-604-001567	1.6749
hsa-miR-544-002265	0.6997	hsa-miR-605-001568	1.6749

hsa-miR-545-002267	0.6997	hsa-miR-606-001569	1.6749
hsa-miR-548a-001538	0.6997	hsa-miR-607-001570	1.6749
hsa-miR-548a-5p-002412	0.6997	hsa-miR-608-001571	1.6749
hsa-miR-548b-001541	0.6997	hsa-miR-609-001573	1.6749
hsa-miR-548b-5p-002408	0.6997	hsa-miR-613-001586	1.6749
hsa-miR-548c-001590	0.6997	hsa-miR-614-001587	1.6749
hsa-miR-548c-5p-002429	0.6997	hsa-miR-616-001589	1.6749
hsa-miR-548d-001605	0.6997	hsa-miR-617-001591	0.448
hsa-miR-548d-5p-002237	0.6997	hsa-miR-620-002672	1.6749
hsa-miR-551b-001535	0.6997	hsa-miR-621-001598	1.6749
hsa-miR-556-3p-002345	0.6997	hsa-miR-622-001553	1.6749
hsa-miR-556-5p-002344	0.6997	hsa-miR-623-001555	1.6749
hsa-miR-561-001528	0.5065	hsa-miR-624-001557	13.9503
hsa-miR-570-002347	0.6997	hsa-miR-625#-002432	1.4797
hsa-miR-574-3p-002349	0.0001	hsa-miR-626-001559	1.6749
hsa-miR-576-3p-002351	0.1049	hsa-miR-628-3p-002434	1.6749
hsa-miR-576-5p-002350	0.6997	hsa-miR-629-001562	2.4453
hsa-miR-579-002398	0.6997	hsa-miR-630-001563	1.6749
hsa-miR-582-3p-002399	0.6997	hsa-miR-631-001564	1.6749
hsa-miR-582-5p-001983	0.6997	hsa-miR-633-001574	1.6749
hsa-miR-589-002409	0.6997	hsa-miR-634-001576	1.6749
hsa-miR-590-5p-001984	0.6997	hsa-miR-635-001578	1.6749
hsa-miR-597-001551	0.2946	hsa-miR-637-001581	1.6749
hsa-miR-598-001988	1.7128	hsa-miR-638-001582	1.3407
hsa-miR-615-5p-002353	0.6997	hsa-miR-639-001583	1.6749
hsa-miR-616-002414	0.2522	hsa-miR-640-001584	1.6749
hsa-miR-618-001593	0.8567	hsa-miR-641-001585	1.6749

hsa-miR-624-002430	0.6997	hsa-miR-643-001594	1.6749
hsa-miR-625-002431	0.9207	hsa-miR-644-001596	1.6749
hsa-miR-627-001560	0.6997	hsa-miR-645-001597	1.4103
hsa-miR-628-5p-002433	1.0034	hsa-miR-646-001599	1.6749
hsa-miR-629-002436	0.8592	hsa-miR-647-001600	1.6749
hsa-miR-636-002088	0.6997	hsa-miR-648-001601	1.6749
hsa-miR-642-001592	1.0664	hsa-miR-649-001602	1.6749
hsa-miR-651-001604	0.6997	hsa-miR-650-001603	1.6749
hsa-miR-652-002352	22.9203	hsa-miR-656-001510	1.6749
hsa-miR-653-002292	0.6997	hsa-miR-657-001512	1.6749
hsa-miR-654-001611	0.808	hsa-miR-658-001513	1.6749
hsa-miR-654-3p-002239	0.2657	hsa-miR-659-001514	1.6749
hsa-miR-655-001612	0.6997	hsa-miR-661-001606	1.6749
hsa-miR-660-001515	0.6997	hsa-miR-662-001607	1.6749
hsa-miR-671-3p-002322	1.0865	hsa-miR-663B-002857	1.6749
hsa-miR-672-002327	0.6997	hsa-miR-664-002897	0.1321
hsa-miR-674-002021	0.6997	hsa-miR-665-002681	1.6749
hsa-miR-708-002341	0.842	hsa-miR-668-001992	1.6749
hsa-miR-744-002324	0.6076	hsa-miR-675-002005	1.6749
hsa-miR-758-001990	0.6997	hsa-miR-708#-002342	1.6749
hsa-miR-871-002354	0.6997	hsa-miR-7-2#-002314	1.6749
hsa-miR-872-002264	0.6997	hsa-miR-720-002895	6.3641
hsa-miR-873-002356	0.6997	hsa-miR-744#-002325	1.6749
hsa-miR-874-002268	0.6997	hsa-miR-765-002643	1.6749
hsa-miR-875-3p-002204	0.6997	hsa-miR-766-001986	2.6832
hsa-miR-876-3p-002225	0.6997	hsa-miR-767-3p-001995	1.6749
hsa-miR-876-5p-002205	0.6997	hsa-miR-767-5p-001993	1.6749

hsa-miR-885-3p-002372	0.6997	hsa-miR-769-3p-002003	1.6749
hsa-miR-885-5p-002296	0.6997	hsa-miR-769-5p-001998	1.2843
hsa-miR-886-3p-002194	0.8041	hsa-miR-770-5p-002002	0.3295
hsa-miR-886-5p-002193	0.9361	hsa-miR-802-002004	1.6749
hsa-miR-887-002374	0.6997	hsa-miR-875-5p-002203	2.1144
hsa-miR-888-002212	143.2352	hsa-miR-888#-002213	0.1604
hsa-miR-889-002202	0.6997	hsa-miR-892b-002214	1.6749
hsa-miR-890-002209	0.6997	hsa-miR-9#-002231	1.6749
hsa-miR-891a-002191	0.6997	hsa-miR-920-002150	1.6749
hsa-miR-891b-002210	0.6997	hsa-miR-921-002151	1.6749
hsa-miR-892a-002195	0.6997	hsa-miR-922-002152	1.6749
hsa-miR-9-000583	0.6997	hsa-miR-924-002154	1.6749
hsa-miR-92a-000431	1.5482	hsa-miR-92a-1#-002137	1.6749
hsa-miR-95-000433	0.9421	hsa-miR-92a-2#-002138	1.6749
hsa-miR-98-000577	0.6997	hsa-miR-92b#-002343	1.6749
hsa-miR-99a-000435	0.4961	hsa-miR-93#-002139	3.5192
hsa-miR-99b-000436	0.5992	hsa-miR-933-002176	1.6749
mmu-miR-124a-001182	0.6997	hsa-miR-934-002177	1.6749
mmu-miR-129-3p-001184	0.0645	hsa-miR-935-002178	1.6749
mmu-miR-134-001186	0.4112	hsa-miR-936-002179	1.6749
mmu-miR-137-001129	0.6997	hsa-miR-937-002180	1.6749
mmu-miR-140-001187	0.5022	hsa-miR-938-002181	1.6749
mmu-miR-153-001191	0.6997	hsa-miR-939-002182	1.6749
mmu-miR-187-001193	0.6997	hsa-miR-941-002183	2.7411
mmu-miR-374-5p-001319	0.7849	hsa-miR-942-002187	0.9784
mmu-miR-379-001138	1.5525	hsa-miR-943-002188	1.6749
mmu-miR-451-001141	0.6997	hsa-miR-944-002189	1.6749

mmu-miR-491-001630	0.4735	hsa-miR-96#-002140	1.0779
mmu-miR-495-001663	0.458	hsa-miR-99a#-002141	0.0339
mmu-miR-496-001953	0.6997	hsa-miR-99b#-002196	1.646
mmu-miR-499-001352	0.6997	mmu-let-7d#-001178	1.6749
mmu-miR-615-001960	0.6997	rno-miR-29c#-001818	0.4655
mmu-miR-93-001090	0.2517	rno-miR-7#-001338	0.7349

	B2M Ct value	U6 Ct value
Untreated Mock	20.71 21.73 21.03	16.54 17.45 16.78
Untreated pre-miR Negative Control	20.35 20.76 20.64	16.88 17.7 17.06
Untreated pre-miR-424-3p	20.72 20.56 20.74	16.44 17.44 18.12
TGF-β1-treated Mock	21.41 22.12 21.39	16.64 16.43 17.1
TGF-β1-treated pre-miR Negative Control	20.50 21.53 21.44	19.36 18.99 19.54
TGF-β1-treated pre-miR-424-3p	20.67 20.99 21.34	17.4 17.44 17

Appendix 2: Comparison of CT values between B2M with U6 in NOF804

NOF804 cells were seeded and transfected with 50 nM of pre-miR negative control or 50 nM of pre-miR-424-3p for 48 h. Following that, cells were serum starved and treated with TGF-β1 or left untreated. RNA was isolated from fibroblasts and later used for cDNA synthesis. The qRT-PCR analysis was done using primers designed to amplify B2M and U6. This table shows B2M has the least variable in CT values between samples than that U